Distribution Agreement

In presenting this thesis or dissertation as a partial fulfillment of the requirements for an advanced degree from Emory University, I hereby grant to Emory University and its agents the non-exclusive license to archive, make accessible, and display my thesis or dissertation in whole or in part in all forms of media, now or hereafter known, including display on the world wide web. I understand that I may select some access restrictions as part of the online submission of this thesis or dissertation. I retain all ownership rights to the copyright of the thesis or dissertation. I also retain the right to use in future works (such as articles or books) all or part of this thesis or dissertation.

Signature:

_____ _____

Aimee R. P. Tierney Date

Characterization of Regulatory Pathways that Control a Virulence-Opacity Switch in

Acinetobacter baumannii

By

Aimee R. P. Tierney

Doctor of Philosophy

Graduate Division of Biological and Biomedical Sciences

Microbiology and Molecular Genetics

_____

Philip N. Rather, Ph.D.
Advisor

_____ _____

Joanna B. Goldberg, Ph.D.
Committee Member

William M. Shafer, Ph.D.
Committee Member

_____ _____

Charles P. Moran, Ph.D.
Committee Member

David S. Weiss, Ph.D.
Committee Member

Accepted:

_____

Kimberly Jacob Arriola, Ph.D., MPH
Dean of the James T. Laney School of Graduate Studies

_____

Date

Characterization of Regulatory Pathways that Control a Virulence-Opacity Switch in *Acinetobacter baumannii*

By

Aimee R. P. Tierney

B.S., Oglethorpe University, 2008

Advisor: Philip N. Rather, Ph.D.

An abstract of

A dissertation submitted to the Faculty of the

James T. Laney School of Graduate Studies of Emory University

in partial fulfillment of the requirements for the degree of

Doctor of Philosophy

in Graduate Division of Biological and Biomedical Sciences

Microbiology and Molecular Genetics

2021

Abstract

Characterization of Regulatory Pathways that Control a Virulence-Opacity Switch in

Acinetobacter baumannii

By: Aimee R. P. Tierney

Acinetobacter baumannii is a Gram-negative nosocomial pathogen that is highly resistant to a wide variety of antibiotics. *A. baumannii* cells exhibit phenotypic heterogeneity and switch rapidly between variants that form opaque or translucent colonies. These variants have unique transcriptional profiles and display differences in quorum sensing signal secretion, surface-associated motility, levels of polysaccharide capsule, biofilm formation, and carbon-source utilization. Most interestingly, the opaque variant is virulent while the translucent variant is avirulent, so they are designated VIR-O and AV-T, respectively. These observations suggest that manipulation of the genetic controls of the switch may attenuate *A. baumannii* virulence, thereby providing new methods of treatment that are not dependent on antibiotic susceptibility. The research described herein details the characterization of several regulatory genes that contribute to the control of the virulence-opacity switch in the clinical isolate AB5075. The stringent response regulator *relA* is one such gene, and upon its deletion cells become locked in the VIR-O state and display a strong increase in quorum sensing signal secretion and motility. The latter two phenotypes are enacted through the LysR-type transcriptional regulator *ABUW_1132*, which becomes overexpressed in the absence of *relA*. Investigation of *ABUW_1132* revealed that its deletion decreases VIR-O to AV-T switching 16-fold, halts quorum sensing signal secretion, and reduces motility. Further, *ABUW_1132* deletion increases levels of polysaccharide capsule and virulence in the AV-T variant. Finally, this work additionally characterizes a family of at least twelve TetR-type transcriptional regulators, some of which constitute the primary pathway through which switching is controlled. As VIR-O cells grow to high density, a stochastic increase in the transcription of one or more of these TetRs occurs, activating the switch to AV-T. The TetRs display high levels of homology to one another and act in a redundant manner such that if one TetR is deleted, others can serve to activate the switch. Four TetRs—*ABUW_1645*, *ABUW_1959*, *ABUW_2818*, and *ABUW_3353*—appear to be the most utilized, and deletion of these four genes results in a 1,245-fold decrease in switching. This research adds significantly to the body of knowledge surrounding switching, quorum sensing, motility, and virulence in AB5075.

Characterization of Regulatory Pathways that Control a Virulence-Opacity Switch in *Acinetobacter baumannii*

By

Aimee R. P. Tierney

B.S., Oglethorpe University, 2008

Advisor: Philip N. Rather, Ph.D.

A dissertation submitted to the Faculty of the

James T. Laney School of Graduate Studies of Emory University

in partial fulfillment of the requirements for the degree of

Doctor of Philosophy

in Graduate Division of Biological and Biomedical Sciences

Microbiology and Molecular Genetics

2021

Acknowledgements

This body of work would not have been possible without the exceptional mentorship of my advisor, Dr. Philip Rather. Phil is completely dedicated to the success of his students and has spent numerous hours providing one-on-one instruction, giving feedback, and generating ideas with me. I am so grateful for his generosity and for the unwavering guidance and support he gave at every step of my academic path.

In addition, I would like to thank my dissertation committee, all of whom have supplied wonderful advice and encouragement. My committee meetings were a source of steady support, perspective, and direction, and I always left with greater clarity and more confidence in myself. I would like to especially recognize Dr. Bill Shafer for the advising and teaching he provided through ARTDTP as well as many opportunities for networking and professional growth. I would further like to thank Dr. David Weiss and Dr. Chui Yoke Chin for their collaboration, which greatly strengthened the impact of this research.

I have been very fortunate to work with a team of excellent scientists and friends in my lab, and I would like to thank them for sharing their ideas, humor, and emotional support with me. To Sarah Anderson, I am so grateful for your encouragement, support, countless literature discussions, and intermittent silliness. To María Pérez-Varela, thank you for all the camaraderie and help as we worked on the TetR mysteries together and for all the semi-chaotic brainstorming sessions. To Jen Colquhoun, thanks for sharing your inimitable sense of humor and valuable advice as I moved through the last year of my PhD.

I would also like to extend my thanks to Dr. Levi Morran and his wife Emily Morran, the former MMG Program Administrator. Levi was my first mentor and gave me the opportunity to volunteer in his lab when I had no research experience. My time in his lab was short, but I remember it very fondly. Emily helped me decide to apply to MMG, and I will never forget the tremendous understanding, support, and advice she gave me at critical junctures and difficult times during my PhD.

I have so many loved ones who have helped me to this point of my life. I send my love and gratitude to my mom, dad, stepmother, sisters, and grandparents, all of whom have given me 36 years of their love, support, and encouragement. A special thanks to my sister Erica Roberts who has become one of my best friends and is always there for me. To my friend of over 20 years Lauralee Hayes, thank you so much for everything. I treasure our friendship and your constant support. To my sister-in-law Ashleigh Tierney, I met you only 18 months into my PhD journey, and you have become my family. Thank you so much for all the conversations that were exactly what I needed. I also must thank my kitties—Bere, Sawyer, and Puca—who have enriched my life with supportive snuggles, comic relief, pesky antics, and unfortunate mishaps for the past eleven years.

Finally, I would like to thank the person who has lived this experience with me more so than anyone else—my amazing husband Brian Tierney. As I have made my way through earning my doctorate, you have been there for every late night, every milestone celebration, and every hard moment. When I stop to think how much work and how many worries you've lifted off my shoulders, I am overwhelmed with gratitude. I love you so much and can't believe my luck at having found such a wonderful partner in life.

Table of Contents

Chapter 1: Introduction

Acinetobacter baumannii

Acinetobacter baumannii is a Gram-negative bacterial pathogen recognized during the 1970s as a particularly troublesome source of pneumonia in nosocomial settings, especially in patients with compromised immune systems and indwelling medical devices [1]. Although *Acinetobacter* infections most commonly occur in the lungs, other sites include the urinary tract, skin and soft tissues, blood, bone, and cerebrospinal fluid [2-4]. Despite a relatively low number of deaths per year attributable to *A. baumannii* infection (700 deaths in the US in 2017) [5], this organism has been deemed a critical priority for research and development of new antimicrobials due to its wide range of resistances to antibiotics, especially carbapenems [3, 5-8], and its impressive ability to persist on surfaces in the clinical setting [9-13]. In recent years, the Rather laboratory discovered that *A. baumannii* displays colony opacity variation that is directly connected to virulence [14, 15], a phenotype that had gone undetected in over 75 years of studies and publications on this species. This phenotype and the transcriptional regulators controlling this process is the primary focus of the research presented herein and will be discussed in greater detail following a summation of *A. baumannii*'s history and other relevant phenotypes.

History of *Acinetobacter baumannii*

The *Acinetobacter* genus has undergone a great deal of taxonomic revisions since its discovery in 1911 by the Dutch microbiologist Beijerinck from soil samples grown in minimal media containing calcium acetate [16]. This first isolate was named *Micrococcus calco-aceticus* and subsequently various other similar species were described and given scientific names under different genera. The designation "Acinetobacter" was later crafted from the Greek "akinetos"

meaning “nonmotile” by Brisou and Prevot in 1954 in an attempt to separate motile and nonmotile species of the *Achromobacter* genus, under which some of the phenotypically similar species to Beijerinck’s *Micrococcus calco-aceticus* had been classified [17]. However, this name was not widely used until 14 years later when Baumann conducted a thorough examination of this assortment of similar species. He determined that they could not be further phenotypically subcategorized and should be classified under the same genus: *Acinetobacter* [18], which was officially accepted in 1971 [19]. Prior to this revision, *A. baumannii* was known mostly by the name *Bacterium anitratum* or *Hellerea vaginicola* [20], and after as *Acinetobacter anitratum* or *Acinetobacter calcoaceticus* var. *anitratum*. Dozens of publications as early as 1949 document this pathogen’s presence, using these older names, in cases of septicemia, pneumonia, pleurisy, meningitis, and urinary tract, wound, and ocular infections [21-34] as well as its resistance to antibiotics [35-42] and its predilection for ventilator-associated infections [43]. Finally, in 1987, Bouvet and Grimont assayed 343 *Acinetobacter* strains, 299 of which were clinical isolates, and found that 253 of these represented the same species, which they named *Acinetobacter baumannii* [44].

As previously mentioned, *A. baumannii* was already a known to exhibit high resistance to a variety of antibiotics, but clinicians became increasingly concerned as resistance to imipenem, a carbapenem to which *A. baumannii* had previously been susceptible, began to be widely documented in the mid-1990s [45-49]. Starting around 2005, publications on *A. baumannii* began to increase exponentially, surpassing 1000 manuscripts in 2019 alone (PubMed search: *Acinetobacter baumannii*). This escalation of publications coincided with increased incidences of nosocomial infections as well as a surge in wound infections with multidrug resistant *A. baumannii* in U.S. soldiers during the Iraq War and later the Afghanistan War, earning it the name

"Iraqibacter" [50-54]. Increased interest in *A. baumannii* may also be due to the proliferation of antibiotic resistance as a whole. In 1994, the first paper to mention the idea of a "post-antibiotic era" was published [55] and was followed by a steady trickle of likeminded publications, with the call to action beginning to amplify greatly in the mid-2000s. In light of this crisis, the study of *A. baumannii* became critical due to its antibiotic resistance profile and ability to gain resistance elements from other bacteria.

Species and Strain General Characteristics

The strain used for this research is AB5075, a clinical isolate recovered from a case of tibial osteomyelitis in 2008. AB5075 is highly virulent and multidrug resistant while still amenable to genetic manipulations by high-copy expression vectors, Tn7 chromosomal insertions, transposon insertional deletions and in-frame null allele deletions [88]. Together these phenotypes make AB5075 an excellent model strain with high clinical relevance.

A. baumannii are aerobic, gram-negative coccobacilli that are catalase-positive, oxidase-negative, non-flagellated, and non-glucose-fermenting [2, 3]. While most *Acinetobacter* species inhabit soil and form part of human skin flora [56-58], the natural habitat of *A. baumannii* is not yet determined, though many potential reservoirs have been identified [59]. Among them are farmed vegetables in the United Kingdom [60], soil in Hong Kong, India, and France [61-63], frequently-touched surfaces in South Korea [64], domestic animals in veterinary settings [65-69], and a variety of other agriculture and aquaculture sources [70-72]. The carrier rate among humans was observed to be generally low (0.5% to 3%) in Europe [57, 58]. Predictably, medical workers exhibit higher rates of colonization [73, 74]; however, a study conducted among New York

community members showed 10.4% *A. baumannii* skin carriage [75], and other studies have shown a strong presence of this species in human head and body lice [76-78].

Colonies appear whitish-beige on solid media and are slightly mucoid due to their production of capsular polysaccharide [79-81]. The outer leaflet of *A. baumannii*'s outer membrane is composed of the endotoxin lipid A onto which a core oligosaccharide is anchored, forming lipooligosaccharide (LOS) [82]. In many species of Gram-negative bacteria, the carbohydrate chain is further elongated by WaaL ligase which connects repeating O-antigen sugar structures onto the core oligosaccharide, forming lipopolysaccharide (LPS) [83]. However, microbiologists debate whether *A. baumannii* cell surfaces display LOS or LPS, due to inconsistencies in silver staining of LPS extractions and the lack of a clear WaaL ligase ortholog [84]. Interestingly, in either case, LOS/LPS is not an essential structure for *A. baumannii*, as demonstrated in mutants for the lipid A biosynthetic pathway [85-87].

Quorum Sensing

A. baumannii uses a LuxI-LuxR type quorum sensing system known as AbaI-AbaR, which employs an N-acyl-homoserine lactone (AHL) molecular signal, primarily N-(3-hydroxydodecanoyl)-L-homoserine lactone. [89]. The autoinducer synthase encoded by *abaI* produces AHL, which exits the cell through an unknown mechanism. At high population density, the AHL signal reenters cells and binds the AbaR transcriptional regulator, encoded upstream of *abaI*, which then brings about global transcriptional changes. AbaR may also promote *abaI* expression based on the presence of a putative *lux*-box 67 bp upstream of *abaI*, indicating a likely binding site for AbaR [89]. Quorum sensing increases surface-associated motility and biofilm

production in *A. baumannii* [89, 90]. It is also thought to contribute to virulence, possibly through regulation of the Type VI secretion system and modulation of host immunity [91, 92].

Motility

Acinetobacters do not encode flagellar genes and were once thought to be nonmotile, as indicated by the Greek etymology "akinetos," meaning "nonmotile." We now recognize that *A. baumannii* exhibits both twitching motility and surface-associated motility [90, 93, 94]. The twitching motility requires a functioning Type IV pilus, which is also necessary for natural transformation [93].

Surface-associated motility can be seen on low concentration agar (~0.3%) and likely employs a gliding mechanism with the assistance of a surfactant. Surface motility in *A. baumannii* is dependent on the AbaI-AbaR quorum sensing system [90]. Briefly, when a quorum is reached, AbaR activates an operon required for biosynthesis of lipopeptide acinetin-505, which acts as a surfactant. Genetic modifications that cause increased AHL production result in a several-fold increase in motility.

Stringent Response

The stringent response is a type of stress response utilized by bacteria in reaction to environmental conditions lacking in nutrients such as amino acids and fatty acids. Activation of the stringent response enacts global transcriptional changes that halts most translational elements of the cell [95, 96]. As a result, the cell undergoes multiple phenotypic changes often including slow growth and changes to motility, virulence, persister cell formation, cell division, and biofilm formation [97].

The stringent response is orchestrated by the RelA and SpoT enzymes [98], the alarmone (p)ppGpp (guanosine tetra- or pentaphosphate), and the transcription factor DskA [95]. RelA synthesizes (p)ppGpp from ATP, GTP or GDP while SpoT acts mainly as a hydrolase of (p)ppGpp, but also has weak synthetase activity [95, 96]. RelA senses amino acid depletion when its C-terminal binds to an uncharged tRNA in the ribosomal A site [99]. The binding event triggers RelA activation, and synthesis of (p)ppGpp initiates. (p)ppGpp binds RNA polymerase (RNAP) at two sites: the β′–ω interface and at a second site that requires DskA assistance—the DskA-β′ interface [100]. The result of this binding is a change in global promoter activity, some increased and some decreased, though the large reduction of transcription at rRNA promoters is most notable and formed the basis of the research that determined (p)ppGpp and DskA interactions with RNAP [95].

Pathogenesis and Virulence Factors

A. baumannii is a hospital pathogen often associated with cases of ventilator-associated pneumonia in ICU settings. However, it is capable of enacting a wide range of other infections, most prominently septicemia, urinary tract infections, skin and soft tissue infections, and meningitis [101, 102]. Often these infections coincide with patients who have a history of long length of stays in the hospital or ICU, major surgery, depressed immune system, alcoholism, or involvement in war or a large-scale disaster such as a tsunami or earthquake. While infections are typically nosocomial, potential reservoirs now exist in the environment and community (as discussed above). Community-associated cases are sporadically reported, often involving individuals suffering from alcoholism or homelessness, or in tropical regions [103-111]. Interestingly, *A. baumannii* has recently been identified as an inhabitant of oral biofilms and a possible oral

pathogen associated with cases of chronic or aggressive periodontitis, especially in HIV-positive patients [112]. Individuals with oral colonization by *A. baumannii* may be at increased risk for ventilator-associated pneumonia.

Persistence in the Clinical Environment

One of *A. baumannii*'s most problematic traits is its ability to withstand long periods of desiccation while retaining virulence [8, 9]. In one study, five clinical isolates survived 60 days on glass or plastic at rates of 40% to 70% [11]. Desiccation resistance is not yet fully understood in *A. baumannii* but is influenced by a variety of factors. A recent study showed that capsule-minus mutants were 2.5-fold less resistant to desiccation, indicating capsule polysaccharide as a possible shield to cell dehydration [113]. Adequate acylation of lipid A is also required for outer membrane integrity in periods of osmotic stress [114]. Additionally, mutations in the coding sequence for the BfmR response regulator gives rise to a desiccation-sensitive phenotype that appears to result from the loss of BfmR-controlled stress responses [115].

Disinfectants used against Gram-negative bacteria are not consistently successful when applied to *A. baumannii* [116]. Here again, the bacterial capsule increases resistance to the common hospital disinfectants benzethonium chloride (BZT), benzalkonium chloride (BAC), and chlorhexidine gluconate (CHG) [113]. Additionally, a variety of efflux pumps also contribute to disinfectant resistance. Deletion of the RND (resistance nodulation division) efflux pumps AdeABC and AdeIJK increase susceptibility to BAC, CHG, Synergize disinfectant, and Wex-Cide [117]. Futher, the efflux pumps AvmA and AdeS both confer resistance to BAC and CHG [118, 119], and yet another, AceI, specifically binds CHG and transports it out of the cell [120].

Another mechanism that promotes environmental persistence is the formation of biofilms on both biotic and abiotic surfaces. This strengthens resistance to desiccation and disinfectants, promotes infection of wounds, and allows colonization of indwelling medical devices [121-123]. The BfmS/BfmR two-component system mediates biofilm formation through its regulation of the csu pilus operon, the quorum sensing system, the OmpA outer membrane protein, the biofilm-associated (Bap) protein, and the *pgaABCD* operon required for the production of PNAG (poly-β-1,6-N-acetylglucosamine) [124].

Host Interaction

A. baumannii employs a wide variety of virulence factors that allow it to colonize, invade, and survive inside a host. The initial adherence to host cells is an essential step to infection, carried out in large part by the OmpA outer membrane protein, a β-barrel porin that binds to the fibronectin component of epithelial cells' extracellular matrix [125-127]. OmpA also promotes serum resistance through the binding and sequestration of factor H, the primary regulator of the alternative complement pathway [128, 129]. Further, OmpA can target both the mitochondria and nucleus, releasing apoptosis-inducing factors and causing cell death [130-132].

Components of the bacterial cell envelope, primarily the polysaccharide capsule, glycosylated proteins, and LOS/LPS, also contribute to pathogenicity [3, 8]. The capsule is possibly *A. baumannii*'s most important contributor to survival in host serum, as loss of capsule causes avirulence due to a large increase in both complement-mediated killing and susceptibility to lysozyme [79, 113]. The precise role of glycosylated proteins in pathogenicity is still unknown, but disruption of the O-linked glycosylation system leads to loss of normal biofilm formation and attenuation of virulence in *Galleria mellonella* larvae [133]. Additionally, a separate O-linked

glycosylation system has been shown to glycosylate Type IV pili, which may shield them from antigenic recognition [80, 134]. Finally, the lipid A moiety of LOS/LPS is a known endotoxin, and the blocking of lipid A and LOS/LPS synthesis decreases virulence significantly through increased opsonophagocytosis [135].

Phospholipases are enzymes that metabolize membrane phospholipids and are crucial for normal cell maintenance. Phospholipases have long been recognized as virulence factors in many species of bacteria, as they can disrupt host cell membranes and interfere with immune-related cell signaling [136, 137]. There are three known classes in bacteria: phospholipase A (PLA), phospholipase C (PLC), and phospholipase D (PLD), of which *A. baumannii* possesses only PLC and PLD [3, 137]. Deletion of PLC or PLD diminishes host cell invasion, serum resistance, cytolysis, and overall virulence [138-142].

A. baumannii employs a variety of methods for secretion, some of which contribute to pathogenicity. The study of outer membrane vesicles (OMVs) in *A. baumannii* has increased in the past ten years, revealing a putative role in virulence [143]. OMVs are capable of transporting a variety of effectors into host cells, including OmpA, phospholipases, and proteases [144-146]. Due to their ability to elicit a strong immune response, OMVs have been considered for use in vaccines, and were shown to provide protection in a mouse model [147, 148]. Additionally, *A. baumannii* possesses multiple classic secretion systems: Types I, II, IV, V, and VI, though only Types II, V, and VI are known to contribute to virulence [149, 150]. The Type II SS secretes several effectors including lipases and a metalloprotease required to colonize and propagate throughout the host [151-153]. The Ata autotransporter is a Type V SS that contributes to adhesion by binding to components of the epithelial extra cellular matrix and basal membrane, including

collagen and laminin [154, 155]. *A. baumannii*'s Type VI SS is primarily used for interspecies competition, but its deletion in one study led to failed infection of *G. mellonella* [156].

Like all organisms, bacteria need trace metals for survival, and during infection they must combat host attempts to prevent their acquisition. Hosts sequester these metals as a protective measure known as nutritional immunity, and *A. baumannii* has evolved multiple mechanisms to overcome this defense [128, 157, 158]. Production and utilization of siderophores, small molecules with a high affinity for iron, is the primary means of iron acquisition. Of several *A. baumannii* siderophores, acinetobactin is the best characterized and is essential to virulence in *G. mellonella* and mouse models [159-161]. Zinc is another key trace metal and a prominent cofactor for enzymatic function. The transcriptional regulator Zur reacts to zinc depletion by upregulation of the high-affinity zinc acquisition system ZnuABC [162-164]. This system also reacts to the presence of calprotectin, a host-affiliated molecule released in the lungs for the entire course of a pulmonary infection, that chelates and sequesters zinc and manganese [165, 166]. Acquisition of manganese, another essential cofactor, relies on the coordinated action of a manganese transporter and urea carboxylase [167]. The urea carboxylase is required for calprotectin resistance, though the mechanism for this interaction is currently unknown.

Antibiotic Resistance

A. baumannii's high resistance levels to a wide range of antibiotics are undeniably its most worrisome characteristic. Globally, over 45% of strains are multidrug resistant, with increasing rates of extreme drug resistant and even pan-resistant organisms [8, 168]. Moreover, the ability of this pathogen to distribute and receive genetic elements encoding resistance through horizontal gene transmission has been extensively documented [169-176]. Resistance to antimicrobials may

be encoded chromosomally or on plasmids and mediated by a variety of mechanisms including, production of antibiotic degrading or modifying enzymes, efflux pumps, changes in permeability, and alteration of antibiotic targets among others [3, 168].

A. baumannii primarily uses antibiotic degrading enzymes, and some isolates carry all four classes of β-lactamases [3]. β-lactamases are a large family of hydrolases that inactivate β-lactam antibiotics such as penicillin and cephalosporin through cleavage of their β-lactam ring. Carbapenems are generally less susceptible to degradation by β-lactamases and until recently were regarded as the weapon of choice in treating MDR *A. baumannii* infections [177]. The aforementioned clinical change in susceptibility to the carbapenem imipenem was later shown to be the result of carbapenemase activity [178-180]. *A. baumannii* possesses three clavulanic acid-resistant carbapenemases: OXA-23, OXA-24, and OXA-58 [181]. Additionally, most clinical isolates of *A. baumannii* are resistant to aminoglycosides, which is primarily achieved through the use of a variety of aminoglycoside-modifying enzymes [182-185].

Efflux pumps can rid the cell of a variety of antibiotics and other toxins. Clinical isolates of *A. baumannii* often overexpress efflux pumps, contributing to their overall resistance [186]. The Ade pumps (AdeABC AdeFGH, AdeIJK), which belong to the RND family, aid in resistance to aminoglycosides, tigecycline, β-lactams, macrolides, tetracycline, fluoroquinolones, trimethoprim, and chloramphenicol [186-191]. Other major facilitator superfamily (MFS) members confer resistance to tetracycline (TetA and TetS) [192], chloramphenicol (CraA, CmlA, FloR) [193, 194], and erythromycin (AmvA) [119]. The EmrAB-TolC pump was recently implicated in reduced susceptibility to the last-line drug colistin as well as netilmicin, tobramycin, and imipenem [195, 196]. While a comprehensive listing of the many efflux pumps utilized in *A.*

baumannii antibiotic resistance is beyond the scope of this introduction, the broad-spectrum protection provided by efflux pumps is evident even among the few examples given here.

A. baumannii may reduce its susceptibility to an antibiotic by modifying the drug's cellular target to prevent its action. Alteration of GyrA and ParC, components of DNA gyrase and topoisomerase IV, respectively, leads to quinolone resistance [197, 198]. *A. baumannii* can also overexpress altered penicillin binding proteins (PBPs), repetitive constituents of bacterial cell walls, to which imipenem can no longer bind [199]. In addition to the aminoglycoside resistance achieved through aminoglycoside-modifying enzymes, the ArmA protein found in many clinical isolates methylates the 16S RNA ribosomal subunit, blocking the drug's point of action [200]. Finally, modification or loss of LOS/LPS removes the electrostatic attraction that allows colistin permeation, thereby promoting resistance [85, 201].

Finally, changes that reduce the ability of antibiotics to permeate cells understandably complicate treatment. Downregulation of outer membrane porins has been shown to enact or further increase resistance to carbapenems by preventing their entry into cells [3]. Furthermore, the slow diffusion of antibiotics through biofilms as well as the major changes to gene expression that occurs in cells within them can prevent antibiotic action [187].

Phenotypic Heterogeneity

The majority of work to be discussed herein centers on *A. baumannii*'s phenotypic heterogeneity, which manifests as cells that can form either opaque or translucent colonies [14]. The difference in colony opacity must be visualized on 0.8% agar plates using a dissecting microscope with an oblique light source from beneath the stage. Opaque colonies are bright yellow-orange in color with a distinct golden sheen and are slightly smaller than translucent colonies, which have a blue-

tinged periphery surrounding a concentric muted beige center. Microscopically, translucent cells are more elongated than opaque cells when grown to stationary phase.

Cells within these opaque and translucent colonies interconvert at frequencies between 4-13% at 24 hours of growth and 20-40% at 48 hours, indicating a high-frequency phenotypic switch between the two variants [14, 15]. Switching in opaque colonies is visibly apparent in the form of translucent sectors that begin to form in the outer edges of the colony after 14-16 hours of growth at 37°C. However, translucent colonies do not display a reliable visual marker indicating switching to the opaque form. The switch only begins to occur at high cell density, so pure glycerol stocks of each variant can be obtained by growing low density cultures from very small, well-isolated colonies. Switching frequencies are quantified by extracting a whole colony with its underlying agar, resuspending the colony in broth, and plating serial dilutions.

Cells that form either opaque or translucent colonies exhibit multiple phenotypic differences, and among the most important of these is virulence. The variant forming opaque colonies is virulent (VIR-O) and those forming translucent colonies are avirulent (AV-T), which has been confirmed in *G. mellonella* and mouse models [14, 15]. When pure cultures of VIR-O are inoculated into mice intranasally, complete lethality occurs by the second day of infection, with recovery of 100% VIR-O variants from the lungs, spleens, and livers at titers of 10^9, 10^6, and 10^6 CFU/g, respectively [15]. By contrast, 100% of mice survived when inoculated with pure cultures of AV-T, and only 70% of the recovered cells from the lungs were the AV-T variant. This indicates that the host environment enriched for the 0.01% of VIR-O variants that were present in the starting culture, resulting in a 3,000-fold increase. Moreover, the bacterial loads recovered from AV-T-infected mouse lungs were 10,000-fold lower and 1,000-fold lower in the spleens and livers

compared with VIR-O-infected mice. Additionally, in humans with *A. baumannii* septicemia, only VIR-O variants are recovered from blood [15].

Other phenotypic distinctions between the two colony types include increases in capsular polysaccharide, secretion of AHL quorum sensing signal, and surface-associated motility of the VIR-O variant [14, 113]. Higher capsule volume of the VIR-O variant constitutes part of the explanation for its increased virulence as well as its increased resistance to desiccation and lysozyme compared to AV-T [15, 113]. However, the visual distinction in opacity between VIR-O and AV-T colony variants is not the result of their capsular differences, as capsule-minus mutants (Δ*wzc*) still exhibit opaque and translucent colony morphotypes [113]. VIR-O cells are also more resistant to hydrogen peroxide and the host antimicrobial peptide LL-37 [15]. Together, these qualities contribute to the virulence of VIR-O and the selection of this variant in the nosocomial environment and in host organisms.

The AV-T variant activates a number of metabolic pathways not expressed in the VIR-O variant and also exhibits increased biofilm formation [14]. Due to these features, the AV-T state is hypothesized to be better adapted for survival in the non-hospital/host environment; however, experiments to better define this role are currently lacking. Despite the typical avirulence of AV-T, experiments suggest that the basic ability to switch from VIR-O to AV-T may be important to virulence. LSOs (low switching VIR-Os) are isogenic populations of VIR-O cells that switch at rates up to 1,000-fold lower than normal VIR-O cells. In mouse pneumonia models, infection with pure LSO cultures results in attenuated virulence with at least 10^3 lower bacterial loads recovered from the lungs at 24 hours post-inoculation than normal VIR-O cells [202].

Regulation of the Switch

The ultimate goal of this research is to contribute to the understanding of the genetic mechanisms underlying the phenotypic switch. Our group has identified upwards of 20 key genes that affect the switch when deleted and/or overexpressed, though at this time their interactions have not been ascertained and a great deal of redundancy appears to exist. Most of these genes encode TetR-type transcriptional regulators (TTTRs), a family of DNA-binding proteins described in detail in a following section. One in particular, *ABUW_1645* (*1645*), appears to be crucial to the maintenance of the AV-T state [15]. This gene was discovered through RNA sequencing of the wild-type VIR-O and AV-T, which revealed a 60-fold upregulation of *1645* in AV-T. Deletion of *1645* in either VIR-O or AV-T backgrounds does not significantly alter rates of switching, but its overexpression completely drives VIR-O cells to AV-T state where they are locked. Other TTTRs were also noted as differentially regulated between the two variants [15]. Some, like *ABUW_1959* and *ABUW_2818*, have identical outcomes to *1645* when deleted and overexpressed (unpublished data). Investigation of many other TTTRs is ongoing.

The OmpR/EnvZ two-component system also plays a role in the phenotypic switch [203]. Deletion of either *ompR* or *envZ* results in a roughly 400-fold increase in VIR-O to AV-T switching. However, deletion of *ompR* or *envZ* in the AV-T background causes a 9-fold reduction or a 5-fold increase in switching, respectively. These outcomes were among the first that strongly indicated the presence of unique regulatory pathways controlling switching in the two variants.

Additionally, transposon mutagenesis screens identified two genes *arpA* and *arpB*, predicted to encode components of RND type efflux systems. Deletion of *arpA* in the VIR-O background caused a 70-fold reduction in switching, while deletion of *arpB* in VIR-O caused a 769-fold reduction [204]. However, neither gene appears to affect the AV-T to VIR-O switch

when deleted. Intriguingly, neither the OmpR/EnvZ nor the ArpAB pathways seem to work through *1645*.

Opacity Variation in Other Organisms

Variation of colony opacity among isogenic populations has also been well documented and described in *Neisseria gonorrhoeae* and *Streptococcus pneumoniae*, both of which result from phase variation. In the case of *N. gonorrhoeae*, cells encode opacity ("Opa" or "P.II") proteins at 11 loci [205-207]. Opa proteins are outer membrane proteins that impart an increased colony opacity that scales with the number of loci that are active in expressing Opa proteins [208]. The 5' ends of the *opa* loci contain several pentameric repeats (CTCTT) that can cause slipped-strand mispairing during DNA replication [209, 210]. When these mispairing events result in a frameshift that brings an ATG start codon into frame, the *opa* gene is expressed [209, 210]. Consequently, any number from 0 to all 11 of the *opa* loci may be expressed in a given gonococcal cell.

S. pneumoniae's opacity variation arises due to large DNA inversions in the $hsdS_A$ gene, one of three genes that encode portions of the HsdS protein of a Type I restriction-modification (R-M) system [211-213]. Typically, R-M systems endeavor to prevent bacteriophage infection through the action of an endonuclease that cleaves phage genetic material [214]. A methyltransferase protects the host genome by methylation of host DNA, which is recognized in a site-specific manner. In a Type I R-M, neither the endonuclease (HsdR) nor the methyltransferase (HsdM) has site-recognition abilities, and a separate protein (HsdS) carries out this function [215]. Three genes with high sequence homology—$hsdS_A$, $hsdS_B$, and $hsdS_C$—encode the subunits of HsdS [213]. Inversions of these genes generate new allelic versions, and among them, the $hsdS_{A1}$ allele was shown to alter sequence recognition of HsdS such that new patterns of methylation by

HsdM emerges, bringing about phenotypic heterogeneity [213]. Specifically, opaque cells carry the $hsdS_{A1}$ allele, while translucent cells lack this allele.

Bistability

It is likely that the opacity variation of *A. baumannii* is dependent on a bistable switch that toggles formation of the two cell types. Bistability refers to the emergence of two phenotypically distinct subpopulations within a clonal population of bacteria [216, 217]. The states of these subpopulations are bimodal, with no notable transitional state that cells can stably inhabit. Characteristic to bistable systems is the role of "noise," the natural stochastic fluctuations of gene products, metabolites, and other molecules that may impact the expression of a master regulatory gene or genes, known as the "switch." At this time, there is not a clear candidate gene that may act as the master regulatory gene for *A. baumannii*'s opacity switch, and it may be that there are multiple, redundant switches.

There are two generally accepted models for the arrangement and mechanism of action for bistable switches [216, 217]. The first system is constituted by an autoregulatory master gene (*abcD*) whose product (AbcD) both activates its own expression as well as that of target genes that bring about phenotypic changes. Bistability occurs when large-scale upregulation of *abcD* drives major changes in global regulation due to synergistic activation of *abcD*'s promoter by AbcD, possibly through cooperative binding to the promoter or multimerization. The stochastic nature of the switch is imparted by random variations in the rates of transcription, translation and degradation of AbcD. The second system involves a pair of mutually repressing repressors (X and Y). In this case, the phenotype associated with constitutive expression of X will persist until an antagonizing element, such as an additional gene product or other molecule whose concentration

in the cell varies stochastically, disrupts X's repression of Y. Once Y is expressed, its product will repress X, hence relieving repression of other downstream regulatory targets of X. These changes bring about the constitutive expression of Y and its associated phenotype.

Bistable systems that promote phenotypic heterogeneity within isogenic populations of bacterial constitute a form of bet-hedging [216, 217]. This strategy ensures that when bacteria are faced with an environmental change, some members of the population will already have committed to a differential state that is more adaptive to the new pressures. For example, in *Staphylococcus aureus*, some cells randomly commit to the persister state, marked by very slow or no growth. When treated with penicillin, these cells survive and once the antibiotic is withdrawn, they serve to reestablish the population. The clear benefit of such a strategy is that the challenge is immediately met, whereas a sole reliance on cells attempting to respond by enacting transcriptional changes may be too slow for population survival. Additionally, specialized subpopulations prevent the need for population-wide use of energy and resources in the generation of gene products that are only tentatively beneficial in the face of a very specific environmental change.

LysR-type Transcriptional Regulators (LTTRs)

A considerable amount of the work described herein centers on the role of a specific LysR-type transcriptional regulator (LTTR): *ABUW_1132*. LTTRs constitute the largest family of prokaryotic transcriptional regulators and are two-domain proteins whose C-terminal binds a co-inducer molecule and whose N-terminal contains a winged helix-turn-helix (HTH) DNA binding domain [218, 219]. The first described LTTRs were negatively autoregulatory and activated a divergently transcribed gene. However, this rule has not persisted over the years as additional members have been characterized. Autoregulation is not a given, and LTTRs are frequently global

regulators that may serve as repressors or activators of their target genes or operons. In many instances the LTTR may be divergently transcribed from its target(s), but this is not always the case. LTTRs have been shown to regulate a wide variety of cellular functions including metabolism, quorum sensing, motility, virulence, oxidative stress response, secretion, cell division, and attachment [219]. A co-inducer molecule is often required to carry out some of their functions, and this molecule may be a product or intermediate of a metabolic pathway regulated by the LTTR. The family's namesake is LysR, a transcriptional activator of the *lysA* gene, which encodes an enzyme that catalyzes production of lysine from the precursor diaminopimelate, which is the co-inducer for LysR [219].

LTTRs usually function as tetramers [219]. The current model for the mechanism by which these regulators function is as follows: LTTR homodimers bind at regions -20 bp to +35 bp and at -20 bp to -40 bp relative to the target gene. The two dimers form a tetramer, causing DNA bending. Upon introduction of the co-inducer, the LTTRs undergo a conformational change that allows complexing with RNA polymerase at the promoter in a manner that may promote or hinder transcription. It is also possible that tetramers may not form until the co-inducer is bound.

The -20 bp to +35 bp binding site typically contains an "LTTR box" consisting of a semi-palindromic dyadic sequence to which the dimer's HTH binds [219, 220]. The consensus for this site is T-N_{11}-A, but this may vary in length and composition. The preference for the LTTR box may be stronger when the LTTR is unbound by its co-inducer, which may also lead to differing affinities for the two binding sites when the LTTR is bound or unbound. Further, there are examples of LTTRs that bind at additional sites even further upstream (-55 bp to -218 bp) or within the target gene (+350 bp).

TetR-type Transcriptional Regulators (TTTRs)

TetR-type transcriptional regulators (TTTRs) are a group of one-component transcriptional regulators that carry out a variety of functions in response to environmental changes. In *A. baumannii* AB5075, there are 36 genes annotated as encoding TTTRs. These homodimeric regulators sense changes through a ligand-binding domain and enact local or global transcriptional regulation through a DNA-binding domain containing a helix-turn-helix (HTH) motif [221, 222]. TTTRs are named for the first and best characterized member: TetR in *E. coli*, which reacts to the presence of tetracycline [221, 222]. TetR normally represses both its own expression and that of *tetA*, a gene encoding a tetracycline efflux pump. Upon binding tetracycline, complexed with Mg^{2+}, TetR undergoes a conformational change that alters its HTH and can no longer bind the *tetR* and *tetA* operators, allowing their expression and the expulsion of tetracycline from the cell via TetA.

Over 240 TTTRs had been at least partially characterized by 2013, promoting a clearer picture of the class as a whole and allowing recognition of common themes among them [221]. Like TetR, a large number of TTTRs are involved in antibiotic or toxin resistance. Others regulate processes including antibiotic biosynthesis, virulence, osmotic stress response, cell to cell signaling, cell division, and metabolism of carbon, lipids, or proteins. Most TTTRs are autoregulatory and act as repressors of their target genes, but exceptions to both of these have been documented. Additionally, the DNA sequences targeted by their HTH tend to be semi-palindromic repeats.

The following research documents the discovery of a link between the stringent response and motility, quorum sensing, and opacity variation in *A. baumannii*. It further presents unpublished data detailing a recent leap in the understanding of the genetic regulation of the opacity-virulence switch. As a whole, this work builds on several prior years of research in the Rather laboratory and adds valuable insight into key facets of *A. baumannii* biology.

References

1. Glew, R.H. et al. (1977) Infections with Acinetobacter calcoaceticus (Herellea vaginicola): clinical and laboratory studies. Medicine (Baltimore) 56 (2), 79-97.

2. Peleg, A.Y. et al. (2008) Acinetobacter baumannii: emergence of a successful pathogen. Clin Microbiol Rev 21 (3), 538-82.

3. Lee, C.R. et al. (2017) Biology of Acinetobacter baumannii: Pathogenesis, Antibiotic Resistance Mechanisms, and Prospective Treatment Options. Front Cell Infect Microbiol 7, 55.

4. Ayoub Moubareck, C. and Hammoudi Halat, D. (2020) Insights into Acinetobacter baumannii: A Review of Microbiological, Virulence, and Resistance Traits in a Threatening Nosocomial Pathogen. Antibiotics (Basel) 9 (3).

5. Control, C.f.D. (2019) Antibiotic Resistance Threats in the United States.

6. Clark, N.M. et al. (2016) Emergence of antimicrobial resistance among Acinetobacter species: a global threat. Curr Opin Crit Care 22 (5), 491-9.

7. World Health Organization (2017) Global Priority List of Antibiotic-Resistant Bacteria to Guide Research, Discovery, and Development of New Antibiotics. https://www.who.int/medicines/publications/WHO-PPL-Short_Summary_25Feb-ET_NM_WHO.pdf, (accessed August 2 2021).

8. Harding, C.M. et al. (2018) Uncovering the mechanisms of Acinetobacter baumannii virulence. Nat Rev Microbiol 16 (2), 91-102.

9. Jawad, A. et al. (1998) Survival of Acinetobacter baumannii on dry surfaces: comparison of outbreak and sporadic isolates. J Clin Microbiol 36 (7), 1938-41.

10. Rocha, I.V. et al. (2018) Multidrug-resistant Acinetobacter baumannii clones persist on hospital inanimate surfaces. Braz J Infect Dis 22 (5), 438-441.

11. Chapartegui-Gonzalez, I. et al. (2018) Acinetobacter baumannii maintains its virulence after long-time starvation. PLoS One 13 (8), e0201961.

12. D'Souza, A.W. et al. (2019) Spatiotemporal dynamics of multidrug resistant bacteria on intensive care unit surfaces. Nat Commun 10 (1), 4569.

13. Bravo, Z. et al. (2019) Analysis of Acinetobacter baumannii survival in liquid media and on solid matrices as well as effect of disinfectants. J Hosp Infect 103 (1), e42-e52.

14. Tipton, K.A. et al. (2015) Phase-Variable Control of Multiple Phenotypes in Acinetobacter baumannii Strain AB5075. J Bacteriol 197 (15), 2593-9.

15. Chin, C.Y. et al. (2018) A high-frequency phenotypic switch links bacterial virulence and environmental survival in Acinetobacter baumannii. Nat Microbiol 3 (5), 563-569.

16. Beijerinck, M. (1911) Pigmenten als oxydatieproducten gevormd door bacterien. Versl. Koninklijke Akad. Wetensch. Amsterdam 19, 1092-1103.

17. Brisou, J. and Prevot, A.R. (1954) [Studies on bacterial taxonomy. X. The revision of species under Acromobacter group]. Ann Inst Pasteur (Paris) 86 (6), 722-8.

18. Baumann, P. et al. (1968) A study of the Moraxella group. II. Oxidative-negative species (genus Acinetobacter). J Bacteriol 95 (5), 1520-41.

19. Lessel, E.F. (1971) Subcommittee on nomenclature of Moraxella and allied bacteria. Int. J. Syst. Bacteriol. 21, 213-214.

20. Brzin, B. (1969) Synonymy of herellea vaginicola and Bacterium anitratum. Zentralbl Bakteriol Orig 209 (3), 409-12.

21. Moor, W.A. (1949) The possible occurrence of Bacterium anitratum in several cases of conjunctivitis. Am J Ophthalmol 32 (11), 1593.

22. Waage, R. (1953) Bacterium anitratum (B5W) isolated from cerebral abscesses. Acta Pathol Microbiol Scand 33 (3), 268-70.

23. De Lavergne, E. et al. (1958) [Pleural infections caused by B5W (Bacterium anitratum)]. Presse Med 66 (9), 177-8.

24. Schneegans, E. et al. (1958) [3 Cases of septicemia caused by Bacterium anitratum in premature infants]. Arch Fr Pediatr 15 (1), 126-8.

25. Glick, L.M. et al. (1959) Lobar pneumonia with bacteremia caused by Bacterium anitratum. Am J Med 27 (1), 183-6.

26. Opsahl, R., Jr. (1961) Bacterium anitratum (Acinetobacter anitratum) isolated from a case with cerebral abscess and purulent meningitis. Acta Pathol Microbiol Scand 51, 72-4.

27. Metelka, M. and Vancurik, J. (1963) [Bacterium anitratum as the pathogen of postoperative infection of the central nervous system]. Zentralbl Neurochir 23, 176-81.

28. Hirsch, S.R. and Koch, M.L. (1964) Herellea (Bacterium Anitratum) Endocarditis. Report of a Case. JAMA 187, 148-50.

29. Matsuda, S. et al. (1964) [Case Report of Septicemia Caused by Bacterium Anitratum]. Nihon Densenbyo Gakkai Zasshi 38, 137-43.

30. Presley, G.D. and Hale, L.M. (1968) Corneal ulcer due to Bacterium anitratum. Am J Ophthalmol 65 (4), 571-2.

31. Kumar, N. et al. (1970) Bacterium anitratum meningitis. A case report. Indian Pediatr 7 (11), 632-4.

32. Marton, E. et al. (1970) [Bacterium anitratum septicemia]. Orv Hetil 111 (23), 1354-5.

33. Umsawasdi, T. et al. (1975) Bacterium anitratum bacteremia in a chronic myelogenous leukemia with blastic transformation patients. J Med Assoc Thai 58 (12), 628-31.

34. Altman, K.A. and Sacks, F. (1979) Bronchopneumonia and endocarditis: caused by Acinetobacter anitratum (Herellea vaginicola). N Y State J Med 79 (9), 1434-5.

35. Grootten, O. et al. (1956) [Studies on bacteria of the type Bacterium anitratum (B 5 W) and their sensitivity to sulfonamides and antibiotics]. Rev Immunol Ther Antimicrob 20 (4), 215-30.

36. Lothe, F. and Griffin, E. (1965) Bacterium Anitratum and Mima Polymorpha Infection in Uganda. J Clin Pathol 18, 301-6.

37. Davis, B. et al. (1969) Gram-negative bacilli in burns. J Clin Pathol 22 (6), 634-41.

38. Lecocq, E. and Linz, R. (1975) [A hospital epidemic due to Achromobacter calcoaceticus]. Pathol Biol (Paris) 23 (4), 277-82.

39. Moellering, R.C., Jr. et al. (1976) Emergence of gentamicin-resistant bacteria: experience with tobramycin therapy of infections due to gentamicin-resistant organisms. J Infect Dis 134 Suppl, S40-9.

40. Morohoshi, T. and Saito, T. (1977) beta-Lactamase and beta-lactam antibiotics resistance in acinetobacter anitratum (syn: A. calcoaceticus). J Antibiot (Tokyo) 30 (11), 969-73.

41. Igari, J. et al. (1978) [Clinical and bacteriological studies on infections due to Acinetobacter calco aceticus (author's transl)]. Jpn J Antibiot 31 (4), 191-9.

42. Overbeek, B.P. et al. (1985) Interaction between ciprofloxacin and tobramycin or azlocillin against multiresistant strains of Acinetobacter anitratum in vitro. Eur J Clin Microbiol 4 (2), 140-1.

43. Perea, E.J. et al. (1975) Mechanical ventilators as vehicles of infection. Acta Anaesthesiol Scand 19 (3), 180-6.

44. Bouvet, P.J. and Grimont, P.A. (1987) Identification and biotyping of clinical isolates of Acinetobacter. Ann Inst Pasteur Microbiol 138 (5), 569-78.

45. Go, E.S. et al. (1994) Clinical and molecular epidemiology of acinetobacter infections sensitive only to polymyxin B and sulbactam. Lancet 344 (8933), 1329-32.

46. Tankovic, J. et al. (1994) Characterization of a hospital outbreak of imipenem-resistant Acinetobacter baumannii by phenotypic and genotypic typing methods. J Clin Microbiol 32 (11), 2677-81.

47. Fass, R.J. et al. (1995) Emergence of bacterial resistance to imipenem and ciprofloxacin in a university hospital. J Antimicrob Chemother 36 (2), 343-53.

48. Lyytikainen, O. et al. (1995) Outbreak caused by two multi-resistant Acinetobacter baumannii clones in a burns unit: emergence of resistance to imipenem. J Hosp Infect 31 (1), 41-54.

49. Clark, R.B. (1996) Imipenem resistance among Acinetobacter baumannii: association with reduced expression of a 33-36 kDa outer membrane protein. J Antimicrob Chemother 38 (2), 245-51.

50. Centers for Disease, C. and Prevention (2004) Acinetobacter baumannii infections among patients at military medical facilities treating injured U.S. service members, 2002-2004. MMWR Morb Mortal Wkly Rep 53 (45), 1063-6.

51. Zapor, M.J. and Moran, K.A. (2005) Infectious diseases during wartime. Curr Opin Infect Dis 18 (5), 395-9.

52. Davis, K.A. et al. (2005) Multidrug-resistant Acinetobacter extremity infections in soldiers. Emerg Infect Dis 11 (8), 1218-24.

53. Stuart, T.L. et al. (2007) Acinetobacter baumannii in casualties returning from Afghanistan. Can J Infect Control 22 (3), 152-4.

54. Calhoun, J.H. et al. (2008) Multidrug-resistant organisms in military wounds from Iraq and Afghanistan. Clin Orthop Relat Res 466 (6), 1356-62.

55. Niemeyer, D.M. (1994) Regulation of beta-lactamase induction in gram-negative bacteria: a key to understanding the resistance puzzle. Mil Med 159 (12), 732-5.

56. Baumann, P. (1968) Isolation of Acinetobacter from soil and water. J Bacteriol 96 (1), 39-42.

57. Seifert, H. et al. (1997) Distribution of Acinetobacter species on human skin: comparison of phenotypic and genotypic identification methods. J Clin Microbiol 35 (11), 2819-25.

58. Berlau, J. et al. (1999) Distribution of Acinetobacter species on skin of healthy humans. Eur J Clin Microbiol Infect Dis 18 (3), 179-83.

59. Eveillard, M. et al. (2013) Reservoirs of Acinetobacter baumannii outside the hospital and potential involvement in emerging human community-acquired infections. Int J Infect Dis 17 (10), e802-5.

60. Berlau, J. et al. (1999) Isolation of Acinetobacter spp. including A. baumannii from vegetables: implications for hospital-acquired infections. J Hosp Infect 42 (3), 201-4.

61. Houang, E.T. et al. (2001) Epidemiology and infection control implications of Acinetobacter spp. in Hong Kong. J Clin Microbiol 39 (1), 228-34.

62. Sarma, P.M. et al. (2004) Assessment of intra-species diversity among strains of Acinetobacter baumannii isolated from sites contaminated with petroleum hydrocarbons. Can J Microbiol 50 (6), 405-14.

63. Bordenave, S. et al. (2007) Effects of heavy fuel oil on the bacterial community structure of a pristine microbial mat. Appl Environ Microbiol 73 (19), 6089-97.

64. Choi, J.Y. et al. (2012) Acinetobacter species isolates from a range of environments: species survey and observations of antimicrobial resistance. Diagn Microbiol Infect Dis 74 (2), 177-80.

65. Francey, T. et al. (2000) The role of Acinetobacter baumannii as a nosocomial pathogen for dogs and cats in an intensive care unit. J Vet Intern Med 14 (2), 177-83.

66. Vaneechoutte, M. et al. (2000) Acinetobacter baumannii-infected vascular catheters collected from horses in an equine clinic. J Clin Microbiol 38 (11), 4280-1.

67. Brachelente, C. et al. (2007) A case of necrotizing fasciitis with septic shock in a cat caused by Acinetobacter baumannii. Vet Dermatol 18 (6), 432-8.

68. Zordan, S. et al. (2011) Multidrug-resistant Acinetobacter baumannii in veterinary clinics, Germany. Emerg Infect Dis 17 (9), 1751-4.

69. Endimiani, A. et al. (2011) Acinetobacter baumannii isolates from pets and horses in Switzerland: molecular characterization and clinical data. J Antimicrob Chemother 66 (10), 2248-54.

70. Huys, G. et al. (2007) Biodiversity of chloramphenicol-resistant mesophilic heterotrophs from Southeast Asian aquaculture environments. Res Microbiol 158 (3), 228-35.

71. Byrne-Bailey, K.G. et al. (2009) Prevalence of sulfonamide resistance genes in bacterial isolates from manured agricultural soils and pig slurry in the United Kingdom. Antimicrob Agents Chemother 53 (2), 696-702.

72. Hamouda, A. et al. (2011) Epidemiology of Acinetobacter baumannii of animal origin. Int J Antimicrob Agents 38 (4), 314-8.

73. Chu, Y.W. et al. (1999) Skin carriage of acinetobacters in Hong Kong. J Clin Microbiol 37 (9), 2962-7.

74. Bayuga, S. et al. (2002) Prevalence and antimicrobial patterns of Acinetobacter baumannii on hands and nares of hospital personnel and patients: the iceberg phenomenon again. Heart Lung 31 (5), 382-90.

75. Zeana, C. et al. (2003) The epidemiology of multidrug-resistant Acinetobacter baumannii: does the community represent a reservoir? Infect Control Hosp Epidemiol 24 (4), 275-9.

76. La Scola, B. and Raoult, D. (2004) Acinetobacter baumannii in human body louse. Emerg Infect Dis 10 (9), 1671-3.

77. Bouvresse, S. et al. (2011) No evidence of Bartonella quintana but detection of Acinetobacter baumannii in head lice from elementary schoolchildren in Paris. Comp Immunol Microbiol Infect Dis 34 (6), 475-7.

78. Kempf, M. et al. (2012) Detection of Acinetobacter baumannii in human head and body lice from Ethiopia and identification of new genotypes. Int J Infect Dis 16 (9), e680-3.

79. Russo, T.A. et al. (2010) The K1 capsular polysaccharide of Acinetobacter baumannii strain 307-0294 is a major virulence factor. Infect Immun 78 (9), 3993-4000.

80. Lees-Miller, R.G. et al. (2013) A common pathway for O-linked protein-glycosylation and synthesis of capsule in Acinetobacter baumannii. Mol Microbiol 89 (5), 816-30.

81. Singh, J.K. et al. (2018) Diversity and Function of Capsular Polysaccharide in Acinetobacter baumannii. Front Microbiol 9, 3301.

82. Raetz, C.R. and Whitfield, C. (2002) Lipopolysaccharide endotoxins. Annu Rev Biochem 71, 635-700.

83. Whitfield, C. et al. (1997) Modulation of the surface architecture of gram-negative bacteria by the action of surface polymer:lipid A-core ligase and by determinants of polymer chain length. Mol Microbiol 23 (4), 629-38.

84. Weber, B.S. et al. (2015) Pathogenic Acinetobacter: from the Cell Surface to Infinity and Beyond. J Bacteriol 198 (6), 880-7.

85. Moffatt, J.H. et al. (2010) Colistin resistance in Acinetobacter baumannii is mediated by complete loss of lipopolysaccharide production. Antimicrob Agents Chemother 54 (12), 4971-7.

86. Powers, M.J. and Trent, M.S. (2018) Expanding the paradigm for the outer membrane: Acinetobacter baumannii in the absence of endotoxin. Mol Microbiol 107 (1), 47-56.

87. Richie, D.L. et al. (2018) A pathway-directed positive growth restoration assay to facilitate the discovery of lipid A and fatty acid biosynthesis inhibitors in Acinetobacter baumannii. PLoS One 13 (3), e0193851.

88. Jacobs, A.C. et al. (2014) AB5075, a Highly Virulent Isolate of Acinetobacter baumannii, as a Model Strain for the Evaluation of Pathogenesis and Antimicrobial Treatments. mBio 5 (3), e01076-14.

89. Niu, C. et al. (2008) Isolation and characterization of an autoinducer synthase from Acinetobacter baumannii. J Bacteriol 190 (9), 3386-92.

90. Clemmer, K.M. et al. (2011) Genetic analysis of surface motility in Acinetobacter baumannii. Microbiology 157 (Pt 9), 2534-2544.

91. Bhuiyan, M.S. et al. (2016) Acinetobacter baumannii phenylacetic acid metabolism influences infection outcome through a direct effect on neutrophil chemotaxis. Proc Natl Acad Sci U S A 113 (34), 9599-604.

92. Lopez, M. et al. (2017) Response to Bile Salts in Clinical Strains of Acinetobacter baumannii Lacking the AdeABC Efflux Pump: Virulence Associated with Quorum Sensing. Front Cell Infect Microbiol 7, 143.

93. Harding, C.M. et al. (2013) Acinetobacter baumannii strain M2 produces type IV pili which play a role in natural transformation and twitching motility but not surface-associated motility. mBio 4 (4).

94. Perez-Varela, M., Tierney, A.R.P., Kim, J., Vazquez-Torres, A., Rather, P.N. (2020) Characterization of RelA in Acinetobacter baumannii. Journal of Bacteriology.

95. Gourse, R.L. et al. (2018) Transcriptional Responses to ppGpp and DksA. Annu Rev Microbiol 72, 163-184.

96. Irving, S.E. and Corrigan, R.M. (2018) Triggering the stringent response: signals responsible for activating (p)ppGpp synthesis in bacteria. Microbiology 164 (3), 268-276.

97. Hauryliuk, V. et al. (2015) Recent functional insights into the role of (p)ppGpp in bacterial physiology. Nat Rev Microbiol 13 (5), 298-309.

98. Cashel, M. (1969) The control of ribonucleic acid synthesis in Escherichia coli. IV. Relevance of unusual phosphorylated compounds from amino acid-starved stringent strains. J Biol Chem 244 (12), 3133-41.

99. Winther, K.S. et al. (2018) Activation of the Stringent Response by Loading of RelA-tRNA Complexes at the Ribosomal A-Site. Mol Cell 70 (1), 95-105 e4.

100. Ross, W. et al. (2016) ppGpp Binding to a Site at the RNAP-DksA Interface Accounts for Its Dramatic Effects on Transcription Initiation during the Stringent Response. Mol Cell 62 (6), 811-823.

101. Sievert, D.M. et al. (2013) Antimicrobial-resistant pathogens associated with healthcare-associated infections: summary of data reported to the National Healthcare Safety Network at the Centers for Disease Control and Prevention, 2009-2010. Infect Control Hosp Epidemiol 34 (1), 1-14.

102. Weiner, L.M. et al. (2016) Antimicrobial-Resistant Pathogens Associated With Healthcare-Associated Infections: Summary of Data Reported to the National Healthcare Safety Network at the Centers for Disease Control and Prevention, 2011-2014. Infect Control Hosp Epidemiol 37 (11), 1288-1301.

103. Falagas, M.E. et al. (2007) Community-acquired Acinetobacter infections. Eur J Clin Microbiol Infect Dis 26 (12), 857-68.

104. Asplund, M.B. et al. (2013) Alcohol impairs J774.16 macrophage-like cell antimicrobial functions in Acinetobacter baumannii infection. Virulence 4 (6), 467-72.

105. Eugenin, E.A. (2013) Community-acquired pneumonia infections by Acinetobacter baumannii: how does alcohol impact the antimicrobial functions of macrophages? Virulence 4 (6), 435-6.

106. Porter, K.A. et al. (2014) Acinetobacter bacteraemia in Thailand: evidence for infections outside the hospital setting. Epidemiol Infect 142 (6), 1317-27.

107. Dexter, C. et al. (2015) Community-acquired Acinetobacter baumannii: clinical characteristics, epidemiology and pathogenesis. Expert Rev Anti Infect Ther 13 (5), 567-73.

108. Alividza, V. et al. (2018) Investigating the impact of poverty on colonization and infection with drug-resistant organisms in humans: a systematic review. Infect Dis Poverty 7 (1), 76.

109. Mittal, J. et al. (2018) An unusual cause of community-acquired pneumonia. IDCases 11, 41-43.

110. Chen, C.T. et al. (2018) Community-acquired bloodstream infections caused by Acinetobacter baumannii: A matched case-control study. J Microbiol Immunol Infect 51 (5), 629-635.

111. Ly, T.D.A. et al. (2019) The Presence of Acinetobacter baumannii DNA on the Skin of Homeless People and Its Relationship With Body Lice Infestation. Preliminary Results. Front Cell Infect Microbiol 9, 86.

112. Richards, A.M. et al. (2015) Code blue: Acinetobacter baumannii, a nosocomial pathogen with a role in the oral cavity. Mol Oral Microbiol 30 (1), 2-15.

113. Tipton, K.A. et al. (2018) Role of Capsule in Resistance to Disinfectants, Host Antimicrobials, and Desiccation in Acinetobacter baumannii. Antimicrob Agents Chemother 62 (12).

114. Boll, J.M. et al. (2015) Reinforcing Lipid A Acylation on the Cell Surface of Acinetobacter baumannii Promotes Cationic Antimicrobial Peptide Resistance and Desiccation Survival. mBio 6 (3), e00478-15.

115. Farrow, J.M., 3rd et al. (2018) Desiccation tolerance in Acinetobacter baumannii is mediated by the two-component response regulator BfmR. PLoS One 13 (10), e0205638.

116. Otter, J.A. et al. (2011) The role played by contaminated surfaces in the transmission of nosocomial pathogens. Infect Control Hosp Epidemiol 32 (7), 687-99.

117. Rajamohan, G. et al. (2010) Novel role of Acinetobacter baumannii RND efflux transporters in mediating decreased susceptibility to biocides. J Antimicrob Chemother 65 (2), 228-32.

118. Srinivasan, V.B. et al. (2009) Role of AbeS, a novel efflux pump of the SMR family of transporters, in resistance to antimicrobial agents in Acinetobacter baumannii. Antimicrob Agents Chemother 53 (12), 5312-6.

119. Rajamohan, G. et al. (2010) Molecular and functional characterization of a novel efflux pump, AmvA, mediating antimicrobial and disinfectant resistance in Acinetobacter baumannii. J Antimicrob Chemother 65 (9), 1919-25.

120. Hassan, K.A. et al. (2013) Transcriptomic and biochemical analyses identify a family of chlorhexidine efflux proteins. Proc Natl Acad Sci U S A 110 (50), 20254-9.

121. Greene, C. et al. (2016) The influence of biofilm formation and multidrug resistance on environmental survival of clinical and environmental isolates of Acinetobacter baumannii. Am J Infect Control 44 (5), e65-71.

122. Greene, C. et al. (2016) Evaluation of the ability of Acinetobacter baumannii to form biofilms on six different biomedical relevant surfaces. Lett Appl Microbiol 63 (4), 233-9.

123. Thompson, M.G. et al. (2014) Validation of a novel murine wound model of Acinetobacter baumannii infection. Antimicrob Agents Chemother 58 (3), 1332-42.

124. Longo, F. et al. (2014) Biofilm formation in Acinetobacter baumannii. New Microbiol 37 (2), 119-27.

125. Smani, Y. et al. (2012) Role of fibronectin in the adhesion of Acinetobacter baumannii to host cells. PLoS One 7 (4), e33073.

126. Gaddy, J.A. et al. (2009) The Acinetobacter baumannii 19606 OmpA protein plays a role in biofilm formation on abiotic surfaces and in the interaction of this pathogen with eukaryotic cells. Infect Immun 77 (8), 3150-60.

127. Choi, C.H. et al. (2008) Acinetobacter baumannii invades epithelial cells and outer membrane protein A mediates interactions with epithelial cells. BMC Microbiol 8, 216.

128. Wang, N. et al. (2014) Genome-wide identification of Acinetobacter baumannii genes necessary for persistence in the lung. mBio 5 (3), e01163-14.

129. Kim, S.W. et al. (2009) Serum resistance of Acinetobacter baumannii through the binding of factor H to outer membrane proteins. FEMS Microbiol Lett 301 (2), 224-31.

130. Choi, C.H. et al. (2008) Acinetobacter baumannii outer membrane protein A targets the nucleus and induces cytotoxicity. Cell Microbiol 10 (2), 309-19.

131. Lee, J.S. et al. (2010) Acinetobacter baumannii outer membrane protein A induces dendritic cell death through mitochondrial targeting. J Microbiol 48 (3), 387-92.

132. Choi, C.H. et al. (2005) Outer membrane protein 38 of Acinetobacter baumannii localizes to the mitochondria and induces apoptosis of epithelial cells. Cell Microbiol 7 (8), 1127-38.

133. Iwashkiw, J.A. et al. (2012) Identification of a general O-linked protein glycosylation system in Acinetobacter baumannii and its role in virulence and biofilm formation. PLoS Pathog 8 (6), e1002758.

134. Piepenbrink, K.H. et al. (2016) Structural Diversity in the Type IV Pili of Multidrug-resistant Acinetobacter. J Biol Chem 291 (44), 22924-22935.

135. Lin, L. et al. (2012) Inhibition of LpxC protects mice from resistant Acinetobacter baumannii by modulating inflammation and enhancing phagocytosis. mBio 3 (5).

136. Songer, J.G. (1997) Bacterial phospholipases and their role in virulence. Trends Microbiol 5 (4), 156-61.

137. Flores-Diaz, M. et al. (2016) Bacterial Sphingomyelinases and Phospholipases as Virulence Factors. Microbiol Mol Biol Rev 80 (3), 597-628.

138. Fiester, S.E. et al. (2016) Iron-Regulated Phospholipase C Activity Contributes to the Cytolytic Activity and Virulence of Acinetobacter baumannii. PLoS One 11 (11), e0167068.

139. Kareem, S.M. et al. (2017) Acinetobacter baumannii virulence is enhanced by the combined presence of virulence factors genes phospholipase C (plcN) and elastase (lasB). Microb Pathog 110, 568-572.

140. Camarena, L. et al. (2010) Molecular mechanisms of ethanol-induced pathogenesis revealed by RNA-sequencing. PLoS Pathog 6 (4), e1000834.

141. Stahl, J. et al. (2015) Acinetobacter baumannii Virulence Is Mediated by the Concerted Action of Three Phospholipases D. PLoS One 10 (9), e0138360.

142. Jacobs, A.C. et al. (2010) Inactivation of phospholipase D diminishes Acinetobacter baumannii pathogenesis. Infect Immun 78 (5), 1952-62.

143. Jha, C. et al. (2017) In vitro study of virulence potential of Acinetobacter baumannii outer membrane vesicles. Microb Pathog 111, 218-224.

144. Jin, J.S. et al. (2011) Acinetobacter baumannii secretes cytotoxic outer membrane protein A via outer membrane vesicles. PLoS One 6 (2), e17027.

145. Moon, D.C. et al. (2012) Acinetobacter baumannii outer membrane protein A modulates the biogenesis of outer membrane vesicles. J Microbiol 50 (1), 155-60.

146. Kwon, S.O. et al. (2009) Proteome analysis of outer membrane vesicles from a clinical Acinetobacter baumannii isolate. FEMS Microbiol Lett 297 (2), 150-6.

147. Huang, W. et al. (2014) Immunization against multidrug-resistant Acinetobacter baumannii effectively protects mice in both pneumonia and sepsis models. PLoS One 9 (6), e100727.

148. Jun, S.H. et al. (2013) Acinetobacter baumannii outer membrane vesicles elicit a potent innate immune response via membrane proteins. PLoS One 8 (8), e71751.

149. Elhosseiny, N.M. and Attia, A.S. (2018) Acinetobacter: an emerging pathogen with a versatile secretome. Emerg Microbes Infect 7 (1), 33.

150. Weber, B.S. et al. (2017) The Secrets of Acinetobacter Secretion. Trends Microbiol 25 (7), 532-545.

151. Harding, C.M. et al. (2016) Medically Relevant Acinetobacter Species Require a Type II Secretion System and Specific Membrane-Associated Chaperones for the Export of Multiple Substrates and Full Virulence. PLoS Pathog 12 (1), e1005391.

152. Johnson, T.L. et al. (2015) Acinetobacter baumannii Is Dependent on the Type II Secretion System and Its Substrate LipA for Lipid Utilization and In Vivo Fitness. J Bacteriol 198 (4), 711-9.

153. Kinsella, R.L. et al. (2017) Defining the interaction of the protease CpaA with its type II secretion chaperone CpaB and its contribution to virulence in Acinetobacter species. J Biol Chem 292 (48), 19628-19638.

154. Weidensdorfer, M. et al. (2019) The Acinetobacter trimeric autotransporter adhesin Ata controls key virulence traits of Acinetobacter baumannii. Virulence 10 (1), 68-81.

155. Bentancor, L.V. et al. (2012) Identification of Ata, a multifunctional trimeric autotransporter of Acinetobacter baumannii. J Bacteriol 194 (15), 3950-60.

156. Repizo, G.D. et al. (2015) Differential Role of the T6SS in Acinetobacter baumannii Virulence. PLoS One 10 (9), e0138265.

157. Subashchandrabose, S. et al. (2016) Acinetobacter baumannii Genes Required for Bacterial Survival during Bloodstream Infection. mSphere 1 (1).

158. Antunes, L.C. et al. (2011) Genome-assisted identification of putative iron-utilization genes in Acinetobacter baumannii and their distribution among a genotypically diverse collection of clinical isolates. Res Microbiol 162 (3), 279-84.

159. Proschak, A. et al. (2013) Structure and biosynthesis of fimsbactins A-F, siderophores from Acinetobacter baumannii and Acinetobacter baylyi. Chembiochem 14 (5), 633-8.

160. Penwell, W.F. et al. (2015) Discovery and Characterization of New Hydroxamate Siderophores, Baumannoferrin A and B, produced by Acinetobacter baumannii. Chembiochem 16 (13), 1896-1904.

161. Gaddy, J.A. et al. (2012) Role of acinetobactin-mediated iron acquisition functions in the interaction of Acinetobacter baumannii strain ATCC 19606T with human lung epithelial cells, Galleria mellonella caterpillars, and mice. Infect Immun 80 (3), 1015-24.

162. Nairn, B.L. et al. (2016) The Response of Acinetobacter baumannii to Zinc Starvation. Cell Host Microbe 19 (6), 826-36.

163. Mortensen, B.L. et al. (2014) Acinetobacter baumannii response to host-mediated zinc limitation requires the transcriptional regulator Zur. J Bacteriol 196 (14), 2616-26.

164. Hood, M.I. et al. (2012) Identification of an Acinetobacter baumannii zinc acquisition system that facilitates resistance to calprotectin-mediated zinc sequestration. PLoS Pathog 8 (12), e1003068.

165. Corbin, B.D. et al. (2008) Metal chelation and inhibition of bacterial growth in tissue abscesses. Science 319 (5865), 962-5.

166. Moore, J.L. et al. (2014) Imaging mass spectrometry for assessing temporal proteomics: analysis of calprotectin in Acinetobacter baumannii pulmonary infection. Proteomics 14 (7-8), 820-828.

167. Juttukonda, L.J. et al. (2016) Acinetobacter baumannii Coordinates Urea Metabolism with Metal Import To Resist Host-Mediated Metal Limitation. mBio 7 (5).

168. Wong, D. et al. (2017) Clinical and Pathophysiological Overview of Acinetobacter Infections: a Century of Challenges. Clin Microbiol Rev 30 (1), 409-447.

169. Ramirez, M.S. et al. (2010) Naturally competent Acinetobacter baumannii clinical isolate as a convenient model for genetic studies. J Clin Microbiol 48 (4), 1488-90.

170. Mussi, M.A. et al. (2011) Horizontal gene transfer and assortative recombination within the Acinetobacter baumannii clinical population provide genetic diversity at the single carO gene, encoding a major outer membrane protein channel. J Bacteriol 193 (18), 4736-48.

171. Rumbo, C. et al. (2011) Horizontal transfer of the OXA-24 carbapenemase gene via outer membrane vesicles: a new mechanism of dissemination of carbapenem resistance genes in Acinetobacter baumannii. Antimicrob Agents Chemother 55 (7), 3084-90.

172. Hamidian, M. et al. (2013) Horizontal transfer of an ISAba125-activated ampC gene between Acinetobacter baumannii strains leading to cephalosporin resistance. J Antimicrob Chemother 68 (1), 244-5.

173. Partridge, S.R. et al. (2018) Mobile Genetic Elements Associated with Antimicrobial Resistance. Clin Microbiol Rev 31 (4).

174. Da Silva, G.J. and Domingues, S. (2016) Insights on the Horizontal Gene Transfer of Carbapenemase Determinants in the Opportunistic Pathogen Acinetobacter baumannii. Microorganisms 4 (3).

175. Valenzuela, J.K. et al. (2007) Horizontal gene transfer in a polyclonal outbreak of carbapenem-resistant Acinetobacter baumannii. J Clin Microbiol 45 (2), 453-60.

176. Tanner, W.D. et al. (2017) Horizontal transfer of the blaNDM-1 gene to Pseudomonas aeruginosa and Acinetobacter baumannii in biofilms. FEMS Microbiol Lett 364 (8).

177. Doi, Y. et al. (2015) Acinetobacter baumannii: evolution of antimicrobial resistance-treatment options. Semin Respir Crit Care Med 36 (1), 85-98.

178. Da Silva, G.J. et al. (1999) Emergence of carbapenem-hydrolyzing enzymes in Acinetobacter baumannii clinical isolates. J Clin Microbiol 37 (6), 2109-10.

179. Bou, G. et al. (2000) OXA-24, a novel class D beta-lactamase with carbapenemase activity in an Acinetobacter baumannii clinical strain. Antimicrob Agents Chemother 44 (6), 1556-61.

180. Takahashi, A. et al. (2000) Detection of carbapenemase-producing Acinetobacter baumannii in a hospital. J Clin Microbiol 38 (2), 526-9.

181. Poirel, L. and Nordmann, P. (2006) Carbapenem resistance in Acinetobacter baumannii: mechanisms and epidemiology. Clin Microbiol Infect 12 (9), 826-36.

182. Zhu, J. et al. (2009) A novel aminoglycoside-modifying enzyme gene aac(6')-Ib in a pandrug-resistant Acinetobacter baumannii strain. J Hosp Infect 73 (2), 184-5.

183. Nemec, A. et al. (2004) Diversity of aminoglycoside-resistance genes and their association with class 1 integrons among strains of pan-European Acinetobacter baumannii clones. J Med Microbiol 53 (Pt 12), 1233-1240.

184. Atasoy, A.R. et al. (2015) Modifying enzymes related aminoglycoside: analyses of resistant Acinetobacter isolates. Int J Clin Exp Med 8 (2), 2874-80.

185. Doi, Y. et al. (2004) Spread of novel aminoglycoside resistance gene aac(6')-Iad among Acinetobacter clinical isolates in Japan. Antimicrob Agents Chemother 48 (6), 2075-80.

186. Coyne, S. et al. (2011) Efflux-mediated antibiotic resistance in Acinetobacter spp. Antimicrob Agents Chemother 55 (3), 947-53.

187. Shin, B. and Park, W. (2017) Antibiotic resistance of pathogenic Acinetobacter species and emerging combination therapy. J Microbiol 55 (11), 837-849.

188. Coyne, S. et al. (2010) Overexpression of resistance-nodulation-cell division pump AdeFGH confers multidrug resistance in Acinetobacter baumannii. Antimicrob Agents Chemother 54 (10), 4389-93.

189. Damier-Piolle, L. et al. (2008) AdeIJK, a resistance-nodulation-cell division pump effluxing multiple antibiotics in Acinetobacter baumannii. Antimicrob Agents Chemother 52 (2), 557-62.

190. Ruzin, A. et al. (2007) AdeABC multidrug efflux pump is associated with decreased susceptibility to tigecycline in Acinetobacter calcoaceticus-Acinetobacter baumannii complex. J Antimicrob Chemother 59 (5), 1001-4.

191. Magnet, S. et al. (2001) Resistance-nodulation-cell division-type efflux pump involved in aminoglycoside resistance in Acinetobacter baumannii strain BM4454. Antimicrob Agents Chemother 45 (12), 3375-80.

192. Ribera, A. et al. (2003) Partial characterization of a transposon containing the tet(A) determinant in a clinical isolate of Acinetobacter baumannii. J Antimicrob Chemother 52 (3), 477-80.

193. Roca, I. et al. (2009) CraA, a major facilitator superfamily efflux pump associated with chloramphenicol resistance in Acinetobacter baumannii. Antimicrob Agents Chemother 53 (9), 4013-4.

194. Fournier, P.E. et al. (2006) Comparative genomics of multidrug resistance in Acinetobacter baumannii. PLoS Genet 2 (1), e7.

195. Lin, M.F. et al. (2017) Contribution of EmrAB efflux pumps to colistin resistance in Acinetobacter baumannii. J Microbiol 55 (2), 130-136.

196. Nowak-Zaleska, A. et al. (2016) Correlation between the number of Pro-Ala repeats in the EmrA homologue of Acinetobacter baumannii and resistance to netilmicin, tobramycin, imipenem and ceftazidime. J Glob Antimicrob Resist 7, 145-149.

197. Vila, J. et al. (1997) Quinolone-resistance mutations in the topoisomerase IV parC gene of Acinetobacter baumannii. J Antimicrob Chemother 39 (6), 757-62.

198. Vila, J. et al. (1995) Mutation in the gyrA gene of quinolone-resistant clinical isolates of Acinetobacter baumannii. Antimicrob Agents Chemother 39 (5), 1201-3.

199. Gehrlein, M. et al. (1991) Imipenem resistance in Acinetobacter baumanii is due to altered penicillin-binding proteins. Chemotherapy 37 (6), 405-12.

200. Yu, Y.S. et al. (2007) Widespread occurrence of aminoglycoside resistance due to ArmA methylase in imipenem-resistant Acinetobacter baumannii isolates in China. J Antimicrob Chemother 60 (2), 454-5.

201. Adams, M.D. et al. (2009) Resistance to colistin in Acinetobacter baumannii associated with mutations in the PmrAB two-component system. Antimicrob Agents Chemother 53 (9), 3628-34.

202. Anderson, S.E. et al. (2020) Copy Number of an Integron-Encoded Antibiotic Resistance Locus Regulates a Virulence and Opacity Switch in Acinetobacter baumannii AB5075. mBio 11 (5).

203. Tipton, K.A. and Rather, P.N. (2016) An ompR/envZ Two-Component System Ortholog Regulates Phase Variation, Osmotic Tolerance, Motility, and Virulence in Acinetobacter baumannii strain AB5075. J Bacteriol.

204. Tipton, K.A. et al. (2017) Multiple roles for a novel RND-type efflux system in Acinetobacter baumannii AB5075. Microbiologyopen 6 (2).

205. Connell, T.D. et al. (1990) Characterization of the repertoire of hypervariable regions in the Protein II (opa) gene family of Neisseria gonorrhoeae. Mol Microbiol 4 (3), 439-49.

206. Dempsey, J.A. et al. (1991) Physical map of the chromosome of Neisseria gonorrhoeae FA1090 with locations of genetic markers, including opa and pil genes. J Bacteriol 173 (17), 5476-86.

207. Bhat, K.S. et al. (1991) The opacity proteins of Neisseria gonorrhoeae strain MS11 are encoded by a family of 11 complete genes. Mol Microbiol 5 (8), 1889-901.

208. Swanson, J. (1978) Studies on gonococcus infection. XIV. Cell wall protein differences among color/opacity colony variants of Neisseria gonorrhoeae. Infect Immun 21 (1), 292-302.

209. Murphy, G.L. et al. (1989) Phase variation of gonococcal protein II: regulation of gene expression by slipped-strand mispairing of a repetitive DNA sequence. Cell 56 (4), 539-47.

210. Stern, A. et al. (1986) Opacity genes in Neisseria gonorrhoeae: control of phase and antigenic variation. Cell 47 (1), 61-71.

211. Weiser, J.N. et al. (1994) Phase variation in pneumococcal opacity: relationship between colonial morphology and nasopharyngeal colonization. Infect Immun 62 (6), 2582-9.

212. Weiser, J.N. (1998) Phase variation in colony opacity by Streptococcus pneumoniae. Microb Drug Resist 4 (2), 129-35.

213. Li, J. et al. (2016) Epigenetic Switch Driven by DNA Inversions Dictates Phase Variation in Streptococcus pneumoniae. PLoS Pathog 12 (7), e1005762.

214. Loenen, W.A. et al. (2014) Highlights of the DNA cutters: a short history of the restriction enzymes. Nucleic Acids Res 42 (1), 3-19.

215. Dryden, D.T. et al. (1997) The in vitro assembly of the EcoKI type I DNA restriction/modification enzyme and its in vivo implications. Biochemistry 36 (5), 1065-76.

216. Veening, J.W. et al. (2008) Bistability, epigenetics, and bet-hedging in bacteria. Annu Rev Microbiol 62, 193-210.

217. Dubnau, D. and Losick, R. (2006) Bistability in bacteria. Mol Microbiol 61 (3), 564-72.

218. Schell, M.A. (1993) Molecular biology of the LysR family of transcriptional regulators. Annu Rev Microbiol 47, 597-626.

219. Maddocks, S.E. and Oyston, P.C.F. (2008) Structure and function of the LysR-type transcriptional regulator (LTTR) family proteins. Microbiology 154 (Pt 12), 3609-3623.

220. Parsek, M.R. et al. (1994) Interaction of two LysR-type regulatory proteins CatR and ClcR with heterologous promoters: functional and evolutionary implications. Proc Natl Acad Sci U S A 91 (26), 12393-7.

221. Cuthbertson, L. and Nodwell, J.R. (2013) The TetR family of regulators. Microbiol Mol Biol Rev 77 (3), 440-75.

222. Ramos, J.L. et al. (2005) The TetR family of transcriptional repressors. Microbiol Mol Biol Rev 69 (2), 326-56.

Chapter 2: Characterization of RelA in *Acinetobacter baumannii*

María Pérez-Varela,[a,c] Aimee R. P. Tierney,[a,c] Ju-Sim Kim,[d] Andrés Vázquez-Torres,[d,e] and Philip Rather [a,b,c]

[a]Department of Microbiology and Immunology, Emory University School of Medicine, Atlanta, Georgia, USA

[b]Research Service, Veterans Affairs Medical Center, Decatur, Georgia, USA

[c]Emory Antibiotic Resistance Center, Emory University School of Medicine, Atlanta, Georgia, USA

[d]Department of Immunology and Microbiology, University of Colorado School of Medicine, Aurora, Colorado, USA

[e]Veterans Affairs Eastern Colorado Health Care System, Denver, Colorado, USA

Published in:

Journal of Bacteriology, 2020

202(12): e00045-20

The manuscript was primarily written by PR and MPV with revisions from all authors. The *relA* experiments were primarily carried out by MPV and PR, with the exception of the TLC autoradiography experiments which were carried out by JSK and AVT. ARPT carried out the *ABUW_1132* experiments.

Abstract

In response to nutrient depletion, the RelA and SpoT proteins generate the signaling molecule (p)ppGpp, which then controls a number of downstream effectors to modulate cell physiology. In *Acinetobacter baumannii* strain AB5075, a *relA* ortholog (*ABUW_3302*) was identified by a transposon insertion that conferred an unusual colony phenotype. An in-frame deletion in *relA* (Δ*relA*) failed to produce detectable levels of ppGpp when amino acid starvation was induced with serine hydroxamate. The Δ*relA* mutant was blocked from switching from the virulent opaque colony variant (VIR-O) to the avirulent translucent colony variant (AV-T), but the rate of AV-T to VIR-O switching was unchanged. In addition, the Δ*relA* mutation resulted in a pronounced hypermotile phenotype on 0.35% agar plates. This hypermotility was dependent on the activation of a LysR regulator ABUW_1132, which was required for expression of AbaR, a LuxR family quorum-sensing regulator. In the Δ*relA* mutant, ABUW_1132 was also required for the increased expression of an operon composed of the *ABUW_3766-ABUW_3773* genes required for production of the surfactant-like lipopeptide acinetin 505. Additional phenotypes identified in the Δ*relA* mutant included (i) cell elongation at high density, (ii) reduced formation of persister cells tolerant to colistin and rifampin, and (iii) decreased virulence in a *Galleria mellonella* model.

Importance

Acinetobacter baumannii is a pathogen of worldwide importance. Due to the increasing prevalence of antibiotic resistance, these infections are becoming increasingly difficult to treat. New therapies are required to combat multidrug-resistant isolates. The role of RelA in *A. baumannii* is largely unknown. This study demonstrates that like in other bacteria, RelA controls a variety of functions, including virulence. Strategies to inhibit the activity of RelA and the resulting production of ppGpp could inhibit virulence and may represent a new therapeutic approach.

Introduction

Acinetobacter baumannii is a nosocomial pathogen responsible for a variety of human infections (1–5). The incidence of these infections is increasing worldwide, and the inability to effectively treat these infections with antibiotics is a worrisome development, as recently emphasized by both the U.S. Centers for Disease Control and Prevention and the World Health Organization (6–9). Furthermore, *A. baumannii* infections can be seen in the community and can cause a severe rapidly fatal disease (10, 11).

A. baumannii strain AB5075 and many clinical isolates can switch between two cell types, those that form opaque colonies on 0.5× Luria-Bertani (LB) agar plates when viewed by oblique lighting and those that form translucent colonies (12). These two cell types exhibit marked differences in virulence in both *Galleria mellonella* and mouse lung models of infection, where the opaque form is virulent (VIR-O) and the translucent form is avirulent (AV-T) (12, 13). Several regulatory genes can influence the rate of VIR-O to AV-T switching. For example, mutations in *arpAB* encoding an RND-type efflux system decrease the rate of switching, and mutations in orthologs of the EnvZ/OmpR two-component system increase the rate of VIR-O to AV-T switching (14, 15). In addition, overexpression of a TetR-type transcriptional regulator, ABUW_1645, can drive cells from the VIR-O to the AV-T state. However, a null allele in *ABUW_1645* had no effect on VIR-O to AV-T switching (13).

Bacteria respond to starvation for carbon, fatty acid, phosphate, iron, and amino acids and other stress responses by inducing synthesis of the alarmone molecule (p)ppGpp via the RelA or SpoT protein, reviewed in references 16 to 20. RelA and SpoT comprise the RSH superfamily, in which RelA synthesizes (p)ppGpp using ATP and GDP/GTP and SpoT has both weak synthetase activity and strong hydrolase (ppGpp degrading) activity. The effect of ppGpp accumulation in

cells is multifactorial. Global transcription is reprogrammed utilizing ppGpp together with the DksA protein to alter the activity of RNA polymerase (RNAP), resulting in both decreased and increased transcription at various promoters (16, 19, 21, 22). A second mechanism for transcriptional reprogramming by ppGpp involves decreasing the affinity of σ^{70} for RNAP and allowing other sigma factors to bind (23). RelA and the resulting production of ppGpp impacts additional cellular functions, including growth rate, translation, and DNA replication (16, 20). A requirement for ppGpp in bacterial virulence has been demonstrated in a wide variety of Gram-negative bacteria, including *Pseudomonas aeruginosa*, *Legionella pneumophila*, *Burkholderia pseudomallei*, *Francisella novicida*, *Vibrio cholerae*, *Yersinia pestis*, *Salmonella enterica*, and *Escherichia coli* (24–32). The role of RelA and ppGpp in the formation of antibiotic-tolerant persister cells has also been described (33–38). Reviews on this subject highlight the multiple roles attributed to RelA, including examples in Gram-positive bacteria (16, 39, 40).

In *A. baumannii*, the role of RelA is largely unknown. A screen for transposon insertions that resulted in sensitivity to ascites fluid or human serum identified *relA*, but no additional characterization was reported (41, 42). A recent study demonstrated a role for RelA in the regulation of efflux genes, such as *adeB* and *adeJ* (43). In this study, we report a transposon insertion in *relA* that was initially identified by the resulting change in colony morphology. Further characterization of an in-frame *relA* deletion revealed that a number of phenotypes were impacted by the mutation, including (i) loss of ppGpp synthesis, (ii) loss of switching from the VIR-O to the AV-T variant, (iii) increased surface motility, and (iv) elongated cell morphology at high density. Furthermore, like in many other bacteria, the loss of *relA* decreased virulence when assessed in a *Galleria mellonella* model. This study reveals for the first time the multiple roles for RelA in the physiology of *A. baumannii*.

Results

Identification of an *A. baumannii relA* ortholog.

A. baumannii strain AB5075 can rapidly switch between two cell types, virulent and avirulent, that are distinguished by their opaque (VIR-O) or translucent (AV-T) colony phenotypes when viewed with a light source that illuminates the colonies from below (oblique lighting) (12, 13). In the course of screening a transposon insertion library (EZ-Tn*5* <Tet-1>) in the avirulent translucent (AV-T) variant of AB5075, a colony with an unusual phenotype was observed that exhibited a metallic sheen and an irregular colony surface when viewed by oblique lighting. This colony phenotype was similar to that of mutants we had previously observed, where cells were highly filamentous (44). When this colony was restreaked, it gave rise to a second colony phenotype that was larger and flat with irregular edges. To identify this mutation, the transposon insertion was cloned out along with flanking DNA, and the insertion site was determined to be within the *ABUW_3302* gene. The protein encoded by *ABUW_3302* exhibited 40% identity and 62% amino acid similarity to the *E. coli* RelA protein. RelA functions as a ppGpp synthetase that generates the secondary messenger molecule (p)ppGpp in response to nutrient starvation and other stressors (19, 45). To confirm that the insertion in *ABUW_3302* was responsible for the observed colony phenotypes, a nonpolar in-frame deletion in *ABUW_3302* was constructed in both the VIR-O and AV-T variants. The AV-T Δ*ABUW_3302* mutant exhibited the same unusual colony phenotype as the original transposon insertion, and this phenotype is shown compared to a wild-type AV-T colony (Fig. 1A). In addition, the AV-T Δ*ABUW_3302* mutant was capable of switching at high frequency (~5% to 10%) to cells that now formed large flat colonies with irregular borders that were identical in appearance to colonies observed arising in the original AV-T transposon mutant. Moreover, these colonies were identical in appearance to

the VIR-O Δ*ABUW_3302* mutant, confirming that these represented VIR-O variants (Fig. 1B). Taken together, these data indicate that the Δ*ABUW_3302* mutation significantly alters colony morphology in both the VIR-O and AV-T variants.

A deletion of *ABUW_3302* blocks the VIR-O to AV-T switch.

As noted above, the AV-T Δ*ABUW_3302* mutant gave rise at high frequency to colonies identical in appearance to the VIR-O Δ*ABUW_3302* mutant. However, the VIR-O Δ*ABUW_3302* mutant did not give rise to colonies of the AV-T morphology when restreaked. To determine if the rate of VIR-O to AV-T switching was reduced by the Δ*ABUW_3302* mutation, the frequency of switching in 24-h colonies was determined (Table 1). While the rate of VIR-O to AV-T was measured at 6.6% in wild-type cells, we could not detect any AV-T colonies arising from the VIR-O mutant in the Δ*ABUW_3302* mutant background. The lower limit of detection in these switching assays is estimated to be $1/10^5$ to $1/10^6$ cells, making the decrease in switching at least 5,000-fold. Interestingly, when the rate of AV-T to VIR-O switching was determined, the levels were similar in wild-type cells and the Δ*ABUW_3302* mutant, 7.5% ± 1.7% and 10.9% ± 6.8%, respectively. To determine whether providing the Δ*ABUW_3302* gene in *trans* could complement the Δ*ABUW_3302* mutation, an isopropyl-β-D-thiogalactopyranoside (IPTG)-inducible copy of Δ*ABUW_3302* was introduced into the chromosome at the *glmS* site on a Tn*7* derivative. In the presence of 2 mM IPTG, the Δ*ABUW_3302*/Tn*7*::*ABUW_3302* cells now exhibited a normal colony morphology, and the rate of VIR-O to AV-T switching was restored to 20.5% ± 8.6%.

The *ABUW_3302* gene encodes a RelA ortholog.

To determine whether the *ABUW_3302* gene encoded a ppGpp synthetase, the production of ppGpp was examined by thin-layer chromatography in the presence or absence of serine hydroxamate, an inducer of the RelA-dependent stringent response. In wild-type cells, the presence of serine hydroxamate induced the production of ppGpp. However, the Δ*relA* mutant was unable to produce ppGpp, confirming that it functioned as a ppGpp synthetase (Fig. 2). Based on this result and the amino acid similarity of the *ABUW_3302* gene product to those of the RelA proteins of other bacteria, the *ABUW_3302* gene will be referred to here as *relA*.

The Δ*relA* mutation results in cell elongation at high density.

Cells of the wild-type VIR-O and AV-T variants and the corresponding isogenic Δ*relA* mutants were examined by phase-contrast microscopy at mid-log phase and at early stationary phase. In mid-log-phase cultures, both wild-type and Δ*relA* cells from either VIR-O or AV-T backgrounds exhibited similar morphologies (Fig. 3). However, at high cell density, the Δ*relA* mutation in both the VIR-O and AV-T backgrounds resulted in elongated cells relative to the wild type, which was restored by a wild-type copy of *relA* (Fig. 3).

The Δ*relA* mutation results in a hypermotile phenotype.

Based on the flat, irregular, and spreading colonies formed by the VIR-O Δ*relA* mutant on 0.5× LB agar plates, we predicted that cells would be hypermotile, as a similar colony phenotype and hypermotility was previously observed in an *arpB* mutant (14). When motility was measured on 0.35% agar plates, the VIR-O Δ*relA* mutant was indeed hypermotile relative to wild-type cells (Fig. 4A). However, this increase in motility was specific to the VIR-O form. When the AV-T Δ*relA* mutant was tested for motility, it was similar to wild-type AV-T cells (data not shown).

Introduction of the wild-type *relA* gene under the control of an IPTG-inducible *tac* promoter in single copy (Tn*7*) into the VIR-O Δ*relA* mutant reduced motility back to wild-type levels when *relA* expression was induced with IPTG (Fig. 4A).

RelA represses quorum sensing.

Previous studies have indicated that surface motility in *A. baumannii* and *Acinetobacter nosocomialis* is dependent on a number of factors, including (i) production of the quorum-sensing signal 3-OH C_{12}-homoserine lactone (HSL) mediated by the AbaI autoinducer synthase, which is activated by the AbaR transcriptional regulator (46), (ii) 1, 3-diaminopropane produced by the combined activity of the Dat and Ddc proteins (47), (iii) acinetin 505, a surfactant-like molecule produced by proteins encoded by a large operon, *ABUW_3766-ABUW_3773* (46, 48), and (iv) loss of the histone-like protein H-NS (49). To determine if the Δ*relA* mutation altered the expression of genes encoding these motility-related factors, we used quantitative real-time PCR (qRT-PCR) to measure expression of these genes in wild-type VIR-O and isogenic Δ*relA* backgrounds. Expression of *abaI*, *abaR*, and *ABUW_3770*, a representative gene in the *ABUW_3766-ABUW_3773* operon, were upregulated 3.9-fold, 41.3-fold, and 55.6-fold, respectively, in the Δ*relA* mutant (Table 2). In contrast, expression of *ABUW_1109* (*dat*) and *ABUW_3609* (*hns*) was not significantly altered in the Δ*relA* mutant (Table 2). Introduction of a wild-type copy of *relA* on a Tn*7* derivative into the Δ*relA* mutant reduced the levels of *abaI*, *abaR*, and *ABUW_3770* expression back to wild-type levels (Table 2).

Next, to evaluate if hypermotility in the Δ*relA* mutant was dependent on overexpression of the *abaI*, *abaR*, or *ABUW_3770* gene, *abaI*::*T26*, *abaR*::*T26*, and *ABUW_3770*::*T26* mutations were individually introduced into the Δ*relA* background, and all these mutations resulted in loss of the hypermotile phenotype (Fig. 4A).

RelA controls motility and quorum sensing via ABUW_1132, a LysR-type regulator.

In the course of screening an *A. baumannii* plasmid library for a separate study, a transformant was identified that produced large flat colonies with irregular edges on 0.5× LB agar plates. This phenotype was very similar to that seen in the Δ*relA* mutant and suggested a hypermotile phenotype. The only functional gene within this insert was *ABUW_1132*, encoding a predicted LysR-type transcriptional regulator. To verify that motility was increased in this transformant, surface motility was examined on 0.35% Eiken agar plates. The presence of *ABUW_1132* in multicopy (p1132) resulted in a 3.8-fold increase in motility compared to that of the vector control (Fig. 4B). In a manner similar to that seen in the Δ*relA* mutant, the hypermotile phenotype resulting from *ABUW_1132* overexpression was lost in *abaI*::T26 and *ABUW_3770*::T26 mutants, indicating that a functional quorum-sensing pathway and acinetin 505 synthesis were required (Fig. 4B).

Since the motility phenotype resulting from *ABUW_1132* overexpression and that of the Δ*relA* mutant were similar, two additional experiments were conducted to determine if the increased motility in the Δ*relA* mutant was due to *ABUW_1132* overexpression. First, qRT-PCR analysis of *ABUW_1132* mRNA levels in a wild-type VIR-O and the isogenic Δ*relA* mutant verified that expression of *ABUW_1132* was increased 14.2 ± 1.0-fold in the Δ*relA* mutant (Table 2). The increased *ABUW_1132* expression was brought back to wild-type levels in the Δ*relA* mutant containing a wild-type copy of *relA* (Tn*7relA*). Next, to determine if the increased *ABUW_1132* expression in the Δ*relA* mutant was responsible for activation of the downstream *abaI*, *abaR*, and *ABUW_3770* genes, the expression of these genes was examined by qRT-PCR in the Δ*relA* mutant and in a Δ*relA ABUW_1132*::*T26* double mutant. The increased expression of *abaI*, *abaR*, and *ABUW_3770* in the Δ*relA* mutant was now lost or significantly

reduced in the Δ*relA ABUW_1132*::*T26* double mutant (Table 2). In addition, the hypermotile phenotype observed in the *relA* mutant was now lost in the Δ*relA ABUW_1132*::*T26* double mutant (Fig. 4C).

Role of RelA in persister cell formation.

Strain AB5075 is highly resistant to most antibiotics and only exhibits sensitivity to a limited number of bactericidal antibiotics, such as colistin and rifampin. The MICs for colistin and rifampin were similar in both the wild-type VIR-O and the Δ*relA* mutant, with the rifampin MIC at 2 μg/ml and the colistin MIC at 0.38 μg/ml. Next, to determine if RelA contributed to the development of persister cells tolerant to high levels of antibiotic, cell survival was assayed after 1 h of exposure to 50× the MIC for colistin or 80× the MIC for rifampin. For wild-type VIR-O with rifampin, the percentage of surviving VIR-O cells was 22.3% ± 10.9%, and for the Δ*relA* mutant it was 6.3% ± 5.9%, representing a 3.5-fold decrease. For wild-type VIR-O, the percentage of cells surviving colistin was 7.9% ± 1.9%. For the Δ*relA* mutant, the percentage of surviving cells was 1.7% ± 0.5%, a 4.6-fold decrease ($P < 0.05$ versus the wild type).

RelA is required for virulence in *Galleria mellonella*.

To investigate the role of RelA in virulence, larvae of the Galleria mellonella moth were utilized. Larvae (n = 30/strain) were infected with 9 × 105 cells of the wild-type VIR-O or isogenic ΔrelA mutant, and survival was monitored over a 5-day period. The ΔrelA mutant exhibited reduced virulence, as indicated by the increased overall survival after 5 days relative to that of larvae infected with wild-type VIR-O cells ($P < 0.001$) (Fig. 5). The reduced virulence of the ΔrelA mutant was restored when a copy of relA (Tn7relA) was introduced (Fig. 5).

Discussion

In this study, we have identified and characterized a RelA ortholog in *A. baumannii* and demonstrated that it regulates multiple cellular functions. Our initial identification of the Δ*relA* mutation resulted from a transposon insertion in the avirulent translucent (AV-T) colony variant that gave an unusual colony phenotype when viewed by oblique lighting under a dissecting microscope. This phenotype was likely the result of elongated cells that changed the colony appearance. This finding is consistent with previous studies that have shown that *relA* mutations and the resulting loss of ppGpp can also result in cell elongation (50–52). Additional changes in colony morphology due to loss of *relA* were evident in virulent opaque (VIR-O) cells, where colonies exhibited a spreading morphology on 0.5× agar plates, a phenotype consistent with increased surface motility.

The Δ*relA* mutation in a VIR-O background resulted in a 3-fold increase in surface motility (Fig. 4A). This increased motility was dependent on the LysR-type transcriptional regulator ABUW_1132, AbaI (autoinducer synthase), AbaR (LuxR-type regulator), and ABUW_3770. Previous studies in *A. nosocomialis* M2 have shown that *abaI*, encoding an autoinducer synthase responsible for the production of 3-OH C_{12}-HSL, was required for surface motility (46). In addition, the AbaI-dependent quorum-sensing pathway in *A. nosocomialis* was responsible for activating a large operon highly similar to *A1S_0112-A1S_0119* in *A. baumannii* strain ATCC 17978 and to *ABUW_3766-ABUW_3773* in *A. baumannii* AB5075 (46). Recent work has shown the *A1S_0112-A1S_0119* gene products direct the production of acinetin 505, a surfactant-like lipopeptide (48). In the Δ*relA* mutant, expression of *abaR* and *ABUW_3770* (a representative gene for the *ABUW_3766-ABUW_3773* operon) were upregulated 41-fold and 56-fold, respectively. This suggests the following mechanism to

explain the hypermotile phenotype in the Δ*relA* mutant (Fig. 6). First, loss of *relA* increases ABUW_1132 expression, which directly or indirectly activates AbaR. In turn, together with 3-OH C_{12}-HSL, AbaR then activates the *ABUW_3766-ABUW_3773* operon, which increases acinetin 505 production and aids cell motility by its surfactant-like qualities. However, the loss of *relA* may also increase *abaR* expression in a manner independent of ABUW_1132, as the levels of expression in the *relA ABUW_1132*::*T26* double mutant are still elevated above wild-type levels (Table 2). Interestingly, the effect of RelA on the quorum-sensing response in *A. baumannii* differs from that seen in *Pseudomonas aeruginosa*, where quorum sensing is activated in a RelA-dependent manner (53).

The Δ*relA* mutation completely blocked the ability of *A. baumannii* AB5075 to switch from the virulent opaque form (VIR-O) to the avirulent translucent form (AV-T). This phenotype was fully complemented by expressing a single copy of the *relA* gene from an IPTG-inducible promoter. Interestingly, the reciprocal AV-T to VIR-O switch was unaffected by the Δ*relA* mutation. A similar effect on switching was also observed in *arpAB* mutants, where switching was decreased in the VIR-O to AV-T direction only (14). This adds support to the hypothesis that separate pathways can control the directionality of this virulence switch. Since *arpAB* mutants exhibited a defect in switching, we determined if the Δ*relA* mutation decreased expression of these genes, but similar levels were observed in the wild type and the Δ*relA* mutant (M. Perez-Varela and P. Rather, unpublished data). Despite being locked in the virulent opaque form, the Δ*relA* mutant exhibited a significant decrease in virulence when tested in a *Galleria mellonella* model. Reduced virulence is a common phenotype resulting from loss of RelA in other bacteria (24–32). The contribution of decreased switching from the VIR-O to the AV-T form to the overall levels of virulence *in vivo* are likely to be minimal, as the majority of

cells will be in the VIR-O form either way. Therefore, in the absence of other genetic changes, simply locking a strain in the VIR-O state may not increase virulence. The reduced virulence of the Δ*relA* mutant is likely due to global pleiotropic changes that negatively impact virulence.

The mechanism by which the Δ*relA* mutation results in loss of switching from the VIR-O to AV-T state is under investigation. However, a Δ*relA ABUW_1132* double mutant did not exhibit restored switching, indicating that the RelA-mediated upregulation of *ABUW_1132* was not involved (Perez-Varela and Rather, unpublished). It is possible that ppGpp directly influences the activity of a transcriptional regulatory protein in a manner similar to that seen with SlyA in *S. enterica* serovar Typhimurium and PigR in *Francisella tularensis* (54, 55). Alternatively, the loss of switching may result from a more general mechanism due to the global changes in gene expression brought about by reprogramming RNA polymerase. We are currently investigating these possibilities by conducting suppressor screens to identify mutations or high-copy-number suppressors that restore VIR-O to AV-T switching in the Δ*relA* mutant. Additionally, a SpoT ortholog (ABUW_0309) is present in *A. baumannii*, and its role in *A. baumannii* is under investigation.

Materials and Methods

Strains and growth conditions.

A. baumannii AB5075 was grown in modified Luria-Bertani (LB) broth (10 g tryptone, 5 g yeast extract, 5 g NaCl per liter) at 37°C with shaking at 270 rpm. LB agar plates were prepared either full strength (1× LB), using 10 g tryptone, 5 g yeast extract, and 5 g NaCl per liter and 1.5% agar, or half strength (0.5× LB), using 5 g tryptone, 2.5 g yeast extract, and 2.5 g NaCl per liter and 0.8% agar. To prepare competent AB5075 AV-T, cells were grown to an optical density at 600 nm (OD_{600}) of 0.8, pelleted by centrifugation, and washed twice with 1 ml of ice-cold 10% glycerol. Competent cells were resuspended in 70 µl of ice-cold 10% glycerol per electroporation. Following electroporation, cells were resuspended in 1 ml of LB broth and recovered by stationary incubation at 37°C for 30 min followed by 30 min of incubation at 270 rpm. Isopropyl-β-D-thiogalactopyranoside (IPTG) was added at a final concentration of 2 µM to media.

Measurement of (p)ppGpp pools.

Nucleotides were measured as described previously (56, 57). *A. baumannii* cells were grown in morpholinepropanesulfonic acid (MOPS) minimal medium supplemented with 0.4% D-glucose, 40 µg/ml of each amino acid except serine, and 0.4 mM phosphate. MOPS minimal medium consisted of 40 mM MOPS buffer, 4 mM tricine, 0.4% D-glucose, 40 µg/ml of each amino acid except serine, 2 mM K_2HPO_4, 10 µM $FeSO_4 \cdot 7H_2O$, 9.5 mM NH_4Cl, 276 µM K_2SO_4, 500 nM $CaCl_2$, 50 mM NaCl, 525 µM $MgCl_2$, 2.9 nM $(NH_4)_6Mo_7O_{24} \cdot 4H_2O$, 400 nM H_3BO_3, 30 nM $CoCl_2$, 9.6 nM $CuSO_4$, 80.8 nM $MnCl_2$, and 9.74 nM $ZnSO_4$ (pH 7.2) (58). Logarithmically grown bacterial cultures (OD_{600} of 0.25) were labeled with 10 µCi/ml of [^{32}P]phosphorous

(PerkinElmer, Waltham, MA) for approximately 1.5 doubling times (60 min). Cells were treated with 0.4 mg/ml serine hydroxamate for 5 min before 0.4 ml of ice-cold 50% formic acid was added to the cultures. Samples incubated on ice for at least 20 min were centrifuged at 13,000 rpm for 5 min. Five microliters of formic acid extracts was spotted along the bottom of polyethyleneimine-cellulose thin-layer chromatography (TLC) plates (20 cm by 20 cm; Millipore, Billerica, MA), and air-dried plates were separated with a 1.25 M KH_2PO_4 (pH 3.4) solvent system in a TLC chamber for 1 h. TLC autoradiograms were visualized using a phosphorimager (Bio-Rad, Hercules, CA).

Transposon mutagenesis.

The AB5075 AV-T variant was mutagenized with EZ-Tn*5* <Tet-1> (Lucigen) per the manufacturer's instructions. The transposon solution (0.5 µl transposon, 0.5 µl transposase, 1.5 µl 10% glycerol) was incubated at 37°C for 1 h prior to electroporation into competent AB5075 AV-T cells. Electroporations were performed in Bio-Rad Gene Pulser 0.2-cm-gap cuvettes with a MicroPulser electroporator (Bio-Rad, Hercules, CA). Cells were plated on LB agar plates with tetracycline and incubated at 37°C for 24 h. Plates were inspected using a dissecting microscope with oblique lighting.

Identification of the EZ-Tn5 <Tet-1> insertion site.

To identify the insertion site of the EZ-Tn*5* <Tet-1> insertion, total genomic DNA from the mutant was partially digested with Sau3A, and fragments in the 2- to 4-kb range were gel purified, ligated into the BamHI site of pBC SK(−), and electroporated into EC100D competent cells (Lucigen, Middleton, WI). Cells were plated on LB agar plates containing 10 µg/ml tetracycline and incubated overnight at 37°C. To confirm that the insertions were present,

plasmid DNA was purified from Tet^r colonies using the QIAprep Spin Miniprep kit (Qiagen, Hilden, Germany) prior to digestion with XbaI. Plasmids containing insertions were sequenced with primers FP1 and RP1 provided by the EZ-Tn*5* <Tet-1> insertion kit (Lucigen, Middleton, WI).

Microscopy.

Cells were grown in LB to either mid-log phase (OD_{600} of 0.3) or to early stationary phase (OD_{600} of 1.3). Cells at mid-log phase were concentrated 10-fold prior to phase-contrast microscopy at ×1,000 magnification under an oil immersion lens.

Construction of an in-frame deletion in *relA*.

To create an in-frame deletion mutant, a fragment upstream of the *relA* gene (RelA Up) which contains the first few codons of *relA* and flanking DNA was PCR amplified using primers Up-1 (5′-AAAAAGGATCCGCTTGAGCCTTTTTCTCACC-3′) and Up-2 (5′-GCACGACGCATGATTCAAG-3′). A second fragment downstream of *relA* (RelA Down) containing the last few *relA* codons and flanking DNA was PCR amplified using primers Down-1 (5′-CTGTTCACGTACTGTGACCAT-3′) and Down-2 (5′-AAAAAGGATCCTAAGCGCCATCCAACTTTAGT-3′). Primers Up-2 and Down-1 were previously phosphorylated using T4 polynucleotide kinase (New England BioLabs, Beverly, MA). RelA Up and RelA Down were ligated for 2 h, run on a 0.8% Tris-acetate-EDTA (TAE) gel, and the gel section corresponding to the size of the combined fragments was gel purified. The fragment was PCR amplified using primers Up-1 and Down-2 to create the *ΔrelA* fragment, which was digested and ligated into the BamHI site of pEX18Tc. The ligation was transformed into EC100D cells and plated on LB plates containing tetracycline (10 μg/ml). Plasmid DNA was

isolated from Tet^r colonies and digested to confirm the presence of pEX18Tc-*ΔrelA* construct. pEX18Tc-*ΔrelA* was electroporated and maintained in *E. coli* SM10 λpir. *E. coli* SM10 λpir pEX18Tc-*ΔrelA* was conjugated to the VIR-O variant of AB5075, and an Amp^r Tet^r Suc^s AB5075 exconjugant was grown in LB broth at 37°C for 1.5 h at 250 rpm. Cells were plated on LB (without NaCl) containing 10% sucrose and incubated at room temperature. Sucrose-resistant colonies were screened via PCR using primers Up-1 and Down-2 to confirm the deletion of *relA*.

Construction of a *relA*-complemented strain.

A wild-type copy of the *relA* gene with its native ribosome binding site was generated by PCR using the primers AGGAGAATGGTATGGTCACAGTACG and ACTCTCAACAATAAGTCCCCAG. This PCR-generated fragment was then cloned into the SmaI site of pUC18Tn7 LAC Apr (kindly provided by Ayush Kumar at the University of Manitoba) (59). A recombinant containing the *relA* gene in the correct orientation such that expression could be driven by the IPTG-inducible *tac* promoter was electroporated along with a plasmid containing the Tn*7* transposase (pTNS2) into the Δ*relA* mutant. A strain with the correct insertion of the Tn*7/relA* into the *glmS* region of the chromosome was verified by PCR. This strain was then grown in the presence of IPTG at the indicated concentrations for complementation experiments.

Moving T26 transposon insertions into new backgrounds.

A recent study reported that chromosomal markers could be moved between A. baumannii strains by phage-mediated generalized transduction (60). Based on this study, we determined that insertions from the comprehensive insertion library constructed by Colin Manoil's group at the

University of Washington could be moved between strains by the same procedure. Overnight saturated cultures containing a given transposon insertion were spun down, and 1 ml of supernatant was filter sterilized (0.22 μm) to generate a phage lysate. To transduce the recipient strain, 20 μl of a mid-log-phase culture was mixed with 20 μl of lysate and spotted on the surface of a well-dried LB plate to allow the spot to quickly soak into the agar. After incubation at 37°C for 4 h, cells were scraped from the plate, resuspended in 2 ml of LB broth, and plated on LB plus tetracycline (5 μg/ml). Colonies were screened by PCR for the correct insertion.

Plasmid p1132 construction.

Plasmid pQF1266 is a derivative of pQF50 (61) and contains a hygromycin resistance cassette cloned into the ScaI site of the β-lactamase gene and an origin of replication from pWH1266. A partial Sau3A digest of AB5075 chromosomal DNA was performed, and fragments in the size range of 3 to 6 kb were cloned into the BamHI site of pQF1266 (62). This genomic library was used in a variety of genetic screens, and a recombinant plasmid that generated a hypermotile colony was designated p1132. The only complete gene within this plasmid was ABUW_1132.

Analysis of VIR-O and AV-T switching frequencies.

Aliquots of AB5075 VIR-O and AV-T variants in the wild-type and *ΔrelA* mutant backgrounds were serially diluted, plated on 0.5× LB plates, and incubated at 37°C for 24 h. Plates containing fewer than 50 colonies were used, and 6 well-isolated colonies from each strain were removed from the plate as agar plugs and resuspended in 2 ml LB broth. Serial dilutions of 10^{-4}, 10^{-5}, and 10^{-7} were plated on 0.5× LB plates and incubated at 37°C for 24 h. Plates were inspected under a dissecting microscope via indirect light, and VIR-O and AV-T variants were quantified.

Motility assays.

Motility assays were carried out on Eiken agar motility plates consisted of 10 g tryptone, 5 g yeast extract, 5 g NaCl, and 3.5 g Eiken agar (Eiken Chemical Ltd., Tokyo, Japan) per liter. The plates were prepared the same day of the assay and they were allowed to dry for 30 min before use. Strains were inoculated in LB broth medium and grown at 37°C with shaking until an OD_{600} of 0.5 was reached. A 1-µl aliquot of the corresponding strain culture was spotted onto the 0.35% Eiken agar motility plates, and the plates were incubated at 37°C for approximately 8 h, which was previously determined to be the time required for the Δ*relA* mutant strain to reach the plate border under experimental conditions. Wild-type and Δ*relA* mutant strains were compared on the same plates. Motility diameters were measured after the designated time, and statistical analysis was performed using Student's *t* test. The relative migration was calculated as the ratio of the motility diameter of the studied strain to that of the corresponding control strain in each case. All assays were conducted a minimum of two independent times.

Galleria mellonella infections.

G. mellonella larvae were purchased from Speedy Worm, Alexandria, MN. For larval infections, the wild-type VIR-O variant of AB5075 and isogenic Δ*relA* mutant cultures were grown in 2 ml of LB broth at 37°C with shaking to an optical density (OD_{600}) of approximately 0.5. Serial dilutions were prepared in LB with 20% glycerol and stored in aliquots at −80°C. For infections, 9×10^5 cells were injected in an 8-µl volume with IPTG (10 mM) into the last proleg of *G. mellonella* larvae weighing between 200 and 250 mg. Larvae were incubated in a petri plate at 37°C in a humidified incubator for up to 5 days. The number of dead larvae was evaluated at 24-h intervals; larvae were considered dead when they were dark brown to black and showed no movement in response to touch with a pipette tip. Injections of LB alone did not result in killing.

For all experiments, the serial dilutions used were plated onto regular LB plates to determine CFU per milliliter for each bacterial strain. The reported data correspond to three independent experiments carried out with 10 larvae for each strain.

RNA extraction and quantitative real-time PCR.

Cultures of wild-type VIR-O strain AB5075 and the ΔrelA mutant were grown in 2 ml of LB broth at 37°C with shaking to an OD600 of approximately 1.500. The cultures were centrifuged, and the RNA was isolated using the MasterPure RNA isolation kit (Lucigen, Middleton, WI) according to the manufacturer's instructions. The samples were treated with Turbo DNA-free DNase (Ambion) to remove the contaminating DNA. The RNA concentration was determined using a NanoDrop ND-1000 spectrophotometer, and cDNA was obtained by using the iScript cDNA synthesis kit (Bio-Rad, Hercules, CA) with random primers. The reverse transcription reaction was performed as follows: 25°C for 5 min, 42°C for 45 min, and 85°C for 5 min. Diluted cDNA (1:10) was used as the template for experimental reactions. Specific oligonucleotides pairs for quantitative real-time PCR (qRT-PCR) to amplify approximately 150-bp fragments from each gene of study were generated by using the Primer-BLAST program (www.ncbi.nlm.nih.gov/tools/primer-blast/). Gene expression was determined using iQ SYBR green Supermix (Bio-Rad, Hercules, CA) on a CFX Connect cycler (Bio-Rad). Cycle conditions to amplify and quantify fragments were the following: 95°C for 3 min and then 95°C for 10 s, 55°C for 10 s, and 72°C for 20 s, repeated 40 times. Melt curve data were then collected to confirm the specificity of the oligonucleotide primer set. Data were generated from two independent RNA isolation and cDNA preparations and three replicates for each primer pair. The expression level of the target genes was standardized relative to the transcription level of the housekeeping gene clpX using the threshold cycle ($2^{-\Delta\Delta CT}$) method (63). The statistical

significance of the observed differences was confirmed by the analysis of variance (ANOVA) test.

Persister cell assays.

Wild-type and *ΔrelA* cells were grown to an OD_{600} of 1.1 and incubated for 1 h at 37°C with either rifampin at a final concentration of 160 μg/ml or colistin at a final concentration of 20 μg/ml. Dilutions were then plated for CFU on LB agar plates.

Acknowledgements

This work was supported by funding from the Department of Veterans Affairs (I01BX001725 and IK6BX004470) and NIH (R21AI142489 to P.N.R., and R01AI36520, R01AI05449 and VAI01BX002073 to A.V.T.).

We thank Ayush Kumar at the University of Manitoba for providing pUC18-miniTn*7*-Lac-Apra. We are grateful to Sarah Dayman, Marjan Farokhyfar, and Daniel Knight for help with strain and plasmid constructions.

References

1. Gootz TD, Marra A. 2008. *Acinetobacter baumannii*: an emerging multidrug-resistant threat. Expert Rev Anti Infect Ther **6**:309–325. doi:10.1586/14787210.6.3.309.

2. Joly-Guillou ML. 2005. Clinical impact and pathogenicity of *Acinetobacter*. Clin Microbiol Infect **11**:868–873. doi:10.1111/j.1469-0691.2005.01227.x.

3. Peleg AY, Seifert H, Paterson DL. 2008. *Acinetobacter baumannii*: emergence of a successful pathogen. Clin Microbiol Rev **21**:538–582. doi:10.1128/CMR.00058-07.

4. Visca P, Seifert H, Towner KJ. 2011. *Acinetobacter* infection–an emerging threat to human health. IUBMB Life **63**:1048–1054. doi:10.1002/iub.534.

5. Wong D, Nielsen TB, Bonomo RA, Pantapalangkoor P, Luna B, Spellberg B. 2017. Clinical and pathophysiological overview of *Acinetobacter* infections: a century of challenges. Clin Microbiol Rev **30**:409–447. doi:10.1128/CMR.00058-16.

6. Tacconelli E, Carrara E, Savoldi A, Harbarth S, Mendelson M, Monnet DL, Pulcini C, Kahlmeter G, Kluytmans J, Carmeli Y, Ouellette M, Outterson K, Patel J, Cavaleri M, Cox EM, Houchens CR, Grayson ML, Hansen P, Singh N, Theuretzbacher U, Magrini N, Aboderin AO, Al-Abri SS, Awang Jalil N, Benzonana N, Bhattacharya S, Brink AJ, Burkert FR, Cars O, Cornaglia G, Dyar OJ, Friedrich AW, Gales AC, Gandra S, Giske CG, Goff DA, Goossens H, Gottlieb T, Guzman Blanco M, Hryniewicz W, Kattula D, Jinks T, Kanj SS, Kerr L, Kieny M-P, Kim YS, Kozlov RS, Labarca J, Laxminarayan R, Leder K, et al. . 2018. Discovery, research, and development of new antibiotics: the WHO priority list of antibiotic-resistant bacteria and tuberculosis. Lancet Infect Dis **18**:318–327. doi:10.1016/S1473-3099(17)30753-3.

7. Sievert DM, Ricks P, Edwards JR, Schneider A, Patel J, Srinivasan A, Kallen A, Limbago B, Fridkin S, National Healthcare Safety Network (NHSN) Team and Participating NHSN Facilities. 2013. Antimicrobial-resistant pathogens associated with healthcare-associated infections: summary of data reported to the National Healthcare Safety Network at the Centers for Disease Control and Prevention, 2009-2010. Infect Control Hosp Epidemiol **34**:1–14. doi:10.1086/668770.

8. Dijkshoorn L, Nemec A, Seifert H. 2007. An increasing threat in hospitals: multidrug-resistant *Acinetobacter baumannii*. Nat Rev Microbiol **5**:939–951. doi:10.1038/nrmicro1789.

9. Rice LB. 2006. Challenges in identifying new antimicrobial agents effective for treating infections with *Acinetobacter baumannii* and *Pseudomonas aeruginosa*. Clin Infect Dis **43**:S100–S105. doi:10.1086/504487.

10. Telang NV, Satpute MG, Dhakephalkar PK, Niphadkar KB, Joshi SG. 2011. Fulminating septicemia due to persistent pan-resistant community-acquired metallo-beta-lactamase (IMP-1)-positive *Acinetobacter baumannii*. Indian J Pathol Microbiol **54**:180–182. doi:10.4103/0377-4929.77397.

11. Lowman W, Kalk T, Menezes CN, John MA, Grobusch MP. 2008. A case of community-acquired *Acinetobacter baumannii* meningitis - has the threat moved beyond the hospital? J Med Microbiol **57**:676–678. doi:10.1099/jmm.0.47781-0.

12. Tipton KA, Dimitrova D, Rather PN. 2015. Phase-variable control of multiple phenotypes in *Acinetobacter baumannii* strain AB5075. J Bacteriol **197**:2593–2599. doi:10.1128/JB.00188-15.

13. Chin CY, Tipton KA, Farokhyfar M, Burd EM, Weiss DS, Rather PN. 2018. A high-frequency phenotypic switch links bacterial virulence and environmental survival in *Acinetobacter baumannii*. Nat Microbiol **3**:563–569. doi:10.1038/s41564-018-0151-5.
14. Tipton KA, Farokhyfar M, Rather PN. 2017. Multiple roles for a novel RND-type efflux system in *Acinetobacter baumannii* AB5075. Microbiologyopen **6**:e00418. doi:10.1002/mbo3.418.
15. Tipton KA, Rather PN. 2017. An ompR/envZ two-component system ortholog regulates phase variation, osmotic tolerance, motility, and virulence in *Acinetobacter baumannii* strain AB5075. J Bacteriol **199**:e00705-16. doi:10.1128/jb.00705-16.
16. Potrykus K, Cashel M. 2008. (p)ppGpp: still magical? Annu Rev Microbiol **62**:35–51. doi:10.1146/annurev.micro.62.081307.162903.
17. Irving SE, Corrigan RM. 2018. Triggering the stringent response: signals responsible for activating (p)ppGpp synthesis in bacteria. Microbiology **164**:268–276. doi:10.1099/mic.0.000621.
18. Atkinson GC, Tenson T, Hauryliuk V. 2011. The RelA/SpoT homolog (RSH) superfamily: distribution and functional evolution of ppGpp synthetases and hydrolases across the tree of life. PLoS One **6**:e23479. doi:10.1371/journal.pone.0023479.
19. Hauryliuk V, Atkinson GC, Murakami KS, Tenson T, Gerdes K. 2015. Recent functional insights into the role of (p)ppGpp in bacterial physiology. Nat Rev Microbiol **13**:298–309. doi:10.1038/nrmicro3448.
20. Srivatsan A, Wang JD. 2008. Control of bacterial transcription, translation and replication by (p)ppGpp. Curr Opin Microbiol **11**:100–105. doi:10.1016/j.mib.2008.02.001.

21. Paul BJ, Barker MM, Ross W, Schneider DA, Webb C, Foster JW, Gourse RL. 2004. DksA: a critical component of the transcription initiation machinery that potentiates the regulation of rRNA promoters by ppGpp and the initiating NTP. Cell **118**:311–322. doi:10.1016/j.cell.2004.07.009.

22. Paul BJ, Berkmen MB, Gourse RL. 2005. DksA potentiates direct activation of amino acid promoters by ppGpp. Proc Natl Acad Sci U S A **102**:7823–7828. doi:10.1073/pnas.0501170102.

23. Jishage M, Kvint K, Shingler V, Nystrom T. 2002. Regulation of sigma factor competition by the alarmone ppGpp. Genes Dev **16**:1260–1270. doi:10.1101/gad.227902.

24. Erickson DL, Lines JL, Pesci EC, Venturi V, Storey DG. 2004. *Pseudomonas aeruginosa relA* contributes to virulence in *Drosophila melanogaster*. Infect Immun **72**:5638–5645. doi:10.1128/IAI.72.10.5638-5645.2004.

25. Hammer BK, Swanson MS. 1999. Co-ordination of *Legionella pneumophila* virulence with entry into stationary phase by ppGpp. Mol Microbiol **33**:721–731. doi:10.1046/j.1365-2958.1999.01519.x.

26. Muller CM, Conejero L, Spink N, Wand ME, Bancroft GJ, Titball RW. 2012. Role of RelA and SpoT in *Burkholderia pseudomallei* virulence and immunity. Infect Immun **80**:3247–3255. doi:10.1128/IAI.00178-12.

27. Dean RE, Ireland PM, Jordan JE, Titball RW, Oyston PC. 2009. RelA regulates virulence and intracellular survival of *Francisella novicida*. Microbiology **155**:4104–4113. doi:10.1099/mic.0.031021-0.

28. Haralalka S, Nandi S, Bhadra RK. 2003. Mutation in the *relA* gene of *Vibrio cholerae* affects *in vitro* and *in vivo* expression of virulence factors. J Bacteriol **185**:4672–4682. doi:10.1128/JB.185.16.4672-4682.2003.

29. Sun W, Roland KL, Branger CG, Kuang X, Curtiss R III. 2009. The role of relA and spoT in *Yersinia pestis* KIM5 pathogenicity. PLoS One **4**:e6720. doi:10.1371/journal.pone.0006720.

30. Pizarro-Cerdá J, Tedin K. 2004. The bacterial signal molecule, ppGpp, regulates *Salmonella* virulence gene expression. Mol Microbiol **52**:1827–1844. doi:10.1111/j.1365-2958.2004.04122.x.

31. Nakanishi N, Abe H, Ogura Y, Hayashi T, Tashiro K, Kuhara S, Sugimoto N, Tobe T. 2006. ppGpp with DksA controls gene expression in the locus of enterocyte effacement (LEE) pathogenicity island of enterohaemorrhagic *Escherichia coli* through activation of two virulence regulatory genes. Mol Microbiol **61**:194–205. doi:10.1111/j.1365-2958.2006.05217.x.

32. Tapscott T, Kim J-S, Crawford MA, Fitzsimmons L, Liu L, Jones-Carson J, Vázquez-Torres A. 2018. Guanosine tetraphosphate relieves the negative regulation of *Salmonella* pathogenicity island-2 gene transcription exerted by the AT-rich *ssrA* discriminator region. Sci Rep **8**:9465. doi:10.1038/s41598-018-27780-9.

33. Korch SB, Henderson TA, Hill TM. 2003. Characterization of the *hipA7* allele of *Escherichia coli* and evidence that high persistence is governed by (p)ppGpp synthesis. Mol Microbiol **50**:1199–1213. doi:10.1046/j.1365-2958.2003.03779.x.

34. Fung DK, Chan EW, Chin ML, Chan RC. 2010. Delineation of a bacterial starvation stress response network which can mediate antibiotic tolerance development. Antimicrob Agents Chemother **54**:1082–1093. doi:10.1128/AAC.01218-09.

35. Amato SM, Brynildsen MP. 2015. Persister heterogeneity arising from a single metabolic stress. Curr Biol **25**:2090–2098. doi:10.1016/j.cub.2015.06.034.

36. Cohen NR, Lobritz MA, Collins JJ. 2013. Microbial persistence and the road to drug resistance. Cell Host Microbe **13**:632–642. doi:10.1016/j.chom.2013.05.009.

37. Nguyen D, Joshi-Datar A, Lepine F, Bauerle E, Olakanmi O, Beer K, McKay G, Siehnel R, Schafhauser J, Wang Y, Britigan BE, Singh PK. 2011. Active starvation responses mediate antibiotic tolerance in biofilms and nutrient-limited bacteria. Science **334**:982–986. doi:10.1126/science.1211037.

38. Betts JC, Lukey PT, Robb LC, McAdam RA, Duncan K. 2002. Evaluation of a nutrient starvation model of *Mycobacterium tuberculosis* persistence by gene and protein expression profiling. Mol Microbiol **43**:717–731. doi:10.1046/j.1365-2958.2002.02779.x.

39. Dalebroux ZD, Svensson SL, Gaynor EC, Swanson MS. 2010. ppGpp conjures bacterial virulence. Microbiol Mol Biol Rev **74**:171–199. doi:10.1128/MMBR.00046-09.

40. Dalebroux ZD, Swanson MS. 2012. ppGpp: magic beyond RNA polymerase. Nat Rev Microbiol **10**:203–212. doi:10.1038/nrmicro2720.

41. Umland TC, Schultz LW, MacDonald U, Beanan JM, Olson R, Russo TA. 2012. *In vivo*-validated essential genes identified in *Acinetobacter baumannii* by using human ascites overlap poorly with essential genes detected on laboratory media. mBio **3**:e00113-12. doi:10.1128/mBio.00113-12.

42. Sanchez-Larrayoz AF, Elhosseiny NM, Chevrette MG, Fu Y, Giunta P, Spallanzani RG, Ravi K, Pier GB, Lory S, Maira-Litrán T. 2017. Complexity of complement resistance factors expressed by *Acinetobacter baumannii* needed for survival in human serum. J Immunol **199**:2803–2814. doi:10.4049/jimmunol.1700877.

43. Jung H-W, Kim K, Islam MM, Lee JC, Shin M. 12 February 2020. Role of ppGpp-regulated efflux genes in *Acinetobacter baumannii*. J Antimicrob Chemother doi:10.1093/jac/dkaa014.

44. Knight D, Dimitrova DD, Rudin SD, Bonomo RA, Rather PN. 2016. Mutations decreasing intrinsic beta-lactam resistance are linked to cell division in the nosocomial pathogen *Acinetobacter baumannii*. Antimicrob Agents Chemother **60**:3751–3758. doi:10.1128/AAC.00361-16.

45. Brown DR, Barton G, Pan Z, Buck M, Wigneshweraraj S. 2014. Nitrogen stress response and stringent response are coupled in *Escherichia coli*. Nat Commun **5**:4115. doi:10.1038/ncomms5115.

46. Clemmer KM, Bonomo RA, Rather PN. 2011. Genetic analysis of surface motility in *Acinetobacter baumannii*. Microbiology **157**:2534–2544. doi:10.1099/mic.0.049791-0.

47. Skiebe E, de Berardinis V, Morczinek P, Kerrinnes T, Faber F, Lepka D, Hammer B, Zimmermann O, Ziesing S, Wichelhaus TA, Hunfeld KP, Borgmann S, Grobner S, Higgins PG, Seifert H, Busse HJ, Witte W, Pfeifer Y, Wilharm G. 2012. Surface-associated motility, a common trait of clinical isolates of *Acinetobacter baumannii*, depends on 1,3-diaminopropane. Int J Med Microbiol **302**:117–128. doi:10.1016/j.ijmm.2012.03.003.

48. Rumbo-Feal S, Perez A, Ramelot TA, Alvarez-Fraga L, Vallejo JA, Beceiro A, Ohneck EJ, Arivett BA, Merino M, Fiester SE, Kennedy MA, Actis LA, Bou G, Poza M.

2017. Contribution of the *A. baumannii* A1S_0114 gene to the interaction with eukaryotic cells and virulence. Front Cell Infect Microbiol **7**:108. doi:10.3389/fcimb.2017.00108.

49. Eijkelkamp BA, Stroeher UH, Hassan KA, Elbourne LD, Paulsen IT, Brown MH. 2013. H-NS plays a role in expression of *Acinetobacter baumannii* virulence features. Infect Immun **81**:2574–2583. doi:10.1128/IAI.00065-13.
50. Xiao H, Kalman M, Ikehara K, Zemel S, Glaser G, Cashel M. 1991. Residual guanosine 3′,5′-bispyrophosphate synthetic activity of *relA* null mutants can be eliminated by *spoT* null mutations. J Biol Chem **266**:5980–5990.
51. Dahl JL, Arora K, Boshoff HI, Whiteford DC, Pacheco SA, Walsh OJ, Lau-Bonilla D, Davis WB, Garza AG. 2005. The *relA* homolog of *Mycobacterium smegmatis* affects cell appearance, viability, and gene expression. J Bacteriol **187**:2439–2447. doi:10.1128/JB.187.7.2439-2447.2005.
52. Chatnaparat T, Li Z, Korban SS, Zhao Y. 2015. The bacterial alarmone (p)ppGpp is required for virulence and controls cell size and survival of *Pseudomonas syringae* on plants. Environ Microbiol **17**:4253–4270. doi:10.1111/1462-2920.12744.
53. van Delden C, Comte R, Bally AM. 2001. Stringent response activates quorum sensing and modulates cell density-dependent gene expression in *Pseudomonas aeruginosa*. J Bacteriol **183**:5376–5384. doi:10.1128/JB.183.18.5376-5384.2001.
54. Zhao G, Weatherspoon N, Kong W, Curtiss R III, Shi Y. 2008. A dual-signal regulatory circuit activates transcription of a set of divergent operons in *Salmonella typhimurium*. Proc Natl Acad Sci U S A **105**:20924–20929. doi:10.1073/pnas.0807071106.

55. Charity JC, Blalock LT, Costante-Hamm MM, Kasper DL, Dove SL. 2009. Small molecule control of virulence gene expression in *Francisella tularensis*. PLoS Pathog **5**:e1000641. doi:10.1371/journal.ppat.1000641.

56. Fitzsimmons LF, Liu L, Kim J-S, Jones-Carson J, Vázquez-Torres A. 2018. *Salmonella* reprograms nucleotide metabolism in its adaptation to nitrosative stress. mBio **9**:e00211-18. doi:10.1128/mBio.00211-18.

57. Cashel M. 1974. Preparation of guanosine tetraphosphate (ppGpp) and guanosine pentaphosphate (pppGpp) from *Escherichia coli* ribosomes. Anal Biochem **57**:100–107. doi:10.1016/0003-2697(74)90056-6.

58. Neidhardt FC, Bloch PL, Smith DF. 1974. Culture medium for enterobacteria. J Bacteriol **119**:736–747. doi:10.1128/JB.119.3.736-747.1974.

59. Ducas-Mowchun K, De Silva PM, Crisostomo L, Fernando DM, Chao T-C, Pelka P, Schweizer HP, Kumar A. 2019. Next generation of Tn*7*-based single-copy insertion elements for use in multi- and pan-drug-resistant strains of *Acinetobacter baumannii*. Appl Environ Microbiol **85**:e00066-19. doi:10.1128/AEM.00066-19.

60. Wachino J-I, Jin W, Kimura K, Arakawa Y. 2019. Intercellular transfer of chromosomal antimicrobial resistance genes between *Acinetobacter baumannii* strains mediated by prophages. Antimicrob Agents Chemother **63**:e00334-19. doi:10.1128/AAC.00334-19.

61. Farinha MA, Kropinski AM. 1990. Construction of broad-host-range plasmid vectors for easy visible selection and analysis of promoters. J Bacteriol **172**:3496–3499. doi:10.1128/JB.172.6.3496-3499.1990.

62. Hunger M, Schmucker R, Kishan V, Hillen W. 1990. Analysis and nucleotide sequence of an origin of DNA replication in *Acinetobacter calcoaceticus* and its use for *Escherichia coli* shuttle plasmids. Gene **87**:45–51. doi:10.1016/0378-1119(90)90494-C.

63. Schmittgen TD, Livak KJ. 2008. Analyzing real-time PCR data by the comparative *CT* method. Nat Protoc **3**:1101–1108. doi:10.1038/nprot.2008.73.

Table 1: Analysis of switching frequency between VIR-O and AV-T variants

Strain or genotype	VIR-O to AV-T (%)	AV-T to VIR-O (%)
Wild type	6.6 ± 2.9	7.5 ± 1.7
Δ*ABUW_3302*	None detected	10.9 ± 6.8
Δ*ABUW_3302*/Tn*7*::*ABUW_3302*	20.5 ± 8.6	Not determined

Table 2: Real-time qRT-PCR analysis of gene expression

Strain or genotype	Relative expression of[a]:					
	abaI	*abaR*	*ABUW_3770*	*dat* (*ABUW_1109*)	*hns* (*ABUW_3609*)	*ABUW_1132*
Wild type	1	1	1	1	1	1
Δ*relA*	3.9 ± 1.3	41.3 ± 10.4[b]	55.6 ± 17.1[b]	1.7 ± 0.3	1.5 ± 0.3	14.2 ± 1.0[b]
Δ*relA/ABUW_1132*::*T26*	1.7 ± 0.7	7.9 ± 3.0[c]	0.9 ± 0.3[c]			
Δ*relA* Tn*7relA*[d]	0.8 ± 0.1	1.2 ± 0.2	0.9 ± 0.2			0.8 ± 0.1

[a]Values represent the means from three biological replicates with standard errors. Values for each strain were calculated using the $2^{-\Delta\Delta CT}$ method with *clpX* as an internal control.
[b]$P < 0.05$ versus wild type.
[c]$P < 0.05$ versus Δ*relA*.
[d]Cells with Tn*7relA* were grown with 5 mM IPTG.

Figure Legends

Figure 1: Colony morphology of wild-type and Δ*3302* mutants. (A) Colonies of the wild-type AV-T and the isogenic AV-T Δ*3302* mutant are shown after 24 h of growth on a 0.5× LB agar plate. **(B)** Colonies of the VIR-O wild type and the isogenic VIR-O Δ*3302* mutant are shown after 24 h of growth on a 0.5× LB agar plate. Because of the larger size of the VIR-O Δ*3302* colony, the relative picture size in panel B is approximately 50% smaller than in panel A.

Figure 2: TLC autoradiogram of ^{32}P-labeled nucleotides from the AB5075 VIR-O wild type (WT) and the Δ*ABUW_3302* (relA) mutant after exposure to 0.4 mg/ml serine hydroxamate (SHX) for 5 min. The autoradiogram shown is representative of three independent experiments.

Figure 3: Cell morphology at low and high cell densities. Cells were grown in LB and examined microscopically at early log phase (OD600 of 0.3) or at high density (OD600 of 1.3).

Figure 4: Surface motility of A. baumannii strains. Cultures of strains to be tested were grown to an optical density of 0.5, and a 1-µl aliquot was placed on the surface of a 0.35% Eiken agar plate. Plates were incubated at 37°C for 8 h. The reported values represent the averages from 6 measurements per strain, 2 from three independent experiments. *, $P < 0.05$ versus wild-type control determined by Student's *t* test.

Figure 5: Virulence assays using Galleria mellonella. Larvae weighing between 200 and 250 mg were injected with 9×10^5 cells of the indicated strains. Larvae were monitored daily for survival for a period of 5 days. The reported values represent the averages from 30 larvae from a total of three independent experiments where 10 larvae/strain were used. *, $P < 0.001$ by the Mantel-Cox test.

Figure 6: A model for the RelA-dependent control of downstream pathways. RelA is predicted to act as a negative regulator of both the LysR-type regulator ABUW_1132 and the LuxR-type regulator AbaR. ABUW_1132 then activates the *abaR* gene and, together with 3-OH C12-HSL, AbaR then activates the *abaI* gene and the *ABUW_3766-ABUW_3773* operon.

Figure 1

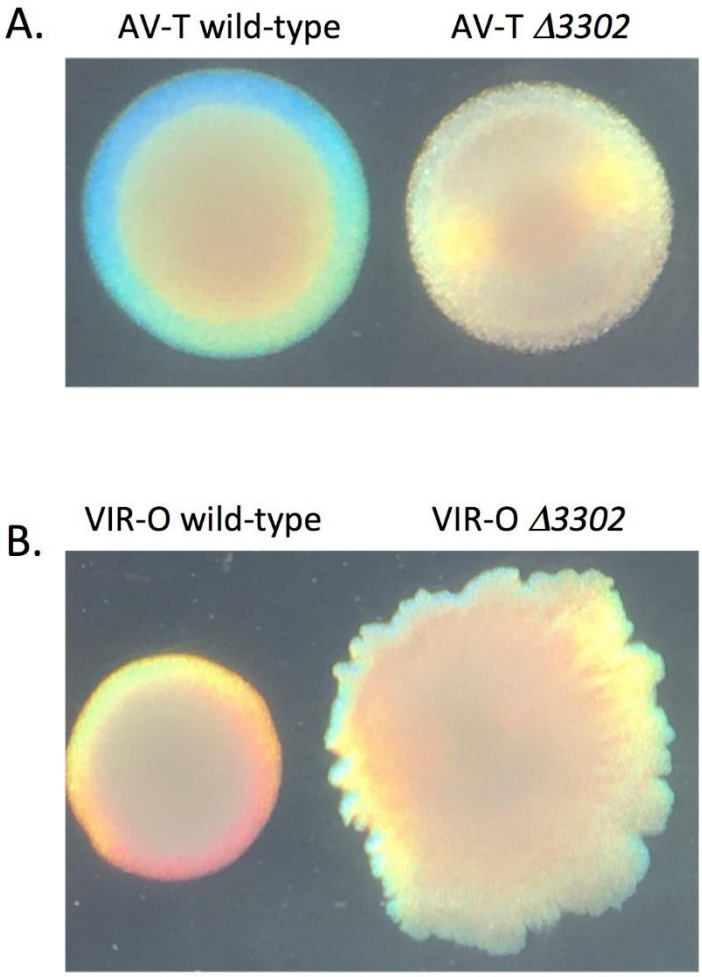

Figure 1: Colony morphology of wild-type and Δ*3302* mutants. (A) Colonies of the wild-type AV-T and the isogenic AV-T Δ*3302* mutant are shown after 24 h of growth on a 0.5× LB agar plate. **(B)** Colonies of the VIR-O wild type and the isogenic VIR-O Δ*3302* mutant are shown after 24 h of growth on a 0.5× LB agar plate. Because of the larger size of the VIR-O Δ*3302* colony, the relative picture size in panel B is approximately 50% smaller than in panel A.

Figure 2

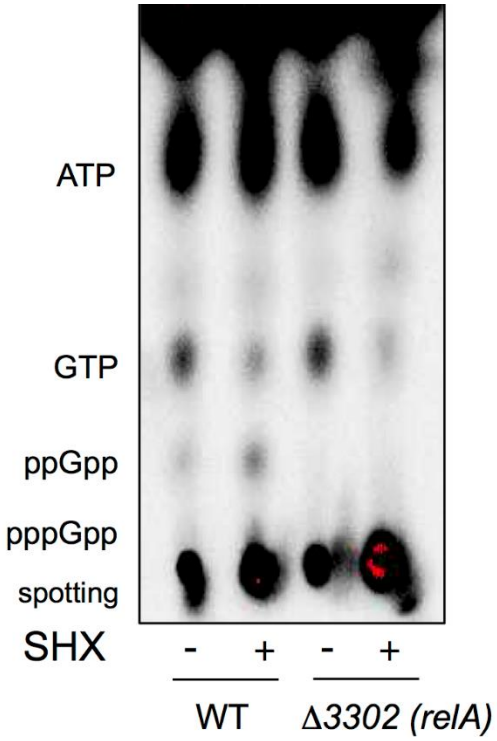

Figure 2: TLC autoradiogram of ^{32}P-labeled nucleotides from the AB5075 VIR-O wild type (WT) and the Δ*ABUW_3302* (relA) mutant after exposure to 0.4 mg/ml serine hydroxamate (SHX) for 5 min. The autoradiogram shown is representative of three independent experiments.

Figure 3

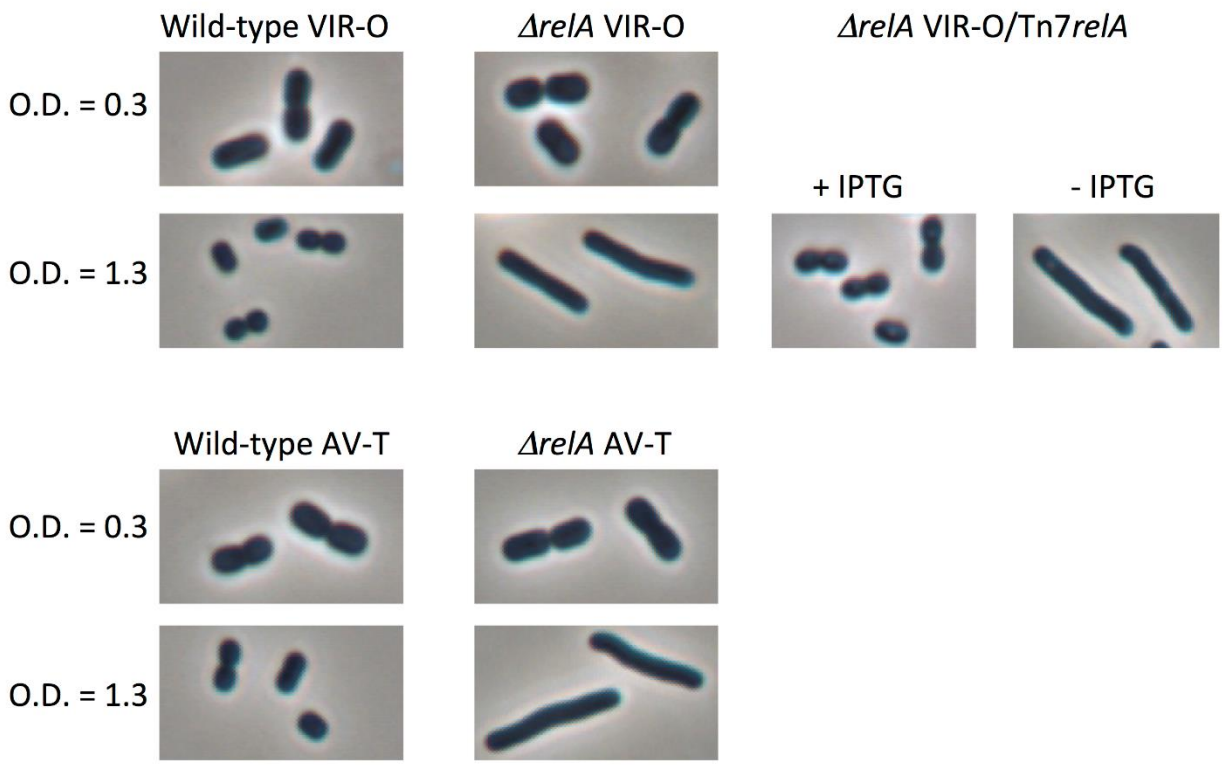

Figure 3: Cell morphology at low and high cell densities. Cells were grown in LB and examined microscopically at early log phase (OD600 of 0.3) or at high density (OD600 of 1.3).

Figure 4

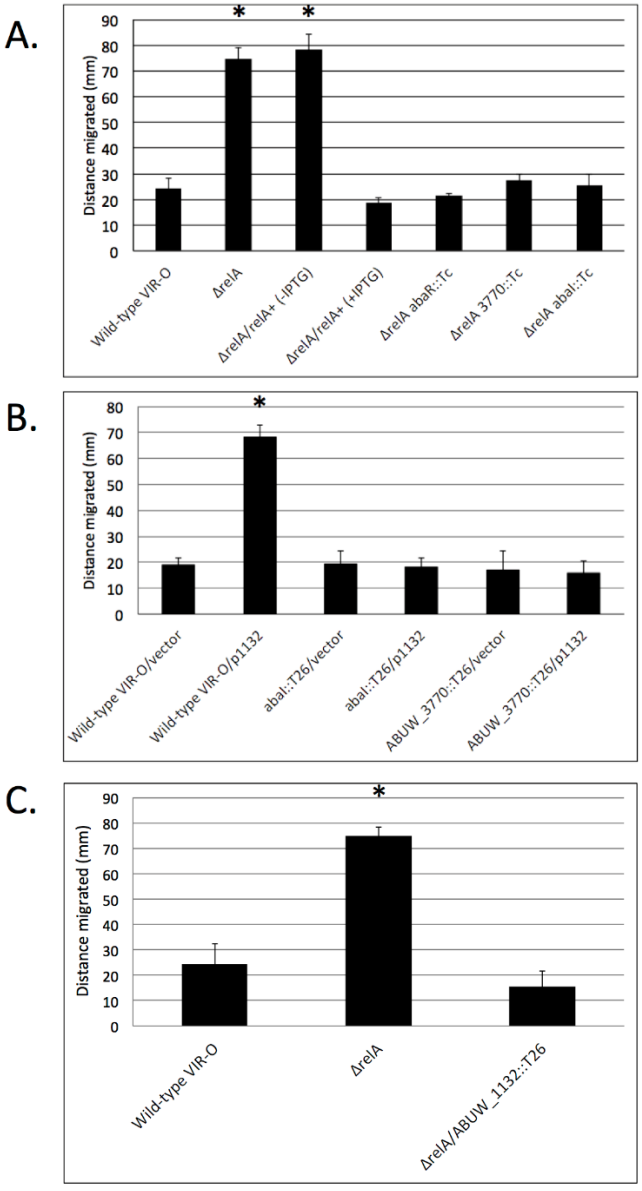

Figure 4: Surface motility of *A. baumannii* strains. Cultures of strains to be tested were grown to an optical density of 0.5, and a 1-µl aliquot was placed on the surface of a 0.35% Eiken agar plate. Plates were incubated at 37°C for 8 h. The reported values represent the averages from 6 measurements per strain, 2 from three independent experiments. *, $P < 0.05$ versus wild-type control determined by Student's *t* test.

Figure 5

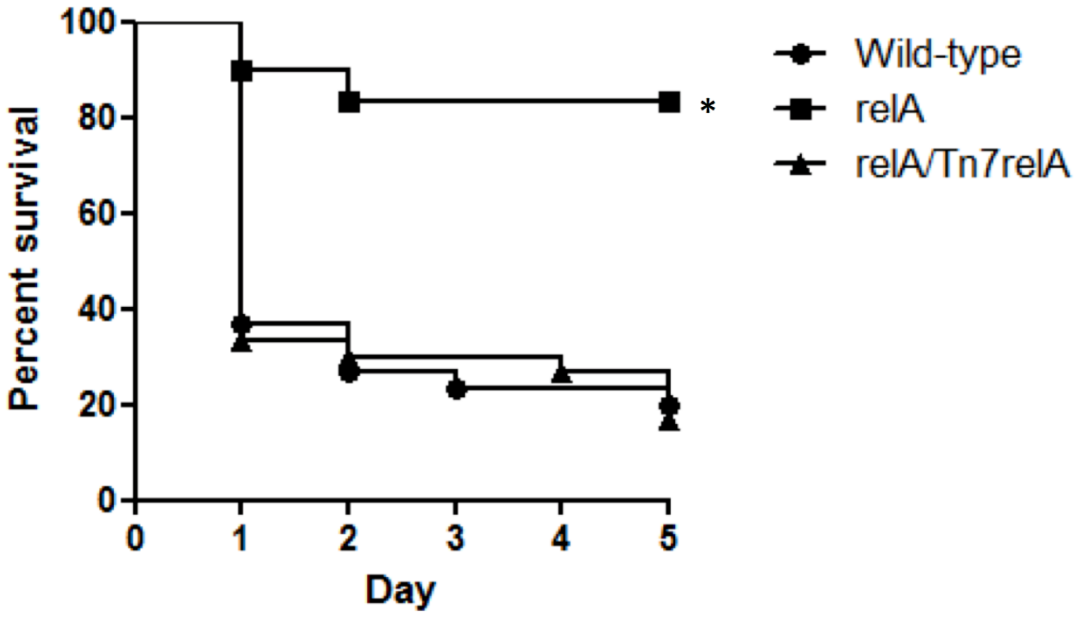

Figure 5: Virulence assays using *Galleria mellonella*. Larvae weighing between 200 and 250 mg were injected with 9×10^5 cells of the indicated strains. Larvae were monitored daily for survival for a period of 5 days. The reported values represent the averages from 30 larvae from a total of three independent experiments where 10 larvae/strain were used. *, $P < 0.001$ by the Mantel-Cox test.

Figure 6

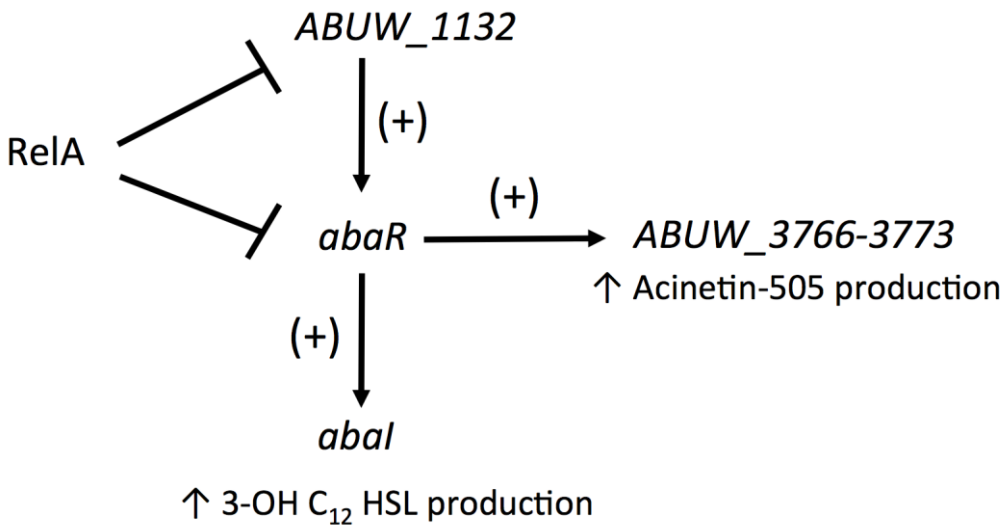

Figure 6: A model for the RelA-dependent control of downstream pathways. RelA is predicted to act as a negative regulator of both the LysR-type regulator ABUW_1132 and the LuxR-type regulator AbaR. ABUW_1132 then activates the *abaR* gene and, together with 3-OH C12-HSL, AbaR then activates the *abaI* gene and the *ABUW_3766-ABUW_3773* operon.

Chapter 3: A LysR-Type Transcriptional Regulator Controls Multiple Phenotypes in *Acinetobacter baumannii*

Aimee R. P. Tierney[1], Chui Yoke Chin[1,2,3,4,5], David S. Weiss[1,2,3,4,5,6], and Philip N. Rather[1,6]

[1] Department of Microbiology and Immunology, Emory University School of Medicine, Atlanta, Georgia, USA

[2] Emory Vaccine Center, Atlanta, Georgia, USA

[3] Yerkes National Primate Research Center, Atlanta, Georgia, USA

[4] Division of Infectious Diseases, Department of Medicine, Emory University School of Medicine, Atlanta, Georgia, USA

[5] Emory Antibiotic Resistance Center, Atlanta, Georgia, USA

[6] Research Service, Department of Veterans Affairs, Atlanta VA Medical Center, Decatur, Georgia, USA

Published in:

Frontiers in Cellular and Infection Microbiology, 2021

11 (1076)

PR and ARPT conceptualized and designed the study and experiments. ARPT carried out all of the experiments except the RNA sequencing, mouse experiments, and electron microscopy. CYC performed the mouse experiments and subsequent data analysis. ARPT analyzed all other data with guidance from PR. ARPT wrote the original manuscript, with the exception of the “Mouse Virulence Assays” methods, which was contributed by CYC. All authors contributed to the article and approved the submitted version.

Abstract

Acinetobacter baumannii is a multidrug-resistant, Gram-negative nosocomial pathogen that exhibits phenotypic heterogeneity resulting in virulent opaque (VIR-O) and avirulent translucent (AV-T) colony variants. Each variant has a distinct gene expression profile resulting in multiple phenotypic differences. Cells interconvert between the VIR-O and AV-T variants at high frequency under laboratory conditions, suggesting that the genetic mechanism underlying the phenotypic switch could be manipulated to attenuate virulence. Therefore, our group has focused on identifying and characterizing genes that regulate this switch, which led to the investigation of *ABUW_1132* (*1132*), a highly conserved gene predicted to encode a LysR-type transcriptional regulator. ABUW_1132 was shown to be a global regulator as the expression of 74 genes was altered > 2-fold in an *1132* deletion mutant. The *1132* deletion also resulted in a 16-fold decrease in VIR-O to AV-T switching, loss of 3-OH-C12-HSL secretion, and reduced surface-associated motility. Further, the deletion of *1132* in the AV-T background caused elevated capsule production, which increased colony opacity and altered the typical avirulent phenotype of translucent cells. These findings distinguish 1132 as a global regulatory gene and advance our understanding of *A. baumannii*'s opacity-virulence switch.

Importance

The increase of antibiotic-resistant infections and the implications for its detrimental impact on healthcare and the economy have been well documented. Consequently, the need to unravel the virulence and resistance-associated genetic pathways of pathogens and pursue alternative avenues for treatment has never been more pressing. *Acinetobacter baumannii* is a nosocomial pathogen that is both highly resistant to antibiotics and extremely persistent in hospital settings. Our group's previous discovery that only the opaque variant can establish an infection has opened doors to new methods of prevention and treatment but necessitates clarification of the genetic regulation of the switching mechanism between the two variants. This report details a rigorous characterization of 1132, a key global regulator that impacts this phenotypic switch as well as other known virulence factors including capsule expression, quorum sensing, and motility. These findings constitute crucial information for the continued elucidation of virulence in *A. baumannii*.

Introduction

The Gram-negative pathogen *Acinetobacter baumannii* poses a major threat to hospitalized patients. Cases of ventilator-associated pneumonia are among the most common *A. baumannii* infections, but incidences of skin and soft tissue infections, urinary tract infections, and sepsis are on the rise (Davis et al., 2005;Dijkshoorn et al., 2007;Peleg et al., 2008;Peleg and Hooper, 2010;Doyle et al., 2011;Weiner et al., 2016;Wong et al., 2017). Of primary concern is *A. baumannii*'s increasing resistance to treatment with antimicrobials, with 63% of infections caused by multidrug-resistant (MDR) strains (Clark et al., 2016;Lee et al., 2017;Centers for Disease Control and Prevention, 2019). In particular, *A. baumannii*'s rapidly growing resistance to carbapenem antibiotics and its ability to widely disseminate resistance via mobile genetic elements prompted the World Health Organization to name this organism as a critical priority for the research and development of new antimicrobial drugs in 2017 (World Health Organization, 2017). Further, its extreme resistance to desiccation and disinfectants makes it notoriously difficult to eradicate in hospital environments (Jawad et al., 1998;Chapartegui-Gonzalez et al., 2018;Rocha et al., 2018;Bravo et al., 2019;D'Souza et al., 2019). In the face of such problematic phenotypes, an understanding of pathogenesis and virulence in this species is imperative. To meet this need, experiments conducted by our group have been carried out in the strain AB5075 (GenBank Accession Number CP008706.1), a highly virulent MDR clinical isolate that is genetically tractable (Jacobs et al., 2014;Gallagher et al., 2015).

Our group has sought to better understand the genetic mechanisms regulating *A. baumannii* virulence in light of our findings that clinical isolates of this species exhibit phenotypic heterogeneity resulting in virulent and avirulent colony opacity variants (Tipton et al., 2015;Chin et al., 2018). The virulent variant has a golden, opaque colony morphotype under oblique lighting

and is termed VIR-O, while the avirulent variant is translucent and is termed AV-T (Fig. 1A). In addition to differences in virulence, the VIR-O variant displays higher levels of capsule production, quorum sensing signal secretion, and surface-associated motility, while AV-T demonstrates greater production of biofilm and is able to utilize multiple carbon sources. Both variants switch back and forth at high frequency, with rates of approximately 4-13% conversion at 24 hours of colony growth and 20-40% at 48 hours (Chin et al., 2018). The two types have distinctly different genomic expression profiles as revealed by RNA sequencing, and a variety of gene products—including transcriptional regulators, a two-component system (OmpR/EnvZ), an efflux pump (ArpB), and a putative sRNA located upstream of a plasmid-encoded antibiotic resistance locus—appear to contribute to interconversion between VIR-O and AV-T (Tipton and Rather, 2016;Tipton et al., 2017;Chin et al., 2018;Anderson et al., 2020).

One such regulator, *ABUW_1645* (*1645*), is a TetR-type transcriptional regulator (TTTR) whose rate of expression is 150-fold higher in the AV-T state and whose overexpression in the VIR-O background drives conversion to the AV-T state (Chin et al., 2018). Although *1645* is crucial to the maintenance of the AV-T variant and is a key regulator of the VIR-O to AV-T switch, it does not appear to act in the same pathways as other previously discovered regulators of the switch such as *arpB* or *ompR* (Tipton and Rather, 2016;Tipton et al., 2017), a fact which emphasizes the complexity of the switching mechanism and the probable functional redundancy of many of the regulatory elements.

We continued to investigate additional genes to better understand the VIR-O and AV-T variants and the processes that regulate their interconversion. This led to the characterization of *ABUW_1132* (*1132*), a LysR-type transcriptional regulator (LTTR) that influences the VIR-O to AV-T switch. LTTRs are highly abundant in Proteobacteria (Reen et al., 2015) and are the most

common type of transcriptional regulator in AB5075 at 24% (59/243) (Casella et al., 2017). They often function as global regulators and act in conjunction with a ligand molecule to repress and/or activate target genes (Maddocks and Oyston, 2008). Prototypical LTTRs are self-repressing and regulate gene(s) divergently transcribed from their own coding sequence, though these need not be the case.

A recent publication by our group detailed the identification of *1132* and its role in a *relA* mutant (*ΔrelA*), which exhibits increased quorum sensing signal secretion and hyper-motility (Perez-Varela et al., 2020). Quorum sensing in *A. baumannii* is carried out by a LuxI-LuxR type system composed of *abaI*, the autoinducer synthase, and *abaR*, the signal receptor and transcriptional regulator (Niu et al., 2008). We reported that the quorum sensing and motility phenotypes of *ΔrelA* were largely enacted through *1132*, which is overexpressed 14-fold in the absence of *relA* (Perez-Varela et al., 2020). Specifically, *1132* overexpression results in upregulation of the autoinducer synthase *abaI*, resulting in a large increase to secretion of the quorum sensing signal 3-OH-C_{12}-homoserine lactone. Expression of the *abaR* transcriptional regulator is also increased, resulting in strong upregulation of one of AbaR's targets: the *ABUW_3766-ABUW_3773* operon. This operon promotes production of the lipopeptide acinetin-505, which acts as a surfactant and gives rise to a hyper-motile phenotype.

This study builds on these findings and details multiple phenotypic changes resulting from the deletion of *1132;* including quorum sensing signal secretion, surface-associated motility, the virulence-opacity switch, capsule expression, and virulence in a mouse pneumonia model of infection.

Results

ABUW 1132 is a global regulator

To identify genes and pathways regulated by *1132*, we carried out genome-wide transcriptional profiling by RNA sequencing of VIR-O Δ*1132* vs. wild-type VIR-O, which revealed a total of 74 differentially regulated genes in VIR-O Δ*1132* (greater than 2-fold change, p value less than 0.05) (Supp. Table 1). These results showed that 1132 impacts transcription of a variety of genes involved in regulation, metabolism, protein synthesis, and possibly the cell stress response. Genes that encode ribosomal proteins, RNA polymerase, translation initiation factors, and both transcriptional and translational elongation factors are among genes that are upregulated in VIR-O Δ*1132*. On the other hand, several genes that are downregulated in the absence of *1132* encode a variety of enzymes involved in oxidative stress protection including catalases, peroxidases and others that interact with glutathione.

Deletion of *1132* Impacts Quorum Sensing Signal Secretion and Motility

Deletion of *1132* results in loss of secretion of the quorum sensing signal 3-OH-C_{12}-HSL (AHL) (Fig. 1B). This is based on the inability to activate an *Agrobacterium tumefaciens traG*::*lacZ* fusion when grown on a soft agar lawn containing this biosensor strain and X-Gal (Niu et al., 2008;Paulk Tierney and Rather, 2019). We utilized a Tn7 transposon system (Ducas-Mowchun et al., 2019a) to provide single-copy complementation of *1132* (VIR-O Δ*1132*-Tn7/*1132*), which restored AHL secretion. This restoration is lost again if the Tn7 copy of *1132* is disrupted (Fig. 1B). The loss of AHL secretion also occurs in the AV-T Δ*1132* mutant (Fig. 1C).

Considering our previously published findings that *1132* overexpression activates the *abaI-abaR* system (Perez-Varela et al., 2020), we hypothesized that loss of AHL secretion was due to

downregulation of *abaI* when *1132* is deleted. Surprisingly, our RNA sequencing analysis indicated wild-type levels of *abaI* expression in VIR-O Δ*1132*, which we confirmed by qRT-PCR (Supp. Fig. 1). This result suggested that the mutant cells synthesize AHL, but do not secrete it. To investigate this possibility, we conducted an assay utilizing the *A. tumefaciens* biosensor in which 10% SDS was added to a well at the center of the plate (Supp. Fig. 2). Cultures of wild-type VIR-O, an *abaI* mutant (VIR-O *abaI*::T26), and VIR-O Δ*1132* were then added to the plate in lines going toward the SDS-containing well. As expected, we saw that the wild-type VIR-O cells uniformly activate the biosensor. However, the VIR-O Δ*1132* cells show activation of the biosensor only at the point where the VIR-O Δ*1132* cells have been lysed by the SDS in the presence of non-lysed biosensor cells, which confirmed our hypothesis that AHL is synthesized but cannot exit the cell. Since there is no activation by an *abaI* mutant near the SDS, the activating signal in the *1132* mutant is 3-OH-C_{12}-HSL and not a released metabolite. These results indicate a more complicated role for *1132* in quorum sensing than simple regulation of *abaI*, which is further considered in the Discussion section.

We previously reported that overexpression of *1132* increases surface-associated motility 3.8-fold and that this effect requires both *abaI* and the *ABUW_3766-ABUW_3773* operon (Perez-Varela et al., 2020). As expected, both VIR-O Δ*1132* and AV-T Δ*1132* demonstrate a significant decrease in motility compared to their wild-type counterparts, both which are complemented by the single-copy chromosomal insertion of *1132* (Fig. 1D, only VIR-O results shown).

The *1132* deletion behaves in a manner opposite to *1132* overexpression with respect to motility, but the mechanism for this is unclear. As previously mentioned, *abaI* mRNA levels are unaffected by *1132* deletion, and although the RNA sequencing data shows a 1.5-fold

downregulation of *abaR*, there are no transcriptional differences in the *ABUW_3766-ABUW_3773* operon (Supp. Table 1). We also considered the possibility that AHL itself acts as a surfactant to some extent and that the loss of AHL secretion could reduce motility. To test this, we constructed a double mutant of *1132* and *abaR*—to control for quorum sensing-directed motility—and measured motility on 0.3% Eiken agar plates containing 1 mM synthetic 3-OH-C_{12}-HSL. However, motility was similar between the solvent control (38.75 mm $\pm$ 0.83) and the plate with AHL added (41.0 $\pm$ 1.73) p = 0.11.

Role of *1132* in Regulation of the VIR-O to AV-T Switch

VIR-O Δ*1132* exhibited lower levels of colony sectoring than observed for the wild-type VIR-O on 0.5X LB agar (Fig. 2A). This lack of sectoring indicated a decreased rate of switching to the AV-T variant, and we subsequently quantified a 16.4-fold decrease in the switching frequency (Fig. 2B). To confirm these effects were due to *1132* deletion, we provided single-copy complementation of *1132* using the Tn7 transposon system. This strain exhibited the wild-type phenotype of colony sectoring and restored VIR-O to AV-T switching to wild-type levels (Fig. 2B).

Deletion of *1132* in the AV-T Background Increases Capsule

We further noted that AV-T Δ*1132* colonies are more opaque than wild-type AV-T colonies, although AV-T Δ*1132* is still translucent compared to VIR-O Δ*1132* colonies (Fig. 3A, 3B). Single-copy chromosomal complementation of the AV-T Δ*1132* mutant restored wild-type levels of translucence (Fig. 3A). We first hypothesized that the increased opacity indicated hyper-switching from AV-T to VIR-O within the colony; however, the rate of switching was the same as

the wild-type AV-T (Supp. Fig. 3). We then considered that the AV-T Δ*1132* mutant's increased opacity may be due to increased levels of capsule.

Previous work revealed that wild-type VIR-O cells exhibit a 2-fold increase in capsule compared with the wild-type AV-T (Chin et al., 2018). We utilized a Percoll density gradient, a method that was recently described as a method to separate *A. baumannii* strains by capsule level (Kon et al., 2020), to compare capsular polysaccharide levels in AV-T Δ*1132* to wild-type VIR-O and AV-T cells. As seen in Fig. 3C, the gradient is able to distinguish between capsule levels of the wild-type VIR-O and AV-T variants, with the AV-T cells migrating significantly further than the VIR-O cells. Intriguingly, AV-T Δ*1132* cells exhibited a high degree of heterogeneity and occupied a space in the gradient layer that was intermediate to that of the wild-type VIR-O and AV-T. We interpret this result as indication that deletion of *1132* causes a dysregulation and increase of capsule in the AV-T state, which imparts the more opaque appearance of AV-T Δ*1132*.

To confirm the effect of *1132* deletion on capsule, we next carried out TEM imaging of cell samples of wild-type VIR-O, wild-type AV-T, and AV-T Δ*1132* stained with Ruthenium red (Fig. 3D). We used ImageJ to measure capsule width in 100 cells per strain with 3 measurements taken per cell, which revealed average capsule widths of 0.142 μM ± 0.010, 0.072 μM ± 0.008, and 0.092 μM ± 0.008 in VIR-O, AV-T, and AV-T Δ*1132*, respectively (Fig. 3E). The resulting ratio of these values is 1.96:1.00:1.28, which demonstrates the 2-fold difference in capsule previously seen in the VIR-O vs. AV-T (Chin et al., 2018) and confirms a 28% increase in capsule in the AV-T background when *1132* is deleted. The difference between the wild-type AV-T and AV-T Δ*1132* is highly significant at $p < 0.0001$ as determined by a Student's two-tailed *t* test.

In light of these results, we considered that, in the AV-T state, *1132* may regulate the K locus genes that encode the proteins largely responsible for the biosynthesis and export of capsular

polysaccharide (CPS). We assessed representative genes from the K locus—*manB, galE, ABUW_3818, ABUW_3820, ABUW_3821, ABUW_3830, wza, wzb,* and *wzc*—by qRT-PCR across three sets of samples (Supp. Fig. 4). These results indicated that *1132* did not transcriptionally regulate the K locus genes.

The Δ*1132* mutation increases virulence in the AV-T background

Capsule is a known virulence factor in *A. baumannii*, and presumably contributes to virulent phenotype of the VIR-O variant relative to AV-T (Russo et al., 2010;Chin et al., 2018;Singh et al., 2018;Tipton et al., 2018;Talyansky et al., 2021). The intermediate capsular levels of AV-T Δ*1132* therefore suggested that this deletion may increase virulence. Before initiating virulence studies, we first tested the growth rates of the AV-T and AV-T Δ*1132* strains and found no significant differences under laboratory conditions (Supp. Fig. 5A. Using the *Galleria mellonella* (waxworm) model of infection, a modest, but statistically significant increase in AV-T Δ*1132* virulence was observed (Fig. 4A). Waxworms injected with the wild-type AV-T control showed a 23.3% survival rate after five days, while only 10% of those injected with AV-T Δ*1132* survived. Complementation of AV-T Δ*1132* with the single-copy chromosomal insertion of *1132* (AV-T Δ*1132*/Tn7-*1132*) reversed the increase in virulence, bringing the rate of survival back up to 30%.

We next examined the virulence of AV-T Δ*1132* in a mouse pneumonia model of infection. In three experiments, mice were intranasally inoculated with 1 x 10^8 CFU/mL of VIR-O (n=10), AV-T (n=17), or AV-T Δ*1132* (n=17). At 24 hours post-inoculation, lungs were harvested, and the CFU/g for each tissue was calculated where a significant increase in CFU/g in AV-T Δ*1132* was observed compared to wild-type AV-T in the lungs (Fig. 4B). Both strains exhibited a similar number of VIR-O variants recovered from the lungs (approximately 0.1%). The highly virulent

VIR-O variant was unaffected by the Δ*1132* mutation in both a *Galleria mellonella* waxworm model and in a mouse pneumonia model (Supp. Fig. 5B, 5C), and both strains exhibited similar growth rates in-vitro (Supp. Fig. 5A).

Discussion

This study confirms 1132 as a global transcriptional regulator that impacts multiple pathways: surface-associated motility, AHL secretion, regulation of the opacity-virulence switch, and capsule expression. Most importantly, our work demonstrates that an *1132* deletion, and possibly its natural downregulation, has the potential to increase virulence of the typically avirulent translucent colony variant in the clinical isolate AB5075. The *1132* gene was highly conserved in all completed *A. baumannii* genome sequences (n = 330), where at least 98.7% nucleotide homology was observed. The gene was also conserved in *A. nosocomialis* (91.7% or greater nucleotide identity), *A. seifertii* (89.8% or greater identity) and *A. pittii* (83.7% or greater identity). Given the high conservation of *1132* among *A. baumannii* strains, it is likely that the *1132*-associated phenotypes we have reported here and in a previous publication (Perez-Varela et al., 2020) will also be conserved in other strains.

Some questions remain regarding the mechanisms through which 1132 acts in the described phenotypes. As previously mentioned, in our earlier publication we determined that overexpression of *1132* causes large increases in AHL secretion and surface-associated motility. This occurs through activation of the *abaI-abaR* system and follows a well-defined downstream pathway ending with overproduction of the surfactant acinetin-505 (Perez-Varela et al., 2020) Perplexingly, although the deletion of *1132* results in phenotypes opposite to that of *1132* overexpression—loss of both AHL secretion and motility—our experiments show that neither of these phenotypes are due to transcriptional downregulation of the *abaI-abaR* system or the *ABUW_3766-ABUW_3773* operon. A post-transcriptional effect of *1132* on *abaI* also seems unlikely, as VIR-O Δ*1132* cells lysed in the presence of the AHL-detecting biosensor are able to activate the *traG*::*lacZ* fusion, indicating a functional AbaI protein (Supp. Fig 2). It is possible that

the length of the *N*-acyl chain of the AHL molecule is altered due to the global changes that occur when *1132* is deleted. Both shortened and elongated chains could affect the hydrophobicity of the AHL molecule and therefore have the potential to disrupt diffusion or export of the autoinducer across the membrane. Due to the trapping of signal within the cell, it is possible that the quorum sensing response is altered, possibly being activated earlier in cell density, or being constitutive. With respect to capsule, the effect of 1132 on capsule thickness did not involve transcriptional changes in representative genes within the capsule locus. Therefore, the *1132* mutation may alter biosynthetic pathways that impact precursors for capsule synthesis in a manner that increases their abundance and results in enhanced capsule thickness.

This work revealed that *1132* positively regulated the VIR-O to AV-T switch, and experiments to address the mechanism for this increase are ongoing. It is possible that one or more of several regulatory genes revealed by the RNA sequencing as differentially regulated by 1132 is involved. However, it is intriguing that other known regulators of the switch, including the OmpR/EnvZ two-component system and the ArpB efflux pump, were not regulated by 1132. A possibility is that the *1132* deletion creates a cellular metabolome that withholds ligands or other molecules required by other known regulators of the switch, such as the TetR regulator *ABUW_1645* (Chin et al., 2018). It is important to note that the lack of AHL secretion is not expected to impact the switch, as deletion of *abaI* does not cause alteration of switching frequency (Tipton et al., 2015).

Our work here has important implications for the characterizations of VIR-O cells as virulent and AV-T cells as avirulent. While the increase in virulence in the AV-T variant caused by *1132* deletion was modest, this finding demonstrates that stochastic downregulation of *1132*—potentially mediated by RelA's repression of *1132*—may allow an AV-T cell to be moderately

virulent in a mammalian host without necessitating a switch to the VIR-O state. We have previously hypothesized that AV-T cells possess an advantage in natural environments due to their versatility in utilization of carbon sources and their improved formation of biofilm (Chin et al., 2018). Combined, these observations suggest that AB5075, and possibly other *A. baumannii* strains, could survive in a natural environment while existing in a virulent state.

Materials and Methods

Bacterial strains and growth conditions

All experiments were conducted using the clinical isolate AB5075. For all experiments, cultures were started from frozen glycerol stocks containing at least 99.5% of the desired colony variant (VIR-O or AV-T). Cultures were grown in either broth or on solid media containing LB (10 g tryptone, 5 g yeast extract, and 5 g NaCl per liter) and 1.5% agar (Difco) ("1X" LB agar) or 0.8% agar ("0.5X" LB agar).

Methods to distinguish colony variants

Cultures were plated or streaked on 0.5X LB agar and viewed under a dissecting microscope, illuminated from underneath at an oblique angle. Colonies must be viewed at high colony density (at least 100 colonies per plate) to effectively distinguish VIR-O and AV-T colonies.

Detection of 3-OH-C_{12}-HSL

Plates containing the *Agrobacterium tumefaciens traG*::*lacZ* biosensor and X-Gal were prepared as described in Paulk Tierney and Rather, 2019. AB5075 cell cultures were grown in 2 mL LB to OD_{600} ~ 0.3, and 1 µL was spotted onto the soft agar lawn. Plates were incubated at 28°C overnight.

Quantification of VIR-O and AV-T switching

Dilutions were plated from frozen pure stocks of the strains to be assessed, and plates were incubated at 37°C for a set number of growth hours. High density plates were used to verify the

purity of the stock. Isolated colonies were extracted from the plate by cutting out a section of agar underlying the colony and then resuspended and dilutions plated. The percent variant was then determined for each set of resuspended colonies from each strain. All experiments were performed twice with three colonies each for a total of six colonies.

Electroporation

Cell cultures for competent cells were grown in 2 mL LB to OD_{600} ~ 0.5 (mid-log phase) at 37°C, shaking from frozen stocks. Cultures were pelleted and washed twice in sterile dH_2O, then resuspended to accommodate a volume of approximately 50 µL of cell per electroporation. Plasmid minipreps or ligation products mixed with cells were added to 2 mm cuvettes and electroporated at 2.5 kV. Cells were recovered in 1 mL LB at 37°C, shaking for one hour, then plated onto media containing selective antibiotics.

Construction of deletion mutations

In-frame deletion of *ABUW_1132* was generated using sucrose counterselection and a suicide vector containing the *sacB* marker (pEX18Tc) using methods previously described (Hoang et al., 1998). Briefly, PCR amplification (Phusion polymerase, Thermo-Fisher Scientific) was used to amplify the 2-kb regions upstream and downstream of the gene to be deleted, gel purified (UltraClean 15 DNA Purification Kit, MO BIO Laboratories), and ligated (Fast-Link DNA Ligation Kit, Epicentre Biotechnologies). The 4-kb ligation product was PCR amplified, gel purified, and ligated into the pEX18Tc vector MCS. The product vector was verified by sequencing and then transformed into competent *E. coli* Transformax EC100D cells (Epicentre Biotechnologies) by electroporation. The resulting suicide vector was confirmed by PCR and

transformed by electroporation into AB5075, grown to OD_{600} of 0.5 in 2-mL LB and washed twice in 10% glycerol. Transformants were plated on 1X LB agar plus Tetracycline (5-µg/mL) to yield single-crossover mutants. Counterselection was carried out at room temperature on 1X LB plates with 10% sucrose and no NaCl, and colonies were screened by PCR for the deletion. Primer sequences are recorded in Supp. Table 2.

To construct the Δ*1132*, *abaR*::T26 double mutant, genomic DNA was purified from an *abaR*::T26 mutant obtained from the University of Washington AB5075 transposon mutant library. Genomic DNA was then electroporated into VIR-O Δ*1132*. Transformants were selected on 1X LB plus Tetracycline (5-µg/mL) and confirmed by PCR.

Construction of single-copy complementation in deletion mutants

We utilized a Tn7-based single-copy insertion element system (Ducas-Mowchun et al., 2019a;Ducas-Mowchun et al., 2019b) to reintroduce *1132* into the VIR-O Δ*1132* and AV-T Δ*1132* deletion mutants. We opted to use a segment of *1132* that includes a large portion of the up and downstream regions (GenBank Accession NZ_CP008706.1:1152309-1156236). This is the portion of the genome contained within the original *1132*-containing fragment isolated from a high-copy AB5075 chromosomal library during the screen that led to our first discovery of *1132* (Perez-Varela et al., 2020), and previous experiments showed that this fragment allows for optimal expression of *1132*. A modified version of this construct containing a T26 transposon (tetracycline) in *1132* had also been made to confirm loss of the phenotypes presumably caused by *1132* overexpression. This was made by digestion of the plasmid with PmlI, which cuts once near the beginning of the *1132* ORF, and re-ligation with a PCR-amplified T26 transposon. The original *1132*-containing fragment and the modified version with *1132*::T26 were excised from these

plasmids by digestion with XbaI, which flanks the site into which the library was cloned, and gel purified to be used in construction of the suicide vector.

The pUC18T-mini-Tn7T-Apr-LAC construct was digested with SpeI and ligated with the *1132*- or *1132*::T26-containing fragment (Fast-Link DNA Ligation Kit, Epicentre Biotechnologies). The ligation product was transformed into competent *E. coli* Transformax EC100D cells (Epicentre Biotechnologies) by electroporation. The resulting constructs—pUC18T-mini-Tn7T-Apr-LAC/*1132* and pUC18T-mini-Tn7T-Apr-LAC/*1132*::T26—were confirmed by PCR and sequencing then transformed into pure cultures of VIR-O Δ*1132* and AV-T Δ*1132* by electroporation along with the helper plasmid pTNS2. Transformant colonies were screened by PCR for insertion into the *att*Tn7 site and those containing the correct insertion were again verified by sequencing. Wild-type Tn7 and Δ*1132*-Tn7 control strains were also made in both VIR-O and AV-T backgrounds using the same methods with an empty pUC18T-mini-Tn7T-Apr-LAC construct. Primer sequences are recorded in Supp. Table 2.

RNA preparation and qRT-PCR analysis

Strains for qRT-PCR analysis in Supp. Fig. 1 were prepared for RNA isolation by growing them from pure frozen stocks to OD_{600} ~ 0.15 then plating 100 µL on a 1X LB plate. Plates were incubated at 37°C for 6 hours, then pooled with 3 mL ice cold LB. Resuspensions were normalized to within OD_{600} of 0.01, then 1 mL of the resuspension was pelleted, flash frozen in an ethanol-dry ice bath and stored at -80°C. The resuspension cultures were streaked on 0.5X LB to ensure sample purity.

Strains for qRT-PCR analysis in Supp. Fig. 4 were grown up to match the growth conditions of the cells prepared for electron microscopy (see below). Samples were grown from pure frozen

stocks in overnight cultures of 2 mL LB and were then shaken at 37°C to the same OD_{600} of 0.3. 20 µL of each culture was then plated as a line onto a 0.5X plate, allowed to incubate at 37°C for 4 hours, and then harvested off the plate. Scraped cells were resuspended to an OD_{600} of 0.6 in 2 mL LB. 1 mL of cells was pelleted, flash frozen in an ethanol-dry ice bath, then stored at -80°C. The resuspension cultures were streaked on 0.5X LB to ensure sample purity.

RNA was prepared using the Epicentre MasterPure RNA Purification kit according to the manufacturer's protocols. The resulting nucleic acid product was purified to remove DNA contamination using the Invitrogen TURBO DNA-*free* kit according to the manufacturer's instructions. Following quantification of RNA concentration using a NanoDrop ND-1000 spectrophotometer, cDNA was prepared from 1 µg of RNA using the High-Capacity cDNA Reverse Transcription Kit by Applied Biosystems and subsequently diluted 1:10 in nuclease-free water. qRT-PCR experiments were carried out on a Bio-Rad CFX Connect Real-Time PCR Detection System using iQ SYBR Green Supermix reverse transcriptase from Bio-Rad. RNA purity was confirmed by qRT-PCR through the inclusion of template controls made without reverse transcriptase. qRT-PCR data was analyzed by the delta-delta Ct method ($2^{-\Delta\Delta Ct}$) with comparison to *16S* as an internal control. This method was carried out for three biological replicates. Each biological replicate had three technical replicates for each primer set. Primer sequences are recorded in Supp. Table 2.

RNA sequencing and analysis

Three independent sets of RNA were prepared from each of AB5075 strains VIR-O and VIR-O Δ*1132*. Cultures were grown in 2 mL LB from pure frozen stocks to OD_{600} ~ 0.5 (shaking, 37°C) and were streaked on 0.5X LB to ensure purity of samples. 1 mL of cells was pelleted and flash

frozen in a dry ice bath before being stored at -80°C. RNA was prepared using the Epicentre MasterPure RNA Purification kit according to the manufacturer's protocols.

RNA quality control, sequencing, and analysis was carried out by the Yerkes Non-Human Primate Genomics Core at Emory University. RNA quantity and quality assessments were carried out using a Thermo Nanodrop2000 and Agilent 2100 Bioanalyzer, respectively. RNA sequencing was carried out using an Illumina HiSeq 3000, and reads were normalized and mapped using Cufflinks software. The data discussed in this publication have been deposited in NCBI's Gene Expression Omnibus and are accessible through GEO Series accession number GSE185730 (https://www.ncbi.nlm.nih.gov/geo/query/acc.cgi?acc=GSE185730).

Percoll density gradient

Method slightly modified from Kon et al 2020. Cell cultures of VIR-O, AV-T, and AV-T Δ*1132* were grown in 2 mL LB from pure frozen stocks to OD_{600} ~ 0.6 (shaking, 37°C). For each strain, 600 µL of cells was pelleted and washed in PBS 1X, then resuspended in 100 µL PBS 1X. Percoll solutions were prepared by first mixing 9 parts Percoll (Sigma Aldrich Cat. P4937) and 1 part 1.5 M NaCl, which was further diluted using 0.15 M NaCl to make 40% and 50% Percoll solutions. For each cell sample to be tested, 1 mL of 40% Percoll was added to a 12x75 mm glass tube (Fisherbrand 14958C), and 1 mL 50% Percoll was gently layered underneath using a 1cc syringe and a 1.5 in. 23G needle (BD 305194). 100 µL of cells were gently layered at the top of the gradient. Samples were spun at 3,000 xg for 30 minutes at room temperature and then visually assessed. This protocol was repeated 6 times.

Electron Microscopy

Ruthenium red-lysine fixation and cell staining and subsequent transmission electron microscopy were performed by the Robert P. Apkarian Integrated Electron Microscopy Core at Emory University using previously described techniques (Fassel et al., 1997;1998;Beaussart et al., 2014). Samples were provided to the EM Core as follows: cells grown from pure frozen stocks in overnight cultures were shaken at 37°C until OD ~ 0.30, and 20 µL of each culture was plated as a line onto the same 0.5X LB plate. Plates were then incubated at 37°C for 4 hours and stored overnight at 4°C before being transported to the EM Core.

Capsule widths in the electron micrographs were measured by ImageJ 1.53e (Rasband, W.S., ImageJ, U. S. National Institutes of Health, Bethesda, Maryland, USA, https://imagej.nih.gov/ij/, 1997-2018). Three measurements were taken for 100 cells of each strain at the same magnification, which were averaged and then converted to micrometers.

Galleria mellonella larvae (Waxworm) virulence assays

Waxworms were purchased from Speedy Worm (www.speedyworm.com). Cultures of AV-T, AV-T Δ*1132*, and AV-T Δ*1132*/Tn7-*1132* were grown in 2 mL LB from pure frozen stocks to OD_{600} ~ 0.5 (shaking, 37°C). 5 µL of a LB control, AV-T, AV-T Δ*1132*, or AV-T Δ*1132*/Tn7-*1132* was injected into the hemolymph of a larvae of mass 150-200 mg (n=30 per condition; approximately 1.2×10^6 CFU were administered per strain). Larvae were then housed in petri dishes in a humidified incubator at 37°C for 5 days. Each day, dead larvae were removed and surviving larvae counted.

Mouse virulence assays

Approximately 1×10^8 CFU were administered per mouse for infections to quantify the bacterial load. For mouse infections, overnight standing bacterial cultures at room temperature were sub-cultured in LB broth and grown at 37°C with shaking to an OD600 ~0.15, washed and re-suspended in PBS. Each mouse was inoculated intranasally with 50 µL of bacteria. Mice were anesthetized with isoflurane immediately prior to intranasal inoculation. At 24 hours, the mice were sacrificed and the lungs were harvested, homogenized, and ten-fold serial dilutions plated for CFU on 0.5X LB plates. The mouse strain used was C57BL/6J (females at 8-10 weeks of age) from Jackson Laboratories (JAX stock #000664). Experiments were carried out under the Institutional Animal Care and Use Committee guidelines.

Statistics

Statistics were performed using GraphPad Prism 9.2.0 software for Windows (GraphPad Software, San Diego, California USA, www.graphpad.com). The following statistical tests were utilized: (1) Mann-Whitney test for the mouse experiments (two-tailed), two-sample switching assays (two-tailed), motility assays (two-tailed), and qRT-PCR experiments (two-tailed or multiple, as indicated); (2) Log-Rank (Mantel-Cox) test for the *Galleria mellonella* experiments; (3) Welch's ANOVA analysis for three-sample switching assays; and (4) Student's two-tailed *t* test for capsule width measurements from the TEM micrographs. The Mann-Whitney test was utilized instead of a Student's *t* test to allow for the possibility or reality of a non-Gaussian distribution. Welch's ANOVA was chosen over standard ANOVA to allow for unequal variance between samples.

Acknowledgments

We thank Dr. M. Pérez-Varela for critical reading of this manuscript and Drs. K.A. Tipton, S.E. Anderson, J.M. Colquhoun, and M. Pérez-Varela for their valuable input. We are grateful to Dr. Ayush Kumar at the University of Manitoba for providing pUC18T-mini-Tn7T-Apr-LAC. This work was supported in part by the Robert P. Apkarian Integrated Electron Microscopy Core at Emory University, and we especially thank Jeannette Taylor and Dr. Ricardo C. Guerrero for conducting the electron microscopy.

Research in the PNR Laboratory is supported by T32 AI106699 to ARPT and NIH R01 AI72219 and R21 AI115183 and Department of Veterans Affairs awards I01 BX001725 and IK6BX004470 to PNR. Research in the DSW Laboratory is supported by a Department of Veteran's Affairs award BX002788. DSW is also supported by a Burroughs Wellcome Fund Investigators in the Pathogenesis of Infectious Disease award. The content expressed herein is solely the responsibility of the authors and does not necessarily represent the official views of the NIH or the Department of Veterans Affairs.

The authors declare that the research was conducted in the absence of any commercial or financial relationships that could be construed as a potential conflict of interest.

References

1. Anderson, S.E., Chin, C.Y., Weiss, D.S., and Rather, P.N. (2020). Copy Number of an Integron-Encoded Antibiotic Resistance Locus Regulates a Virulence and Opacity Switch in Acinetobacter baumannii AB5075. *mBio* 11.

2. Beaussart, A., Péchoux, C., Trieu-Cuot, P., Hols, P., Mistou, M.Y., and Dufrêne, Y.F. (2014). Molecular mapping of the cell wall polysaccharides of the human pathogen Streptococcus agalactiae. *Nanoscale* 6**,** 14820-14827.

3. Bravo, Z., Orruno, M., Navascues, T., Ogayar, E., Ramos-Vivas, J., Kaberdin, V.R., and Arana, I. (2019). Analysis of Acinetobacter baumannii survival in liquid media and on solid matrices as well as effect of disinfectants. *J Hosp Infect* 103**,** e42-e52.

4. Casella, L.G., Weiss, A., Pérez-Rueda, E., Antonio Ibarra, J., and Shaw, L.N. (2017). Towards the complete proteinaceous regulome of Acinetobacter baumannii. *Microb Genom* 3**,** mgen000107.

5. Centers for Disease Control and Prevention (2019). *Antibiotic Resistance Threats in the United States, 2019. Atlanta, GA* [Online]. Available: https://www.cdc.gov/drugresistance/pdf/threats-report/2019-ar-threats-report-508.pdf [Accessed August 2 2021].

6. Chapartegui-Gonzalez, I., Lazaro-Diez, M., Bravo, Z., Navas, J., Icardo, J.M., and Ramos-Vivas, J. (2018). Acinetobacter baumannii maintains its virulence after long-time starvation. *PLoS One* 13**,** e0201961.

7. Chin, C.Y., Tipton, K.A., Farokhyfar, M., Burd, E.M., Weiss, D.S., and Rather, P.N. (2018). A high-frequency phenotypic switch links bacterial virulence and environmental survival in Acinetobacter baumannii. *Nat Microbiol* 3**,** 563-569.

8. Clark, N.M., Zhanel, G.G., and Lynch, J.P., 3rd (2016). Emergence of antimicrobial resistance among Acinetobacter species: a global threat. *Curr Opin Crit Care* 22**,** 491-499.

9. D'souza, A.W., Potter, R.F., Wallace, M., Shupe, A., Patel, S., Sun, X., Gul, D., Kwon, J.H., Andleeb, S., Burnham, C.D., and Dantas, G. (2019). Spatiotemporal dynamics of multidrug resistant bacteria on intensive care unit surfaces. *Nat Commun* 10**,** 4569.

10. Davis, K.A., Moran, K.A., Mcallister, C.K., and Gray, P.J. (2005). Multidrug-resistant Acinetobacter extremity infections in soldiers. *Emerg Infect Dis* 11**,** 1218-1224.

11. Dijkshoorn, L., Nemec, A., and Seifert, H. (2007). An increasing threat in hospitals: multidrug-resistant Acinetobacter baumannii. *Nat Rev Microbiol* 5**,** 939-951.

12. Doyle, J.S., Buising, K.L., Thursky, K.A., Worth, L.J., and Richards, M.J. (2011). Epidemiology of infections acquired in intensive care units. *Semin Respir Crit Care Med* 32**,** 115-138.

13. Ducas-Mowchun, K., De Silva, P.M., Crisostomo, L., Fernando, D.M., Chao, T.C., Pelka, P., Schweizer, H.P., and Kumar, A. (2019a). Next Generation of Tn7-Based Single-Copy Insertion Elements for Use in Multi- and Pan-Drug-Resistant Strains of Acinetobacter baumannii. *Appl Environ Microbiol* 85.

14. Ducas-Mowchun, K., De Silva, P.M., Patidar, R., Schweizer, H.P., and Kumar, A. (2019b). Tn7-Based Single-Copy Insertion Vectors for Acinetobacter baumannii. *Methods Mol Biol* 1946**,** 135-150.

15. Fassel, T.A., Mozdziak, P.E., Sanger, J.R., and Edmiston, C.E. (1997). Paraformaldehyde effect on ruthenium red and lysine preservation and staining of the staphylococcal glycocalyx. *Microsc Res Tech* 36**,** 422-427.
16. Fassel, T.A., Mozdziak, P.E., Sanger, J.R., and Edmiston, C.E. (1998). Superior preservation of the staphylococcal glycocalyx with aldehyde-ruthenium red and select lysine salts using extended fixation times. *Microsc Res Tech* 41**,** 291-297.
17. Gallagher, L.A., Ramage, E., Weiss, E.J., Radey, M., Hayden, H.S., Held, K.G., Huse, H.K., Zurawski, D.V., Brittnacher, M.J., and Manoil, C. (2015). Resources for Genetic and Genomic Analysis of Emerging Pathogen Acinetobacter baumannii. *J Bacteriol* 197**,** 2027-2035.
18. Hoang, T.T., Karkhoff-Schweizer, R.R., Kutchma, A.J., and Schweizer, H.P. (1998). A broad-host-range Flp-FRT recombination system for site-specific excision of chromosomally-located DNA sequences: application for isolation of unmarked Pseudomonas aeruginosa mutants. *Gene* 212**,** 77-86.
19. Jacobs, A.C., Thompson, M.G., Black, C.C., Kessler, J.L., Clark, L.P., Mcqueary, C.N., Gancz, H.Y., Corey, B.W., Moon, J.K., Si, Y., Owen, M.T., Hallock, J.D., Kwak, Y.I., Summers, A., Li, C.Z., Rasko, D.A., Penwell, W.F., Honnold, C.L., Wise, M.C., Waterman, P.E., Lesho, E.P., Stewart, R.L., Actis, L.A., Palys, T.J., Craft, D.W., and Zurawski, D.V. (2014). AB5075, a Highly Virulent Isolate of Acinetobacter baumannii, as a Model Strain for the Evaluation of Pathogenesis and Antimicrobial Treatments. *mBio* 5**,** e01076-01014.
20. Jawad, A., Seifert, H., Snelling, A.M., Heritage, J., and Hawkey, P.M. (1998). Survival of Acinetobacter baumannii on dry surfaces: comparison of outbreak and sporadic isolates. *J Clin Microbiol* 36**,** 1938-1941.

21. Kon, H., Schwartz, D., Temkin, E., Carmeli, Y., and Lellouche, J. (2020). Rapid identification of capsulated Acinetobacter baumannii using a density-dependent gradient test. *BMC Microbiol* 20**,** 285.
22. Lee, C.R., Lee, J.H., Park, M., Park, K.S., Bae, I.K., Kim, Y.B., Cha, C.J., Jeong, B.C., and Lee, S.H. (2017). Biology of Acinetobacter baumannii: Pathogenesis, Antibiotic Resistance Mechanisms, and Prospective Treatment Options. *Front Cell Infect Microbiol* 7**,** 55.
23. Maddocks, S.E., and Oyston, P.C.F. (2008). Structure and function of the LysR-type transcriptional regulator (LTTR) family proteins. *Microbiology* 154**,** 3609-3623.
24. Niu, C., Clemmer, K.M., Bonomo, R.A., and Rather, P.N. (2008). Isolation and characterization of an autoinducer synthase from Acinetobacter baumannii. *J Bacteriol* 190**,** 3386-3392.
25. Paulk Tierney, A.R., and Rather, P.N. (2019). Methods for Detecting N-Acyl Homoserine Lactone Production in Acinetobacter baumannii. *Methods Mol Biol* 1946**,** 253-258.
26. Peleg, A.Y., and Hooper, D.C. (2010). Hospital-acquired infections due to gram-negative bacteria. *N Engl J Med* 362**,** 1804-1813.
27. Peleg, A.Y., Seifert, H., and Paterson, D.L. (2008). Acinetobacter baumannii: emergence of a successful pathogen. *Clin Microbiol Rev* 21**,** 538-582.
28. Perez-Varela, M., Tierney, A.R.P., Kim, J., Vazquez-Torres, A., Rather, P.N. (2020). Characterization of RelA in *Acinetobacter baumannii*. *Journal of Bacteriology*.
29. Reen, F.J., Romano, S., Dobson, A.D., and O'gara, F. (2015). The Sound of Silence: Activating Silent Biosynthetic Gene Clusters in Marine Microorganisms. *Mar Drugs* 13**,** 4754-4783.

30. Rocha, I.V., Xavier, D.E., Almeida, K.R.H., Oliveira, S.R., and Leal, N.C. (2018). Multidrug-resistant Acinetobacter baumannii clones persist on hospital inanimate surfaces. *Braz J Infect Dis* 22**,** 438-441.
31. Russo, T.A., Luke, N.R., Beanan, J.M., Olson, R., Sauberan, S.L., Macdonald, U., Schultz, L.W., Umland, T.C., and Campagnari, A.A. (2010). The K1 capsular polysaccharide of Acinetobacter baumannii strain 307-0294 is a major virulence factor. *Infect Immun* 78**,** 3993-4000.
32. Singh, J.K., Adams, F.G., and Brown, M.H. (2018). Diversity and Function of Capsular Polysaccharide in Acinetobacter baumannii. *Front Microbiol* 9**,** 3301.
33. Talyansky, Y., Nielsen, T.B., Yan, J., Carlino-Macdonald, U., Di Venanzio, G., Chakravorty, S., Ulhaq, A., Feldman, M.F., Russo, T.A., Vinogradov, E., Luna, B., Wright, M.S., Adams, M.D., and Spellberg, B. (2021). Capsule carbohydrate structure determines virulence in Acinetobacter baumannii. *PLoS Pathog* 17**,** e1009291.
34. Tipton, K.A., Chin, C.Y., Farokhyfar, M., Weiss, D.S., and Rather, P.N. (2018). Role of Capsule in Resistance to Disinfectants, Host Antimicrobials, and Desiccation in Acinetobacter baumannii. *Antimicrob Agents Chemother* 62.
35. Tipton, K.A., Dimitrova, D., and Rather, P.N. (2015). Phase-Variable Control of Multiple Phenotypes in Acinetobacter baumannii Strain AB5075. *J Bacteriol* 197**,** 2593-2599.
36. Tipton, K.A., Farokhyfar, M., and Rather, P.N. (2017). Multiple roles for a novel RND-type efflux system in Acinetobacter baumannii AB5075. *Microbiologyopen* 6.
37. Tipton, K.A., and Rather, P.N. (2016). An ompR/envZ Two-Component System Ortholog Regulates Phase Variation, Osmotic Tolerance, Motility, and Virulence in Acinetobacter baumannii strain AB5075. *J Bacteriol*.

38. Weiner, L.M., Webb, A.K., Limbago, B., Dudeck, M.A., Patel, J., Kallen, A.J., Edwards, J.R., and Sievert, D.M. (2016). Antimicrobial-Resistant Pathogens Associated With Healthcare-Associated Infections: Summary of Data Reported to the National Healthcare Safety Network at the Centers for Disease Control and Prevention, 2011-2014. *Infect Control Hosp Epidemiol* 37**,** 1288-1301.

39. Wong, D., Nielsen, T.B., Bonomo, R.A., Pantapalangkoor, P., Luna, B., and Spellberg, B. (2017). Clinical and Pathophysiological Overview of Acinetobacter Infections: a Century of Challenges. *Clin Microbiol Rev* 30**,** 409-447.

40. World Health Organization (2017). *Global Priority List of Antibiotic-Resistant Bacteria to Guide Research, Discovery, and Development of New Antibiotics* [Online]. Available: https://www.who.int/medicines/publications/WHO-PPL-Short_Summary_25Feb-ET_NM_WHO.pdf [Accessed August 2 2021].

Figure Legends

Figure 1: (A) AB5075 Wild-type opaque (VIR-O) and translucent (AV-T) colonies, viewed under a dissecting microscope with oblique lighting from underneath. **(B)** Qualitative assay of AHL secretion in which cultures of the wild-type (VIR-O), the VIR-O Δ*1132* mutant, the complemented mutant (VIR-O Δ*1132*/Tn7-*1132*), and a version of the complemented mutant disrupted by transposon insertion (VIR-O Δ*1132*/Tn7-*1132*::T26) were spotted onto a soft agar lawn containing X-Gal and an *Agrobacterium tumefaciens traG*::*lacZ* biosensor that reacts to the presence of exogenous AHL by cleaving X-Gal, forming a blue halo. (C) Qualitative assay of AHL secretion in the wild-type (AV-T), the AV-T Δ*1132* mutant, the complemented mutant (AV-T Δ*1132*/Tn7-*1132*), and a version of the complemented mutant disrupted by transposon insertion (AV-T Δ*1132*/Tn7-*1132*::T26). Signal secretion was analyzed as in panel B, except the amount of X-Gal was increased 2-fold. **(D)** Surface-associated motility of wild-type (VIR-O), the VIR-O Δ*1132* mutant, and the complemented mutant (VIR-O Δ*1132*/Tn7-*1132*) measured on 0.3% Eiken Agar plates. A Welch's ANOVA (****$p < 0.00005$) was carried out to assess **(B)**; error bars indicate standard deviation of the mean.

Figure 2: The Reduced Switching Phenotypes in VIR-O Δ*1132*. (A) Micrograph showing the loss of sectoring in VIR-O Δ*1132* colonies compared to wild-type VIR-O colonies at 24 hours of growth. **(B)** Quantification of switching frequencies demonstrating restoration of normal switching of VIR-O Δ*1132* through single copy complementation (VIR-O Δ*1132*/Tn7-*1132)*. The wild-type VIR-O and VIR-O Δ*1132* controls each have integrated an empty version of the pUC18T-mini-Tn7T-Apr-LAC insertion element into the attTn7 site. All micrographs were taken under a dissecting microscope illuminated from below the plate at an angle. All quantitative switching

assays represent six colonies from each strain. A two-tailed Mann-Whitney test (**$p < 0.005$) was carried out for **(B)**, and error bars represent the standard deviation of the mean. ns, not significant. The p value represents a comparison of both wild-type to mutant and mutant to the complemented strain.

Figure 3: Deletion of *1132* in the AV-T background alters the opacity phenotype and capsule expression. (A) Micrographs comparing representative colonies of AV-T, AV-T Δ*1132* and AV-T Δ*1132* Tn7-*1132*. **(B)** Micrographs comparing colonies of AV-T Δ*1132*, indicated by arrows, to VIR-O Δ*1132*. Micrographs were taken under a dissecting scope lit from underneath at an angle. **(C)** Wild-type VIR-O, wild-type AV-T, and AV-T Δ*1132* cells were layered onto a Percoll gradient (top layer 40%, bottom layer 50%) and centrifuged for 30 minutes at 3,000 xg. AV-T Δ*1132* cells migrate between the stopping points for VIR-O and AV-T wild-types, indicating intermediate capsular levels with high levels of heterogeneity in the AV-T Δ*1132* mutant. Photograph shown is one of six experimental replicates. **(D)** Transmission electron micrographs of representative wild-type VIR-O, wild-type AV-T, and AV-T Δ*1132* cells, stained with Ruthenium red. **(E)** Averages ± standard deviation of the mean of capsule widths of these three strains converted to ratios to the wild-type AV-T. The difference between the wild-type AV-T and AV-T Δ*1132* capsule widths is significant at $p < 0.0001$ as determined by a Student's two-tailed *t* test.

Figure 4: Deletion of *1132* in AV-T background increases virulence. (A) *Galleria mellonella* infected with AV-T Δ*1132* are killed at higher rates compared with wild-type AV-T or the complemented mutant (AV-T Δ*1132*/Tn7-*1132*). **(B)** Bacterial CFU/g recovered from mice lungs

24 hours after intranasal inoculation with pure cultures of wild-type VIR-O, wild-type AV-T, or AV-T Δ*1132*. A Log-Rank (Mantel-Cox) test (*$p < 0.05$) was carried out for **(A)** and a two-tailed Mann-Whitney test (*$p < 0.05$; ***$p < 0.0005$) was carried out for **(B)**.

Supplemental Figure 1: **Deletion of *1132* does not affect *abaI* expression.** qRT-PCR experiments comparing wild-type VIR-O and VIR-O Δ*1132* indicate no significant difference in the expression of *abaI*, using *16S* as an internal control (two-tailed Mann-Whitney test, ns = not significant). Results are the average of three biological replicates.

Supplemental Figure 2: **VIR-O Δ*1132* cells contain quorum sensing signal (AHL), but do not secrete it.** Cultures of wild-type VIR-O, VIR-O Δ*1132*, and VIR-O Δ*abaI* were grown to the same OD_{600} and plated as a line onto a soft-agar lawn containing *Agrobacterium tumefaciens* (*traG*::*lacZ*) and X-Gal. 10% SDS was added to a well at the center of the plate, lysing the cells.

Supplemental Figure 3: AV-T Δ*1132* switches to the VIR-O variant at the same frequency as wild-type AV-T. Bars represent averages of six colonies assayed for switching frequency at 18 hours of growth. Error bars indicate standard deviation of the mean, and there is no statistical significance as assessed by Welch's ANOVA.

Supplementary Figure 4: K locus genes for capsule polysaccharide synthesis and export are not transcriptionally regulated by 1132. Bars for AV-T Δ*1132* and AV-T Δ*1132*/Tn7-*1132* represent averages of three biological replicates. Error bars indicate standard deviation of the

mean, and there is no statistical significance in expression across strains as assessed by multiple Mann-Whitney tests.

Supplementary Figure 5: **(A)** Growth curves for VIR-O, AV-T, VIR-O Δ*1132*, and AV-T Δ*1132* in LB media. Data represents two biological replicates, and error bars indicate standard deviation of the mean. **(B)** *Galleria mellonella* infected with VIR-O Δ*1132* show no significant difference in mortality compared with wild-type VIR-O (n=30 per strain) as assessed by a log-rank (Mantel-Cox) test. **(C)** Mice were infected intranasally with either VIR-O or VIR-O Δ*1132*. At 24 hours post-inoculation, bacteria were recovered from the lungs, spleen, and liver tissues and CFU/g quantified. There is no significant difference between the two strains in all tissues as assessed by a Mann-Whitney test. ns, not significant.

Supplementary Table 1: RNA Sequencing Data for VIR-O Δ*1132*

Supplementary Table 2: Primers used in this study

Figure 1

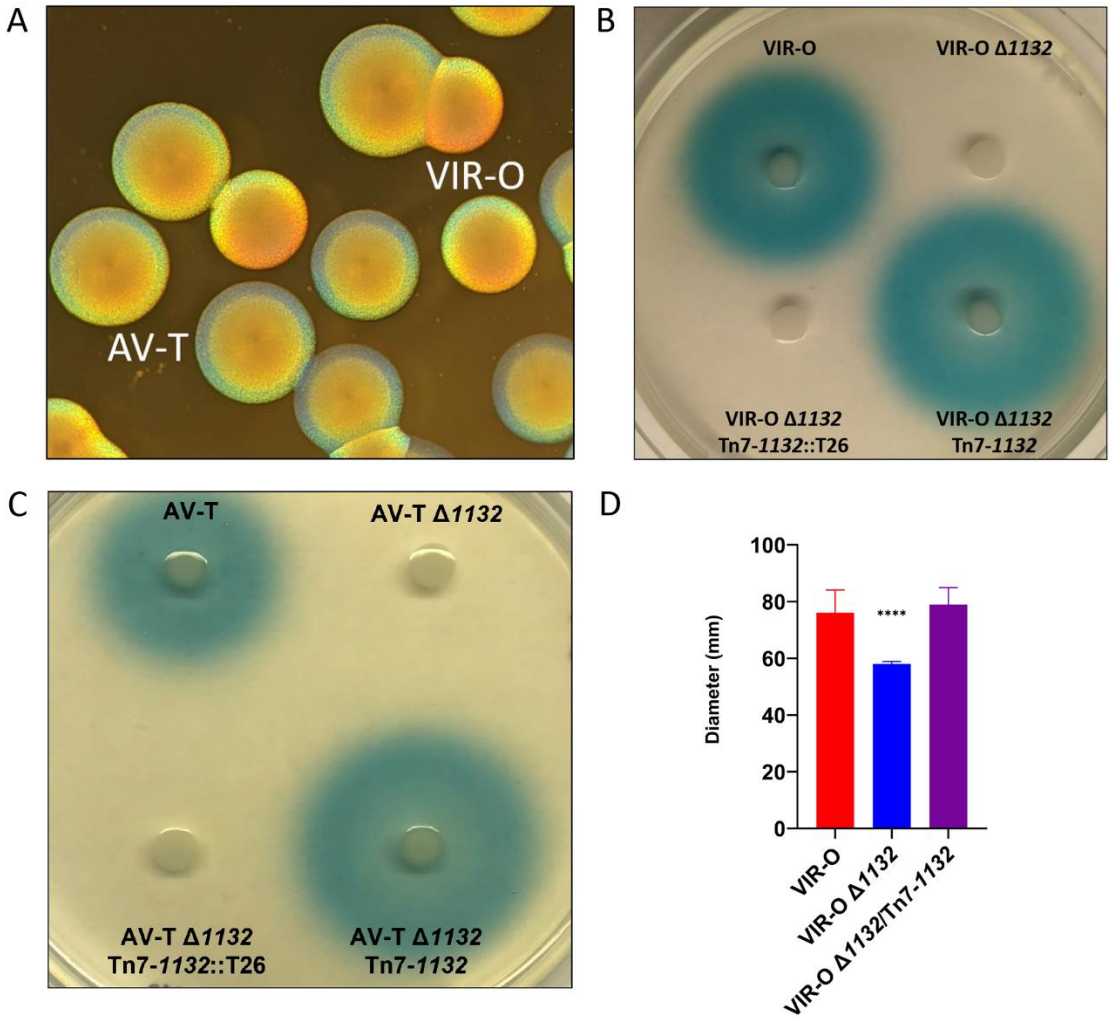

Figure 1: (A) AB5075 Wild-type opaque (VIR-O) and translucent (AV-T) colonies, viewed under a dissecting microscope with oblique lighting from underneath. **(B)** Qualitative assay of AHL secretion in which cultures of the wild-type (VIR-O), the VIR-O Δ*1132* mutant, the complemented mutant (VIR-O Δ*1132*/Tn7-*1132*), and a version of the complemented mutant disrupted by transposon insertion (VIR-O Δ*1132*/Tn7-*1132*::T26) were spotted onto a soft agar lawn containing X-Gal and an *Agrobacterium tumefaciens traG*::*lacZ* biosensor that reacts to the presence of exogenous AHL by cleaving X-Gal, forming a blue halo. (C) Qualitative assay of AHL secretion

in the wild-type (AV-T), the AV-T Δ*1132* mutant, the complemented mutant (AV-T Δ*1132*/Tn7-*1132*), and a version of the complemented mutant disrupted by transposon insertion (AV-T Δ*1132*/Tn7-*1132*::T26). Signal secretion was analyzed as in panel B, except the amount of X-Gal was increased 2-fold. **(D)** Surface-associated motility of wild-type (VIR-O), the VIR-O Δ*1132* mutant, and the complemented mutant (VIR-O Δ*1132*/Tn7-*1132*) measured on 0.3% Eiken Agar plates. A Welch's ANOVA (****$p < 0.00005$) was carried out to assess **(B)**; error bars indicate standard deviation of the mean.

Figure 2

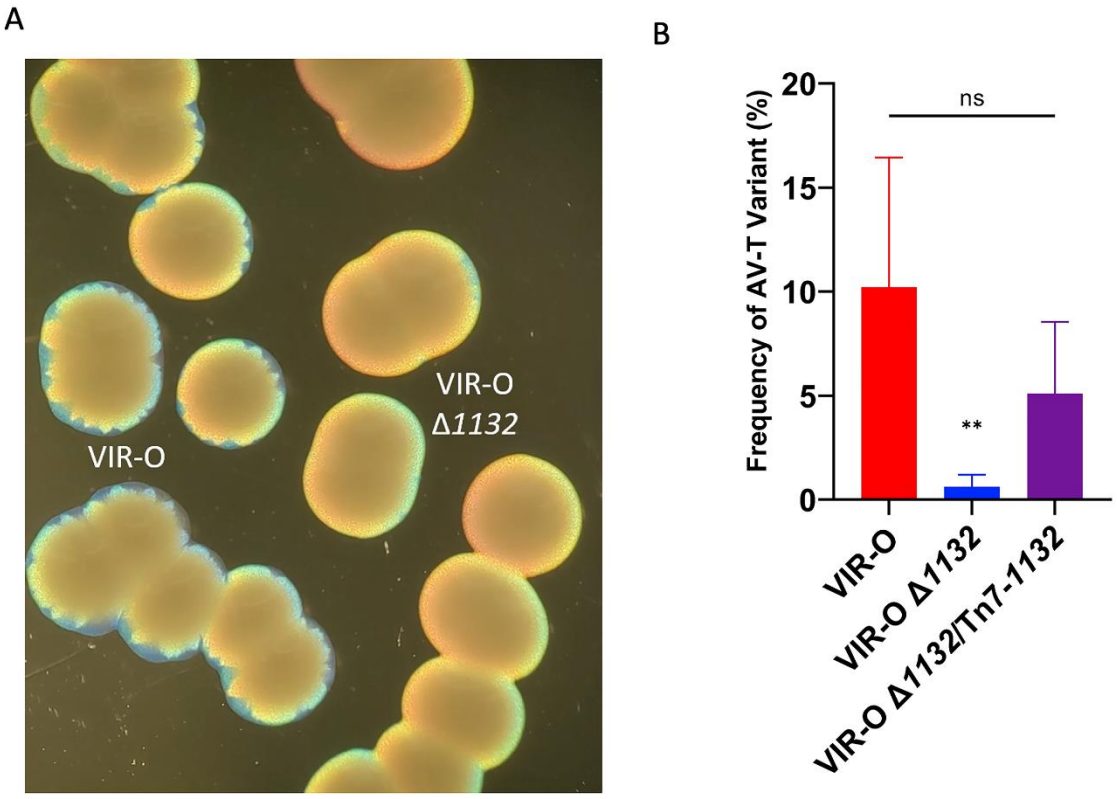

Figure 2: The Reduced Switching Phenotypes in VIR-O Δ*1132*. (A) Micrograph showing the loss of sectoring in VIR-O Δ*1132* colonies compared to wild-type VIR-O colonies at 24 hours of growth. **(B)** Quantification of switching frequencies demonstrating restoration of normal switching of VIR-O Δ*1132* through single copy complementation (VIR-O Δ*1132*/Tn7-*1132)*. The wild-type VIR-O and VIR-O Δ*1132* controls each have integrated an empty version of the pUC18T-mini-Tn7T-Apr-LAC insertion element into the attTn7 site. All micrographs were taken under a dissecting microscope illuminated from below the plate at an angle. All quantitative switching assays represent six colonies from each strain. A two-tailed Mann-Whitney test (**$p < 0.005$) was carried out for **(B)**, and error bars represent the standard deviation of the mean. Ns, not significant. The p value represents a comparison of both wild-type to mutant and mutant to the complemented strain.

Figure 3

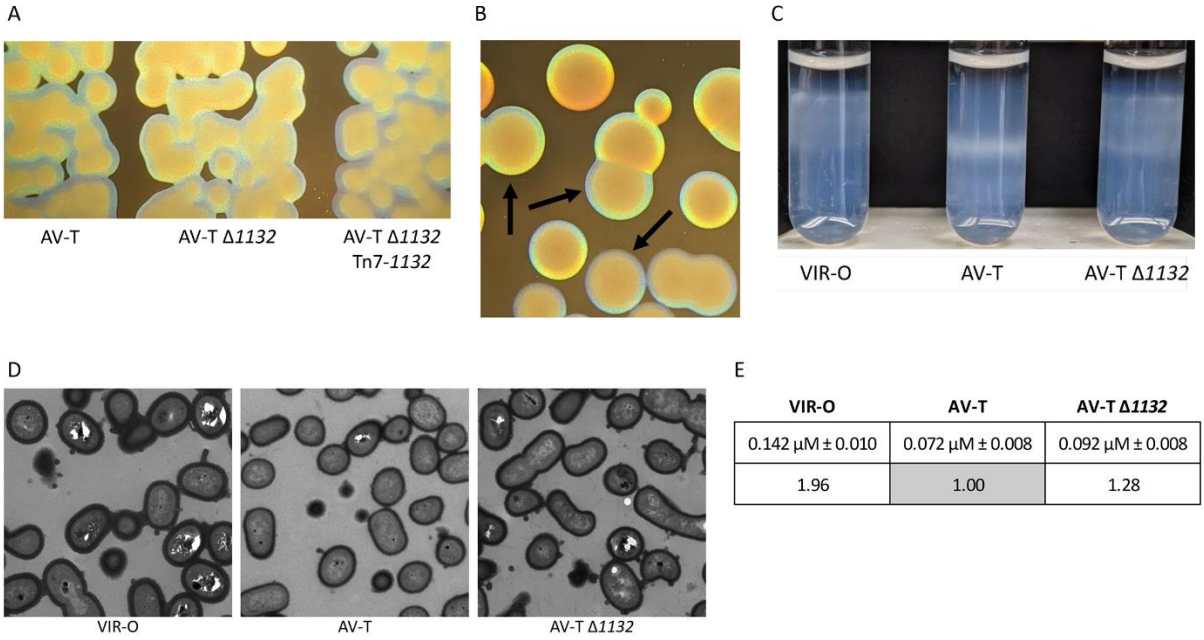

E

VIR-O	AV-T	AV-T Δ*1132*
0.142 µM ± 0.010	0.072 µM ± 0.008	0.092 µM ± 0.008
1.96	1.00	1.28

Figure 3: Deletion of *1132* in the AV-T background alters the opacity phenotype and capsule expression. (A) Micrographs comparing representative colonies of AV-T, AV-T Δ*1132* and AV-T Δ*1132* Tn7-*1132*. **(B)** Micrographs comparing colonies of AV-T Δ*1132*, indicated by arrows, to VIR-O Δ*1132*. Micrographs were taken under a dissecting scope lit from underneath at an angle. **(C)** Wild-type VIR-O, wild-type AV-T, and AV-T Δ*1132* cells were layered onto a Percoll gradient (top layer 40%, bottom layer 50%) and centrifuged for 30 minutes at 3,000 xg. AV-T Δ*1132* cells migrate between the stopping points for VIR-O and AV-T wild-types, indicating intermediate capsular levels with high levels of heterogeneity in the AV-T Δ*1132* mutant. Photograph shown is one of six experimental replicates. **(D)** Transmission electron micrographs of representative wild-type VIR-O, wild-type AV-T, and AV-T Δ*1132* cells, stained with Ruthenium red. **(E)** Averages ± standard deviation of the mean of capsule widths of these three strains converted to ratios to the wild-type AV-T. The difference between the wild-type AV-T and

AV-T Δ*1132* capsule widths is significant at $p < 0.0001$ as determined by a Student's two-tailed *t* test.

Figure 4

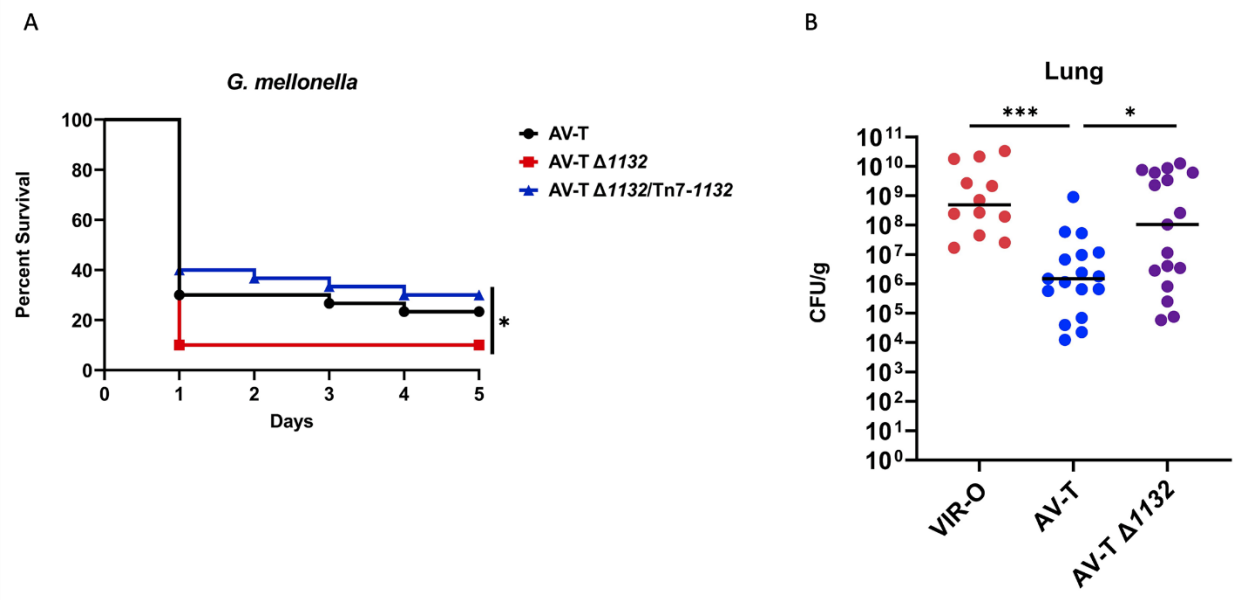

Figure 4: Deletion of *1132* in AV-T background increases virulence. (A) *Galleria mellonella* infected with AV-T Δ*1132* are killed at higher rates compared with wild-type AV-T or the complemented mutant (AV-T Δ*1132*/Tn7-*1132*). **(B)** Bacterial CFU/g recovered from mice lungs 24 hours after intranasal inoculation with pure cultures of wild-type VIR-O, wild-type AV-T, or AV-T Δ*1132*. A Log-Rank (Mantel-Cox) test (*$p < 0.05$) was carried out for **(A)** and a two-tailed Mann-Whitney test (*$p < 0.05$; ***$p < 0.0005$) was carried out for **(B)**.

Supplemental Figure 1

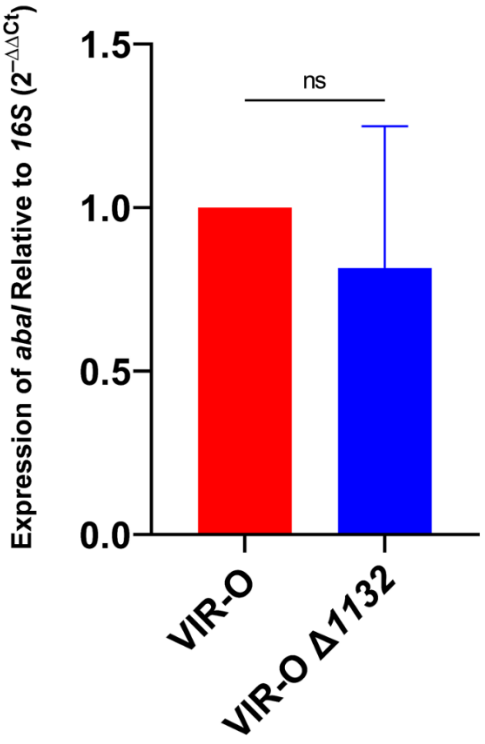

Supplemental Figure 1: **Deletion of *1132* does not affect *abaI* expression.** qRT-PCR experiments comparing wild-type VIR-O and VIR-O Δ*1132* indicate no significant difference in the expression of *abaI*, using *16S* as an internal control (two-tailed Mann-Whitney test, ns = not significant). Results are the average of three biological replicates.

Supplemental Figure 2

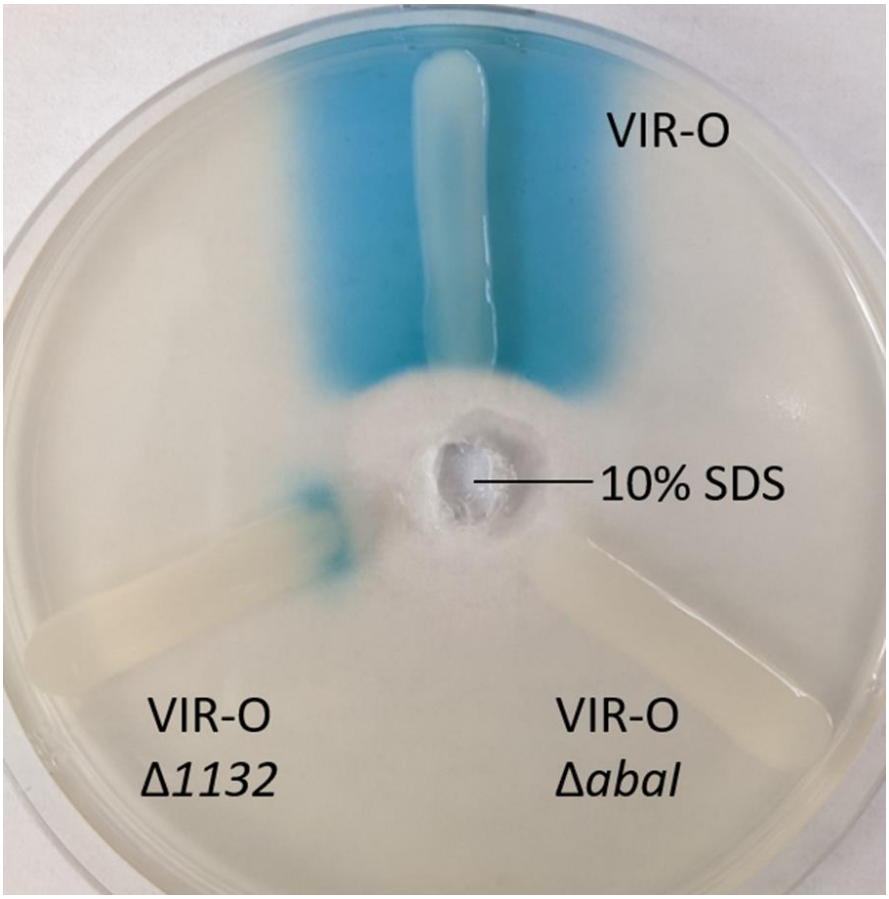

Supplemental Figure 2: **VIR-O Δ*1132* cells contain quorum sensing signal (AHL), but do not secrete it.** Cultures of wild-type VIR-O, VIR-O Δ*1132*, and VIR-O Δ*abaI* were grown to the same OD_{600} and plated as a line onto a soft-agar lawn containing *Agrobacterium tumefaciens* (*traG*::*lacZ*) and X-Gal. 10% SDS was added to a well at the center of the plate, lysing the cells.

Supplemental Figure 3

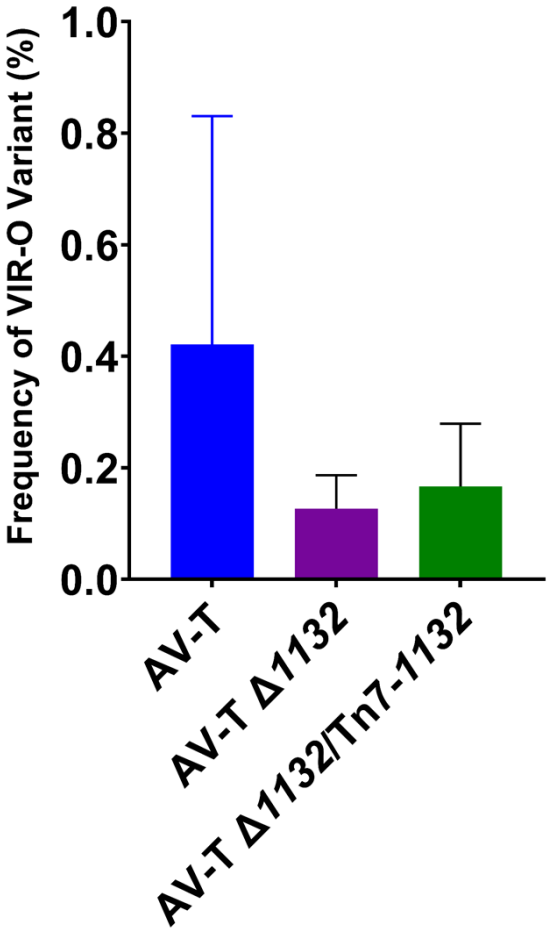

Supplemental Figure 3: AV-T Δ*1132* switches to the VIR-O variant at the same frequency as wild-type AV-T. Bars represent averages of six colonies assayed for switching frequency at 18 hours of growth. Error bars indicate standard deviation of the mean, and there is no statistical significance as assessed by Welch's ANOVA.

Supplemental Figure 4

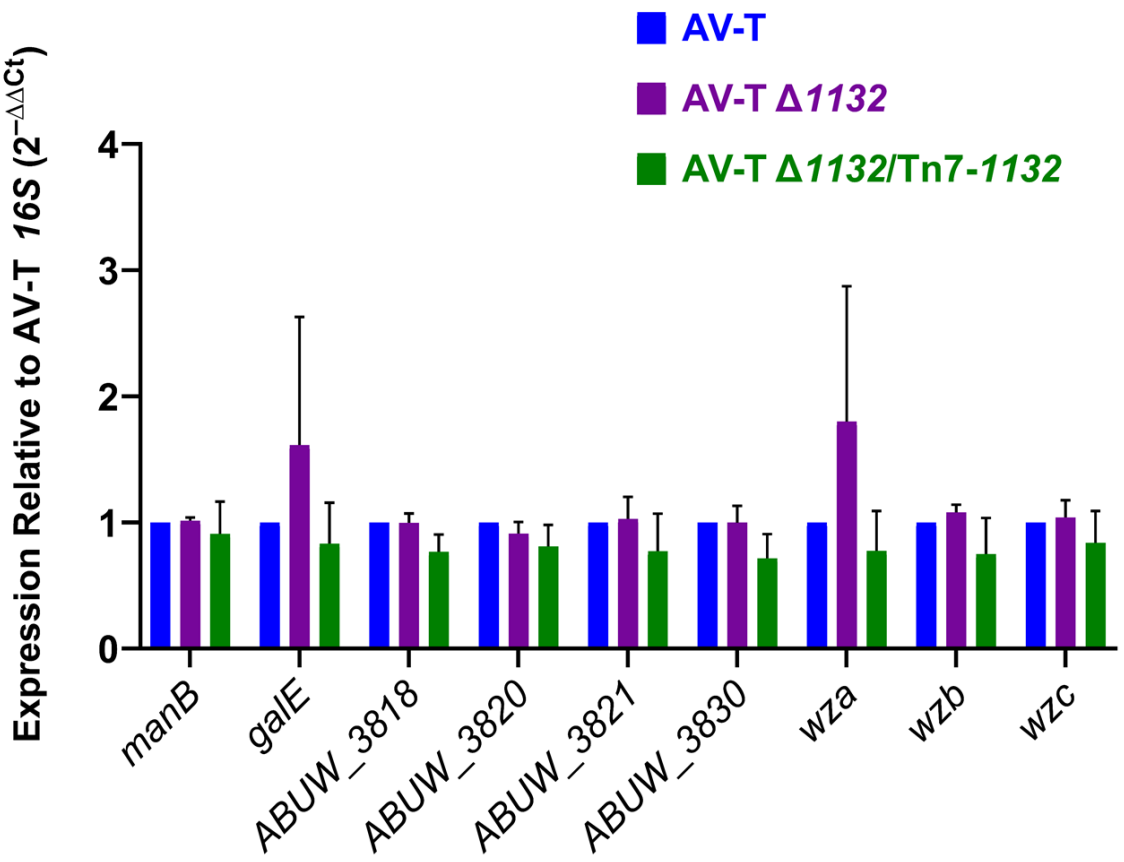

Supplementary Figure 4: K locus genes for capsule polysaccharide synthesis and export are not transcriptionally regulated by 1132. Bars for AV-T Δ*1132* and AV-T Δ*1132*/Tn7-*1132* represent averages of three biological replicates. Error bars indicate standard deviation of the mean, and there is no statistical significance in expression across strains as assessed by multiple Mann-Whitney tests.

Supplementary Figure 5

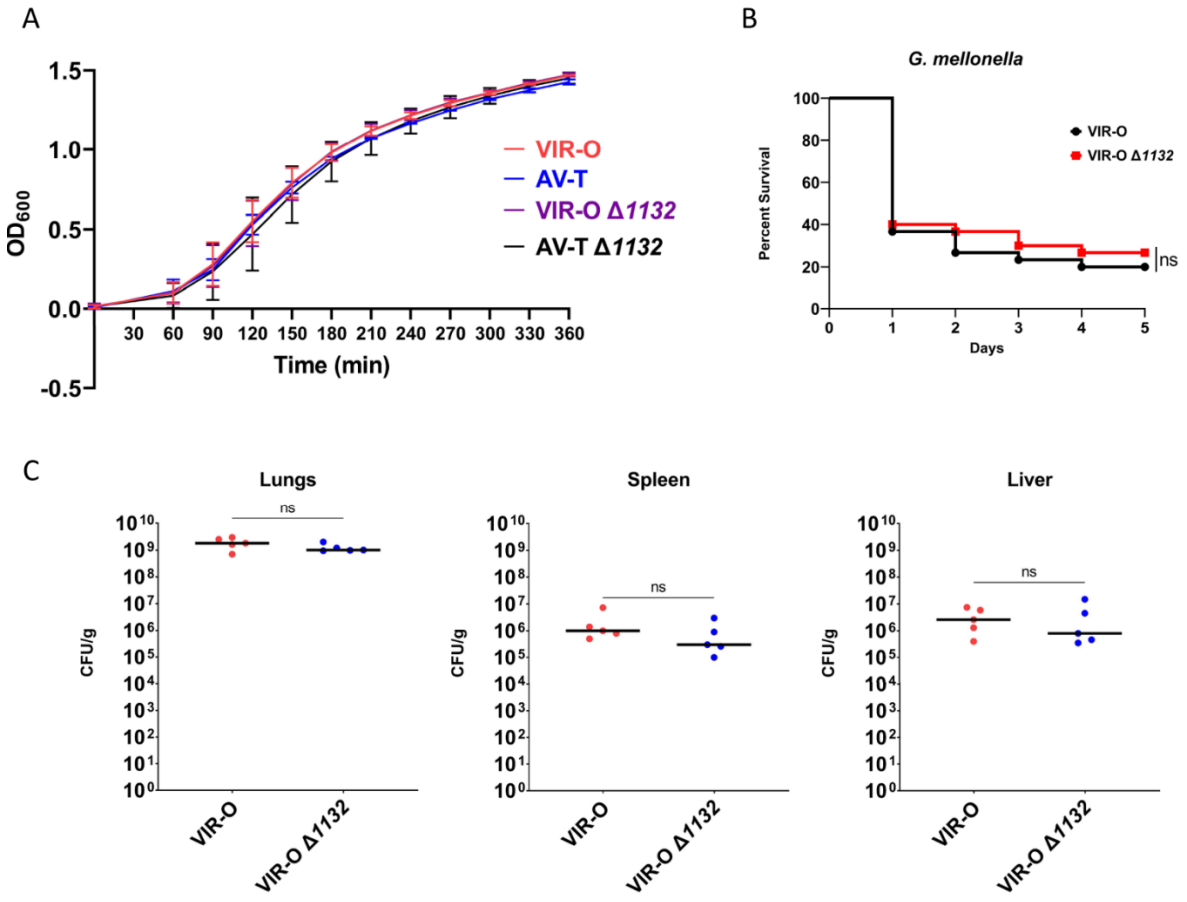

Supplementary Figure 5: **(A)** Growth curves for VIR-O, AV-T, VIR-O Δ*1132*, and AV-T Δ*1132* in LB media. Data represents two biological replicates, and error bars indicate standard deviation of the mean. **(B)** *Galleria mellonella* infected with VIR-O Δ*1132* show no significant difference in mortality compared with wild-type VIR-O (n=30 per strain) as assessed by a log-rank (Mantel-Cox) test. **(C)** Mice were infected intranasally with either VIR-O or VIR-O Δ*1132*. At 24 hours post-inoculation, bacteria were recovered from the lungs, spleen, and liver tissues and CFU/g quantified. There is no significant difference between the two strains in all tissues as assessed by a Mann-Whitney test. ns, not significant.

Supplementary Table 1: RNA Sequencing Data for VIR-O Δ*1132*[1]

Upregulated in VIR-O Δ*1132* (fold change ≥ 2.0, $p < 0.05$)

Gene	Gene function	log2FoldChange	pvalue
ABUW_2965	hypothetical protein	1.961295846	0.000604492
ABUW_0928	lytic transglycosylase, catalytic	1.885129873	1.73994E-16
ABUW_1860	hypothetical protein	1.872882079	3.68519E-10
ABUW_1861	ring hydroxylating dioxygenase, Rieske	1.80387855	9.37852E-12
ABUW_1859	hypothetical protein	1.691026846	4.72958E-10
ABUW_1863	short-chain dehydrogenase/reductase	1.650304412	1.16755E-12
ABUW_1862	aromatic-ring-hydroxylating dioxygenase beta subunit	1.644821317	4.88748E-11
ABUW_1858	acyl-CoA dehydrogenase	1.630758202	0.007110473
pntB	NAD(P) transhydrogenase subunit beta	1.524004574	0.009455886
ABUW_1864	2Fe-2S iron-sulfur cluster binding domain protein	1.515487744	3.4676E-09
ABUW_2103	hypothetical protein	1.396286823	2.5455E-05
rplB	ribosomal protein L2	1.355787742	1.89674E-09
ABUW_2102	hypothetical protein	1.350249007	0.001934095
ABUW_1857	Glu-tRNA amidotransferase	1.33982145	0.025505609
ABUW_1906	transcriptional regulator, LysR family	1.335739688	3.59868E-14
ABUW_2276	transcriptional regulator, ArsR family	1.323953684	1.06455E-09
rplV	ribosomal protein L22	1.30807529	1.1861E-08
rplD	ribosomal protein L4/L1e	1.303068367	1.92527E-08
rpsQ	ribosomal protein S17	1.282013953	6.66588E-07
ABUW_2964	putative cobalamin synthesis protein	1.272754435	1.78629E-10
rpsC	ribosomal protein S3	1.266479373	2.62045E-08
rplC	ribosomal protein L3	1.263234638	4.53774E-08
ABUW_1233	OmpW family protein	1.262713332	0.036401349
rplW	ribosomal protein L23	1.254776138	2.41682E-07
ABUW_1865	P-hydroxyphenylacetate hydroxylase C1:reductase component	1.24279795	1.33877E-08
rpsS	ribosomal protein S19	1.228647212	9.92145E-08
rplP	ribosomal protein L16	1.225814066	1.56763E-07
ABUW_0187	hypothetical protein	1.212161791	6.49337E-09
ABUW_4123	hypothetical protein	1.2083132	0.035957784

[1] Note: The table presented here has been modified to fit this document. The original version was published as a supplementary file in Frontiers in Cellular and Infection Microbiology, which may be downloaded at:
https://www.frontiersin.org/articles/10.3389/fcimb.2021.778331/full#supplementary-material

pntA2	NAD(P) transhydrogenase subunit alpha	1.165429903	4.44522E-05
ABUW_3881	matrixin superfamily	1.149103656	0.000272945
rpsJ	ribosomal protein S10	1.096441337	1.68586E-06
ABUW_1904	antibiotic biosynthesis monooxygenase	1.078130875	7.20481E-07
rplS	ribosomal protein L19	1.076671089	5.65671E-07
rpmD	ribosomal protein L30	1.057307344	2.5436E-08
rpsH	ribosomal protein S8	1.037111677	8.53666E-06
ABUW_0357	hypothetical protein	1.024923147	3.18468E-07
ABUW_1905	isochorismatase hydrolase	1.021068084	6.48871E-09
ABUW_4094	hypothetical protein	1.014348646	2.98844E-07
rpsE	ribosomal protein S5	0.995686106	4.41269E-07
rpsN	ribosomal protein S14	0.995126708	1.80277E-05
rpmC	ribosomal protein L29	0.986109395	6.8819E-05
ABUW_2630	lipid A biosynthesis lauroyl acyltransferase	0.978407351	3.47425E-08
ABUW_1969	alpha/beta hydrolase	0.972366804	0.022710688
rplF	ribosomal protein L6	0.967027259	2.63369E-06
rplI	ribosomal protein L9	0.958856352	5.22331E-06
ABUW_0358	peptidase S8 and S53 subtilisin	0.957647701	2.57894E-06
rplE	ribosomal protein L5	0.955862094	2.71425E-05
ABUW_4093	hypothetical protein	0.946222508	2.42582E-05
ABUW_2806	putrescine importer	0.907138594	0.000387949
gdhB1	quinoprotein glucose dehydrogenase-B	0.903248542	4.39201E-06
rplR	ribosomal protein L18	0.897907562	1.62045E-05
betA	choline dehydrogenase	0.889514936	0.001617127
adeB	multidrug efflux protein AdeB	0.889296503	4.24505E-06
caiB2	L-carnitine dehydrogenase	0.88878961	0.000339542
trmD	tRNA (guanine-N1)-methyltransferase	0.873513148	1.07968E-05
ABUW_4095	Soluble lytic murein transglycosylase	0.86933977	0.002486102
ABUW_4096	hypothetical protein	0.867267919	8.96982E-05
rplA	ribosomal protein L1	0.866215771	3.67415E-06
rplX	ribosomal protein L24	0.860965022	0.000162164
ABUW_2967	MarC family integral membrane protein	0.85992403	0.000109076
rpsR	ribosomal protein S18	0.832990634	1.68847E-05
rplO	ribosomal protein L15	0.816295628	1.47438E-05
rpoA	DNA-directed RNA polymerase, alpha subunit	0.815102053	2.02112E-05
icmF	type VI secretion protein IcmF	0.814766971	7.89476E-05
ABUW_2687	hypothetical protein	0.810904881	1.06268E-05
rpsF	ribosomal protein S6	0.801505068	2.80946E-05

ABUW_1942	ribose-phosphate pyrophosphokinase	0.797481491	0.002227699
ABUW_3149	hypothetical protein	0.794089134	0.00017773
ABUW_1855	general substrate transporter:Major facilitator superfamily	0.785448146	0.012240901
mucK2	cis,cis-muconate transport protein	0.778747363	0.003240104
ABUW_1796	hypothetical protein	0.777744527	0.006928674
traE	conjugative transfer system protein TraE	0.776556425	0.003185619
rplQ	ribosomal protein L17	0.767047784	0.000276798
secY	preprotein translocase, SecY subunit	0.766950964	3.19007E-05
traL	TraL	0.757761981	0.005192332
rplT	ribosomal protein L20	0.757205236	0.000571163
comL	pilus assembly protein, PilQ	0.754751862	0.000906265
ABUW_3891	integral membrane protein TerC	0.750746498	0.00110694
rplL	ribosomal protein L7/L12	0.736147676	1.73998E-05
rplN	ribosomal protein L14	0.728847352	0.000890104
ABUW_0382	hypothetical protein	0.728543923	0.032339649
adeA	multidrug efflux protein AdeA	0.720105309	0.001394626
ABUW_4047	hypothetical protein	0.709473056	0.000140784
rpsI	ribosomal protein S9	0.707628992	0.00148434
rplJ	ribosomal protein L10	0.706744367	3.78135E-05
ABUW_4097	hypothetical protein	0.70507969	0.000697637

Downregulated in VIR-O Δ*1132* (fold change ≥ 2.0, $p < 0.05$)

Gene	Gene function	log2FoldChange	pvalue
ABUW_1132	transcriptional regulator, LysR family	-8.601525249	2.8644E-203
ABUW_0684	coproporphyrinogen III oxidase	-2.363306712	3.68447E-38
ABUW_3351	heme oxygenase-like protein	-1.950460596	3.45166E-24
ABUW_1949	RND family drug transporter	-1.948305873	2.81679E-17
ABUW_1693	heme oxygenase-like protein	-1.747812394	2.92692E-19
ABUW_2679	DUF4142/predicted OMP	-1.647069188	3.76281E-13
ABUW_1692	TetR transcriptional regulator	-1.573162991	1.94712E-13
ABUW_2678	17 kDa surface antigen	-1.511897805	4.63134E-09
ABUW_2627	hypothetical protein	-1.452607384	2.16539E-14
ABUW_1950	multidrug resistance protein VceB	-1.417805103	1.74942E-06
ABUW_1467	acyl-CoA dehydrogenase	-1.396211322	1.0447E-11
ABUW_3352	putative transcriptional regulator	-1.392818929	3.9427E-12
ABUW_1659	hypothetical protein	-1.365607582	1.55582E-08
ABUW_1468	LmbE-like protein	-1.33907148	2.18879E-08
ABUW_0449	hypothetical protein	-1.298891027	5.53946E-12

ABUW_1470	glycosyl transferase, family 2	-1.264654551	5.98952E-07
ABUW_1951	hypothetical protein	-1.257021303	4.66419E-06
ABUW_1952	auxin-responsive GH3-related protein	-1.241366116	1.03625E-07
cinA1	competence/damage-inducible protein cinA	-1.23674542	1.65083E-06
ABUW_1637	oxidoreductase short-chain dehydrogenase/reductase family	-1.22128007	1.02542E-08
ABUW_2434	hypothetical protein	-1.209534993	3.53817E-06
ABUW_2060	hypothetical protein	-1.19856057	2.77049E-08
ABUW_1469	methyltransferase type 12	-1.195009144	1.92606E-06
ABUW_0685	alpha/beta hydrolase fold protein	-1.192625413	1.85883E-10
ABUW_3798	short-chain dehydrogenase/reductase SDR	-1.188344157	1.47717E-10
ABUW_2145	hypothetical protein	-1.147833522	1.41756E-09
ABUW_1635	glutathione S-transferase	-1.088457502	4.46632E-06
ABUW_1636	short chain dehydrogenase	-1.083911193	5.70996E-06
ABUW_2437	heme oxygenase-like protein	-1.073489114	1.70548E-06
ABUW_1632	PapD-like P pilus assembly protein	-1.07111178	3.42114E-09
ABUW_1594	hypothetical protein	-1.070691104	3.41442E-09
otsA	trehalose-6-phosphate synthase	-1.069589423	1.46178E-05
ABUW_2594	glutathione-dependent formaldehyde dehydrogenase	-1.040438182	2.44086E-05
otsB	trehalose-phosphatase	-1.025924201	1.49664E-06
ABUW_2064	hypothetical protein	-0.997635407	1.86714E-06
ABUW_1471	hypothetical protein	-0.948622613	0.000283352
ABUW_2435	oxidoreductase	-0.934741536	9.96414E-05
ABUW_2058	hypothetical protein	-0.923952446	8.84294E-05
ABUW_1633	fimbrial biogenesis outer membrane usher protein	-0.900714393	4.55397E-06
ABUW_2684	phage putative head morphogenesis protein	-0.899364565	2.16863E-06
ABUW_0934	hypothetical protein	-0.884162498	0.008842011
ABUW_1657	hypothetical protein	-0.861729142	0.000217464
ABUW_3322	hypothetical protein	-0.847820865	0.001775124
ABUW_1499	EamA-like transporter family protein	-0.847173036	0.000875339
cysP	thiosulfate-binding protein	-0.847099476	0.004770505
copA	copper resistance protein A	-0.843261422	0.00030549
ABUW_1631	spore coat protein U	-0.838225902	1.45764E-05
ABUW_1379	hypothetical protein	-0.837518919	0.000117946
ABUW_2887	lipoprotein	-0.833223437	4.22943E-05
ABUW_1634	spore coat protein U	-0.82955249	0.001128184
ABUW_0360	hypothetical protein	-0.829405029	3.69036E-05

ABUW_3575	serine hydrolase domain-containing protein	-0.81728765	0.0004209
ABUW_1629	hypothetical protein	-0.814790936	0.001558172
ABUW_0259	sulfate transporter	-0.806046229	0.001457525
ABUW_2685	hypothetical protein	-0.795097191	2.86166E-05
ABUW_0628	peroxidase	-0.794236119	0.000113172
ABUW_3106	peptidoglycan-binding LysM	-0.780207482	2.56877E-05
ABUW_1759	extracellular serine protease	-0.775047034	0.000168497
ABUW_0055	glucose sorbosone dehydrogenase	-0.773228109	0.000174059
ABUW_0916	biofilm-associated protein	-0.769047874	0.000103053
ABUW_1953	outer membrane efflux protein	-0.757553932	0.002696082
algC	phosphomannomutase	-0.75658648	1.47072E-05
ABUW_2321	hypothetical protein	-0.756098829	0.000828061
ABUW_2403	MFS permease	-0.746342328	0.003095028
ABUW_0233	hypothetical protein	-0.742062466	8.74948E-05
ABUW_1227	acyl-CoA dehydrogenase	-0.736772043	0.005493207
ABUW_0921	glycerophosphoryl diester phosphodiesterase	-0.735643343	0.005410306
ABUW_3577	hypothetical protein	-0.729641931	4.09155E-05
manB	phosphomannomutase	-0.727536999	5.24995E-05
ABUW_3708	transglycosylase SLT domain protein	-0.727080036	0.001044547
ABUW_1042	glutathione-dependent formaldehyde-activating enzyme/centromere protein V	-0.723873511	0.000614386
ABUW_1996	hypothetical protein	-0.720830843	0.000971826
ahpF2	alkyl hydroperoxide reductase, F subunit	-0.719192839	0.003271284
ABUW_2554	putative hemolysin	-0.718202468	0.000872036
ABUW_2504	catalase	-0.717479086	0.00083838
ABUW_0210	glutathione-dependent formaldehyde-activating enzyme/centromere protein V	-0.712867017	0.000314544
ABUW_2063	uracil-DNA glycosylase-like protein	-0.710550828	7.67967E-05
ABUW_0359	hypothetical protein	-0.708740233	0.000141777
ABUW_3898	transglycosylase-associated protein	-0.708540871	0.006329618

Supplementary Table 2: Primers used in this study

Primer Name	Sequence	Description/Use
1132 Up 1	GATACCCTCATCAGCAAAAA	Amplifies the 2kb region upstream of *1132*
1132 Up 2	AAAAAATGCTTATTGTTGTAATGAAAG	
1132 Down 1	ATGCAGATTGTTCGTTAACTTT	Amplifies the 2kb region downstream of *1132*
1132 Down 2	ATCAGGTTCAAGAACTGACT	
1132 For	GTTTCCTCGTATAATACAAT	Verification of *1132* deletion
1132 Rev	CTACGCTAAAGCAAAAATAA	
manB qPCR 1	AGCGCTTAACGTACCTGTTGA	qRT-PCR of *manB*
manB qPCR 2	AAACAGCGGTCAAAATCGCC	
galE qPCR 1	CAGTGGGTGAAAGCCAGGAA	qRT-PCR of *galE*
galE qPCR 2	GGCATACCCGTTGGCATTTC	
3818 qPCR 1	TCGGGCATGTTAGCTACTCG	qRT-PCR of *ABUW_3818*
3818 qPCR 2	CACCGCCAAATCCTACACCT	
3820 qPCR 1	AGCATTACCTTCAGTAGGCCG	qRT-PCR of *ABUW_3820*
3820 qPCR 2	AGGGTCACGTCCCAGTAAGT	
3821 qPCR 1	TGGTCATATTGCGGCATGGT	qRT-PCR of *ABUW_3821*
3821 qPCR 2	AAACCTGGTGGGTGCTGTTT	
3830 qPCR 1	CAGGAACTCACAAGGCACCA	qRT-PCR of *ABUW_3830*
3830 qPCR 2	CGCCAACTAAACCTGGACGA	
wza qPCR 1	GTTTCCTCTAGTGGGACGCT	qRT-PCR of *wza*
wza qPCR 2	CGCTGCCTTGAACGGAAAAG	
wzb qPCR 1	CTGCCGGTATTTCAGGGCTT	qRT-PCR of *wzb*
wzb qPCR 2	GCAAAGGGCCAAGTCTGTTC	
wzc qPCR 1	AGATACGGCCGTTGAACCAG	qRT-PCR of *wzc*
wzc qPCR 2	GCGTGGCACAGTTGCATAAA	
16S qPCR 1	GATCTTCGGACCTTGCGCTA	qRT-PCR of *16S*
16S qPCR 2	GTGTCTCAGTCCCAGTGTGG	
abaI qPCR 1	TGCCAGACTACTACCCACCA	qRT-PCR of *abaI*
abaI qPCR 2	ACTAGCAGAGGAAGGCGGAT	
att-Tn7 site 1	TTGCTGATGAAAATAGTGGTGTAG	Amplification of the att-Tn7 insertion site downstream of glmS
att-Tn7 site 2	CACATCTAGAATTGCCTTCCAT	

Chapter 4: A Family of TetR-Type Transcriptional Regulators Controls a Phenotypic Switch in *Acinetobacter baumannii*

Pérez-Varela M*[1], Tierney ARP*[1], Tipton KA[1], Hutcheson AR[6], Chin CY[1,2,3,4,5], Weiss DS[1,2,3,4,5,6], and Rather PN[1,6]

*Authors contributed equally.

[1] Department of Microbiology and Immunology, Emory University, Atlanta, Georgia, USA

[2] Emory Vaccine Center, Atlanta, Georgia, USA

[3] Yerkes National Primate Research Center, Atlanta, Georgia, USA

[4] Division of Infectious Diseases, Department of Medicine, Emory University, Atlanta, Georgia, USA

[5] Emory Antibiotic Resistance Center, Atlanta, Georgia, USA

[6] Research Service, Department of Veterans Affairs, Atlanta VA Medical Center, Decatur, Georgia, USA

Unpublished Results

to be included in a Future Manuscript

PNR, ARPT, and MPV wrote this draft manuscript. ARPT carried out the experiments shown in Figures S5, S6, and S8. MPV carried out the experiments shown in Figures 2, S2, S3, S4. MPV and ARPT carried out the experiments shown in Figure S7. ARPT and ARH carried out the experiments shown in Figure 3. ARPT, MPV, PNR, and KAT all contributed to the work shown in Table 1. PNR conducted the experiments in Figures 1A-1C and S1. CYC conducted the mouse experiments. MPV, ARPT, ARH, PNR, and KAT each made various mutants and/or overexpression constructs.

Abstract

Acinetobacter baumannii cells interconvert at a high frequency between two colony opacity variants termed virulent opaque (VIR-O) and avirulent translucent (AV-T). We have reported on several genes that impact the rate of switching between these two variants, with the TetR-type transcriptional regulator (TTTR) *ABUW_1645* appearing to be a crucial component of the key pathway of VIR-O to AV-T switching. We now report that *ABUW_1645* is one of a large family of at least 12 functionally redundant TTTRs in AB5075 that share high levels of homology in their helix-turn-helix DNA binding region and are all able to mediate conversion of VIR-O cells to the AV-T state when overexpressed. As a VIR-O colony grows, cells within that colony switch to AV-T, forming multiple sectors of translucent cells in the periphery of the colony. In each sector, at least one of these TTTRs has been activated to allow the switch to AV-T and then to maintain the AV-T state. Three of these TTTRs, *ABUW_1645*, *ABUW_1959*, and *ABUW_2818*, are utilized most often, while a fourth—*ABUW_3353*—is required for switching in the absence of the main three. Deletion of the TTTR(s) that is currently maintaining the AV-T state causes cells to switch back to the VIR-O state, which effectively "resets" the system, allowing a different TTTR to activate and mediate the switch from VIR-O to AV-T. Real-time quantitative PCR analysis further revealed that members of this TTTR family do not appear to inter-regulate or autoregulate, and investigations into the conditions and mechanisms that activate these TTTRs are ongoing.

Introduction

Within the last decade, *Acinetobacter baumannii* has become a highly relevant nosocomial pathogen due to its ability to evade treatment with antibiotics and to persist in clinical environments [1-12]. While much research has elucidated the prevalence of multi-drug resistance and the resistance mechanisms employed by *A. baumannii*, there is a much less cohesive picture of its virulence. In 2015, our group published on a phenotypic switch in *A. baumannii* that regulates virulence [13]. At its most basic level, this switch results in a phenotypic heterogeneity that presents as cells forming either opaque or translucent colonies. The translucent variants appear to be important for survival in a natural environment, as they readily form biofilm and are able to utilize a wide variety of carbon sources [13, 14]. The opaque variants secrete higher levels of 3-OH C_{12}-homoserine lactone quorum sensing signal, display increased surface-associated motility, and have greater resistance to desiccation. Further, the opaque variant possesses higher levels of capsule, is virulent in a mouse pneumonia model, and was exclusively recovered from the blood of humans with *A. baumannii* septicemia [13-15]. Due to this difference in virulence between the two colony types, we designated the opaque variant as VIR-O (virulent opaque) and the translucent variant as AV-T (avirulent translucent).

VIR-O and AV-T cells switch to the opposite variant at a high frequency, with rates averaging 4-13% at 24 hours and 20-40% at 48 hours [14]. Many investigations to determine the genetic mechanisms that regulate this switch have been carried out to date, utilizing techniques including RNA sequencing, real-time quantitative PCR, and genetic screens to reveal gene products that promote or preclude switching. These led to the discovery of numerous gene products capable of influencing the switch including but not limited to: an RND-type efflux system, the OmpR-EnvZ two-component system, a plasmid-based antibiotic resistance locus, a LysR-type

transcriptional regulator, and a TetR-type transcriptional regulator (TTTR)—*ABUW_1645*—whose overexpression both completely converts VIR-O to AV-T and serves as a highly effective live attenuated vaccine strain that protects mice from lethal infection [14, 16-19].

TTTRs are a well-defined family of transcriptional regulators named for the founding member TetR, which regulates tetracycline resistance in *Escherichia coli* [20, 21]. These regulators form homodimers and possess both a helix-turn-helix (HTH) DNA-binding domain and a ligand-binding domain whose bound and unbound states alter the conformation of the HTH. We now have evidence that *ABUW_1645* is an important member of a family of at least twelve TTTRs in *A. baumannii* that promote switching from VIR-O to AV-T and maintain the AV-T state. Although work is still underway to elucidate the mechanisms and potential ligands that regulate this subpopulation of TTTRs in a bistable manner, the following findings constitute a novel system of regulation as yet undocumented in bacteria.

Results

Overexpression of the TTTRs *ABUW_1959* or *ABUW_2818* converts VIR-O cells to an AV-T-like state.

Previous work demonstrated the TTTR *ABUW_1645* (*1645*) was upregulated in AV-T cells and its overexpression in VIR-O cells converted them to the AV-T state (**Fig. 1A)** [14]. A recently identified phenotype associated with *1645* overexpression in VIR-O cells was a reduction in surface motility (**Fig. 1B**), a characteristic associated with AV-T cells [13]. In addition, we have found that VIR-O and AV-T cells differ in secretion of the AbaI-dependent quorum sensing signal 3-OH C_{12}-HSL, where VIR-O cells secrete far greater amounts than AV-T cells (**Fig. S1A**) [13]**.** Overexpression of *1645* in VIR-O cells resulted in loss of 3-OH-C_{12}-HSL secretion **(Fig. 1C).** Therefore, overexpression of *1645* converted VIR-O cells to known phenotypes of the AV-T state. This effect was not limited to strain AB5075, as overexpression of *1645* in four other clinical isolates also drove VIR-O cells to a translucent colony phenotype, reduced motility and led to a reduction in 3-OH C_{12}-HSL secretion **(Fig. S1B).** Based on this data, it was hypothesized that the stochastic activation of *1645* in a subset of VIR-O cells was a key step in the switch from the VIR-O to AV-T state. However, as previously reported, an in-frame deletion of *1645* did not impact VIR-O to AV-T switching [14], suggesting the possibility that functionally redundant regulators might be present.

To identify additional regulators that might be stochastically activated in VIR-O cells to drive them to the AV-T state, we re-examined several RNA sequencing data sets between VIR-O and AV-T cells. This revealed two additional TTTRs, *ABUW_1959* (*1959*) and *ABUW_2818* (*2818*), that were strongly upregulated in AV-T cells. This differential expression was confirmed by qRT-PCR analysis, where in AV-T cells *1959* expression was increased 18.5 $\pm$ 7.2-fold and

2818 was increased 28.1 ± 7.7-fold above the levels in VIR-O cells. As a reference, *1645* was upregulated 149.8 ± 34.6-fold by qRT-PCR in these same AV-T cells. To determine if increased expression of *1959* or *2818* in VIR-O cells could convert them to the AV-T state, each gene was cloned in pWH1266, where transcription was driven from the β-lactamase promoter as previously done with *1645* [14]. Constitutive expression of either *1959* or *2818* in the VIR-O variant converted cells to the translucent colony phenotype **(Fig. 1A)**, reduced motility **(Fig. 1B)**, and blocked 3-OH C_{12} –HSL secretion **(Fig. 1C)**. As a control, the overexpression of another TetR-type transcriptional regulator ArpR [17] cloned in an identical manner, did not convert VIR-O cells to any of the AV-T-associated phenotypes (data not shown). Surprisingly, despite their translucent colony appearance, VIR-O cells overexpressing either *1959* or *2818* did not exhibit a statistically significant difference in bacterial CFU/g at 24 hours post-infection in a mouse lung model of infection compared to VIR-O cells containing the pWH1266 vector **(Fig. 1D).** This contrasts with the marked decrease in bacterial CFU/g previously seen with *1645* overexpression [14].

Expression of additional TTTRs can convert VIR-O cells to an AV-T-like state.

A bioinformatic analysis of the 1645, 1959 and 2818 proteins determined that they possessed similar helix-turn-helix DNA binding regions (**Fig. S2**), which likely accounted for their ability to regulate similar phenotypes when overexpressed. During this analysis, it became apparent that nine additional TTTRs were highly similar to 1645 in the DNA-binding helix-turn-helix (HTH) region. These included ABUW_3353, 2596, 1498, 3194, 1163, 0939, 0222, 2629, and 1912 **(Fig. S2)**. Each of these TTTRs was individually overexpressed from the β-lactamase promoter in pWH1266 in an identical manner as was done for *1645*, *1959* and *2818* and introduced into VIR-

O cells. In each case, this resulted in conversion to a translucent colony phenotype, loss of 3-OH C_{12}-HSL secretion, and, in most cases, a reduction in surface motility **(Table 1).**

Individual AV-T variants derived from VIR-O cells exhibit different TTTR expression profiles.

As noted above, in our lab stock of AV-T cells, the TTTRs *1645*, *1959*, and *2818* were upregulated 150, 19 and 28-fold, respectively (**Fig. 2**). Since additional TTTRs were identified that could drive the VIR-O to AV-T switch (**Table 1**), we considered the possibility that one or more of these were also activated in AV-T cells that had switched from the VIR-O state. Each TTTR shown in Table 1 was tested for expression in our lab stock of VIR-O and AV-T variants by qRT-PCR, and all exhibited similar levels of expression between VIR-O and AV-T cells, indicating that they were all in the OFF state in the AV-T cells (**Fig. 2**).

To confirm the expression profile seen in the AV-T variant of our lab stock, a second variant designated AV-T.T1 was independently derived from a VIR-O colony, and expression of the entire panel of TTTR genes in Table 1 was examined by qRT-PCR analysis. Remarkably, when compared to the VIR-O parent, a different pattern of TTTR gene expression was observed in AV-T.T1, with only *1645* upregulated (**Fig 2**). As a control, the TTTR expression profile was similar between the two VIR-O isolates used to derive each AV-T, demonstrating that variations were occurring in the independent AV-T isolates. To determine if *1645* in the "ON" state was required to maintain AV-T.T1 cells in the AV-T form, an *ABUW_1645*::*T26* insertion was introduced into the AV-T.T1 cells. This mutation converted AV-T cells to the VIR-O state based on colony opacity and the restoration of 3-OH C_{12} HSL secretion (**Fig. S3**), indicating that *1645* expression was required to keep AV-T.T1 cells in the AV-T state and its activation in the VIR-O cell drove it to the AV-T state.

The TTTR expression pattern was then examined in a third independent AV-T variant, designated AV-T.T3, and this new variant exhibited a third distinct pattern of TTTR gene expression, where only *1959* was in the ON state and upregulated 19.2 ± 11-fold (**Fig. 2**). In AV-T.T3, introduction of an *ABUW_1959*::*T26* insertion converted cells back to the VIR-O state and restored 3-OH C_{12}-HSL production (**Fig. S3**). As expected, AV-T.T3 cells with *ABUW_1645::T26* or *ABUW_2818:T26* insertions remained in the AV-T state as these TTTRs were OFF in this isolate (**Fig. 2**). Therefore, *1959* expression was required to keep AV-T.T1 cells in the AV-T state.

A fourth independent AV-T variant (AV-T.T6) exhibited a pattern of TTTR gene expression that was distinct from the previous three variants, where *1645* and *2818* were in the ON state (**Fig. 2**). In this AV-T.T6 variant, introduction of individual T26 insertions into either *1645* or *2818* did not result in a conversion to the VIR-O state, indicating that expression of more than one TTTR was maintaining the AV-T state and further demonstrating the functional redundancy of these regulators.

TTTR expression profiles in AV-T cells are reset after passage through the VIR-O state.

In AV-T.T1, the *1645*::*T26* mutation converted cells back to the VIR-O state (**Fig. S3**). However, these VIR-O colonies now formed translucent sectors, indicating they were capable of switching back to the AV-T state, despite the fact that *1645* was no longer functional and its activation initially drove cells into the AV-T state. A similar result was observed in AV-T.T3, where the *1959*::*T26* mutation converted cells back to the VIR-O state, but these VIR-O cells were now capable of switching once again to the AV-T state. This indicated that cells in the new VIR-O state no longer relied on the previous set of TTTRs and activated a different TTTR to switch to the AV-T state.

To determine which TTTR was now activated to drive cells from the VIR-O to AV-T state, the TTTR expression profiles in two independent AV-T colonies derived from AV-T.T1 *1645*::*T26* (opaque) were measured by qRT-PCR. In the first AV-T variant, *2818* was now activated 38.8-fold (**Fig. S4A**). In the second AV-T variant, a new TTTR *ABUW_3353* (*3353*) was activated 34.5-fold (**Fig. S4B**). Interestingly, 3353 was previously identified based on the significant similarity to 1645 in the HTH region, and it was capable of driving VIR-O cells to the AV-T state when overexpressed (**Table 1**).

Next, the TTTR expression profiles in two independent AV-T colonies derived from AV-T.T3 *1959*::*T26* (opaque) were measured. In the first AV-T variant, *1645* was activated 188.9-fold (**Fig. S4C**). In the second AV-T variant, both *1645* and *2818* were now activated, 129.6-fold and 28.6-fold, respectively (**Fig. S4D**).

Role of 1645, 1959, and 2818 in switching between the VIR-O and AV-T states.

The above data demonstrated that 1645, 1959 and 2818 were functionally redundant in their ability to drive VIR-O cells to the AV-T state. To investigate a role in switching, individual null alleles were constructed in the *1959* and *2818* genes. However, neither mutation alone had an effect on VIR-O to AV-T switching (**Fig. 3**). The ratio of switching of a Δ*1959* mutant compared to wild-type was 1.06 and the ratio of a *2818*::*T26* mutant to wild-type was 1.01, which was similar to that previously reported for a *1645* deletion [14]. To determine if all three genes were required for the VIR-O to AV-T switch, a *2818*::*T26* insertion was introduced into a double mutant of *1645* and *1959* (VIR-O Δ*1645*/Δ*1959*) to make a triple mutant in the VIR-O background (VIR-O Δ*1645*/Δ*1959*/*2818*::*T26*). Surprisingly, this triple mutant only exhibited a 2.8-fold decrease in VIR-O to AV-T switching compared to wild-type cells **(Fig. 3).**

Deletion of *1645*, *1959*, and *2818* allows less utilized TTTRs to drive VIR-O to AV-T

We further attempted to construct a triple mutant of *1645*, *1959*, and *2818* in the AV-T background using the same method of moving the *2818*::*T26* into the AV-T Δ*1645*/Δ*1959* double mutant. However, this additional mutation forced the AV-T cells to immediately switch back to the VIR-O state, indicating *2818* as the TTTR that was maintaining the AV-T state in AV-T Δ*1645*/Δ*1959*. We allowed the triple mutants of these VIR-O colonies to sector and obtained a clone of AV-T Δ*1645*/Δ*1959*/*2818*::*T26*. Analysis of the TTTR expression profile in this mutant by qRT-PCR showed that *ABUW_1498* (*1498*) was increased 616-fold. Interestingly, 1498 is yet another TTTR with similarity to the HTH region of 1645, and overexpression of *1498* converts VIR-O cells to the AV-T state (**Table 1, Fig. S2**).

We next wanted to determine whether *1498* was the primary TTTR activated once *1645*, *1959*, and *2818* were nonfunctional. We isolated additional AV-T clones from the strain of VIR-O Δ*1645*/Δ*1959*/*2818*::*T26* that was constructed by introduction of the *2818*::*T26* into the VIR-O Δ*1645*/Δ*1959* double mutant, which had shown only a 2.8-fold decrease in switching (**Fig. 3**). For this experiment, we utilized practices recently identified in our lab that promote maintenance of the AV-T state and allow the currently active TTTRs to stay on. These practices include plating on LB (10 g tryptone, 5 g yeast extract, and 5 g NaCl per liter) containing 1.5% agar and incubating plates at room temperature. Six independent AV-T variants were isolated from VIR-O Δ*1645*/Δ*1959*/*2818*::*T26* colonies, and the expression profile for all the TTTR genes in Table 1 was determined by qRT-PCR. In all six AV-T triple mutant variants, a single TTTR, *ABUW_3353* (*3353*), was in the ON state relative to the VIR-O triple mutant. To determine whether expression of *3353* was required to keep cells in the AV-T state, a *3353*::*T26* insertion was moved into two

of the newly isolated AV-T triple mutant variants. In each case, the loss of *3353* reverted cells back to the VIR-O phenotype and (**Fig. S5**).

3353 is required to drive VIR-O to AV-T switch in the absence of *1645*, *1959*, and *2818*

Since *3353* was confirmed as the primary TTTR activated in the cells of the VIR-O Δ*1645*/Δ*1959*/*2818*::*T26* triple mutant that had switched to the AV-T state, it was predicted that loss of *3353* in this background would impact switching. Indeed, the quadruple mutant of *1645*, *1959*, *2818*, and *3353* exhibited levels of VIR-O to AV-T switching that were decreased an average of 1,245-fold compared to wild-type, a rate equivalent to approximately $1/10^5$ cells of the quadruple mutant (**Fig. 3**). This result demonstrated that *3353* is the TTTR responsible for maintaining the AV-T state when the most commonly used three TTTRs are unavailable.

Regulatory interactions among the TTTRs

The primary TTTRs driving the VIR-O to AV-T switch were 1645, 2818, 1959 and 3353 as indicated by the near complete loss of switching in the quadruple mutant (**Fig. 3**). To determine if regulatory interactions existed between these TTTRs, we measured expression of all twelve homologous TTTRs by qRT-PCR in backgrounds where (1) each of the four main TTTRs were overexpressed using the pWH1266 constructs (**Fig. S6**) and (2) each of the four main TTTRs was disrupted by T26 insertion (**Fig. S7**). Interesting neither of these conditions significantly affected transcription of any of the other TTTRs.

TTTRs often autoregulate [20, 21], so the possibility of autoregulation among the 1645, 1959, and 2818 was also examined by qRT-PCR. These experiments were conducted by probing the region between the predicted promoter and the ORF for *1645*, *1959*, or *2818* while

overexpressing the same TTTR in the pWH1266 construct. The primers targeted the region between the transcriptional start site, as identified by RNA sequencing mapping, and the coding region cloned in pWH1266, so that only expression of the chromosomal promoter site was measured. However, this analysis did not reveal autoregulation among the TTTRs (**Fig. S8**).

The implications of these unpublished results are discussed in

Chapter 6: Discussion on page 197.

Materials and Methods

Bacterial strains and growth conditions

Acinetobacter baumannii strain AB5075 [22] and its derivative strains were routinely grown at 37°C in modified Luria-Bertani (LB) agar or in LB broth stationary at room temperature (RT) or with shaking at 37°C when necessary. Regular agar plates (1xLB) contain 10 g tryptone, 5 g yeast extract, 5 g NaCl per liter and 1.5% agar. For distinguishing opaque and translucent phenotypes, the cells were plated in half strength LB (0.5xLB) constituted by 5 g tryptone, 2.5 g yeast extract, and 2.5 g NaCl per liter and 0.8% agar. Variable amounts of tryptone and yeast extract were used for the starvation assays plates, using 0.25xLB (5 g of tryptone and 2.5 g of yeast extract, 5 g NaCl per liter) or 0.125xLB (1.25 g tryptone and 0.625 g yeast extract, 5 g NaCl per liter) when required.

For counterselection of in-frame deletion mutants 1xLB without NaCl was used. Bacterial strains were stored at -80°C in 15% glycerol and pure stocks obtained as previously described [23]. To prevent opacity switching, VIR-O and AV-T cultures were grown overnight stationary at RT and not more than to OD_{600}: 1.0 (VIR-O) or OD_{600}: 0.8 (AV-T) when shaking at 37°C. Competent cells were prepared by growing the cells to an OD_{600}: 1.0 (VIR-O) or OD_{600}: 0.8 (AV-T) and pelleting them by centrifugation. The cells were washed twice with 1 mL of cold dH_2O and resuspended in 70 µL of cold dH_2O. After electroporation, the cells were recovered in 1mL of LB broth and grown stationary at 37°C followed by 1 hour shaking at 37°C. Freshly prepared competent cells were used for each transformation. *Escherichia coli* EC100 Transformax cells (Lucigen, Middleton, WI) were used for cloning procedures and transformants were selected with tetracycline (5 µg/mL), ampicillin (200 µg/mL) or hygromycin

(150 µg/mL) when required. *A. baumannii* transformants were selected with tetracycline (5 µg/mL) or hygromycin (150 µg/mL) as appropriate.

The pEX18Tc plasmid [24] was used for allelic replacement in *A. baumannii* AB5075, the pWH1266 plasmid [25] was used for overexpression of the target genes.

In silico protein analysis

The amino acid sequence of the proteins annotated as TetR-type transcriptional regulators in the *A. baumannii* AB5075 strain genome were obtained from the NCBI database (GenBank accession number: CP008706.1). The protein sequence alignment of the selected TetR transcriptional regulators proteins was generated using the Clustal Omega website (www.ebi.ac.uk/Tools/msa/clustalo/). The analysis of the secondary structure of the proteins to identify the helix-turn-helix region was carried out using the SOPMA website (npsa-prabi.ibcp.fr/cgi-bin/npsa_automat.pl?page=/NPSA/npsa_sopma.html) and then the sequence similarity analysis of this region was performed using the Clustal Omega website.

Construction of in-frame deletions.

The single or combined in-frame deletion mutant strains of the TetR transcriptional regulators, *ABUW_1645*, *ABUW_1959*, and *ABUW_2818*, were generated as previously described (3). Briefly, approximately 1 kb upstream and downstream fragments containing small portions of the target gene were amplified from the *A. baumannii* AB5075 genome by PCR with the Phusion High-Fidelity DNA Polymerase (Thermo-Fisher Scientific, Waltham, MA). The mutant strains contain deletions corresponding to amino acids 10 to 181 for Δ*1645*, 3 to 208 for Δ*1959*, and 0 to 185 for Δ*2818*. The oligonucleotide pairs used are listed in **Supplementary Table 1**.

The oligonucleotides Up 1 and Down 2 of each set contain *BamHI* restriction sites at the 5' end, except the *ABUW_2818* Up1 and Down 2 pair. In each case, the upstream and downstream fragments were ligated together using the Fast-Link DNA Ligation Kit (Lucigen, Middleton, WI). The resulting fragment of approximately 2 kb was cloned into the *BamHI* site of the pEX18Tc suicide vector. In the case of the *ABUW_2818* fragment, it was cloned into the *SmaI* site. 1 µL of the ligation was transformed into EC100 Transformax cells (Lucigen, Middleton, WI), and selection carried out on 5 µg/mL tetracycline 1xLB plates. The pEX18TcΔ*TetR* vector was introduced into both VIR-O and AV-T *A. baumannii* AB5075 competent cells prepared by washing them twice with dH_2O. The integrant clones were selected on 5 µg/mL tetracycline 1xLB plates at 28°C to prevent cells from switching in the case of the AV-T derivative mutants. Then, counterselection was performed at RT on LB without NaCl and LB without NaCl supplemented with 10% sucrose. Potential mutant clones were screened by PCR using their respective Up 1 and Down 2 oligonucleotide set. Pure cultures of each mutant were obtained as previously described [23].

Construction of strains with T26 transposon insertions.

The T26 insertions were obtained from the transposon mutant library created by Colin Manoil's group at the University of Washington [26]. Cultures of the target insertions were grown overnight at 37°C shaking, centrifuged and the supernatant was filtered using a 0.22 µm pore filter to obtain the phage lysate. 10 µL of the recipient strain grown until an OD_{600}: 0.5 and 10 µL of the lysate were spotted on the surface of a 2 hour-dried 1xLB plate and incubated at 37°C. After 4 hours, the cells were recovered from the plate and resuspended in 1 mL of LB broth. The transductions were plated in 5 µg/mL tetracycline 1xLB plates. Both a negative

control of only the recipient strain cells and other of only the lysate were included. All the insertions were verified by PCR using primers located outside the target gene.

Overexpression of TetR transcriptional regulators

Each of the 10 TetR transcriptional regulators was cloned into the pWH1266 expression vector that was previously digested with *ScaI*. All the constructs contain the full-length gene and a short upstream region from the start codon and a short downstream region from the stop codon of the gene. Each of the fragments was amplified by PCR using the Phusion High-Fidelity DNA Polymerase (Thermo-Fisher Scientific, Waltham, MA). For this PCR, the respective Exp1 and Exp2 oligonucleotides pair listed in Table X and the genomic DNA of *A. baumannii* AB5075 as template were used. The fragment was gel-purified from an agarose gel using the Monarch DNA Gel Extraction Kit (New England Biolabs, Ipswich, MA) and ligated with the *ScaI* digested vector using the Fast-Link Ligation Kit (Lucigen, Middleton, WI). 1 µL of the ligation was transformed into *E. coli* Transformax EC100D competent cells (Lucigen, Middleton, WI) and plated in 5µL/mL tetracycline 1xLB plates. The transformant clones were screened for tetracycline resistance and ampicillin sensitivity and the plasmids with insert were confirmed by DNA sequencing (Genewiz, South Plainfield, NJ). The pWH1266 + *TetR* vectors and the empty pWH1266 vector were transformed into *A. baumannii* AB5075 VIR-O and AV-T competent cells prepared by washing the cells twice with dH_2O. The transformants were selected in 5µL/mL tetracycline 1xLB plates. For determining the opacity of the strains harboring the TetR overexpression plasmids, two colonies from each transformation were grown in LB broth with 5µL/mL tetracycline until turbid and streaked in 0.5xLB plates.

After 24 hours, the opacity phenotype was determined by viewing the cells under a stereo microscope with oblique lighting.

VIR-O and AV-T switching assays

For assessing the opacity switching frequency, tenfold serial dilutions from the frozen stocks of each of the strains were plated in 20 mL 1 hour-dried 0.5xLB plates. Initial dilutions plates were incubated at 37°C. After 24 hours, six well-isolated colonies were lifted as agar plugs from low colony density plates (<50 colonies) and resuspended in 1 mL of LB broth. Serial dilutions were plated in 0.5xLB and incubated at 37°C overnight. The number of each VIR-O and AV-T variant was determined on four independent random sectors of the 10^{-5} plate using a stereo microscope with oblique lighting. The switching frequency was assessed for each initial colony as the total number of colonies of the opposite opacity phenotype divided by the total number of colonies of both phenotypes and expressed as a percentage.

Surface motility assays

Surface motility assays were carried out as previously described [27]. Briefly, a 1-µl drop of the strains grown in LB broth until OD_{600}: 0.5 was inoculated onto a 30 minutes-dried 0.35% Eiken agar motility plate prepared the same day of the experiment. The strains to be compared were spotted on the same motility plates. The plates were incubated at 37°C until the control strain reached the plate border, approximately 8 h. Motility diameters were measured and relative migration determined by calculating the ratio of the motility diameter of the strain of interest to that of the control strain. The differences in motility between strains were determined using the Student's *t* test. All assays were carried out a minimum of two times.

HSL production assays

The HSL secretion of the strains of study was assessed using the soft agar lawn assay [28]. In this method, an *Agrobacterium tumefaciens* biosensor strain containing a plasmid-localized *traG-lacZ* fusion (pZLR4) is utilized. The exogenous HSL produced by *A. baumannii* bind to TraR and coactivates *traG* resulting in the production of β-galactosidase giving rise to the appearance of a blue halo. The soft-agar plates were prepared by adding 60 µL of 20 µg/mL X-gal and 120 µL of an *A. tumefaciens* culture (grown overnight stationary at 28°C in 30 µg/mL gentamicin LB broth) to 20 mL of 0.5xLB cooled to 45°C. The plates were allowed to dry for 30 minutes before use. Strains to test were grown shaking in LB broth medium at 37°C until an OD_{600}: 0.5. A 1 µL drop of each strain was spotted onto the soft-agar plates and incubated at 28°C overnight. The presence of blue halo was determined, and significant images of each experiment were taken. All the assays were carried out a minimum of two times.

RNA Isolation

Bacterial cultures of the strains of interest were grown in 2mL of LB broth at 37°C with shaking to an OD_{600}: 0.5. Cells were collected by centrifugation and RNA was isolated using the MasterPure RNA Purification Kit (Lucigen, Middleton, WI) following the manufacturer's instructions. The total RNA extraction was subjected to two Turbo DNA-free treatments (Thermo-Fisher Scientific, Waltham, MA) to remove contaminating DNA according to the manufacturer's protocol. Absence of DNA was tested by 40xcycles PCR using the RNA samples as template. RNA concentration was measured with a Nanodrop ND-100 spectrophotometer.

Quantitative real-time PCR

cDNA was synthesized from 1 µg of the purified RNA of the strains of interest using the iScript Select cDNA Synthesis Kit (Bio-Rad, Hercules, CA) with random primers. Negative controls were carried out by including reactions without reverse transcriptase. The cDNA synthesis was performed following the cycling parameters: 25°C for 5 min, 42°C for 45 min, and 85°C for 5 min. Reverse transcriptase quantitative PCR (qRT-PCR) was used to assess the expression level of the genes of interest. Diluted cDNAs (1:10 dilution with dH_2O water) were used as template and iQ SYBR Green Supermix (Bio-Rad, Hercules, CA) as fluorescent dye mix. The oligonucleotide pairs were designed to amplify fragments of approximately 150 bp of the gene of study and they were generated using the NCBI Primer-BLAST website (www.ncbi.nlm.nih.gov/tools/primer-blast). The oligonucleotide pairs used for each gene are listed in Table X as qRT-PCR 1 and qRT-PCR 2 primers. The Bio-Rad CFX Connect cycler was used following the program: 95°C for 3 min, followed by 40 cycles of 95°C for 10 s, 55°C for 10 s, and 72°C for 20 s. Three independent biological replicates were analyzed. The fold changes in gene expression were calculated using the threshold cycle ($2-\Delta\Delta CT$) method (9) comparing target gene expression with housekeeping gene (*16S*) expression.

References

1. Peleg, A.Y. et al. (2008) Acinetobacter baumannii: emergence of a successful pathogen. Clin Microbiol Rev 21 (3), 538-82.

2. Lee, C.R. et al. (2017) Biology of Acinetobacter baumannii: Pathogenesis, Antibiotic Resistance Mechanisms, and Prospective Treatment Options. Front Cell Infect Microbiol 7, 55.

3. Ayoub Moubareck, C. and Hammoudi Halat, D. (2020) Insights into Acinetobacter baumannii: A Review of Microbiological, Virulence, and Resistance Traits in a Threatening Nosocomial Pathogen. Antibiotics (Basel) 9 (3).

4. Centers for Disease, C. and Prevention (2004) Acinetobacter baumannii infections among patients at military medical facilities treating injured U.S. service members, 2002-2004. MMWR Morb Mortal Wkly Rep 53 (45), 1063-6.

5. Centers for Disease Control and Prevention (2019) Antibiotic Resistance Threats in the United States, 2019. Atlanta, GA. https://www.cdc.gov/drugresistance/pdf/threats-report/2019-ar-threats-report-508.pdf, (accessed August 2 2021).

6. Clark, N.M. et al. (2016) Emergence of antimicrobial resistance among Acinetobacter species: a global threat. Curr Opin Crit Care 22 (5), 491-9.

7. World Health Organization (2017) Global Priority List of Antibiotic-Resistant Bacteria to Guide Research, Discovery, and Development of New Antibiotics. https://www.who.int/medicines/publications/WHO-PPL-Short_Summary_25Feb-ET_NM_WHO.pdf, (accessed August 2 2021).

8. Jawad, A. et al. (1998) Survival of Acinetobacter baumannii on dry surfaces: comparison of outbreak and sporadic isolates. J Clin Microbiol 36 (7), 1938-41.

9. Rocha, I.V. et al. (2018) Multidrug-resistant Acinetobacter baumannii clones persist on hospital inanimate surfaces. Braz J Infect Dis 22 (5), 438-441.

10. Chapartegui-Gonzalez, I. et al. (2018) Acinetobacter baumannii maintains its virulence after long-time starvation. PLoS One 13 (8), e0201961.

11. D'Souza, A.W. et al. (2019) Spatiotemporal dynamics of multidrug resistant bacteria on intensive care unit surfaces. Nat Commun 10 (1), 4569.

12. Bravo, Z. et al. (2019) Analysis of Acinetobacter baumannii survival in liquid media and on solid matrices as well as effect of disinfectants. J Hosp Infect 103 (1), e42-e52.

13. Tipton, K.A. et al. (2015) Phase-Variable Control of Multiple Phenotypes in Acinetobacter baumannii Strain AB5075. J Bacteriol 197 (15), 2593-9.

14. Chin, C.Y. et al. (2018) A high-frequency phenotypic switch links bacterial virulence and environmental survival in Acinetobacter baumannii. Nat Microbiol 3 (5), 563-569.

15. Tipton, K.A. et al. (2018) Role of Capsule in Resistance to Disinfectants, Host Antimicrobials, and Desiccation in Acinetobacter baumannii. Antimicrob Agents Chemother 62 (12).

16. Tipton, K.A. and Rather, P.N. (2016) An ompR/envZ Two-Component System Ortholog Regulates Phase Variation, Osmotic Tolerance, Motility, and Virulence in Acinetobacter baumannii strain AB5075. J Bacteriol.

17. Tipton, K.A. et al. (2017) Multiple roles for a novel RND-type efflux system in Acinetobacter baumannii AB5075. Microbiologyopen 6 (2).

18. Anderson, S.E. et al. (2020) Copy Number of an Integron-Encoded Antibiotic Resistance Locus Regulates a Virulence and Opacity Switch in Acinetobacter baumannii AB5075. mBio 11 (5).

19. Tierney, A.R.P. et al. (2021) A LysR-Type Transcriptional Regulator Controls Multiple Phenotypes in Acinetobacter baumannii. Frontiers in Cellular and Infection Microbiology 11 (1076).

20. Cuthbertson, L. and Nodwell, J.R. (2013) The TetR family of regulators. Microbiol Mol Biol Rev 77 (3), 440-75.

21. Ramos, J.L. et al. (2005) The TetR family of transcriptional repressors. Microbiol Mol Biol Rev 69 (2), 326-56.

22. Jacobs, A.C. et al. (2014) AB5075, a Highly Virulent Isolate of Acinetobacter baumannii, as a Model Strain for the Evaluation of Pathogenesis and Antimicrobial Treatments. mBio 5 (3), e01076-14.

23. Anderson, S.E. and Rather, P.N. (2019) Distinguishing Colony Opacity Variants and Measuring Opacity Variation in Acinetobacter baumannii. Methods Mol Biol 1946, 151-157.

24. Hoang, T.T. et al. (1998) A broad-host-range Flp-FRT recombination system for site-specific excision of chromosomally-located DNA sequences: application for isolation of unmarked Pseudomonas aeruginosa mutants. Gene 212 (1), 77-86.

25. Hunger, M. et al. (1990) Analysis and nucleotide sequence of an origin of DNA replication in Acinetobacter calcoaceticus and its use for Escherichia coli shuttle plasmids. Gene 87 (1), 45-51.

26. Gallagher, L.A. et al. (2015) Resources for Genetic and Genomic Analysis of Emerging Pathogen Acinetobacter baumannii. J Bacteriol 197 (12), 2027-35.

27. Perez-Varela, M., Tierney, A.R.P., Kim, J., Vazquez-Torres, A., Rather, P.N. (2020) Characterization of RelA in *Acinetobacter baumannii*. Journal of Bacteriology.

28. Paulk Tierney, A.R. and Rather, P.N. (2019) Methods for Detecting N-Acyl Homoserine Lactone Production in Acinetobacter baumannii. Methods Mol Biol 1946, 253-258.

Table 1: Phenotypes of VIR-O cells overexpressing TTTRs.

TTTR	Opacity	QS Signal Secretion	Motility
ABUW_1645	Translucent (AV-T)	-	-
ABUW_2818	Translucent (AV-T)	-	+
ABUW_1959	Translucent (AV-T)	-	+/-
ABUW_3353	Translucent (AV-T)	-	-
ABUW_2596	Translucent (AV-T)	-	-
ABUW_1498	Translucent (AV-T)	-	-
ABUW_3194	Translucent (AV-T)	-	+
ABUW_1163	Translucent (AV-T)	-	-
ABUW_0939	Translucent (AV-T)	-	-
ABUW_0222	Translucent (AV-T)	-	-
ABUW_2629	Translucent (AV-T)	-	+
ABUW_1912	Translucent (AV-T)	-	-

The translucent colony morphotype that results from overexpression of a subpopulation of TetR-type transcriptional regulators in VIR-O exhibits additional AV-T associated phenotypes including a decrease in 3-OH C_{12}-HSL secretion and, in most cases, reduced surface-associated motility. Explanation of symbols: "-" and "+" signs indicate reduced or increased, respectively, 3-OH C_{12}-HSL secretion or reduced motility relative to a VIR-O empty vector (pWH1266) control; "+/-" indicates similar levels to the VIR-O vector control.

Figure Legends

Figure 1: Phenotypes associated with overexpression of *1645, 1959,* and *2818*.

(A) Overexpression of *1645, 1959,* and *2818* in VIR-O causes cells to switch to the AV-T state. Colonies on the left are VIR-O + pWH1266 (empty vector control). Colonies on the right contain pWH1266 constructs overexpressing each TTTR. These constructs were used in all assays shown in this figure. **(B)** Overexpression of *1645, 1959,* and *2818* in VIR-O results in a reduction of surface-associated motility. The motility for each VIR-O + pWH1266/TTTR construct was measured on 0.3% Eiken agar plates relative to a VIR-O + pWH1266 control. Proportion of the distance migrated by each construct relative to the vector control is shown. **(C)** Overexpression of *1645, 1959,* and *2818* in VIR-O results in a loss of 3-OH C_{12}-HSL secretion, qualitatively measured on a soft agar lawn containing *Agrobacterium tumefaciens* with a p*traG*::*LacZ* fusion and X-Gal. **(D)** Strains overexpressing *1959* and *2818* in VIR-O were intranasally inoculated into mice. At 24 hours post-infection, the lungs were harvested, homogenized, and CFU/g determined. The CFU/g of bacteria recovered for the overexpression strains were not significantly different from the vector control.

Figure 2: TTTR activation profiles during VIR-O to AV-T switching. Each AV-T variant shown (AV-T Variant Lab Stock, AV-T.T1, AV-T.T3, and AV-T.T6) was derived from a unique VIR-O sector. The TTTRs that were transcriptionally activated ("ON") in each AV-T were identified by qRT-PCR by comparison to the parent VIR-O and *16S* internal control. In the AV-T Variant Lab Stock, *1645, 1959,* and *2818* were ON, and disruption of any one of these genes by T26 does not alter the opacity phenotype. In AV-T.T1, only *1645* is ON, and introduction of

T26 into this gene results in the inability to maintain the AV-T state and a complete switch to VIR-O. In AV-T.T3, only *1959* is ON, and the disruption of *1959* by *T26* causes a switch to VIR-O. Controls of *1645*::*T26* and *2818*::*T26* in this strain do not change the opacity phenotype. In AV-T.T26, *1645* and *2818* are ON, and neither the *1645*::*T26* and *2818*::*T26* insertions alone cause a reversal to the VIR-O state. Error bars indicated standard error.

Figure 3: Analysis of VIR-O to AV-T switching frequencies in TTTR single, triple, and quadruple mutants. Single deletions of *1959* and *2818* do not significantly affect rates of VIR-O to AV-T switching. A triple mutant ("3KO" = VIR-O Δ*1645*/Δ*1959*/*2818*::*T26*) exhibits a 2.8-fold decrease in switching relative to wild-type VIR-O (*, $p < .05$ as assessed by Mann-Whitney test). A quadruple mutant ("4KO" = VIR-O Δ*1645*/Δ*1959*/*2818*::*T26scar*/*3353*::*T26*) shows a 1,245-fold decrease in switching relative to wild-type VIR-O (**, $p = 0.0001$ to 0.001 as assessed by one-way ANOVA with Welch's Correction). All assays represent the averages of six colonies extracted at 24 hours of growth. Error bars indicate standard deviation of the mean.

Supplementary Figure 1: *ABUW_1645* overexpression converts other *A. baumannii* strains from VIR-O to AV-T. (A) VIR-O and AV-T cells at the same OD_{600} were spotted onto a soft agar lawn containing the *Agrobacterium tumefaciens* biosensor (p*traG*::*lacZ*) and X-Gal. The smaller blue halo around the AV-T cells demonstrates the decrease in of 3-OH C_{12}-HSL secretion in AV-T. **(B)** Overexpression of *1645* in VIR-O backgrounds of the *Acinetobacter baumannii* clinical isolates AB5075, 2050, P2A, EH3, and AB0057 all demonstrate a shift from VIR-O to AV-T. Further, all isolates exhibit a reduction or loss of 3-OH C_{12}-HSL secretion, and all isolates except AB0057 display decreased motility.

Supplementary Figure 2: The DNA-binding HTH region of 1645 is highly homologous to eleven other TetR-type transcriptional regulators in AB5075.

Supplementary Figure 3: Phenotypes of inactivating a TTTR in the ON state in AV-T cells. (Top) In AV-T.T1, *1645* was identified as the only TTTR that activated to cause a switch from VIR-O to AV-T (Fig. 2). Introduction of *T26* into *1645* forces cells to switch back to VIR-O and restores 3-OH C_{12}-HSL secretion, as shown by activation of the *A. tumefaciens* p*traG*::*lacZ* fusion. **(Bottom)** Disruption of *1959* in AV-T.T3 by *T26*, in which *1959* had activated the VIR-O to AV-T switch (Fig. 2), also results in a switch back to VIR-O and restored 3-OH C_{12}-HSL secretion.

Supplementary Figure 4: Passage through the VIR-O state allows TetR-type transcriptional regulators (TTTRs) to reset. (A, B) Introduction of *1645*::*T26* into AV-T.T1 caused cells to switch to the VIR-O state (Fig. S3). Colonies of these VIR-O cells were allowed to grow and sector, and two new AV-T variants were obtained. qRT-PCR analysis showed transcriptional activation of *2818* in the first variant (A), and *3353* in the second variant (B). **(C, D)** Introduction of *1959*::*T26* into AV-T.T3 also caused cells to switch to the VIR-O state (Fig. S3), and two new AV-T variants were derived from VIR-O sectors. qRT-PCR analysis revealed that *1645* had activated in the first variant (C), and both *1645* and *2818* had activated in the second variant (D).

Supplementary Figure 5: Introduction of a *3353*::*T26* insertion in the triple mutant AV-T Δ*1645*/Δ*1959*/*2818*::*T26scar* forces a switch back to the VIR-O state, evidenced by the change in colony opacity and the restoration of 3-OH C_{12}-HSL secretion.

Supplementary Figure 6: Analysis of inter-regulation between TTTRs by overexpression of TTTRs in the AV-T background. Each of the four main TTTRs—*1645, 1959, 2818*, and *3353*—were cloned into the pWH1266 ScaI site, which puts inserted genes under control of the β-lactamase promoter, leading to strong overexpression. Empty pWH1266 vector controls and pWH1266/TTTR constructs were transformed into AV-T cells. Expression levels of all eleven other TTTRs were then measured by qRT-PCR, comparing the overexpression strain to the vector control strain and internal control *16S*. The value shown for each overexpression strain represents the average $2^{-\Delta\Delta Ct}$ of three biological replicates. Error bars indicated standard deviation of the mean. This analysis showed no significant differences in TTTR expression when one of the four main TTTRs is overexpressed as measured by multiple Mann-Whitney tests.

Supplementary Figure 7: Analysis of inter-regulation between TTTRs in single mutants of *1645, 1959, 2818,* and *3353* in the AV-T background. Expression levels of TTTRs were measured by qRT-PCR in strains of AV-T *1645*::*T26*, AV-T *1959*::*T26*, AV-T *2818*::*T26*, and AV-T *3353*::*T26* compared to a wild-type AV-T control strain and a *16S* internal control. The value shown for each overexpression strain represents the average $2^{-\Delta\Delta Ct}$ of two biological replicates. Error bars indicated standard deviation of the mean. This analysis showed no significant differences in TTTR expression when one of the four main TTTRs is overexpressed as measured by multiple Mann-Whitney tests.

Supplementary Figure 8: Analysis of autoregulation of *1645*, *1959*, and *2818*. Two sets of primers were designed to probe the region upstream of each of *1645*, *1959*, and *2818*, between the predicted transcriptional start site (TSS) and the coding region. The "Up A" and "Up B" primers target two portions of the upstream region, with the "Up A" primer probing further upstream and closer to the TSS than the "Up B" primer. These primers were used in qRT-PCR experiments to measure expression of these upstream regions when the same TTTR was being overexpressed in the pWH1266 construct. Autoregulation of *1959* and *2818* were both assayed in strains of AV-T containing either a vector control or the overexpression construct, and each value shown represents the average of three biological replicates. Autoregulation of *1645* was assayed in both VIR-O and AV-T containing either a vector control or the overexpression construct, and each value shown represents a single independent experiment. For *1645* experiments, the fold changes when *1645* was overexpressed are less than two, which does not implicate autoregulation. For *1959* and *2818* experiments, multiple Mann-Whitney tests determined no significant changes in the upstream regions of the TTTRs when the same TTTR was overexpressed.

Supplementary Table 1: Oligonucleotides used in this study.

Figure 1

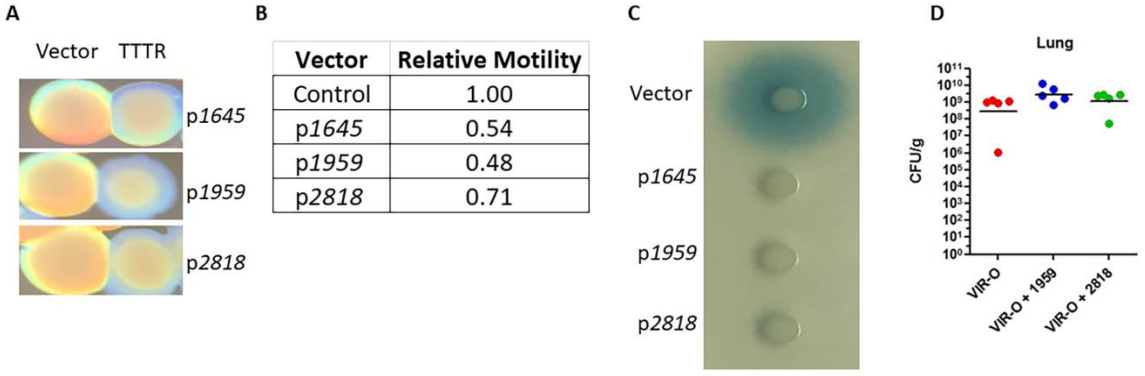

Figure 1: Phenotypes associated with overexpression of *1645, 1959,* and *2818*.

(A) Overexpression of *1645*, *1959*, and *2818* in VIR-O causes cells to switch to the AV-T state. Colonies on the left are VIR-O + pWH1266 (empty vector control). Colonies on the right contain pWH1266 constructs overexpressing each TTTR. These constructs were used in all assays shown in this figure. **(B)** Overexpression of *1645*, *1959*, and *2818* in VIR-O results in a reduction of surface-associated motility. The motility for each VIR-O + pWH1266/TTTR construct was measured on 0.3% Eiken agar plates relative to a VIR-O + pWH1266 control. Proportion of the distance migrated by each construct relative to the vector control is shown. **(C)** Overexpression of *1645*, *1959*, and *2818* in VIR-O results in a loss of 3-OH C_{12}-HSL secretion, qualitatively measured on a soft agar lawn containing *Agrobacterium tumefaciens* with a p*traG*::*LacZ* fusion and X-Gal. **(D)** Strains overexpressing *1959* and *2818* in VIR-O were intranasally inoculated into mice. At 24 hours post-infection, the lungs were harvested, homogenized, and CFU/g determined. The CFU/g of bacteria recovered for the overexpression strains were not significantly different from the vector control.

Figure 2

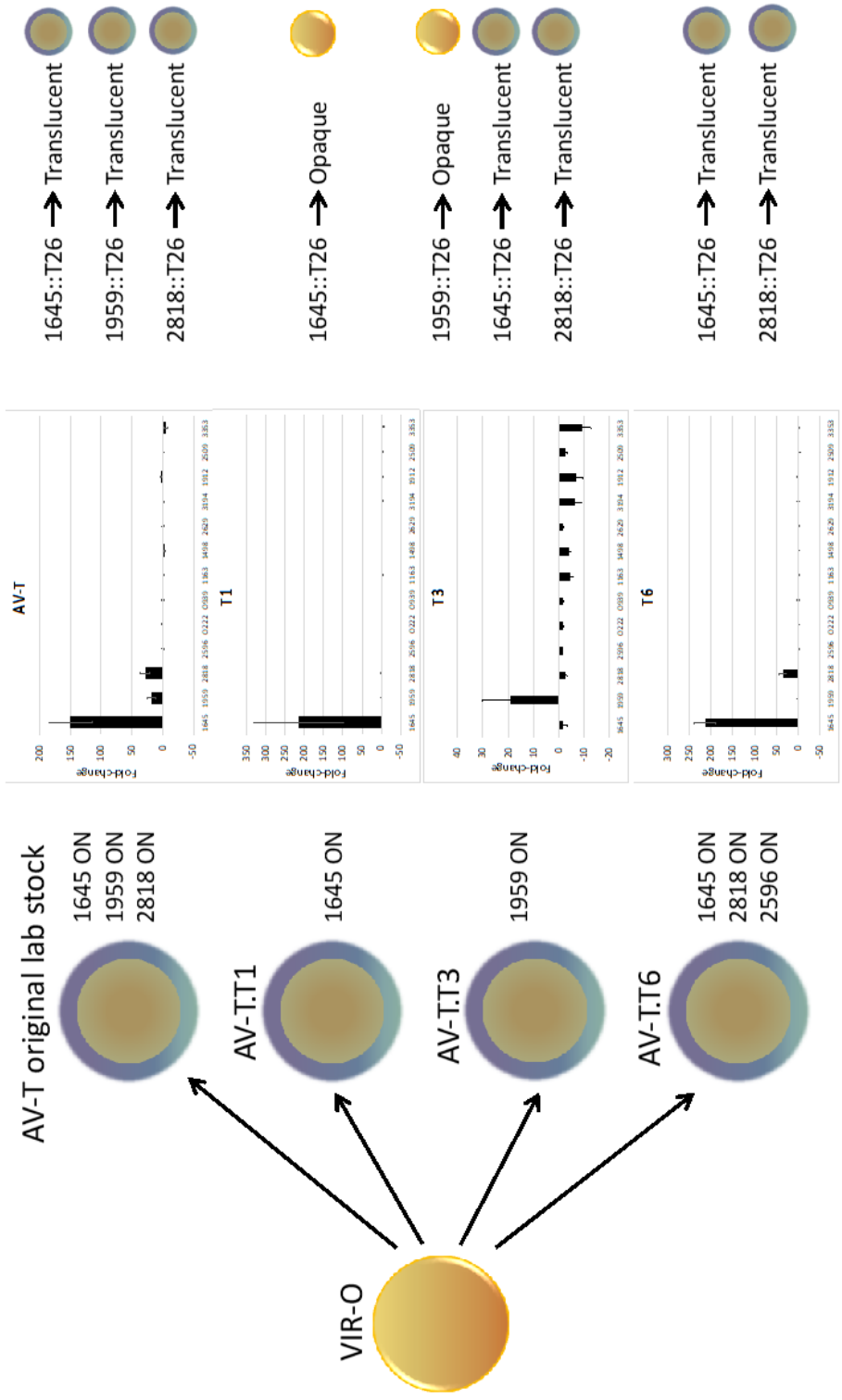
AV-T original lab stock
1645 ON
1959 ON
2818 ON
AV-T.T1
1645 ON
AV-T.T3
1959 ON
AV-T.T6
1645 ON
2818 ON
2596 ON
VIR-O
1645::T26 → Translucent
1959::T26 → Translucent
2818::T26 → Translucent
1645::T26 → Opaque
1959::T26 → Opaque
1645::T26 → Translucent
2818::T26 → Translucent
1645::T26 → Translucent
2818::T26 → Translucent
AV-T
T1
T3
T6
Fold-change

Figure 2: TTTR activation profiles during VIR-O to AV-T switching. Each AV-T variant shown (AV-T Variant Lab Stock, AV-T.T1, AV-T.T3, and AV-T.T6) was derived from a unique VIR-O sector. The TTTRs that were transcriptionally activated ("ON") in each AV-T were identified by qRT-PCR by comparison to the parent VIR-O and *16S* internal control. In the AV-T Variant Lab Stock, *1645*, *1959*, and *2818* were ON, and disruption of any one of these genes by T26 does not alter the opacity phenotype. In AV-T.T1, only *1645* is ON, and introduction of *T26* into this gene results in the inability to maintain the AV-T state and a complete switch to VIR-O. In AV-T.T3, only *1959* is ON, and the disruption of *1959* by *T26* causes a switch to VIR-O. Controls of *1645*::*T26* and *2818*::*T26* in this strain do not change the opacity phenotype. In AV-T.T26, *1645* and *2818* are ON, and neither the *1645*::*T26* and *2818*::*T26* insertions alone cause a reversal to the VIR-O state. Error bars indicate standard error.

Figure 3

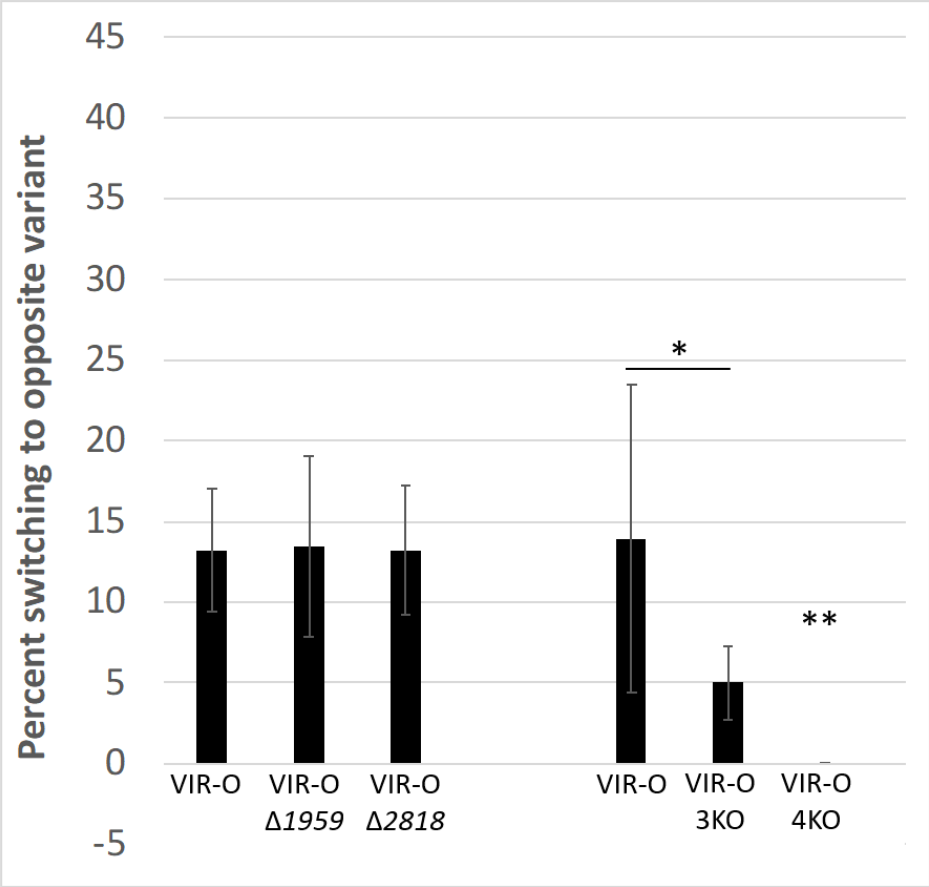

Figure 3: Analysis of VIR-O to AV-T switching frequencies in TTTR single, triple, and quadruple mutants. Single deletions of *1959* and *2818* do not significantly affect rates of VIR-O to AV-T switching. A triple mutant ("3KO" = VIR-O Δ*1645*/Δ*1959*/*2818*::*T26*) exhibits a 2.8-fold decrease in switching relative to wild-type VIR-O (*, $p < .05$ as assessed by Mann-Whitney test). A quadruple mutant ("4KO" = VIR-O Δ*1645*/Δ*1959*/*2818*::*T26scar*/*3353*::*T26*) shows a 1,245-fold decrease in switching relative to wild-type VIR-O (**, $p = 0.0001$ to 0.001 as assessed by one-way ANOVA with Welch's Correction). All assays represent the averages of six colonies extracted at 24 hours of growth. Error bars indicate standard deviation of the mean.

Supplementary Figure 1

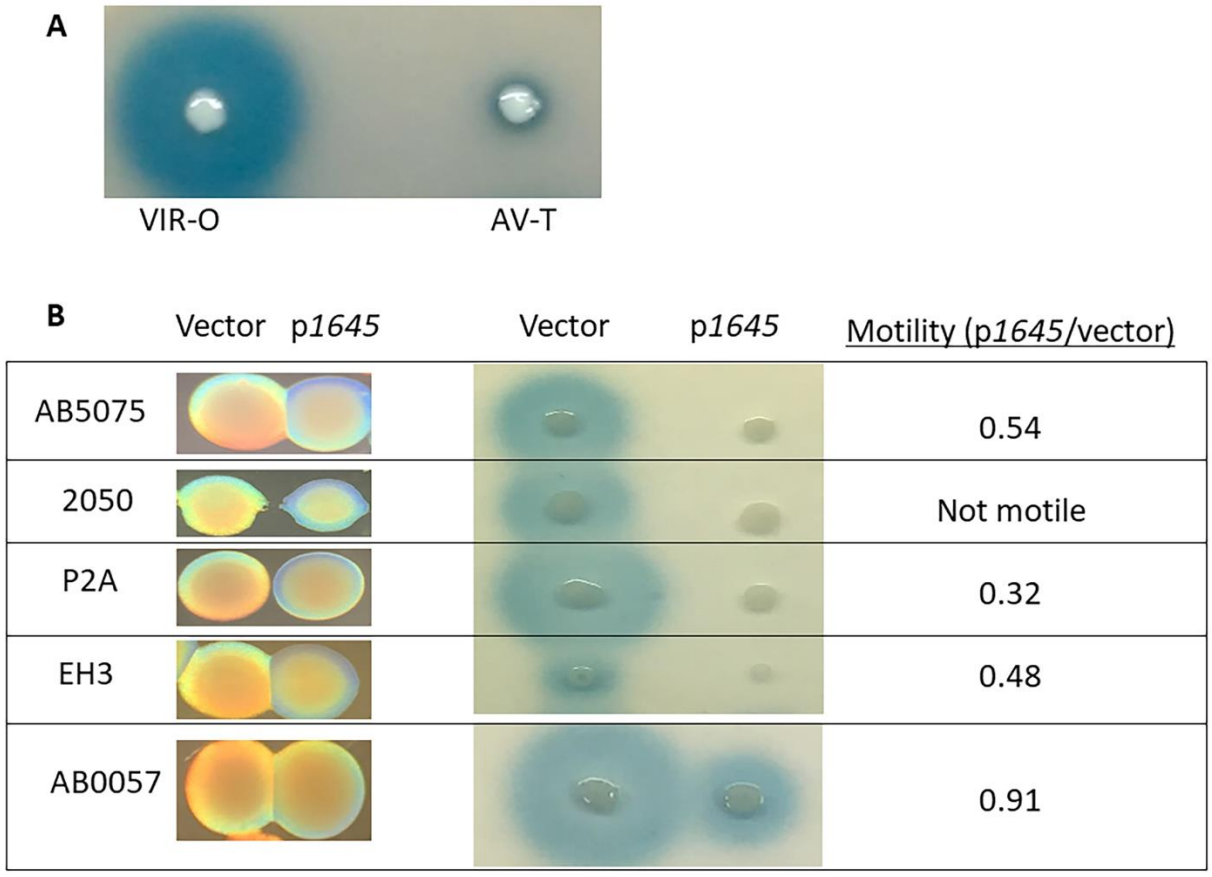

Supplementary Figure 1: *ABUW_1645* overexpression converts other *A. baumannii* strains from VIR-O to AV-T. (A) VIR-O and AV-T cells at the same OD_{600} were spotted onto a soft agar lawn containing the *Agrobacterium tumefaciens* biosensor (p*traG*::*lacZ*) and X-Gal. The smaller blue halo around the AV-T cells demonstrates the decrease in of 3-OH C_{12}-HSL secretion in AV-T. **(B)** Overexpression of *1645* in VIR-O backgrounds of the *Acinetobacter baumannii* clinical isolates AB5075, 2050, P2A, EH3, and AB0057 all demonstrate a shift from VIR-O to AV-T. Further, all isolates exhibit a reduction or loss of 3-OH C_{12}-HSL secretion, and all isolates except AB0057 display decreased motility.

Supplementary Figure 2

Supplementary Figure 2: The DNA-binding HTH region of 1645 is highly homologous to eleven other TetR-type transcriptional regulators in AB5075.

Supplementary Figure 3

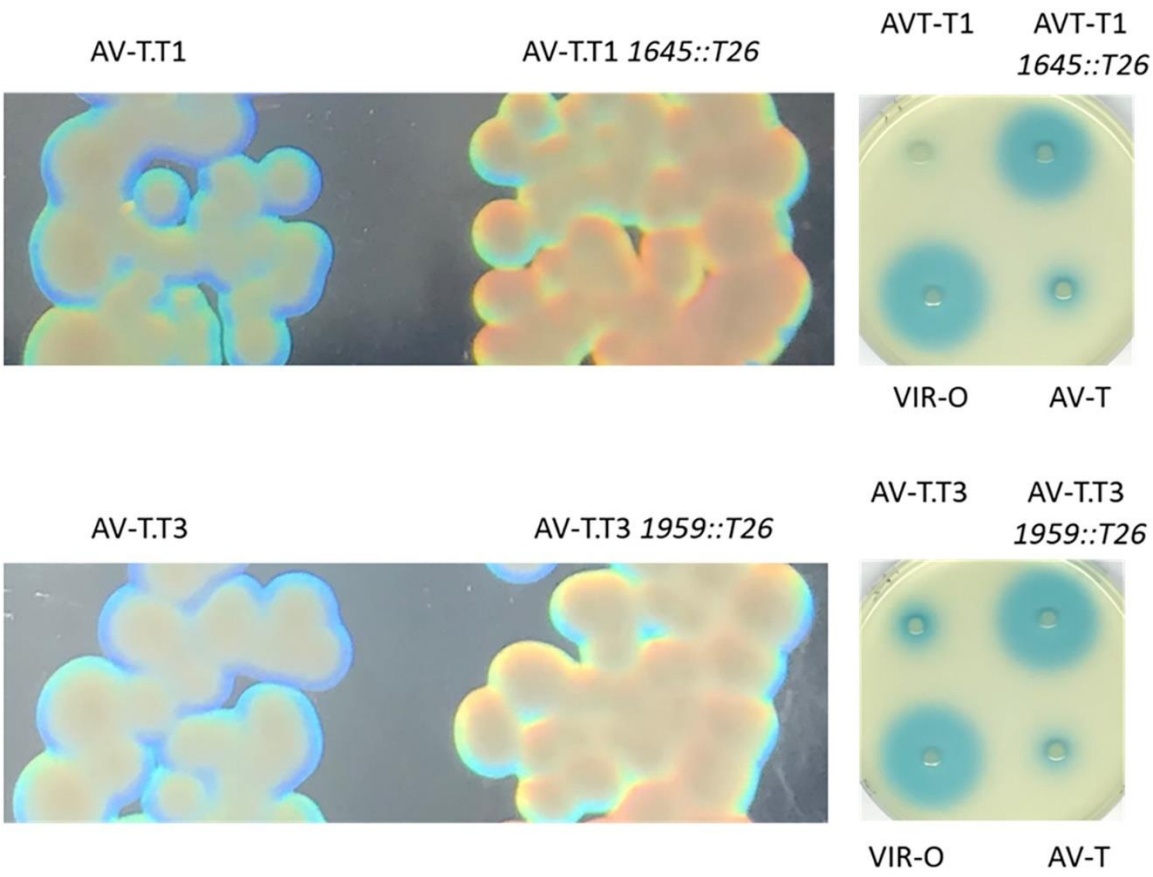

Supplementary Figure 3: Phenotypes of inactivating a TTTR in the ON state in AV-T cells. **(Top)** In AV-T.T1, *1645* was identified as the only TTTR that activated to cause a switch from VIR-O to AV-T (Fig. 2). Introduction of *T26* into *1645* forces cells to switch back to VIR-O and restores 3-OH C_{12}-HSL secretion, as shown by activation of the *A. tumefaciens* p*traG*::*lacZ* fusion. **(Bottom)** Disruption of *1959* in AV-T.T3 by *T26*, in which *1959* had activated the VIR-O to AV-T switch (Fig. 2), also results in a switch back to VIR-O and restored 3-OH C_{12}-HSL secretion.

Supplementary Figure 4

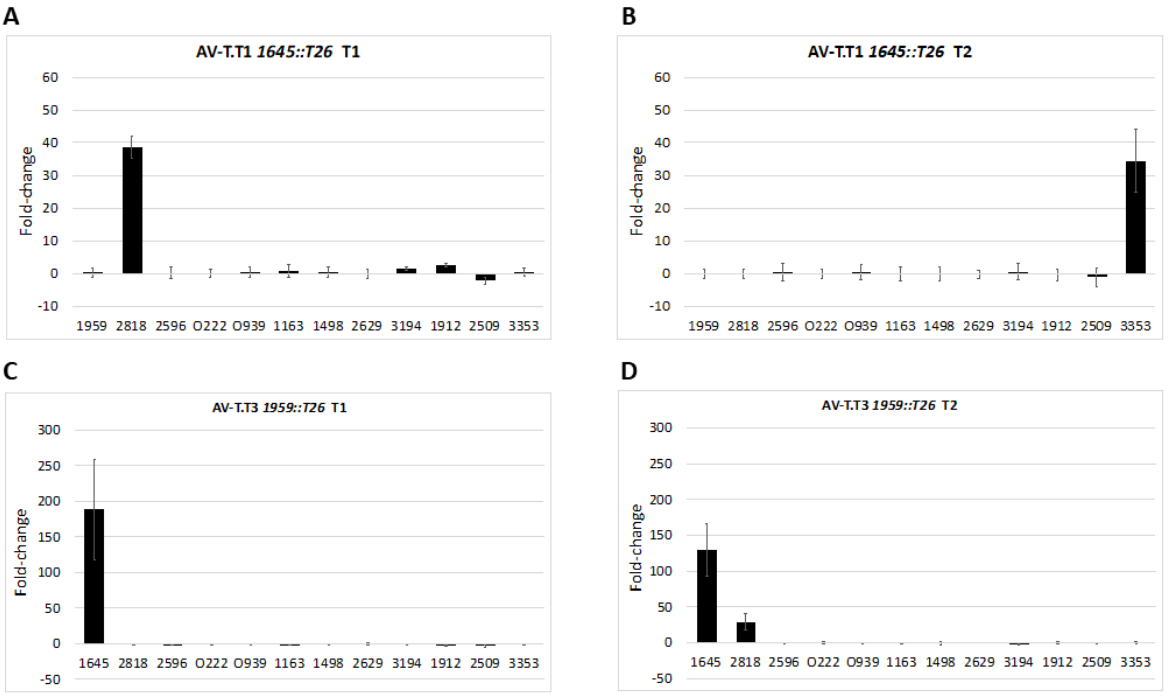

Supplementary Figure 4: Passage through the VIR-O state allows TetR-type transcriptional regulators (TTTRs) to reset. (A, B) Introduction of *1645*::*T26* into AV-T.T1 caused cells to switch to the VIR-O state (Fig. S3). Colonies of these VIR-O cells were allowed to grow and sector, and two new AV-T variants were obtained. qRT-PCR analysis showed transcriptional activation of *2818* in the first variant (A), and *3353* in the second variant (B).

(C, D) Introduction of *1959*::*T26* into AV-T.T3 also caused cells to switch to the VIR-O state (Fig. S3), and two new AV-T variants were derived from VIR-O sectors. qRT-PCR analysis revealed that *1645* had activated in the first variant (C), and both *1645* and *2818* had activated in the second variant (D).

Supplementary Figure 5

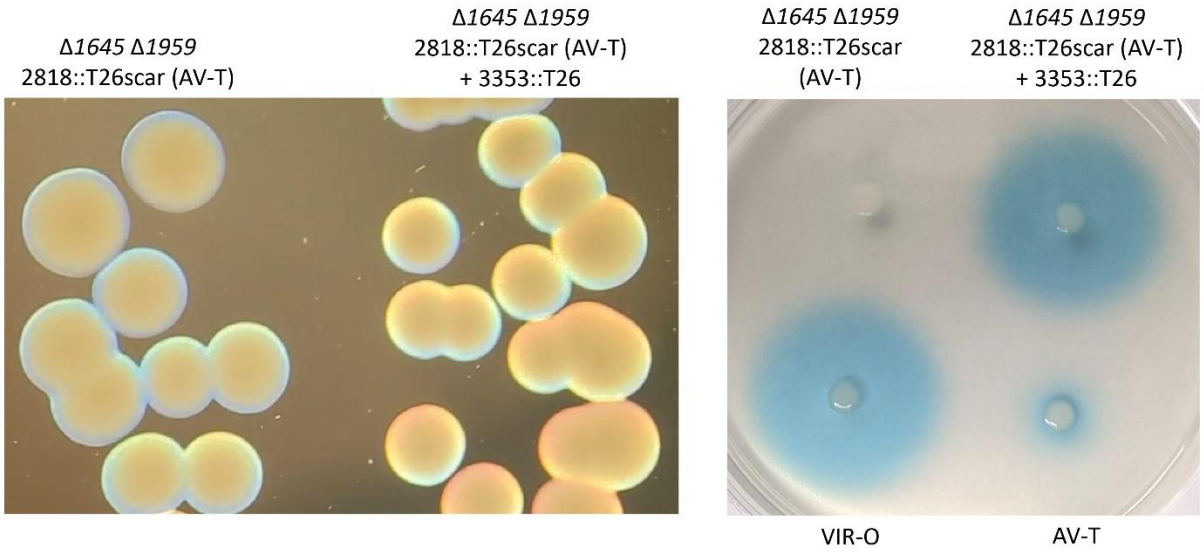

Supplementary Figure 5: Introduction of a *3353*::*T26* insertion in the triple mutant AV-T Δ*1645*/Δ*1959*/*2818*::*T26scar* forces a switch back to the VIR-O state, evidenced by the change in colony opacity and the restoration of 3-OH C_{12}-HSL secretion.

Supplementary Figure 6

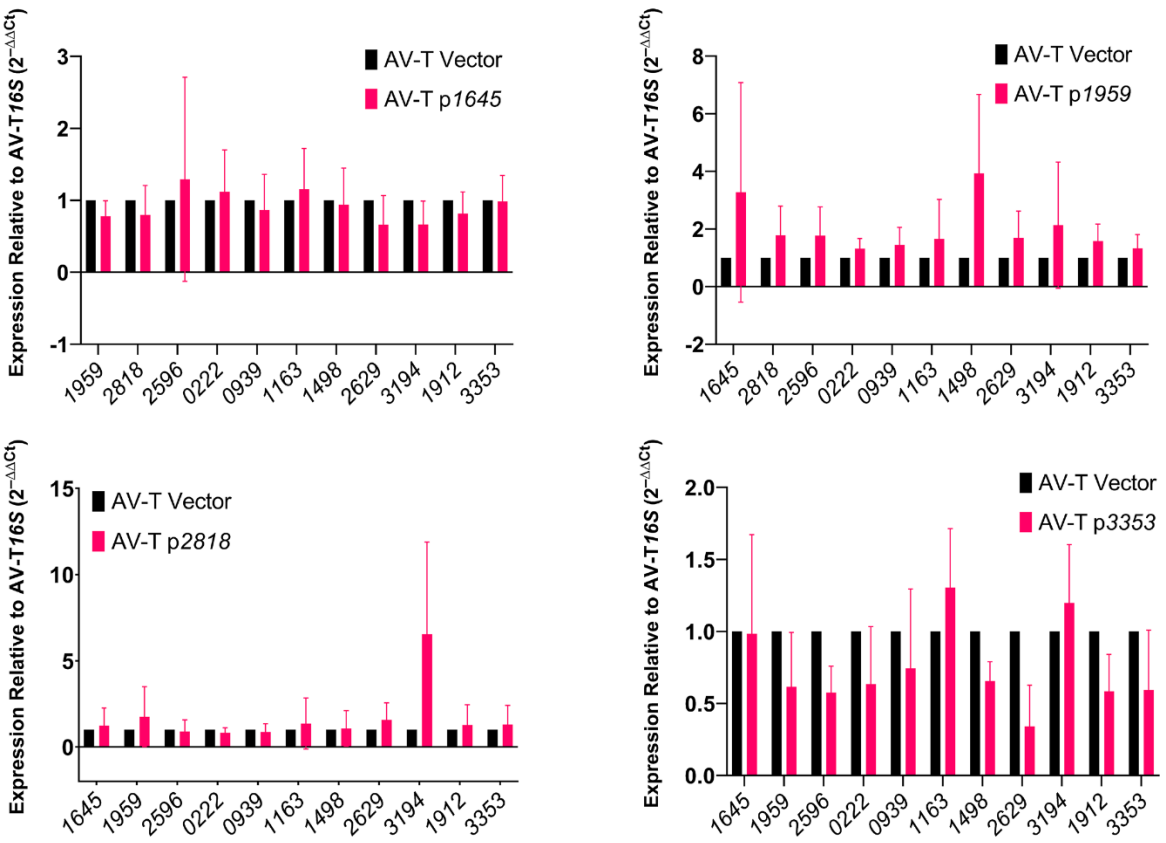

Supplementary Figure 6: Analysis of inter-regulation between TTTRs by overexpression of TTTRs in the AV-T background. Each of the four main TTTRs—*1645*, *1959*, *2818*, and *3353*—were cloned into the pWH1266 ScaI site, which puts inserted genes under control of the β-lactamase promoter, leading to strong overexpression. Empty pWH1266 vector controls and pWH1266/TTTR constructs were transformed into AV-T cells. Expression levels of all eleven other TTTRs were then measured by qRT-PCR, comparing the overexpression strain to the vector control strain and internal control *16S*. The value shown for each overexpression strain represents the average $2^{-\Delta\Delta Ct}$ of three biological replicates. Error bars indicate standard deviation of the mean. This analysis showed no significant differences in TTTR expression when one of the four main TTTRs is overexpressed as measured by multiple Mann-Whitney tests.

Supplementary Figure 7

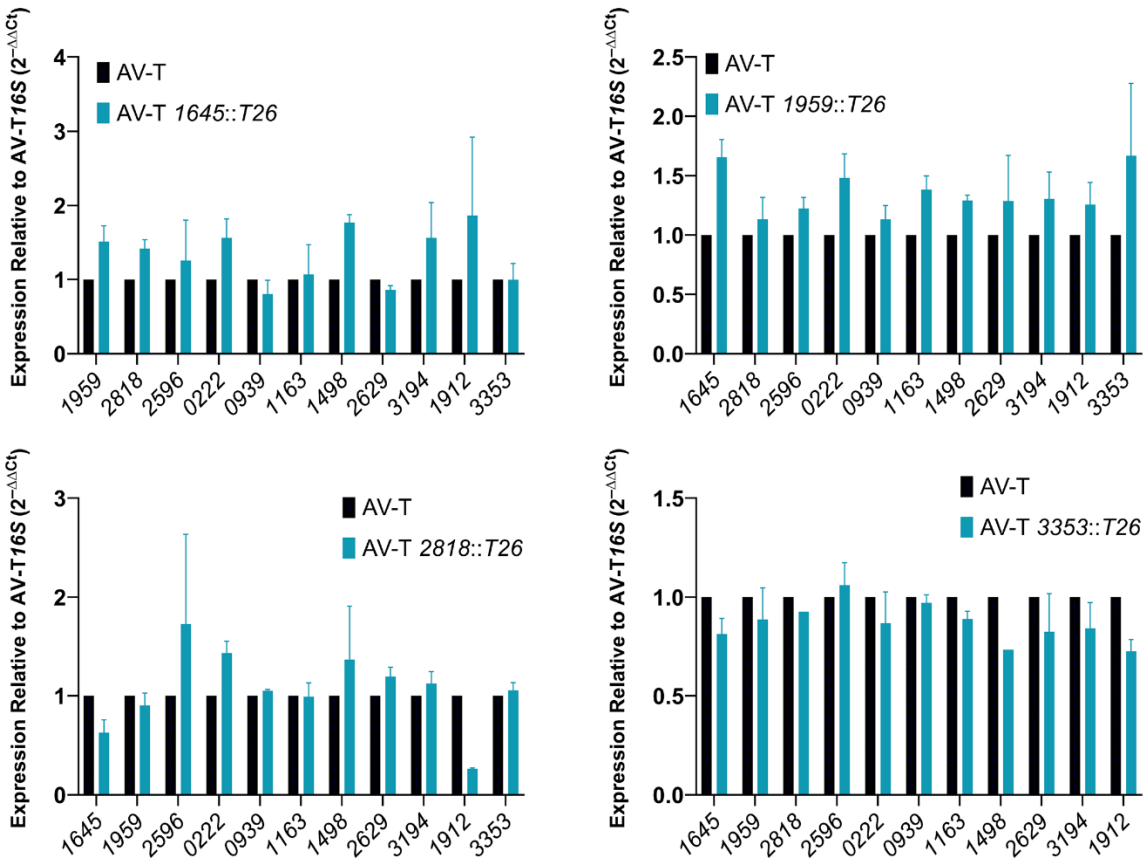

Supplementary Figure 7: Analysis of inter-regulation between TTTRs in single mutants of *1645, 1959, 2818,* and *3353* in the AV-T background. Expression levels of TTTRs were measured by qRT-PCR in strains of AV-T *1645*::*T26*, AV-T *1959*::*T26*, AV-T *2818*::*T26*, and AV-T *3353*::*T26* compared to a wild-type AV-T control strain and a *16S* internal control. The value shown for each overexpression strain represents the average $2^{-\Delta\Delta Ct}$ of two biological replicates. Error bars indicate standard deviation of the mean. This analysis showed no significant differences in TTTR expression when one of the four main TTTRs is overexpressed as measured by multiple Mann-Whitney tests.

Supplementary Figure 8

Fold Change of *1645* Upstream Regions Relative to Vector Control (*16S*)

	AV-T	VIR-O
1645 Up A	1.3	1.2
1645 Up B	-1.2	1.4

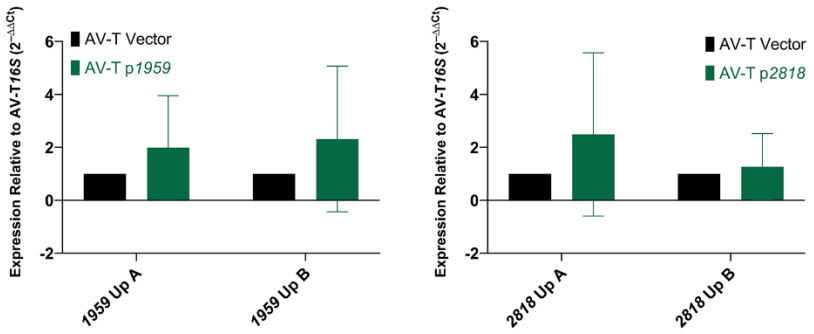

Supplementary Figure 8: Analysis of autoregulation of *1645*, *1959*, and *2818*. Two sets of primers were designed to probe the region upstream of each of *1645*, *1959*, and *2818*, between the predicted transcriptional start site (TSS) and the coding region. The "Up A" and "Up B" primers target two portions of the upstream region, with the "Up A" primer probing further upstream and closer to the TSS than the "Up B" primer. These primers were used in qRT-PCR experiments to measure expression of these upstream regions when the same TTTR was being overexpressed in the pWH1266 construct. Autoregulation of *1645* was assayed in both VIR-O and AV-T containing either a vector control or the overexpression construct, and each value shown represents a single independent experiment. Autoregulation of *1959* and *2818* were both assayed in strains of AV-T containing either a vector control or the overexpression construct, and each value shown represents the average of three biological replicates. For *1645* experiments, the fold changes when *1645* was overexpressed are less than two, which does not implicate autoregulation. For *1959* and *2818* experiments, multiple Mann-Whitney tests determined no significant changes in the upstream regions of the TTTRs when the same TTTR was overexpressed.

Supplementary Table 1: Oligonucleotides used in this study. BamHI sites appear in italics.

Oligonucleotide	Sequence	Use
***1645* Up 1**	*AAAAAGGATCC*TACAGACCTTAAATAACGTTG	Mutant construction
***1645* Up 2**	TGCTCTAAATGAAGCTTCTAA	Mutant construction
***1645* Down 1**	ATAATACTGTCCTAGATTAAAAATAAAAGC	Mutant construction
***1645* Down 2**	*AAAAAGGATCC*TGGTCAAACTTTACGTGGT	Mutant construction
***1959* Up 1**	*AAAAAGGATCC*GGGCTACGCTATTCTATGCA	Mutant construction
***1959* Up 2**	AAAAGGCATAGCAAAGCCCT	Mutant construction
***1959* Down 1**	GGGTGAGGTGGAAATAATGA	Mutant construction
***1959* Down 2**	*AAAAAGGATCC*AGTACTGCGCTTAAACTTTCGTTA	Mutant construction
***2596* Up 1**	*AAAAAGGATCC*ACCGACCTCTTCAACAATGC	Mutant construction
***2596* Up 2**	CTGTCTGAGTGTTAAATCTAGAAACAC	Mutant construction
***2596* Down 1**	AAATGAAGCTTCTAAATTTGG	Mutant construction
***2596* Down 2**	*AAAAAGGATCC*GAGTAGCTAGTTGAGTCGATTG	Mutant construction
***2818* Up 1**	AGTTTTACCGTTATAAATTCTTGTTGTTTC	Mutant construction
***2818* Up 2**	AGCGTGCAAATTCACGGAAG	Mutant construction
***2818* Down 1**	TAACTGGCTTGCACCATGAC	Mutant construction
***2818* Down 2**	AGAGAGGAAAACTAATTAATTGCAC	Mutant construction
***0222* Exp1**	GTAGAACTCCTTTACACACAAG	Overexpression
***0222* Exp2**	GTATTTCTTTAATGGGGGC	Overexpression
***0939* Exp1**	CATTTCATCATTTACCATTTTCATATTC	Overexpression
***0939* Exp2**	GTAATTCAAATTTTAGGCTTTCATTC	Overexpression
***1163* Exp1**	CCAGGTAAACCTAAAACTTCATC	Overexpression
***1163* Exp2**	AACCCTAAACTTTCATTTGCAT	Overexpression
***1498* Exp1**	CACTCATTTTAAGAGTGACGGC	Overexpression
***1498* Exp2**	GCTCAATCAATTTAGTTAACCCTCA	Overexpression
***1645* Exp1**	GAGTGACGGCATGTCTATCT	Overexpression
***1645* Exp2**	CTTATAGCCATAAGTGGTAATTGAG	Overexpression

***1959* Exp1**	GCTATAACGACACAGCTTAAAA	Overexpression
***1959* Exp2**	AGGTTAATGAAATCAGCAGG	Overexpression
***2596* Exp1**	GCGTGAGCCGTGGCCTTAAA	Overexpression
***2596* Exp2**	AAACCCGAGATAGGCGAGCAC	Overexpression
***2629* Exp1**	CTACACCTTAAGAATCGTCACG	Overexpression
***2629* Exp2**	GGTCTGCTCATCTAATAAAAATCAAG	Overexpression
***2818* Exp1**	CAAAAAAAGTATCTCATTTAGAAAC	Overexpression
***2818* Exp2**	AAGAATAAAAACCTAAAATCATATG	Overexpression
***3194* Exp1**	GAAACAACAAGAATTTATAACGG	Overexpression
***3194* Exp2**	GAATGGATTTATTTAGTAACTATTTAATC	Overexpression
322 Bam For	GCAACCGCACCTGTGGCGCCG	pWH1266 sequencing
322 Bam Rev	CCCATTCTGCTATTCTGTATACAC	pWH1266 sequencing
***16S* qRT-PCR 1**	GATCTTCGGACCTTGCGCTA	qRT-PCR
***16S* qRT-PCR 2**	GTGTCTCAGTCCCAGTGTGG	qRT-PCR
***0222* qRT-PCR 1**	AGTGAGTGTGGTGAGTGAGC	qRT-PCR
***0222* qRT-PCR 2**	GCGGTTTGGTAGGCATTTGG	qRT-PCR
***0939* qRT-PCR 1**	CACCGTGGGTTCCACCTTAT	qRT-PCR
***0939* qRT-PCR 2**	TCGACCATTGCGACTACTTGT	qRT-PCR
***1163* qRT-PCR 1**	GCAGGAGTGCTTAAGTCATATTCG	qRT-PCR
***1163* qRT-PCR 2**	GTTTCATCACCGTGGATTTCATCTG	qRT-PCR
***1498* qRT-PCR 1**	TTCGCTCATAAACTCAGGCA	qRT-PCR
***1498* qRT-PCR 2**	CTTCGGCATATGAAACGGCT	qRT-PCR
***1645* qRT-PCR 1**	CTCGAAGGGCTGTACCGTTT	qRT-PCR
***1645* qRT-PCR 2**	TCTTCGAGTGTAGCTGTGGC	qRT-PCR
***1959* qRT-PCR 1**	TGTGGGCGTCGATAGACTTG	qRT-PCR
***1959* qRT-PCR 2**	TGTGCTTGTGTCATGGTCGT	qRT-PCR
***2596* qRT-PCR 1**	TATCGTGAACTTATGGTGTTTG	qRT-PCR

***2596* qRT-PCR 2**	TCAACCACCACTTTATAGGC	qRT-PCR
***2629* qRT-PCR 1**	AAGCCACGTTGTATAACTACT	qRT-PCR
***2629* qRT-PCR 2**	TTCCTTGAGCTTATCGGTTG	qRT-PCR
***2818* qRT-PCR 1**	GCCACTTTCTATACTCGATTGCC	qRT-PCR
***2818* qRT-PCR 2**	CTCAAACCGTTACTGCACGC	qRT-PCR
***3194* qRT-PCR 1**	TTACTCAAGCCGTTACTACA	qRT-PCR
***3194* qRT-PCR 2**	GTATTCAACTGCCATACGGT	qRT-PCR
***1645* P1**	TATTTATGAGTTAATGTGAGTTAAG	lacZ fusion construction
***1645* P2**	TAAATTTGGCATAGTTATACCGC	lacZ fusion construction
***1498* P1**	GTGCGCATATCTAGCCTAAG	lacZ fusion construction
***1498* P2**	AATCCGATGCTATGTGGAGC	lacZ fusion construction
***1959* P1**	GTACAGCTCCATCAGTTTAAAAATC	lacZ fusion construction
***1959* P2**	CATAGCAAAGCCCTAAAGACTGTG	lacZ fusion construction
***2596* P1**	TTTTGAAATGATCACAGGGACAAAAC	lacZ fusion construction
***2596* P2**	GGTTGTAAAACGTGGCTTTGGTC	lacZ fusion construction
***2818* P1**	GGAAGAGGTTTCTAAATTTGGCAT	lacZ fusion construction
***2818* P2**	TTCATGGTTTTCCATTTTTATATTT	lacZ fusion construction
lacZ	CTGCAAGGCGATTAAGTTGG	lacZ fusion verification

Chapter 5: Methods for Detecting N-Acyl Homoserine Lactone Production in *Acinetobacter baumannii*

Aimee R. Paulk Tierney[1] and Philip N. Rather[2]

[1]Department of Microbiology and Immunology, Emory University School of Medicine, Emory University, Atlanta, GA, USA.

[2]Department of Microbiology and Immunology, Emory University, Atlanta, GA, USA.

Published in:

Acinetobacter baumannii Methods and Protocols, Springer Nature 2019

Methods in Molecular Biology vol. 1946

pp. 151-158

ARPT and PR wrote the manuscript. PR provided and prepared the figures.

Abstract

Acinetobacter baumannii cell-cell signaling is mediated by production and release of *N*-acyl homoserine lactones (AHLs), primarily *N*-(3-hydroxydodecanoyl)-l-homoserine lactone (3-hydroxy-C_{12}-HSL). The secretion of this signal can be readily assessed via simple plate-based or thin-layer chromatography-based assays utilizing an *Agrobacterium tumefaciens traG-lacZ* containing biosensor. In this chapter, we describe methods to assay for secreted *N*-acyl homoserine lactone production in *Acinetobacter baumannii*.

Introduction

Similar to other Gram-negative bacteria, *Acinetobacter baumannii* communicates via production and secretion of *N*-acyl homoserine lactone (AHL) autoinducers utilizing a LuxI-/LuxR-type system [1]. In this system, an autoinducer synthase produces the AHL signal, which typically diffuses across the cell membrane, reenters the cell at high concentrations, and then binds and activates a transcriptional regulatory protein to mediate global changes in gene expression [2]. In *A. baumannii*, the autoinducer synthase and transcriptional regulator proteins are termed AbaI and AbaR, respectively [1].

Secretion levels of AHL signal can be qualitatively assessed by plate-based methods that utilize bacterial biosensor strains containing a reporter gene that is transcriptionally activated in the presence of AHL signals. Typical reporters include luminescence (*lux*), β-galactosidase (*lacZ*), or *Chromobacterium violaceum* purple pigment violacein [3, 4]. Here, we demonstrate detection of *A. baumannii* AHL signals using an *Agrobacterium tumefaciens* biosensor containing a plasmid-localized *traG-lacZ* fusion (pZLR4). The host biosensor strain does not make AHL signals, but exogenous AHL from other bacteria will bind to TraR, coactivating *traG* and inducing production of β-galactosidase [4, 5]. Strains of interest can be surveyed for AHL secretion by (a) cross-streaking the *A. tumefaciens* biosensor against the strain of interest on a LB plate containing 5-bromo-4-chloro-3-indolyl-β-d-galactopyranoside (X-gal); (b) direct plating of bacterial culture, cell-free supernatants, or patched colonies onto a soft agar lawn containing the *A. tumefaciens* biosensor and X-gal; or (c) separating extracts on reversed-phase C_{18} thin-layer chromatography plates and overlaying the dried plates with a soft agar lawn containing the *A. tumefaciens* biosensor.

Materials

Prepare all solutions with distilled water prior to daily use. Store reagents at room temperature unless otherwise indicated.

1. Media: Luria broth (LB)—10 g tryptone, 5 g yeast extract, 5 g sodium chloride per liter.
2. Soft agar. Luria broth containing 0.7% agar.
3. Gentamicin stock solution 20 mg/mL in water.
4. Petri dishes and tubes for bacterial culture.
5. X-gal (5-bromo-4-chloro-3-indolyl-β-d-galactopyranoside) solution at 20 μg/mL. Store at −20 °C.
6. Reversed-phase C-18 thin-layer chromatography (TLC) plates.
7. Glass chromatography chamber for developing TLC plates.
8. 60% methanol.

Methods

3.1. Cross-Streak Assay

1. Inoculate 2 mL LB containing gentamicin 30 μg/mL with the *Agrobacterium tumefaciens* biosensor strain. Grow overnight at 28 °C, stationary (*see* Note 1).
2. Prepare a LB agar plate (15 g agar/L) with 80 μL of 20 μg/mL X-gal per 20 mL (*see* Note 2). Dry the plate inverted with the top off at 37 °C for at least 1 h.
3. While holding the plate at an angle, add 30 μL of the *A. tumefaciens* biosensor strain (OD_{600} = 0.2) and allow the culture to run down the surface of the plate to form a line of cells. Streak a loop of *A. baumannii* strain to be tested for AHL production next to the biosensor strain. Alternatively, spot 5 μL of the culture to be tested for signal production adjacent to the biosensor strain and allow the spot to soak into the agar.
4. Incubate plates at 28 °C for 12 h or until a blue color develops in the biosensor strain.

Blue pigmentation of the *A. tumefaciens* biosensor near the strain(s) of interest indicates production of the AHL signal (Fig. 1).

3.2. Soft Agar Assay

1. Inoculate 2 mL LB containing gentamicin (30 μg/mL) with the *Agrobacterium tumefaciens* biosensor strain. Grow overnight at 28 °C, stationary (*see* Note 1).
2. Prepare LB soft agar (0.7 g agar/L). Cool to 45 °C and add 80 μL of 20 μg/mL X-gal per 20 mL melted agar and 250 μL of the A. tumefaciens culture (OD A_{600} = 0.2) per 20 mL melted agar. Mix and pour plate immediately (*see* Notes 2 and 3).
3. Allow plate to set and then dry inverted at 37 °C for 30–45 min.

4. Plate or patch bacterial cultures, colonies, or supernatants as desired. Incubate plates at 28 °C. Strains of interest that are positive for AHL secretion will produce a blue halo (Fig. 2).

3.3 Thin-Layer Chromatography (TLC) Assay

1. Spot samples to be tested on a reversed-phase C_{18} TLC plate. Spots should be approximately 2–3 cm from the bottom of the TLC plate.
2. Allow spots to dry completely.
3. Incubate the TLC plate in a glass chamber with 50 mL of 60% methanol and allow the solvent to completely ascend to the top of the plate.
4. Allow the plate to sit at room temperature for 60 min in a fume hood to allow the methanol to evaporate.
5. Seal all four sides of the TLC plate with tape in a manner that creates a lip of at least 1/2 in. on all sides. Laboratory tape works well for this (Fig. 3A).
6. Prepare 50 mL of LB soft agar (0.7 g agar/L). Cool to 45 °C and add 160 μL of 20 μg/mL X-gal and 400 μL of the *A. tumefaciens* culture. Mix and immediately pour the agar solution over the TLC plate to completely cover the surface. Allow the agar to solidify for 30 min (*see* Note 4).
7. Remove the tape border and place the TLC plate on top of an 8 in. × 8 in. glass Pyrex dish that contains 100 mL of water in the bottom, Fig. 3B (*see* Note 5). Cover the plate with an identical 8 in. × 8 in. glass Pyrex dish (Fig. 3C). Seal the two dishes by using Saran wrap. Place the sealed Pyrex dishes in a 28 °C incubator and incubate for 24–48 h until blue spots appear indicating activation of the biosensor.

8. Air-dry the TLC plate until the soft agar lawn has become completely dehydrated. This can be done at room temperature or in a 37 °C incubator (*see* Note 6).

Notes

1. The *A. tumefaciens* with pZLR4 should be grown at 28 °C as the replication of this plasmid is temperature sensitive.
2. The concentration of X-gal can be adjusted to suit experimental needs.
3. The volume of *A. tumefaciens* culture added varies by culture density. The indicated volume of 250 μL per 20 mL agar is based on a culture at an OD_{600} of at least 0.2. It is generally better to err on the side of using a higher concentration as too low concentration will result in a sparse lawn with poor halo visualization. Troubleshooting the volume of culture needed may be required to suit experimental needs.
4. When the soft agar is added to the TLC plate, it is not necessary to have it at an even thickness in all areas of the plate. Once the plate is done incubating and the agar overlay is dried, all changes in thickness will even out and be invisible.
5. This will allow the soft agar overlay to remain hydrated within the chamber created by the sealed Pyrex dishes.
6. When drying the soft agar lawn on the TLC plate, be aware that the dried agar/TLC matrix can sometime crack and curl up. Photograph the plates immediately after drying.

Acknowledgements

This work is supported by the following awards to P.N.R., VA Merit Award I01 BX001725 and Research Career Scientist Award IK6BX004470, both from the Department of Veterans Affairs, and R01AI072219 from the National Institutes of Health.

References

1. Niu C, Clemmer KM, Bonomo RA, Rather PN (2008) Isolation and characterization of an autoinducer synthase from *Acinetobacter baumannii*. *J Bacteriol* 190(9):3386–3392. Epub 19 Feb 2008. 10.1128/JB.01929-07
2. Bhargava N, Sharma P, Capalash N (2010) Quorum sensing in Acinetobacter: an emerging pathogen. *Crit Rev Microbiol* 36(4):349–360. Epub 18 Sept 2010. 10.3109/1040841X.2010.512269
3. McClean KH, Winson MK, Fish L, Taylor A, Chhabra SR, Camara M, Daykin M, Lamb JH, Swift S, Bycroft BW, Stewart GS, Williams P (1997) Quorum sensing and Chromobacterium violaceum: exploitation of violacein production and inhibition for the detection of N-acylhomoserine lactones. *Microbiology (Reading, England)* 143(Pt 12):3703–3711. Epub 9 Jan 1998. 10.1099/00221287-143-12-3703
4. Shaw PD, Ping G, Daly SL, Cha C, Cronan JE Jr, Rinehart KL, Farrand SK (1997) Detecting and characterizing N-acyl-homoserine lactone signal molecules by thin-layer chromatography. *Proc Natl Acad Sci U S A* 94(12):6036–6041. Epub 10 June 1997
5. Cook DM, Li PL, Ruchaud F, Padden S, Farrand SK (1997) Ti plasmid conjugation is independent of vir: reconstitution of the tra functions from pTiC58 as a binary system. *J Bacteriol* 179(4):1291–1297. Epub 1 Feb 1997

Figure Legends

Figure 1: Cross-streak of *Agrobacterium tumefaciens* indicator strain and *Acinetobacter baumannii*. *A. baumannii* (horizontal line, top of plate) was streaked perpendicular to the *A. tumefaciens* biosensor (vertical line). Blue pigmentation of the biosensor strain near the point of intersection to *A. baumannii* indicates production, secretion, and diffusion of AHL through the medium.

Figure 2: Detection of AHL secretion on a soft agar lawn containing *Agrobacterium tumefaciens* biosensor strain. Colonies of an *A. baumannii* wild-type control (right) and an AHL-deficient mutant (left) were patched onto a soft agar lawn of *A. tumefaciens traG-lacZ* biosensor and X-gal. The plate was incubated for 24 h at 28 °C. The blue halo surrounding the wild-type *A. baumannii* patch indicates production, secretion, and diffusion of AHL through the medium, where it results in activation of the *traG-lacZ* fusion in the biosensor strain.

Figure 3: Methods for incubating TLC plates with a soft agar overlay. This figure demonstrates how an enclosure can be generated with glass Pyrex dishes that can be used to incubate TLC plates in an incubator. Panel **A** demonstrates how tape can be used to create an agar enclosure for the TLC plate. Panels **B** and **C** demonstrate the use of Pyrex dishes to create a humidified enclosure.

Figure 1

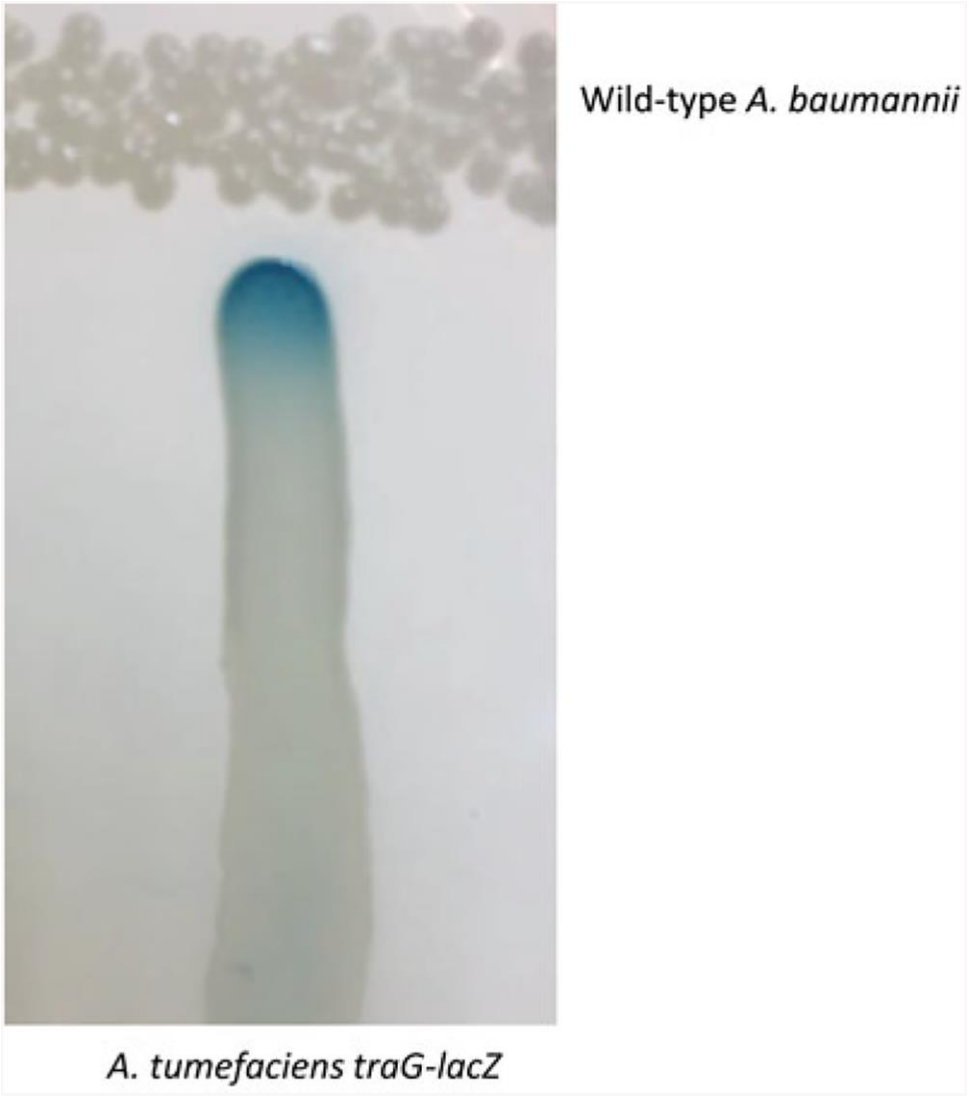

Figure 1: Cross-streak of *Agrobacterium tumefaciens* indicator strain and *Acinetobacter baumannii*. *A. baumannii* (horizontal line, top of plate) was streaked perpendicular to the *A. tumefaciens* biosensor (vertical line). Blue pigmentation of the biosensor strain near the point of intersection to *A. baumannii* indicates production, secretion, and diffusion of AHL through the medium.

Figure 2

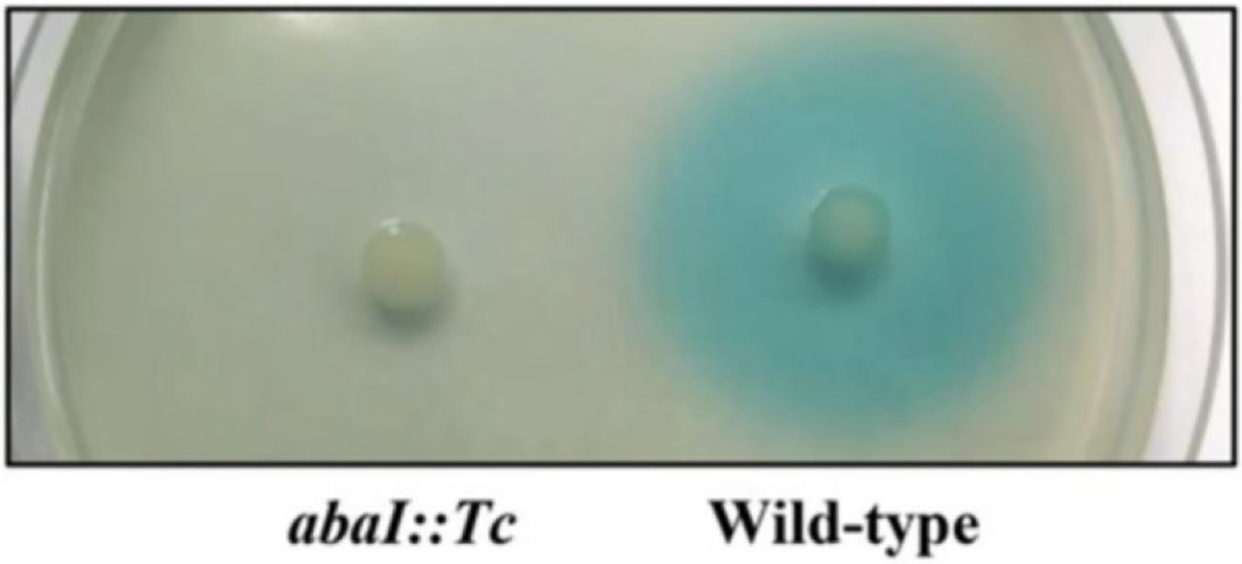

Figure 2: Detection of AHL secretion on a soft agar lawn containing *Agrobacterium tumefaciens* biosensor strain. Colonies of an *A. baumannii* wild-type control (right) and an AHL-deficient mutant (left) were patched onto a soft agar lawn of *A. tumefaciens traG-lacZ* biosensor and X-gal. The plate was incubated for 24 h at 28 °C. The blue halo surrounding the wild-type *A. baumannii* patch indicates production, secretion, and diffusion of AHL through the medium, where it results in activation of the *traG-lacZ* fusion in the biosensor strain.

Figure 3

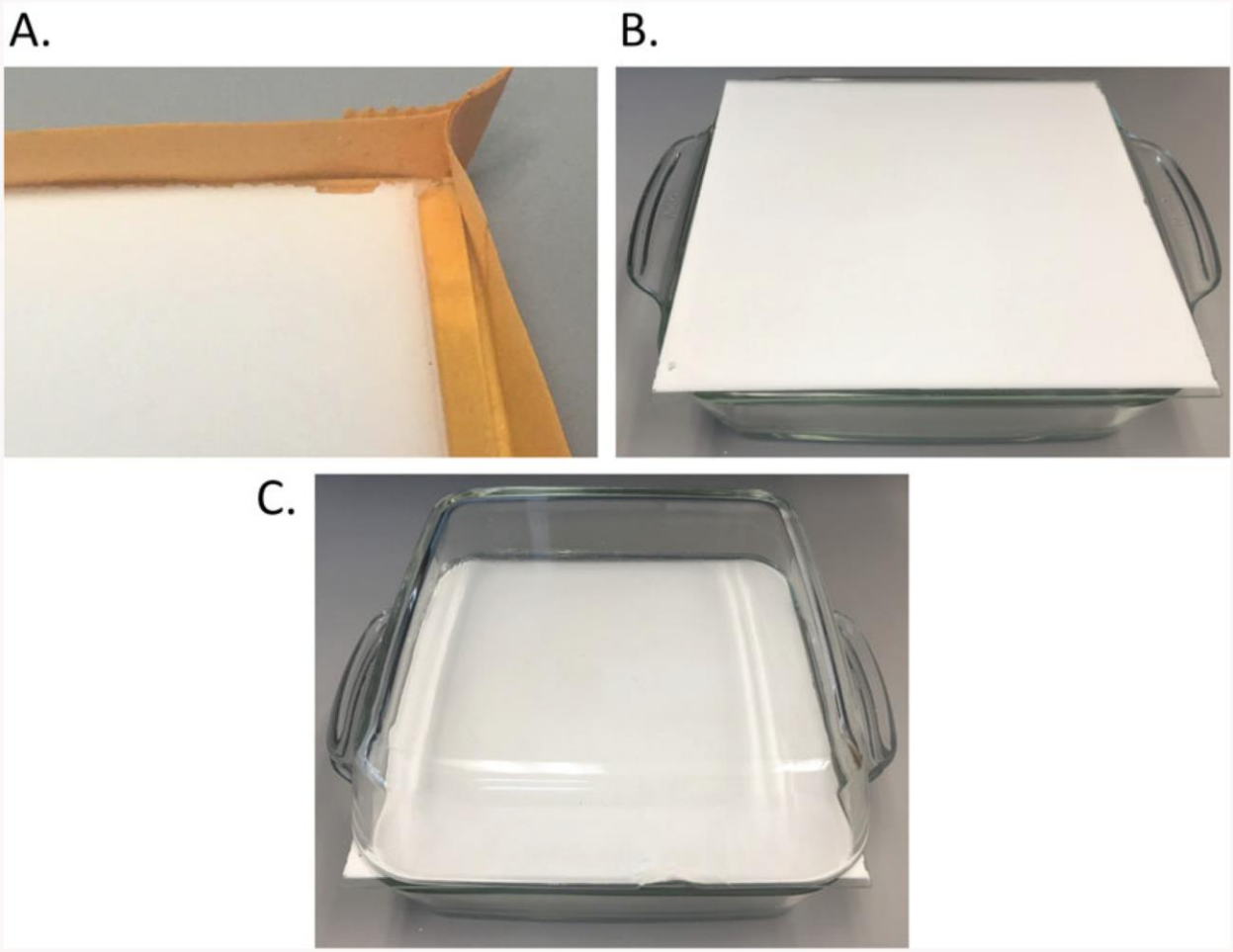

Figure 3: Methods for incubating TLC plates with a soft agar overlay. This figure demonstrates how an enclosure can be generated with glass Pyrex dishes that can be used to incubate TLC plates in an incubator. Panel **A** demonstrates how tape can be used to create an agar enclosure for the TLC plate. Panels **B** and **C** demonstrate the use of Pyrex dishes to create a humidified enclosure.

Chapter 6: Discussion

The discovery of bistable opacity-virulence states in *Acinetobacter baumannii* presents an unprecedented opportunity for the development of future treatments of this notoriously antimicrobial resistant nosocomial pathogen. Given the somewhat discouraging state of antibiotic drug development [1-5] and the prevalence of *A. baumannii* strains that are multidrug resistant [6], exploration of alternative methods of treatment is imperative. The existence of an avirulent translucent (AV-T) state, to which virulent opaque (VIR-O) cells may readily switch, represents an exploitable vulnerability in *A. baumannii* that went undetected until only recently [7]. Importantly, our previous publications demonstrate that many clinical isolates, not solely AB5075, possess the ability to switch between the VIR-O and AV-T states [7, 8], indicating that clinical interventions which target the switch are likely to have broad applicability. While a number of other bacterial species exhibit colony opacity variation, reviewed in Chapter 1, the method by which *A. baumannii* regulates colony opacity does not overlap with any other known systems. Therefore, the characterization of the genetic mechanisms that control the phenotypic switch is a high priority.

This body of work introduces two hitherto unknown regulatory pathways that influence the VIR-O to AV-T switch and adds greatly to the understanding of a previously known pathway involving the TetR-type transcriptional regulator (TTTR) ABUW_1645 [8]. In Chapter 2, we reveal a role for the stringent response regulator RelA in the phenotypic switch, as deletion of *relA* locks cells into the VIR-O state [9]. We further discovered that RelA represses the LysR-type transcriptional regulator *ABUW_1132* (*1132*), whose deletion results in a 16-fold decrease in VIR-O to AV-T switching as shown in Chapter 3 [9, 10]. Finally, Chapter 4 entails the discovery and characterization of a novel regulatory system comprised of a family of at least twelve functionally

redundant TTTRs that appears to constitute the primary pathway that drives the VIR-O to AV-T switch. Importantly, we were able to identify four TTTRs among these that are most crucial to the switch: *ABUW_1645* (*1645*), *ABUW_1959* (*1959*), *ABUW_2818* (*2818*), and *ABUW_3353* (*3353*), as indicated by the near total loss of switching in the VIR-O quadruple mutant.

In addition, this research has increased our knowledge of *A. baumannii* biology as a whole. The genetic pathways that regulate quorum sensing and surface-associated motility are not clearly defined in *Acinetobacter*. Therefore, our findings that RelA and 1132 act as key regulators of both processes provide new insight into these complex systems. In particular, the discovery that RelA represses the AbaI-AbaR quorum sensing system through repression of *1132* is a key finding that will likely be of value in completing our understanding of both the stringent response and quorum sensing in *Acinetobacter* species [9]. It is important to note that the impact of these regulators upon the quorum sensing and motility phenotypes is not due to their simultaneous influence on the opacity-virulence switch. Although both of these phenotypes differ between wild-type VIR-O and AV-T cells, the expression of *abaI* is equal between the opacity variants, indicating that a different mechanism is responsible for the increase in quorum sensing signal (3-OH C_{12}-homoserine lactone; "AHL") secretion and motility seen in VIR-O [7, 8].

This research has also challenged our previously held notion that cells exhibiting a translucent colony appearance are reliably and unequivocally avirulent. As shown in Chapter 3, the deletion of *1132* resulted in "AV-T" variants with increased capsular polysaccharide, a known virulence factor which has been shown in other studies to promote resistances to desiccation, host antimicrobials, and surface disinfectants [8, 10-14]. While these resistances were not tested in the AV-T Δ*1132* mutant, we demonstrated moderately increased virulence of this mutant in both *Galleria mellonella* and mouse lung models of infection [10]. Furthermore, findings in Chapter 4

revealed that although overexpression of the TTTRs *1959* and *2818* in the VIR-O background drives a switch to cells having a translucent colony appearance, these cells are recovered at equal CFU/g counts compared with VIR-O vector controls in a mouse lung model. This is a stark contrast to the greater than 10,000-fold reduction in CFU observed when the TTTR *1645* was overexpressed in the same conditions [8].

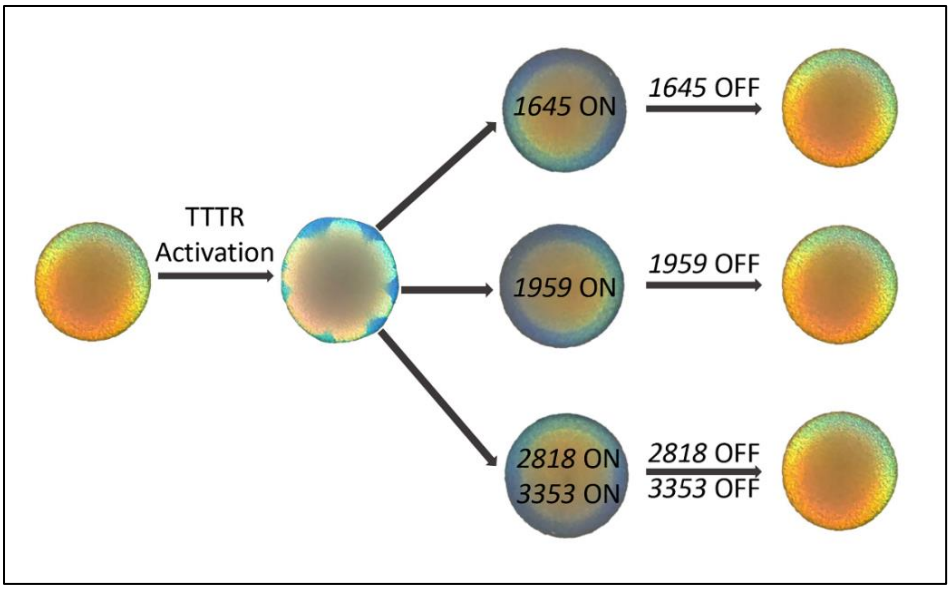

Figure 1: A model for VIR-O to AV-T to VIR-O switching as directed by the stochastic activation and subsequent deactivation of TTTRs.

These findings allow us to construct a model in which the fundamental mechanism for the VIR-O to AV-T switch is the stochastic activation of *1645* and/or at least one other TTTR with homology to the DNA-binding HTH region of *1645* (**Fig. 1**), with a preference for *1645*, *1959*, *2818*, and *3353*. The subsequent deactivation of the TTTR(s) is responsible for the return to the VIR-O state. We hypothesize that other regulatory elements that have been identified in previous publications, ongoing research, and the research presented in this dissertation operate peripherally to the central TTTR pathway. These peripheral entities may function in a variety of ways, such as

to moderate TTTR transcription, to provide necessary ligands for the TTTRs, or to stabilize TTTR transcripts or proteins. It is further possible that they may carry out one of these roles for the genes (or gene products) that are regulated by the TTTRs.

This work has generated a number of interesting questions for further exploration. First, the relationships between RelA, 1132, and the AbaI-AbaR quorum sensing system are not totally clear. Our research would benefit from an analysis of whether RelA directly represses *1132* or if this effect occurs via downstream transcriptional changes brought about by RelA. Further experiments could consider whether 1132 helps to bring about desired changes during the stringent response, which may be possible to assess by measuring *1132* transcripts in cells under protein starvation conditions. As noted in Chapter 3, a portion of *1132*'s regulon includes ribosomal proteins, RNA polymerase, and transcriptional initiation and elongation factors, all of which would be expected to be downregulated during the stringent response.

Intriguingly, deletion of *relA* in the AV-T background did not result in the hyper-motile phenotype observed for VIR-O Δ*relA* [9]. Wild-type AV-T cells overexpressing *1132* from the p*1132* construct described in Chapter 2 exhibit 3.2-fold increased motility relative to vector controls (unpublished data). For comparison, wild-type VIR-O with p*1132* exhibit a 3.8-fold increase in motility (Chapter 2). This observation implies that *1132* may only become overexpressed in the VIR-O Δ*relA*, which would suggest that RelA's repression of *1132* is limited to the VIR-O state. Should a qRT-PCR analysis of AV-T Δ*relA* reveal similar levels of *1132* expression as VIR-O Δ*relA*, it may be the case that the AV-T Δ*relA* cells lack the conditions or necessary ligands for 1132 to activate the quorum sensing genes and the downstream acinetin-505 operon.

Additional experiments could be carried out to determine whether the *abaI* and *abaR* loci are directly regulated by 1132. As discussed in Chapter 2 and 3, we only saw transcriptional changes in *abaI* and *abaR* when *1132* was overexpressed, and *abaR* was only downregulated 1.5-fold when *1132* was deleted. This contrast may indicate that 1132's relationship with the quorum sensing genes, particularly *abaI*, is indirect. One hypothesis that could be considered is whether 1132 mediates a change in the permeability of the membrane to AHL, such that when *1132* is overexpressed, the membrane is highly permeable to AHL. In such a scenario, cells would reach a quorum more quickly, and *abaI* transcripts would increase due to activation by AbaR-AHL, a positive feedback loop that has been verified in *A. nosocomialis* strain M2 [15].

Other future directions entail the clarification of the roles of each of RelA, 1132, and the TTTRs in the phenotypic switch. As previously stated, we consider the TTTR pathway to be central to the switch and the likely mechanism for switching in wild-type cells. This claim is based on the observation that the TTTRs *1645*, *1959*, and *2818* are among the most highly transcriptionally upregulated genes in AV-T relative to VIR-O ([8] and Chapter 4). Moreover, overexpression of *1645* forces a switch to AV-T in nearly all switching-deficient mutant backgrounds that have been discovered to date, including VIR-O Δ*relA* and VIR-O Δ*1132* (unpublished data). We therefore have questioned whether the loss of switching seen when either r*elA* or *1132* is deleted is due to a change in the expression of the TTTRs. qRT-PCR analysis of these strains indicated that neither mutation affects TTTR transcription in a biologically meaningful way. Future experiments could utilize Western blotting to determine whether TTTR protein levels are diminished in either of these mutants. Alternatively, loss of either *relA* or *1132* may impair the unknown process that catalyzes the stochastic activation of the TTTRs or may hamper the activity of a downstream target of the TTTRs. In the case of VIR-O Δ*relA* in particular,

the dysregulation of the stringent response may simply preclude active VIR-O to AV-T switching due to the pleiotropy of this mutation.

The TTTRs are themselves global regulators, as seen by the number of phenotypes they influence including colony opacity, AHL secretion, motility, and potentially virulence. As further evidence, RNA sequencing of VIR-O overexpressing *1645* revealed 335 differentially regulated genes ($p < 0.05$, fold-change ≥ 2.0). Due to the homology of the HTH regions of the TTTRs involved in switching, it is probable that each TTTR has a large regulon. Indeed, this is currently under investigation as we have recently carried out RNA sequencing for VIR-O overexpressing each of *1959* and *2818*, and analysis is under way. We expect to discover many common targets as well as elucidate key differences between these TTTRs, which may aid in the understanding of the evolutionary benefit to the possession of at least a dozen functionally redundant regulators. These data may further indicate genes that are key to the avirulent phenotype of the true AV-T state, as the overexpression of *1959* or *2818* in VIR-O both caused a shift to a translucent colony morphotype without the reversal of virulence (see Chapter 4).

Finally, the most important future direction for this work is to determine the mechanism that regulates the TTTRs, and thereby the switch from VIR-O to AV-T. Such a mechanism should meet the criteria of functioning in a bistable and stochastic manner as well as preferentially targeting one of the most commonly used TTTRs. The most promising candidate for this role at this time is the transcriptional termination factor Rho. Briefly, Rho is an ATP-dependent RNA helicase-translocase that targets selected nascent mRNA transcripts and uncouples RNA polymerase from the DNA [16]. Rho has been implicated as a beneficial generator of noise in stochastic systems, whereby it promotes phenotypic heterogeneity and “bet-hedging” strategies [17]. Preliminary studies indicate that Rho terminates transcription in a long leader region of one

or more of the TTTRs during the VIR-O state, but this termination is prevented in VIR-O cells that switch to the AV-T state. Initial experiments also indicate interaction between Rho and *1645* transcripts (M Pérez-Varela, unpublished data). However, it is also clear that Rho does not function alone in controlling the phenotypic switch, as Rho is not differentially expressed between the two variants, although post-translational modifications may differ between variants [8]. Additional assays will be necessary to identify gene products that regulate the TTTRs and potentially act antagonistically to Rho.

In conclusion, our work has resulted in the identification and characterization of important genetic elements that regulate a novel phenotypic switch impacting several clinically relevant *A. baumannii* phenotypes, including virulence. The discovery of the TTTRs homologous to 1645 and the manner by which they orchestrate the switch constitutes a completely unique system of regulation. We further identified RelA and the LysR-transcriptional regulator 1132 as key contributors to wild-type levels of switching, and also revealed a link between the stringent response, quorum sensing, and motility. Overall, this research has significantly advanced our understanding of *A. baumannii*'s opacity-virulence switch, which will likely be crucial knowledge in the search for new treatments to counter the prevalence of multi-drug resistance in this pathogen.

References

1. Tommasi, R. et al. (2015) ESKAPEing the labyrinth of antibacterial discovery. Nat Rev Drug Discov 14 (8), 529-42.

2. DiMasi, J.A. et al. (2016) Innovation in the pharmaceutical industry: New estimates of R&D costs. J Health Econ 47, 20-33.

3. Renwick, M.J. et al. (2016) A systematic review and critical assessment of incentive strategies for discovery and development of novel antibiotics. J Antibiot (Tokyo) 69 (2), 73-88.

4. Ribeiro da Cunha, B. et al. (2019) Antibiotic Discovery: Where Have We Come from, Where Do We Go? Antibiotics (Basel) 8 (2).

5. Boyd, N.K. et al. (2021) Brief Overview of Approaches and Challenges in New Antibiotic Development: A Focus On Drug Repurposing. Front Cell Infect Microbiol 11, 684515.

6. Centers for Disease Control and Prevention (2019) Antibiotic Resistance Threats in the United States, 2019. Atlanta, GA. https://www.cdc.gov/drugresistance/pdf/threats-report/2019-ar-threats-report-508.pdf, (accessed August 2 2021).

7. Tipton, K.A. et al. (2015) Phase-Variable Control of Multiple Phenotypes in Acinetobacter baumannii Strain AB5075. J Bacteriol 197 (15), 2593-9.

8. Chin, C.Y. et al. (2018) A high-frequency phenotypic switch links bacterial virulence and environmental survival in Acinetobacter baumannii. Nat Microbiol 3 (5), 563-569.

9. Perez-Varela, M., Tierney, A.R.P., Kim, J., Vazquez-Torres, A., Rather, P.N. (2020) Characterization of RelA in *Acinetobacter baumannii*. Journal of Bacteriology.

10. Tierney, A.R.P. et al. (2021) A LysR-Type Transcriptional Regulator Controls Multiple Phenotypes in Acinetobacter baumannii. Frontiers in Cellular and Infection Microbiology 11 (1076).

11. Tipton, K.A. et al. (2018) Role of Capsule in Resistance to Disinfectants, Host Antimicrobials, and Desiccation in Acinetobacter baumannii. Antimicrob Agents Chemother 62 (12).

12. Lee, C.R. et al. (2017) Biology of Acinetobacter baumannii: Pathogenesis, Antibiotic Resistance Mechanisms, and Prospective Treatment Options. Front Cell Infect Microbiol 7, 55.

13. Harding, C.M. et al. (2018) Uncovering the mechanisms of Acinetobacter baumannii virulence. Nat Rev Microbiol 16 (2), 91-102.

14. Russo, T.A. et al. (2010) The K1 capsular polysaccharide of Acinetobacter baumannii strain 307-0294 is a major virulence factor. Infect Immun 78 (9), 3993-4000.

15. Niu, C. et al. (2008) Isolation and characterization of an autoinducer synthase from Acinetobacter baumannii. J Bacteriol 190 (9), 3386-92.

16. Ciampi, M.S. (2006) Rho-dependent terminators and transcription termination. Microbiology (Reading) 152 (Pt 9), 2515-2528.

17. Bidnenko, E. and Bidnenko, V. (2018) Transcription termination factor Rho and microbial phenotypic heterogeneity. Curr Genet 64 (3), 541-546.

Appendix

Roles of two-component regulatory systems in antibiotic resistance

Aimee R. P. Tierney[1] and Philip N. Rather[1,2]

[1]Department of Microbiology & Immunology, Emory University School of Medicine, Atlanta, GA, 30322 USA

[2]Research Service, Department of Veterans' Affairs, Atlanta VA Health Care System, Decatur, GA, 30033 USA

Published in Future Microbiology, 2019

14(6): 533–552.

ARPT wrote the original manuscript followed by guidance, revisions, and editing from PNR.

Abstract

Two-component regulatory systems (TCSs) are a major mechanism by which bacteria sense and respond to changes in their environment. TCSs typically consist of two proteins that bring about major regulation of the cell genome through coordinated action mediated by phosphorylation. Environmental conditions that activate TCSs are numerous and diverse and include exposure to antibiotics as well as conditions inside a host. The resulting regulatory action often involves activation of antibiotic defenses and changes to cell physiology that increase antibiotic resistance. Examples of resistance mechanisms enacted by TCSs contained in this review span those found in both Gram-negative and Gram-positive species and include cell surface modifications, changes in cell permeability, increased biofilm formation, and upregulation of antibiotic-degrading enzymes.

Executive summary

- Bacteria utilize coupled sensory-response proteins known as two-component systems (TCSs) to sense environmental changes, including exposure to antibiotics and conditions inside a host, and to respond with activation of genes that increase antibiotic resistance.
- TCSs are ubiquitous in bacteria and can initiate a variety of antibiotic resistance mechanisms, including modification of the cell surface, increased efflux, decreased influx, biofilm formation and upregulation of antibiotic-degrading enzymes.
- The importance of TCSs to antibiotic resistance, in addition to their role in regulating virulence, has led to the current focus in drug discovery for TCS inhibitors.

The escalating issue of antibiotic resistance

Since the introduction of penicillin in 1942, antibiotics have been nothing short of miracle drugs, prolonging life through treatment of previously lethal infections and permitting advances in healthcare through surgery. However, within 2 years of clinical implementation of penicillin, healthcare workers were already beginning to see a loss of drug efficacy due to bacterial resistance. Now, over 70 years later, a post-antibiotic era is either here or uncomfortably close. Measures must be taken to institute better stewardship of current drugs to dedicate funding to research of new drugs as well as to research the mechanisms of antibiotic resistance. This last point may seem comparatively trivial or too little, too late, but an understanding of how bacteria evade antibiotics is crucial to the success of both the former measures.

The intent of this review is to introduce the primary mechanisms by which bacteria activate antibiotic resistance via two-component regulatory systems (TCSs). TCSs are ubiquitous in bacteria and crucial to the maintenance of homeostasis, allowing bacteria to sense changes in their

environment and respond accordingly. While the primary purpose of many TCSs is to initiate responses to simple criteria such as environmental changes in nutritional availability and osmolarity, others directly respond to the presence of antibiotics or conditions induced by them. In many cases the identity of the signal is not known, and even TCSs that do not directly sense antibiotics may respond to conditions that overlap with those found inside hosts or may indirectly lead to an increased antibiotic-resistant state. Consequently, TCSs are major players in the realm of infectious disease caused by pathogenic bacteria, and so much so that recent years have seen an increase in research of identifying drugs that target TCSs [1–21].

Fundamentals of bacterial two-component signal transduction

Prototypical bacterial TCSs consist of a pair of proteins: a sensor histidine kinase (HK) and a response regulator (RR) (**Figure 1**). The HK constitutes a homodimeric integral membrane protein with an N-terminal domain containing a receptor that faces the extracellular or periplasmic space and a C-terminal kinase domain located in the cytosol. These domains are connected by a series of transmembrane helices, the number of which vary from system to system. The variable HK N-terminal domain senses environmental changes via binding of an extracellular ligand or through other conformational changes, which triggers autophosphorylation of a conserved C-terminal histidine residue through adenosine triphosphate hydrolysis. The histidine-bound phosphate is transferred to an aspartate residue in the conserved N-terminal domain of the RR, a homodimeric protein located in the cytosol, which activates the RR's variable C-terminal output domain, allowing it to regulate genomic expression via targeting of DNA. Through this flow of information through phosphorylation, bacteria are able to effectively sense changes in their surroundings (nutrition, pH, osmotic pressure, antibiotics, etc.) and orchestrate their genetic expression in a way

that permits a rapid, cohesive reaction to a dynamic environment [22–26]. Furthermore, the variable natures of the input domain of the HK and the output domain of the RR can allow adaptation to recognize new signaling molecules and/or regulate different genetic *foci*.

The number and organization of proteins comprising a TCS can vary from the archetypal arrangement described above. For example, certain systems utilize an intramembrane-sensing HK (IM-HK), which is significantly smaller than an average HK and does not extend into the extracellular or periplasmic space (**Figure 1**). The IM-HKs were originally predicted to detect stimuli within or at the surface of the membrane [27,28], but more recent studies indicated that these minimalistic HKs do not carry out sensory functions independently and instead recruit additional proteins that detect membrane stimuli [29–31]. Additionally, despite the name of 'two-component system', the domains that compose the HK and RR may exist on multiple separate proteins, forming a phosphorelay. In particular, it is not uncommon for an independent protein to provide the histidine-containing phosphotransfer (HPt) domain that transfers a phosphate to the RR aspartate [32,33]. Finally, an additional gene product may be required for proper functioning of the HK [34] or act as a second RR [35], forming a 'three-component system'.

A subset of sensor kinases autophosphorylate on a serine or threonine residue, which is similar to signal transduction in eukaryotic cells and has resulted in their being termed eukaryotic-like Ser/Thr kinases (eSTKs). The eSTKs bring about cellular changes by different mechanisms than TCSs, and therefore are not considered to be substitutes of HKs in TCSs. However, interactions in signaling between eSTKs and TCSs can occur [36]. As the purpose of this review is to consider antibiotic resistance controlled specifically by TCSs, eSTKs will not be discussed further.

Mechanisms of TCS-induced antibiotic resistance

In many cases, TCSs respond directly to the presence of antibiotics to bring about a resistant phenotype. In other cases, TCS-enacted global regulation in response to general environmental stressors or changes results in physiological changes that indirectly render the bacteria more resistant to antibiotics. While the types of environmental signals are highly variable, the resulting mechanisms of antibiotic resistance brought about by TCSs will be divided into four categories for the purposes of this review: modification of the cell surface, decreased drug influx or increased drug efflux, upregulation of antibiotic-degrading enzymes and alternative forms of antibiotic resistance, including biofilm production and stress response-induced antibiotic resistance. The following sections will highlight the best characterized TCSs per category of resistance mechanism. Additional TCSs and those that affect antibiotic resistance through an undetermined mechanism can be found in Table 1.

Modification of cell surfaces

Different classes of antibiotics work through a variety of mechanisms that cause bacterial lysis or stasis. However, all antibiotics must first interact with the outermost portion of the cell. In Gram-negative bacteria, this is the outer membrane (OM), and in Gram-positive bacteria, it is the cell wall composed of peptidoglycan. Many antibiotics directly target the OM, peptidoglycan or their biogenesis as their destabilization is lethal to cells [222].

Gram-negative bacteria

Strongly positively charged antibiotics such as polymyxin B, colistin, aminoglycosides, as well as host cationic antimicrobial peptides (CAMPs) take advantage of the net negative charge of the OM

in Gram-negative cells. Polymyxin B, colistin and host CAMPs utilize a self-promoted uptake system in which they interact with the OM to form neutral patches that lead to membrane breakage, thereby permitting drug or peptide passage to the periplasm. Here, the amphipathic portion of the cationic molecules insert into the cytoplasmic membrane to form pores, leading to the breakdown of the membrane and cell death. It is also possible for this insertion to occur at the OM [223,224]. Aminoglycosides use the difference in charge to cross the membrane and reach their target – the bacterial ribosome [225–227]. The anionic nature of the OM is due to the prevalence of lipopolysaccharide, which contains a negatively charged lipid A moiety. Bacteria can reverse this state by covalent modification of the lipid A through which the OM becomes positively charged, resulting in decreased or abolished antibiotic action. The three most common modifications to lipid A are the addition of 4-aminoarabinose (4AA), phosphoethanolamine (PEtN) or palmitic acid, the latter of which reduces membrane fluidity but does not affect charge [151,152].

TCSs play a major role in OM lipid A modification, and the two of the best known and most well-characterized TCSs, PhoPQ and PmrAB are found in many Gram-negative bacterial species including but not limited to: *Salmonella enterica, Enterobacter cloacae, Pseudomonas aeruginosa, Klebsiella pneumoniae,* and *Yersinia pestis* [151–170]. PhoQ is a HK located in the inner membrane (IM) which activates in response to low concentrations of Mg^{2+} or to the presence of polycationic peptides. The SK PhoQ then activates the RR PhoP, which can bring about modifications to the OM via genetic regulation. The path leading to lipid A modification differs from species to species. In *S. enterica,* PhoP can further activate *pmrAB*, which can lead to PEtN and 4AA modifications to lipid A by activation of the *pmrCAB* and *arnBCADTEF-pmrE* operons, respectively [38,164,173,228–232]. In *P. aeruginosa*, the *arnBCADTEF-pmrE* operon can be directly induced by PhoP or else via the PmrAB TCS [154]. Furthermore, PmrAB is capable of

activating independently of PhoPQ through sensing of low pH or high Fe^{3+} levels [39,163,171,231], and a recent study of clinical isolates of *Acinetobacter baumannii*, a multidrug resistant Gram-negative nosocomial pathogen, found mutations in PmrAB could invoke up to a 30-fold increase in transcription of *pmrC*, which encodes the lipid A phosphoethanolamine transferase [233]. Finally, PhoP can also activate *pagB*, a gene encoding a palmitoyltransferase which modifies lipid A by addition of a palmitic acid [158].

Two additional TCSs in *P. aeruginosa*, ParRS and CprRS can activate the *arnBCADTEF* operon, which regulates 4-AA modification of lipid A in response to the detection of subinhibitory concentrations of polymyxins and colistin [83–87,147]. A recent study further demonstrated the critical need to understand these systems, as the researchers found that 4-AA lipid A modifications are a prerequisite to the evolution of colistin resistance in *P. aeruginosa* [234].

Finally, in several Gram-negative organisms, including *E. coli* and *Salmonella* species, the Rcs TCS, also known as the Rcs phosphorelay, regulates expression of *ugd*, which is essential to the production and incorporation of 4-AA into the lipopolysaccharide [158,174–184]. Further, in *E. coli* the Rcs TCS has been shown to increase PagP expression in mature biofilms, leading to increased lipid A palmitoylation and consequently enhanced resistance to treatment with positively charged antibiotics [184,235].

Gram-positive bacteria

The peptidoglycan of bacterial cell walls is formed by alternating sugar residues N-acetylglucosamine (NAG) and N-acetylmuramic acid (NAM), polymers of which are linked together by cross-linked peptide side chains bound to NAM. During cell wall biosynthesis, the

peptide side chains begin as pentapeptides bound to a Lipid II precursor molecule, and in many species the pentapeptide contains a terminal D-Ala moiety. The cross-linkage of peptide side chains on opposite strands of the NAM-NAG polymer is catalyzed by a transpeptidase enzyme that recognizes the D-Ala signature. The transpeptidase cleaves the distal D-Ala from each side chain being cross-linked and forms a bond between the two side chains.

Both the glycopeptide and β-lactam classes of antibiotics attempt to shut down cell wall synthesis by preventing the final cross-linking step of peptidoglycan synthesis. In the case of glycopeptides, such as vancomycin, inhibition is accomplished by binding of the drug to the D-Ala peptides, which simultaneously blocks polymerization of Lipid II through transglycosylation as well as the transpeptidase action [236]. β-lactams, such as penicillin, mimic the D-Ala-D-Ala moiety and bind to the active site of the transpeptidase enzyme, impeding it from binding its true substrate. For this reason, transpeptidase enzymes that cross-link peptidoglycan are called penicillin binding proteins (PBPs) [237].

The TCSs in many bacterial species can sense antimicrobials or antimicrobial-induced cell wall damage and initiate a response. Vancomycin-resistant *Enterococcus* and vancomycin-resistant *Staphylococcus aureus* and several *Streptomyces* species utilize a chromosomal or plasmid encoded VanSR TCS to counteract vancomycin. The VanS, the HK, is located in the plasma membrane and autophosphorylates on exposure to vancomycin. Subsequent activation of the RR VanR results in the activation of several genes – *vanA/B*, *vanH*, *vanX* and *vanY* – whose products collectively negate vancomycin's mechanism of action. The VanA/B ligates D-Lac to D-Ala, lowering the concentration of D-Ala pentapeptides targetable by vancomycin. The VanH reduces pyruvate to D-Lac, further supporting the action of VanA/B. The VanX and VanY work

together to deplete the cell of the normal peptidoglycan precursors displaying the D-Ala moiety required for vancomycin recognition [199–204].

In addition to VanSR defenses, *S. aureus* encodes VraSR and GraRS, both of which prevent antibiotic targeting of cell surfaces. The VraSR acts to mitigate antibiotic degradation of the cell wall specifically during the early and late stages of peptidoglycan synthesis. The system is induced by the action of β-lactams or glycopeptides, increasing resistance to vancomycin, daptomycin and oxacillin [60,211–216]. The VraSR has also been shown to increase expression of PBP2, which plays a role in methicillin and vancomycin resistance [217]. The GraRS, also known as the APS system (antimicrobial peptide sensing), reverses the surface bacterial charge via *D*-alanylation of teichoic acids to repel positively charged antibiotics and host cAMPs [129,130,238,239].

Enterococcus faecalis and *Enterococcus faecium* utilize the CroRS TCS to resist β-lactam antibiotics including ampicillin and cephalosporins. In this case the CroS HK activates in response to antimicrobial-induced cell wall damage, and in response, CroR upregulates PBP5, an alternative PBP which can still carry out transpeptidase activity while having a low-binding affinity for β-lactams [100–106].

Several *Streptococcus* species including *S. pneumoniae, S. mutans, S. agalactiae* (group B *Streptococcus*) utilize LiaSR to respond to cell-envelope stressors such as vancomycin, bacitracin and polymyxin B, resulting in activation of genes involved in cell wall maintenance [34,71,133–136].

TCS regulation of drug influx & efflux

Bacteria regulate entry and exit of many molecules via the expression of porins and efflux pumps. Porins, also called outer membrane proteins (OMPs), are β-barrel proteins embedded in the OM of Gram-negative bacteria that allow passive diffusion of molecules. Hydrophilic antibiotics such as β-lactams, aminoglycosides and fluoroquinolones can enter cells via porins, and therefore, downregulation of porins can reduce permeation and decrease susceptibility to a wide variety of antibiotics [240–244].

Efflux pumps are active transport proteins essential to bacterial homeostasis through expulsion of toxic substances and are found in all types of bacteria. Naturally, bacteria also use them to expel antibiotics, and many drug resistances arise from increased expression or activity of efflux pumps [242,243,245]. Some types of pumps transport a wide variety of structurally dissimilar compounds, and it is these that give rise to multiple drug resistances (MDR) and are therefore termed MDR efflux pumps. Increased expression of efflux pumps is often a first step to high levels of resistance as it allows the bacteria to cope with low to intermediate levels of an antibiotic, thereby giving it a chance to gain additional mutations [246]. It is therefore unsurprising that there are many instances of TCS-mediated upregulation of efflux pumps found across many species of MDR bacteria. Here, we will consider a few examples to appreciate the prevalence and diversity of these resistance mechanisms.

Gram-negative bacteria

One of the best known TCSs in Gram-negatives is the EnvZ/OmpR, which is found in a wide variety of species including *E. coli, A. baumannii, Yersinia* species and *S. enterica* among others [89,90,108–121]. EnvZ is a HK that primarily senses osmolarity changes and modulates the RR

OmpR to regulate expression levels of the OM porins OmpC and OmpF according to levels of certain chemicals in the environment. Reduced expression levels of these OMPs has been seen to upregulate resistance to β-lactams in *E. coli* and *S. enterica* Typhimurium [38,89,90,108–110,112], and furthermore, OmpR has been seen to act in additional regulatory pathways in *Yersinia*, activating the AcrAB-TolC MDR efflux pump [122].

In *P. aeruginosa*, the TCSs CzcRS and CopRS respond to the presence of metals in the environment. The HK CzcS senses zinc, cobalt, cadmium and copper, while the CopS HK senses copper. Both RRs, CzcR and CopR, repress expression of the OrpD porin. As a result, carbapenem antibiotics, a subclass of β-lactams used to treat highly problematic MDR infections, can no longer access their target PBPs due to the lack of an entry route [81,82,107]. Another *P. aeruginosa* sensor kinase SagS, a TCS hybrid, activates the RR BlrR via cyclic-di-GMP to turn on MDR ABC transporters [190–197]. Additionally, the AmgRS TCS responds to membrane stress and damage induced by aminoglycosides by upregulating the *mexAB-oprM* MDR efflux pump [45].

Similarly, *K. pneumoniae* encodes two TCSs, CpxAR and PhoBR, that repress the KpnO porin, decreasing susceptibility to several antibiotics including chloramphenicol, amikacin, nalidixic acid, and tetracycline. Both TCSs activate due to OM stress [91,150]. Furthermore, CpxAR simultaneously upregulates three MDR RND-family efflux pumps in response to OM stress in *K. pneumoniae* [91]. A CpxAR homolog in *E. coli* acts identically, repressing expression of the porins OmpF and OmpC [92,93] and simultaneously activating the *mar* operon which increases expression of the MDR pump AcrAB-TolC [122].

A. baumannii has at least two TCSs that upregulate MDR efflux pumps. The first, AdeRS, activates the AdeABC MDR pump, and the second, BaeSR, also activates AdeABC as well as two

other pumps: AdeIJK and MacAB-TolC [38–44,49]. In *E. coli*, BaeSR acts similarly, activating the mdtABCD gene cluster encoding a multidrug transporter [50,51]. Finally, BaeSR acts in *S. enterica* Typhimurium to upregulate two OMPs, resulting in increased resistance to ceftriaxone [52].

In *Stenotrophomonas maltophilia*, a nosocomial pathogen, the TCS PhoPQ not only contributes to polymyxin resistance through lipid A modification, but also causes resistance to gentamicin, kanamycin, and streptomycin (aminoglycosides) through activation of SmeZ, an efflux protein [172], which is also regulated by an additional *S. maltophilia* TCS called SmeRySy [198].

Gram-positive bacteria

S. aureus encodes two TCSs that increase resistance by upregulation of various ABC transporters in response to low concentrations of antibiotics: GraRS, which has been implicated in vancomycin resistance through upregulation of the VraFG ABC transporter [61,130,131] and BraRS, also called BceRS or NsaRS, which activates the BraDE and VraDE ABC transporters, increasing resistance to nisin and bacitracin [60–64].

Bacillus subtilis, a soil-dwelling model organism, increases expression of BceAB, an ABC-family efflux pump, via its TCS BceRS in response to exposure to the antibiotic bacitracin [65,66]. Similarly, the YvcPQ TCS in *Bacillus thuringiensis*, a member of the *Bacillus cereus* group, modulates efflux via two ABC transporters in response to lantibiotics and bacitracin [221].

Mycobacteria

Finally, *Mycobacterium tuberculosis* encodes an essential TCS called MtrAB that primarily functions in replication and cell wall biosynthesis. However, MtrA also binds and

activates the *iniBAC* promoter, an operon encoding an efflux pump that increases resistance to isoniazid and ethambutol, two first-line antituberculosis drugs [143–145,247–253]. Additionally, mutations to *mtrA* in *M. smegmatis* resulted in decreased resistance to rifampicin and vancomycin, albeit with increased resistance to isoniazid [254]. In the opportunistic pathogen *M. avium*, MtrAB is required for conversion to a virulent, MDR colony morphotype, presumably by decreasing cell permeability [146].

TCS regulation of antibiotic-modifying enzymes

A discussion of antibiotic resistance would not be complete without mention of the first resistance mechanism clinicians encountered after the introduction of penicillin: the production of enzymes that target the antibiotic itself. As their name suggests, β-lactamases are enzymes that degrade β-lactam antibiotics, which they accomplish through hydrolyzation of the β-lactam ring. They are comprised of many subclasses including but not limited to carbapenemases, cephalosporinases and penicillinases. Other classes of enzymes inactivate antibiotics by direct modification, such as aminoglycoside and chloramphenicol acetyltransferases [255].

The CreBC TCS in *P. aeruginosa* not only affects biofilm formation, but also activates the chromosomal *ampC* gene encoding a β-lactamase. The HK CreB directly senses β-lactam activity, making this system particularly effective: it detects a specific threat and responds with a specific countermeasure [96–99].

Another example is the BlrAB TCS found in bacteria of the *Aeromonas* genus (Gram-negative). Analogous to the CreBC TCS, the BlrB HK autophosphorylates in response to accumulation of pentapeptides in the periplasm, the result of β-lactam inhibition of PBP4.

Subsequent phosphorylation of BlrA results in activation of three β-lactamases: a cephalosporinase, a penicillinase and a carbapenemase [57–59].

A final example in the MDR nosocomial pathogen *Providencia stuartii*, the AarG sensor kinase has been implicated in aminoglycoside resistance through regulation of the *aac(2')-Ia* gene encoding an aminoglycoside acetyltransferase. Furthermore, a mutation in *aarG* gave rise to several additional intrinsic resistances to tetracycline, chloramphenicol and ciprofloxacin, a phenotype that was hypothesized to be mediated via derepression of *aarP*, encoding a global transcriptional regulator that targets various MDR-associated genes [37].

Alternative forms of resistance

Upregulation of biofilm formation

Biofilms are structurally complex bacterial communities that present a major obstacle to the treatment of many infections. While a thorough discussion of the issues of antibiotic efficacy in eradication of bacteria contained in biofilms is beyond the scope of this review, it is important to convey that biofilm formation generally results in increased tolerance or resistance to antibiotics in several ways including differential gene expression in biofilms, decreased drug penetration through the matrix and the presence of dormant populations of cells or persisters [256–264].

Several *Streptococcus* species including *S. pyogenes*, *S. mutans* and *S. pneumoniae* utilize the TCS VicKR, which upregulates biofilm formation in response to an as-yet-undetermined environmental signal [137,206–208]. In *S. mutans*, LiaSR also increases biofilm formation in response to cell envelope stress and can directly react to the antibiotic bacitracin [135,137]. At least two other TCSs, ComDE and *hk11*/*rr11* in *S. mutans*, also appear to function in the formation of biofilm [79,80,132].

P. aeruginosa is well known for its role in cystic fibrosis-associated lung infections and the tremendous difficulties encountered in treatment due to the impenetrable nature of its biofilm. Therefore, it is not surprising that *P. aeruginosa* encodes several TCSs that facilitate biofilm formation [187]. The two-component hybrid SagS directs the transition from a planktonic to surface-associated way of life, activating a second TCS, BfiSR, which is essential to the formation of biofilm. As previously noted, SagS simultaneously activates the BrlR RR to upregulate MDR efflux pumps within the biofilm, greatly increasing the biofilm drug tolerance [190–197]. CreBC directly senses β-lactam inhibition of PBP4 and responds by increasing biofilm formation [97]. The GacSA TCS in *P. aeruginosa* is also essential for biofilm formation and is unique among other GacSA systems in that the GacS sensor kinase cannot autophosphorylate. Instead GacS must be activated by the orphan sensor kinase RetS, which functions as both a kinase and phosphatase to GacS [187–189]. Several more TCSs, including the Roc1 system, Rcs/Pvr, PprAB and PilRS, regulate the expression of cup fimbriae and/or type IV *pili* required for surface adhesion and prerequisite to biofilm formation in *P. aeruginosa* [35,185,187,265–268]. Furthermore and finally, small colony variants [269] in this species are known to have increased biofilm production and multidrug resistance [270], and interestingly, a recent study on clinical isolates of *P. aeruginosa* revealed that mutations in *amgRS* as well as *pmrAB* culminated in a highly drug resistant SCV phenotype [46].

BfmRS, a TCS in *A. baumannii*, also upregulates biofilm production, possibly in response to sublethal concentrations of chloramphenicol, and in doing so, becomes increasingly recalcitrant to treatment [1,38,39,53–56]. Finally, the Rcs TCS is also essential to biofilm formation in *E. coli*, *Proteus mirabilis* and *S. enterica* Typhimurium as well as other species [174–182,186,187].

Stress response-associated antibiotic resistance

A number of TCSs induce cellular stress responses in reaction to environmental changes including poor nutrition, fluctuations in temperature, membrane integrity and oxidative stress. Stress responses often bring about global transcriptional changes, some of which alter the efficacy of antibiotic action. Many of the previously discussed TCSs are considered to function in this manner, including PhoPQ, CpxAR, LiaSR, BaeSR, BceRS, BraRS, VraSR, CroRS and ParRS [34,133,271–273]. Other examples include the AmgRS TCS in *P. aeruginosa*, which is believed to respond to membrane stress caused by aminoglycoside-induced accumulation of mistranslated peptides by upregulating certain proteases and otherwise implementing measures that protect the membrane [47,48].

Future perspective

TCSs are incredibly versatile and provide bacteria with an indispensable tool for sensing and reacting to their surroundings. Given the essential role of TCSs in bacterial homeostasis as well as the diverse antibiotic resistance mechanisms that can be activated through them, TCSs are an intriguing target for the development of new antimicrobial therapeutics [1–21]. The ability to use predictive software to identify putative compounds that bind one or more TCSs to render them ineffective would be an essential tool in the pharmaceutical targeting of TCSs [2]. Further, the conserved nature of certain domains of the various HKs and RRs both within and across bacterial species could be exploited to develop new broad-spectrum antimicrobials, although portions of these domains share similarity to eukaryotic proteins and thereby could lead to inhibition of host cell processes. Tiwari *et al.* recently published a review on this topic that covers the benefits and

feasibility of medicinal targeting of TCSs and lists several predicted and validated TCS inhibitors [21].

While this review cannot hope to detail the myriad and often pleiotropic effects of TCSs, one can certainly begin to grasp the scope of their importance in antibiotic resistance from the research compiled herein. The numerous instances of TCS-induced resistance mechanisms across both Gram-negative and Gram-positive species highlights the need for further and continued investigation into targeting TCSs in the future development of antimicrobial therapeutics.

Acknowledgments

Authors would like to thank W Shafer of Emory University for critical reading of this manuscript.

Funding

This work is supported by the following awards to PN Rather, VA Merit Award I01 BX001725 and Research Career Scientist Award IK6BX004470; both from the Department of Veterans Affairs and R01AI072219 from the National Institutes of Health. ARP Tierney is supported by the T32 training grant AI106699 from the National Institutes of Health. The authors have no other relevant affiliations or financial involvement with any organization or entity with a financial interest in or financial conflict with the subject matter or materials discussed in the manuscript apart from those disclosed.

References

Papers of special note have been highlighted as: • of interest; •• of considerable interest

1. Russo TA, Manohar A, Beanan JM. et al. The response regulator BfmR is a potential drug target for *acinetobacter baumannii*. *mSphere* 1(3), pii:e00082–16 (2016).

2. Bem AE, Velikova N, Pellicer MT, Baarlen P, Marina A, Wells JM. Bacterial histidine kinases as novel antibacterial drug targets. *ACS Chem. Biol.* 10(1), 213–224 (2015).

3. Worthington RJ, Blackledge MS, Melander C. Small-molecule inhibition of bacterial two-component systems to combat antibiotic resistance and virulence. *Future Med. Chem.* 5(11), 1265–1284 (2013).

4. Barrett JF, Goldschmidt RM, Lawrence LE. et al. Antibacterial agents that inhibit two-component signal transduction systems. *Proc. Natl Acad. Sci. USA* 95(9), 5317–5322 (1998).

5. Barrett JF, Hoch JA. Two-component signal transduction as a target for microbial anti-infective therapy. *Antimicrob. Agents Chemother.* 42(7), 1529–1536 (1998).

6. Cardona ST, Choy M, Hogan AM. Essential two-component systems regulating cell envelope functions: opportunities for novel antibiotic therapies. *J. Membr. Biol.* 251(1), 75–89 (2018).

7. Cai XH, Zhang Q, Shi SY, Ding DF. Searching for potential drug targets in two-component and phosphorelay signal-transduction systems using three-dimensional cluster analysis. *Acta Biochim. Biophys. Sin. (Shanghai)* 37(5), 293–302 (2005).

8. Dbeibo L, Van Rensburg JJ, Smith SN. et al. Evaluation of CpxRA as a therapeutic target for uropathogenic *Escherichia coli* infections. *Infect. Immun.* 86(3), e00798–17 (2018).

9. Hilliard JJ, Goldschmidt RM, Licata L, Baum EZ, Bush K. Multiple mechanisms of action for inhibitors of histidine protein kinases from bacterial two-component systems. *Antimicrob. Agents Chemother.* 43(7), 1693–1699 (1999).

10. Hlasta DJ, Demers JP, Foleno BD. et al. Novel inhibitors of bacterial two-component systems with Gram-positive antibacterial activity: pharmacophore identification based on the screening hit closantel. *Bioorg. Med. Chem. Lett.* 8(14), 1923–1928 (1998).

11. Milton ME, Minrovic BM, Harris DL. et al. Re-sensitizing multidrug resistant bacteria to antibiotics by targeting bacterial response regulators: characterization and comparison of interactions between 2-aminoimidazoles and the response regulators BfmR from *acinetobacter baumannii* and QseB from *Francisella* spp. *Front. Mol. Biosci* 5, 15 (2018).

12. Stephenson K, Yamaguchi Y, Hoch JA. The mechanism of action of inhibitors of bacterial two-component signal transduction systems. *J. Biol. Chem.* 275(49), 38900–38904 (2000).

13. Stephenson K, Hoch JA. Two-component and phosphorelay signal-transduction systems as therapeutic targets. *Curr. Opin. Pharmacol.* 2(5), 507–512 (2002).

14. Stephenson K, Hoch JA. Virulence- and antibiotic resistance-associated two-component signal transduction systems of Gram-positive pathogenic bacteria as targets for antimicrobial therapy. *Pharmacol. Ther.* 93(2–3), 293–305 (2002).

15. Stephenson K, Hoch JA. Histidine kinase-mediated signal transduction systems of pathogenic microorganisms as targets for therapeutic intervention. *Curr. Drug Targets Infect. Disord.* 2(3), 235–246 (2002).

16. Stephenson K, Hoch JA. Developing inhibitors to selectively target two-component and phosphorelay signal transduction systems of pathogenic microorganisms. *Curr. Med. Chem.* 11(6), 765–773 (2004).

17. Tang YT, Gao R, Havranek JJ, Groisman EA, Stock AM, Marshall GR. Inhibition of bacterial virulence: drug-like molecules targeting the *Salmonella enterica* PhoP response regulator. *Chem. Biol. Drug Des.* 79(6), 1007–1017 (2012).

18. Utsumi R, Igarashi M. [Two-component signal transduction as attractive drug targets in pathogenic bacteria]. *Yakugaku Zasshi* 132(1), 51–58 (2012).

19. Velikova N, Fulle S, Manso AS. et al. Putative histidine kinase inhibitors with antibacterial effect against multi-drug resistant clinical isolates identified by *in vitro* and *in silico* screens. *Sci. Rep.* 6, 26085 (2016).

20. Wilke KE, Francis S, Carlson EE. Inactivation of multiple bacterial histidine kinases by targeting the ATP-binding domain. *ACS Chem. Biol.* 10(1), 328–335 (2015).

21. Tiwari S, Jamal SB, Hassan SS. et al. Two-component signal transduction systems of pathogenic bacteria as targets for antimicrobial therapy: an overview. *Front. Microbiol.* 8, 1878 (2017). •• Review of the benefits and feasibility of medicinal targeting of two-component regulatory systems (TCSs) and lists several predicted and validated TCS inhibitors.

22. Bourret RB, Silversmith RE. Two-component signal transduction. *Curr. Opin. Microbiol.* 13(2), 113–115 (2010).

23. Cheung J, Hendrickson WA. Sensor domains of two-component regulatory systems. *Curr. Opin. Microbiol.* 13(2), 116–123 (2010).

24. Groisman EA. Feedback control of two-component regulatory systems. *Annu. Rev. Microbiol.* 70, 103–124 (2016). •• Detailed review of TCS functionality, regulation and the significance of these systems to bacterial physiology.

25. Nixon BT, Ronson CW, Ausubel FM. Two-component regulatory systems responsive to environmental stimuli share strongly conserved domains with the nitrogen assimilation regulatory genes *ntrB* and *ntrC*. *Proc. Natl Acad. Sci. USA* 83(20), 7850–7854 (1986).

26. Hoch JA. Two-component and phosphorelay signal transduction. *Curr. Opin. Microbiol.* 3(2), 165–170 (2000).

27. Mascher T, Margulis NG, Wang T, Ye RW, Helmann JD. Cell wall stress responses in *Bacillus subtilis*: the regulatory network of the bacitracin stimulon. *Mol. Microbiol.* 50(5), 1591–1604 (2003).

28. Mascher T. Intramembrane-sensing histidine kinases: a new family of cell envelope stress sensors in Firmicutes bacteria. *FEMS Microbiol. Lett.* 264(2), 133–144 (2006).

29. Mascher T. Bacterial (intramembrane-sensing) histidine kinases: signal transfer rather than stimulus perception. *Trends Microbiol.* 22(10), 559–565 (2014).

30. Revilla-Guarinos A, Gebhard S, Mascher T, Zuniga M. Defence against antimicrobial peptides: different strategies in Firmicutes. *Environ. Microbiol.* 16(5), 1225–1237 (2014).

31. Gebhard S, Mascher T. Antimicrobial peptide sensing and detoxification modules: unravelling the regulatory circuitry of *Staphylococcus aureus*. *Mol. Microbiol.* 81(3), 581–587 (2011).

32. Gao R, Stock AM. Biological insights from structures of two-componentrproteins. *Ann. Rev. Microbiol.* 63, 133–154 (2009).

33. Salvado B, Vilaprinyo E, Sorribas A, Alves R. A survey of HK, HPt, and RR domains and their organization in two-component systems and phosphorelay proteins of organisms with fully sequenced genomes. *PeerJ* 3, e1183 (2015).

34. Jordan S, Junker A, Helmann JD, Mascher T. Regulation of LiaRS-dependent gene expression in *Bacillus subtilis*: identification of inhibitor proteins, regulator binding sites, and target genes of a conserved cell envelope stress-sensing two-component system. *J. Bacteriol.* 188(14), 5153–5166 (2006).

35. Kuchma SL, Connolly JP, O'toole GA. A three-component regulatory system regulates biofilm maturation and type III secretion in *Pseudomonas aeruginosa*. *J. Bacteriol.* 187(4), 1441–1454 (2005).

36. Dworkin J. Ser/Thr phosphorylation as a regulatory mechanism in bacteria. *Curr. Opin. Microbiol.* 24(Suppl. C), 47–52 (2015).

37. Rather PN, Paradise MR, Parojcic MM, Patel S. A regulatory cascade involving AarG, a putative sensor kinase, controls the expression of the 2′-N-acetyltransferase and an intrinsic multiple antibiotic resistance (Mar) response in *Providencia stuartii*. *Mol. Microbiol.* 28(6), 1345–1353 (1998).

38. Lee CR, Lee JH, Park M. et al. Biology of *acinetobacter baumannii*: pathogenesis, antibiotic resistance mechanisms, and prospective treatment options. *Front. Cell. Infection Microbiol.* 7, 55 (2017).

39. Kroger C, Kary SC, Schauer K, Cameron AD. Genetic regulation of virulence and antibiotic resistance in *acinetobacter baumannii*. *Genes (Basel)* 8(1), pii:E12 (2016).

40. Richmond GE, Evans LP, Anderson MJ. et al. The *Acinetobacter baumannii* two-component system AdeRS regulates genes required for multidrug efflux, biofilm formation, and virulence in a strain-specific manner. *mBio* 7(2), e00430–e00416 (2016).

41. Adams FG, Stroeher UH, Hassan KA, Marri S, Brown MH. Resistance to pentamidine is mediated by AdeAB, regulated by AdeRS, and influenced by growth conditions in *Acinetobacter baumannii* ATCC 17978. *PLoS ONE* 13(5), e0197412 (2018).

42. Coyne S, Courvalin P, Perichon B. Efflux-mediated antibiotic resistance in *Acinetobacter* spp. *Antimicrob. Agents Chemother.* 55(3), 947–953 (2011).

43. Marchand I, Damier-Piolle L, Courvalin P, Lambert T. Expression of the RND-type efflux pump AdeABC in *Acinetobacter baumannii* is regulated by the AdeRS two-component system. *Antimicrob. Agents Chemother.* 48(9), 3298–3304 (2004).

44. Yoon EJ, Courvalin P, Grillot-Courvalin C. RND-type efflux pumps in multidrug-resistant clinical isolates of *Acinetobacter baumannii*: major role for AdeABC overexpression and AdeRS mutations. *Antimicrob. Agents Chemother.* 57(7), 2989–2995 (2013).

45. Fruci M, Poole K. Aminoglycoside-inducible expression of the mexAB-oprM multidrug efflux operon in *Pseudomonas aeruginosa*: Involvement of the envelope stress-responsive AmgRS two-component system. *PLoS ONE* 13(10), e0205036 (2018).

46. Schniederjans M, Koska M, Haussler S. Transcriptional and mutational profiling of an aminoglycoside-resistant *Pseudomonas aeruginosa* small-colony variant. *Antimicrob. Agents Chemother.* 61(11), pii:e01178–17 (2017).

47. Lee S, Hinz A, Bauerle E. et al. Targeting a bacterial stress response to enhance antibiotic action. *Proc. Natl Acad. Sci. USA* 106(34), 14570–14575 (2009).

48. Lau CH, Fraud S, Jones M, Peterson SN, Poole K. Mutational activation of the AmgRS two-component system in aminoglycoside-resistant *Pseudomonas aeruginosa*. *Antimicrob. Agents Chemother.* 57(5), 2243–2251 (2013).

49. Lin MF, Lin YY, Lan CY. The role of the two-component system BaeSR in disposing chemicals through regulating transporter systems in *acinetobacter baumannii*. *PLoS ONE* 10(7), e0132843 (2015).

50. Baranova N, Nikaido H. The baeSR two-component regulatory system activates transcription of the yegMNOB (mdtABCD) transporter gene cluster in *Escherichia coli* and increases its resistance to novobiocin and deoxycholate. *J. Bacteriol.* 184(15), 4168–4176 (2002).

51. Nagakubo S, Nishino K, Hirata T, Yamaguchi A. The putative response regulator BaeR stimulates multidrug resistance of *Escherichia coli* via a novel multidrug exporter system, MdtABC. *J. Bacteriol.* 184(15), 4161–4167 (2002).

52. Hu WS, Li PC, Cheng CY. Correlation between ceftriaxone resistance of *Salmonella enterica* serovar Typhimurium and expression of outer membrane proteins OmpW and Ail/OmpX-like protein, which are regulated by BaeR of a two-component system. *Antimicrob. Agents Chemother.* 49(9), 3955–3958 (2005).

53. Geisinger E, Isberg RR. Antibiotic modulation of capsular exopolysaccharide and virulence in *Acinetobacter baumannii*. *PLoS Pathog.* 11(2), e1004691 (2015).

54. Gaddy JA, Actis LA. Regulation of *Acinetobacter baumannii* biofilm formation. *Future Microbiol.* 4(3), 273–278 (2009).

55. Qi L, Li H, Zhang C. et al. Relationship between antibiotic resistance, biofilm formation, and biofilm-specific resistance in *Acinetobacter baumannii*. *Front. Microbiol.* 7, 483 (2016).

56. Tomaras AP, Flagler MJ, Dorsey CW, Gaddy JA, Actis LA. Characterization of a two-component regulatory system from *Acinetobacter baumannii* that controls biofilm formation and cellular morphology. *Microbiology* 154(Pt 11), 3398–3409 (2008).

57. Alksne LE, Rasmussen BA. Expression of the AsbA1, OXA-12, and AsbM1 beta-lactamases in *Aeromonas jandaei* AER 14 is coordinated by a two-component regulon. *J. Bacteriol.* 179(6), 2006–2013 (1997).

58. Niumsup P, Simm AM, Nurmahomed K, Walsh TR, Bennett PM, Avison MB. Genetic linkage of the penicillinase gene, *amp*, and blrAB, encoding the regulator of beta-lactamase expression in *Aeromonas* spp. *J. Antimicrob. Chemother.* 51(6), 1351–1358 (2003).

59. Tayler AE, Ayala JA, Niumsup P. et al. Induction of beta-lactamase production in *Aeromonas hydrophila* is responsive to beta-lactam-mediated changes in peptidoglycan composition. *Microbiology* 156(Pt 8), 2327–2335 (2010).

60. Draper LA, Cotter PD, Hill C, Ross RP. Lantibiotic resistance. *Microbiol. Mol. Biol. Rev.* 79(2), 171–191 (2015).

61. Kawada-Matsuo M, Yoshida Y, Zendo T. et al. Three distinct two-component systems are involved in resistance to the class I bacteriocins, Nukacin ISK-1 and nisin A, in *Staphylococcus aureus*. *PLoS ONE* 8(7), e69455 (2013).

62. Blake KL, Randall CP, O'neill AJ. *In vitro* studies indicate a high resistance potential for the lantibiotic nisin in *Staphylococcus aureus* and define a genetic basis for nisin resistance. *Antimicrob. Agents Chemother.* 55(5), 2362–2368 (2011).

63. Kolar SL, Nagarajan V, Oszmiana A. et al. NsaRS is a cell-envelope-stress-sensing two-component system of *Staphylococcus aureus*. *Microbiology* 157(Pt 8), 2206–2219 (2011).

64. Hiron A, Falord M, Valle J, Debarbouille M, Msadek T. Bacitracin and nisin resistance in *Staphylococcus aureus*: a novel pathway involving the BraS/BraR two-component system (SA2417/SA2418) and both the BraD/BraE and VraD/VraE ABC transporters. *Mol. Microbiol.* 81(3), 602–622 (2011).

65. Rietkötter E, Hoyer D, Mascher T. Bacitracin sensing in *Bacillus subtilis*. *Mol. Microbiol.* 68(3), 768–785 (2008).

66. Ohki R, Giyanto, Tateno K. et al. The BceRS two-component regulatory system induces expression of the bacitracin transporter, BceAB, in *Bacillus subtilis*. *Mol. Microbiol.* 49(4), 1135–1144 (2003).

67. Gottschalk S, Bygebjerg-Hove I, Bonde M. et al. The two-component system CesRK controls the transcriptional induction of cell envelope-related genes in Listeria monocytogenes in response to cell wall-acting antibiotics. *J. Bacteriol.* 190(13), 4772–4776 (2008).

68. Nielsen PK, Andersen AZ, Mols M, Van Der Veen S, Abee T, Kallipolitis BH. Genome-wide transcriptional profiling of the cell envelope stress response and the role of LisRK and CesRK in Listeria monocytogenes. *Microbiology* 158(Pt 4), 963–974 (2012).

69. Kallipolitis BH, Ingmer H, Gahan CG, Hill C, Sogaard-Andersen L. CesRK, a two-component signal transduction system in Listeria monocytogenes, responds to the presence of cell wall-acting antibiotics and affects beta-lactam resistance. *Antimicrob. Agents Chemother.* 47(11), 3421–3429 (2003).

70. Martinez B, Zomer AL, Rodriguez A, Kok J, Kuipers OP. Cell envelope stress induced by the bacteriocin Lcn972 is sensed by the Lactococcal two-component system CesSR. *Mol. Microbiol.* 64(2), 473–486 (2007).

71. Gomez-Mejia A, Gamez G, Hammerschmidt S. *Streptococcus pneumoniae* two-component regulatory systems: the interplay of the pneumococcus with its environment. *Int. J. Med. Microbiol.* 308(6), 722–737 (2018).

72. Mascher T, Heintz M, Zahner D, Merai M, Hakenbeck R. The CiaRH system of *Streptococcus pneumoniae* prevents lysis during stress induced by treatment with cell wall inhibitors and by mutations in pbp2x involved in beta-lactam resistance. *J. Bacteriol.* 188(5), 1959–1968 (2006).

73. Lévesque C, Mair R, Perry J, Lau P, Li Y, Cvitkovitch D. Systemic inactivation and phenotypic characterization of two-component systems in expression of Streptococcus mutans virulence properties. *Lett. Appl. Microbiol.* 45(4), 398–404 (2007).

74. Zahner D, Kaminski K, Van Der Linden M, Mascher T, Meral M, Hakenbeck R. The ciaR/ciaH regulatory network of *Streptococcus pneumoniae*. *J. Mol. Microbiol. Biotechnol.* 4(3), 211–216 (2002).

75. Quach D, Van Sorge NM, Kristian SA, Bryan JD, Shelver DW, Doran KS. The CiaR response regulator in group B Streptococcus promotes intracellular survival and resistance to innate immune defenses. *J. Bacteriol.* 191(7), 2023–2032 (2009).

76. Mascher T, Zahner D, Merai M, Balmelle N, De Saizieu AB, Hakenbeck R. The *Streptococcus pneumoniae* cia regulon: CiaR target sites and transcription profile analysis. *J. Bacteriol.* 185(1), 60–70 (2003).

77. Guenzi E, Gasc AM, Sicard MA, Hakenbeck R. A two-component signal-transducing system is involved in competence and penicillin susceptibility in laboratory mutants of *Streptococcus pneumoniae*. *Mol. Microbiol.* 12(3), 505–515 (1994).

78. Giammarinaro P, Sicard M, Gasc AM. Genetic and physiological studies of the CiaH–CiaR two-component signal-transducing system involved in cefotaxime resistance and competence of Streptococcus pneumoniae. *Microbiology* 145(Pt 8), 1859–1869 (1999).

79. Li YH, Tang N, Aspiras MB. et al. A quorum-sensing signaling system essential for genetic competence in Streptococcus mutans is involved in biofilm formation. *J. Bacteriol.* 184(10), 2699–2708 (2002).

80. Li YH, Lau PC, Lee JH, Ellen RP, Cvitkovitch DG. Natural genetic transformation of Streptococcus mutans growing in biofilms. *J. Bacteriol.* 183(3), 897–908 (2001).

81. Caille O, Rossier C, Perron K. A copper-activated two-component system interacts with zinc and imipenem resistance in *Pseudomonas aeruginosa*. *J. Bacteriol.* 189(13), 4561–4568 (2007).

82. Raavi, Mishra S, Singh S. Prevention of OprD regulated antibiotic resistance in *Pseudomonas aeruginosa* biofilm. *Microb. Pathog.* 112, 221–229 (2017).

83. Breidenstein EB, De La Fuente-Nunez C, Hancock RE. *Pseudomonas aeruginosa*: all roads lead to resistance. *Trends Microbiol.* 19(8), 419–426 (2011).

84. Fernandez L, Breidenstein EB, Song D, Hancock RE. Role of intracellular proteases in the antibiotic resistance, motility, and biofilm formation of *Pseudomonas aeruginosa*. *Antimicrob. Agents Chemother.* 56(2), 1128–1132 (2012).

85. Gutu AD, Sgambati N, Strasbourger P. et al. Polymyxin resistance of *Pseudomonas aeruginosa* phoQ mutants is dependent on additional two-component regulatory systems. *Antimicrob. Agents Chemother.* 57(5), 2204–2215 (2013).

86. Muller C, Plesiat P, Jeannot K. A two-component regulatory system interconnects resistance to polymyxins, aminoglycosides, fluoroquinolones, and beta-lactams in *Pseudomonas aeruginosa*. *Antimicrob. Agents Chemother.* 55(3), 1211–1221 (2011).

87. Lee JY, Chung ES, Na IY, Kim H, Shin D, Ko KS. Development of colistin resistance in pmrA-, phoP-, parR- and cprR-inactivated mutants of *Pseudomonas aeruginosa*. *J. Antimicrob. Chemother.* 69(11), 2966–2971 (2014).

88. Fernandez L, Jenssen H, Bains M, Wiegand I, Gooderham WJ, Hancock RE. The two-component system CprRS senses cationic peptides and triggers adaptive resistance in *Pseudomonas aeruginosa* independently of ParRS. *Antimicrob. Agents Chemother.* 56(12), 6212–6222 (2012).

89. Sun S, Berg OG, Roth JR, Andersson DI. Contribution of gene amplification to evolution of increased antibiotic resistance in *Salmonella typhimurium* . . *Genetics* 182(4), 1183–1195 (2009).

90. Hirakawa H, Nishino K, Yamada J, Hirata T, Yamaguchi A. Beta-lactam resistance modulated by the overexpression of response regulators of two-component signal transduction systems in *Escherichia coli*. *J. Antimicrob. Chemother.* 52(4), 576–582 (2003).

91. Srinivasan VB, Vaidyanathan V, Mondal A, Rajamohan G. Role of the two component signal transduction system CpxAR in conferring cefepime and chloramphenicol resistance in *Klebsiella pneumoniae* NTUH-K2044. *PLoS ONE* 7(4), e33777 (2012).

92. Batchelor E, Walthers D, Kenney LJ, Goulian M. The *Escherichia coli* CpxA-CpxR envelope stress response system regulates expression of the porins OmpF and OmpC. *J. Bacteriol.* 187(16), 5723–5731 (2005).

93. Raivio TL, Leblanc SK, Price NL. The *Escherichia coli* Cpx envelope stress response regulates genes of diverse function that impact antibiotic resistance and membrane integrity. *J. Bacteriol.* 195(12), 2755–2767 (2013).

94. Weatherspoon-Griffin N, Yang D, Kong W, Hua Z, Shi Y. The CpxR/CpxA two-component regulatory system up-regulates the multidrug resistance cascade to facilitate *Escherichia coli* resistance to a model antimicrobial peptide. *J. Biol. Chem.* 289(47), 32571–32582 (2014).

95. Hirakawa H, Nishino K, Hirata T, Yamaguchi A. Comprehensive studies of drug resistance mediated by overexpression of response regulators of two-component signal transduction systems in *Escherichia coli*. *J. Bacteriol.* 185(6), 1851–1856 (2003).

96. Moya B, Dotsch A, Juan C. et al. Beta-lactam resistance response triggered by inactivation of a nonessential penicillin-binding protein. *PLoS Pathog.* 5(3), e1000353 (2009).

97. Zamorano L, Moya B, Juan C, Mulet X, Blazquez J, Oliver A. The *Pseudomonas aeruginosa* CreBC two-component system plays a major role in the response to beta-lactams,

fitness, biofilm growth, and global regulation. *Antimicrob. Agents Chemother.* 58(9), 5084–5095 (2014).

98. Tsutsumi Y, Tomita H, Tanimoto K. Identification of novel genes responsible for overexpression of ampC in *Pseudomonas aeruginosa* PAO1. *Antimicrob. Agents Chemother.* 57(12), 5987–5993 (2013).

99. Avison MB, Horton RE, Walsh TR, Bennett PM. *Escherichia coli* CreBC is a global regulator of gene expression that responds to growth in minimal media. *J. Biol. Chem.* 276(29), 26955–26961 (2001).

100. Arbeloa A, Segal H, Hugonnet JE. et al. Role of class A penicillin-binding proteins in PBP5-mediated beta-lactam resistance in *Enterococcus faecalis* . . *J. Bacteriol.* 186(5), 1221–1228 (2004).

101. Comenge Y, Quintiliani R, Jr., Li L. et al. The CroRS two-component regulatory system is required for intrinsic beta-lactam resistance in *Enterococcus faecalis*. *J. Bacteriol.* 185(24), 7184–7192 (2003).

102. Kellogg SL, Kristich CJ. Functional dissection of the CroRS two-component system required for resistance to cell wall stressors in *Enterococcus faecalis*. *J. Bacteriol.* 198(8), 1326–1336 (2016).

103. Kellogg SL, Little JL, Hoff JS, Kristich CJ. Requirement of the CroRS two-component system for resistance to cell wall-targeting antimicrobials in *Enterococcus faecium*. *Antimicrob. Agents Chemother.* 61(5), pii:e02461–16 (2017).

104. Miller WR, Munita JM, Arias CA. Mechanisms of antibiotic resistance in enterococci. *Expert Rev. Anti-infect. Ther* 12(10), 1221–1236 (2014).

105. Hancock LE, Perego M. Systematic inactivation and phenotypic characterization of two-component signal transduction systems of *Enterococcus faecalis* V583. *J. Bacteriol.* 186(23), 7951–7958 (2004).

106. Snyder H, Kellogg SL, Skarda LM, Little JL, Kristich CJ. Nutritional control of antibiotic resistance via an interface between the phosphotransferase system and a two-component signaling system. *Antimicrob. Agents Chemother.* 58(2), 957–965 (2014).

107. Perron K, Caille O, Rossier C, Van Delden C, Dumas JL, Kohler T. CzcR-CzcS, a two-component system involved in heavy metal and carbapenem resistance in *Pseudomonas aeruginosa*. *J. Biol. Chem.* 279(10), 8761–8768 (2004).

108. Jaffe A, Chabbert YA, Derlot E. Selection and characterization of beta-lactam-resistant *Escherichia coli* K-12 mutants. *Antimicrob. Agents Chemother.* 23(4), 622–625 (1983).

109. Mizuno T, Mizushima S. Signal transduction and gene regulation through the phosphorylation of two regulatory components: the molecular basis for the osmotic regulation of the porin genes. *Mol. Microbiol.* 4(7), 1077–1082 (1990).

110. Cai SJ, Inouye M. EnvZ-OmpR interaction and osmoregulation in *Escherichia coli*. *J. Biol. Chem.* 277(27), 24155–24161 (2002).

111. Tipton KA, Rather PN. An ompR/envZ two-component system ortholog regulates phase variation, osmotic tolerance, motility, and virulence in *Acinetobacter baumannii* strain AB5075. *J. Bacteriol.* (2016) (Epub ahead of print).

112. Viveiros M, Dupont M, Rodrigues L. et al. Antibiotic stress, genetic response and altered permeability of *E. coli*. *PLoS ONE* 2(4), e365 (2007).

113. Russo FD, Silhavy TJ. EnvZ controls the concentration of phosphorylated OmpR to mediate osmoregulation of the porin genes. *J. Mol. Biol.* 222(3), 567–580 (1991).

114. Raczkowska A, Skorek K, Brzostkowska M, Lasinska A, Brzostek K. Pleiotropic effects of a *Yersinia enterocolitica* ompR mutation on adherent-invasive abilities and biofilm formation. *FEMS Microbiol. Lett.* 321(1), 43–49 (2011).

115. Brzostkowska M, Raczkowska A, Brzostek K. OmpR, a response regulator of the two-component signal transduction pathway, influences *inv* gene expression in *Yersinia enterocolitica* O9. *Front. Cell. Infect. Microbiol.* 2, 153 (2012).

116. Gao H, Zhang Y, Han Y. et al. Phenotypic and transcriptional analysis of the osmotic regulator OmpR in *Yersinia pestis*. *BMC Microbiol.* 11, 39 (2011).

117. Dorman CJ, Chatfield S, Higgins CF, Hayward C, Dougan G. Characterization of porin and ompR mutants of a virulent strain of *Salmonella typhimurium*: ompR mutants are attenuated *in vivo*. *Infect. Immun.* 57(7), 2136–2140 (1989).

118. Alphen WV, Lugtenberg B. Influence of osmolarity of the growth medium on the outer membrane protein pattern of *Escherichia coli*. *J. Bacteriol.* 131(2), 623–630 (1977).

119. Liljestrom P, Maattanen PL, Palva ET. Cloning of the regulatory locus ompB of *Salmonella typhimurium* LT-2. II. Identification of the *envZ* gene product, a protein involved in the expression of the porin proteins. *Mol. Gen. Genet.* 188(2), 190–194 (1982).

120. Liljestrom P, Laamanen I, Palva ET. Structure and expression of the ompB operon, the regulatory locus for the outer membrane porin regulon in *Salmonella typhimurium* LT-2. *J. Mol. Biol.* 201(4), 663–673 (1988).

121. Forst SA, Roberts DL. Signal transduction by the EnvZ-OmpR phosphotransfer system in bacteria. *Res. Microbiol.* 145(5–6), 363–373 (1994).

122. Raczkowska A, Trzos J, Lewandowska O, Nieckarz M, Brzostek K. Expression of the AcrAB components of the AcrAB-TolC multidrug efflux pump of *yersinia enterocolitica* is subject to dual regulation by OmpR. *PLoS ONE* 10(4), e0124248 (2015).

123. Eguchi Y, Oshima T, Mori H. et al. Transcriptional regulation of drug efflux genes by EvgAS, a two-component system in *Escherichia coli*. *Microbiology* 149(Pt 10), 2819–2828 (2003).

124. Nishino K, Yamaguchi A. EvgA of the two-component signal transduction system modulates production of the yhiUV multidrug transporter in *Escherichia coli*. *J. Bacteriol.* 184(8), 2319–2323 (2002).

125. Nishino K, Yamaguchi A. Overexpression of the response regulator evgA of the two-component signal transduction system modulates multidrug resistance conferred by multidrug resistance transporters. *J. Bacteriol.* 183(4), 1455–1458 (2001).

126. Kato A, Ohnishi H, Yamamoto K, Furuta E, Tanabe H, Utsumi R. Transcription of emrKY is regulated by the EvgA–EvgS two-component system in *Escherichia coli* K-12. *Biosci. Biotechnol. Biochem.* 64(6), 1203–1209 (2000).

127. Hancock LE, Perego M. The *Enterococcus faecalis* fsr two-component system controls biofilm development through production of gelatinase. *J. Bacteriol.* 186(17), 5629–5639 (2004).

128. Cerqueira GM, Kostoulias X, Khoo C. et al. A global virulence regulator in *Acinetobacter baumannii* and its control of the phenylacetic acid catabolic pathway. *J. Infect. Dis.* 210(1), 46–55 (2014).

129. Herbert S, Bera A, Nerz C. et al. Molecular basis of resistance to muramidase and cationic antimicrobial peptide activity of lysozyme in staphylococci. *PLoS Pathog.* 3(7), e102 (2007).

130. Yang SJ, Bayer AS, Mishra NN. et al. The *Staphylococcus aureus* two-component regulatory system, GraRS, senses and confers resistance to selected cationic antimicrobial peptides. *Infect. Immun.* 80(1), 74–81 (2012).

131. Meehl M, Herbert S, Gotz F, Cheung A. Interaction of the GraRS two-component system with the VraFG ABC transporter to support vancomycin-intermediate resistance in *Staphylococcus aureus*. *Antimicrob. Agents Chemother.* 51(8), 2679–2689 (2007).

132. Li YH, Lau PC, Tang N, Svensater G, Ellen RP, Cvitkovitch DG. Novel two-component regulatory system involved in biofilm formation and acid resistance in Streptococcus mutans. *J. Bacteriol.* 184(22), 6333–6342 (2002).

133. Mascher T, Zimmer SL, Smith TA, Helmann JD. Antibiotic-inducible promoter regulated by the cell envelope stress-sensing two-component system LiaRS of *Bacillus subtilis*. *Antimicrob. Agents Chemother.* 48(8), 2888–2896 (2004).

134. Pietiainen M, Gardemeister M, Mecklin M, Leskela S, Sarvas M, Kontinen VP. Cationic antimicrobial peptides elicit a complex stress response in *Bacillus subtilis* that involves ECF-type sigma factors and two-component signal transduction systems. *Microbiology* 151(Pt 5), 1577–1592 (2005).

135. Suntharalingam P, Senadheera MD, Mair RW, Levesque CM, Cvitkovitch DG. The LiaFSR system regulates the cell envelope stress response in Streptococcus mutans. *J. Bacteriol.* 191(9), 2973–2984 (2009).

136. Klinzing DC, Ishmael N, Dunning Hotopp JC. et al. The two-component response regulator LiaR regulates cell wall stress responses, *pili* expression and virulence in group B Streptococcus. *Microbiology* 159(Pt 7), 1521–1534 (2013).

137. Kawada-Matsuo M, Komatsuzawa H. Role of Streptococcus mutans two-component systems in antimicrobial peptide resistance in the oral cavity. *Jpn. Dent. Sci. Rev.* 53(3), 86–94 (2017).

138. Kallipolitis BH, Ingmer H. Listeria monocytogenes response regulators important for stress tolerance and pathogenesis. *FEMS Microbiol. Lett.* 204(1), 111–115 (2001).

139. Cotter PD, Guinane CM, Hill C. The LisRK signal transduction system determines the sensitivity of Listeria monocytogenes to nisin and cephalosporins. *Antimicrob. Agents Chemother.* 46(9), 2784–2790 (2002).

140. Tzeng YL, Datta A, Ambrose K. et al. The MisR/MisS two-component regulatory system influences inner core structure and immunotype of lipooligosaccharide in *Neisseria meningitidis*. *J. Biol. Chem.* 279(33), 35053–35062 (2004).

141. Kandler JL, Holley CL, Reimche JL. et al. The MisR response regulator is necessary for intrinsic cationic antimicrobial peptide and aminoglycoside resistance in *Neisseria gonorrhoeae*. *Antimicrob. Agents Chemother.* 60(8), 4690–4700 (2016).

142. Johnson CR, Newcombe J, Thorne S. et al. Generation and characterization of a PhoP homologue mutant of *Neisseria meningitidis*. *Mol. Microbiol.* 39(5), 1345–1355 (2001).

143. Li Y, Zeng J, Zhang H, He ZG. The characterization of conserved binding motifs and potential target genes for M. tuberculosis MtrAB reveals a link between the two-component system and the drug resistance of *M. smegmatis*. *BMC Microbiol.* 10, 242 (2010).

144. Moker N, Brocker M, Schaffer S, Kramer R, Morbach S, Bott M. Deletion of the genes encoding the MtrA–MtrB two-component system of *Corynebacterium glutamicum* has a strong influence on cell morphology, antibiotics susceptibility and expression of genes involved in osmoprotection. *Mol. Microbiol.* 54(2), 420–438 (2004).

145. Nguyen HT, Wolff KA, Cartabuke RH, Ogwang S, Nguyen L. A lipoprotein modulates activity of the MtrAB two-component system to provide intrinsic multidrug resistance, cytokinetic control and cell wall homeostasis in Mycobacterium. *Mol. Microbiol.* 76(2), 348–364 (2010).

146. Cangelosi GA, Do JS, Freeman R, Bennett JG, Semret M, Behr MA. The two-component regulatory system mtrAB is required for morphotypic multidrug resistance in Mycobacterium avium. *Antimicrob. Agents Chemother.* 50(2), 461–468 (2006).

147. Fernandez L, Gooderham WJ, Bains M, Mcphee JB, Wiegand I, Hancock RE. Adaptive resistance to the 'last hope' antibiotics polymyxin B and colistin in *Pseudomonas aeruginosa* is mediated by the novel two-component regulatory system ParR–ParS. *Antimicrob. Agents Chemother.* 54(8), 3372–3382 (2010).

148. Dadura K, Plocinska R, Rumijowska-Galewicz A. et al. PdtaS deficiency affects resistance of mycobacteria to ribosome targeting antibiotics. *Front. Microbiol.* 8, 2145 (2017).

149. Morth JP, Gosmann S, Nowak E, Tucker PA. A novel two-component system found in Mycobacterium tuberculosis. *FEBS Lett.* 579(19), 4145–4148 (2005).

150. Srinivasan VB, Venkataramaiah M, Mondal A, Vaidyanathan V, Govil T, Rajamohan G. Functional characterization of a novel outer membrane porin KpnO, regulated by PhoBR two-component system in *Klebsiella pneumoniae* NTUH-K2044. *PLoS ONE* 7(7), e41505 (2012).

151. Olaitan AO, Morand S, Rolain JM. Mechanisms of polymyxin resistance: acquired and intrinsic resistance in bacteria. *Front. Microbiol.* 5, 643 (2014).

152. Raetz CR, Reynolds CM, Trent MS, Bishop RE. Lipid A modification systems in Gram-negative bacteria. *Ann. Rev. Bio.* 76, 295–329 (2007).

153. Cheng HY, Chen YF, Peng HL. Molecular characterization of the PhoPQ-PmrD-PmrAB mediated pathway regulating polymyxin B resistance in *Klebsiella pneumoniae* CG43. *J. Biomed. Sci.* 17, 60 (2010).

154. Gooderham WJ, Hancock RE. Regulation of virulence and antibiotic resistance by two-component regulatory systems in *Pseudomonas aeruginosa*. *FEMS Microbiol. Rev.* 33(2), 279–294 (2009).

155. Guo L, Lim KB, Gunn JS. et al. Regulation of lipid A modifications by *Salmonella typhimurium* virulence genes phoP–phoQ. *Science* 276(5310), 250–253 (1997).

156. Macfarlane EL, Kwasnicka A, Hancock RE. Role of *Pseudomonas aeruginosa* PhoP–phoQ in resistance to antimicrobial cationic peptides and aminoglycosides. *Microbiology* 146(Pt 10), 2543–2554 (2000).

157. Mcphee JB, Bains M, Winsor G. et al. Contribution of the PhoP–PhoQ and PmrA–PmrB two-component regulatory systems to Mg2+-induced gene regulation in *Pseudomonas aeruginosa*. *J. Bacteriol.* 188(11), 3995–4006 (2006).

158. Richards SM, Strandberg KL, Gunn JS. Salmonella-regulated lipopolysaccharide modifications. *Subcell. Biochem.* 53, 101–122 (2010).

159. Zhou D, Han Y, Qin L. et al. Transcriptome analysis of the Mg2+-responsive PhoP regulator in *Yersinia pestis*. *FEMS Microbiol. Lett.* 250(1), 85–95 (2005).

160. Band VI, Crispell EK, Napier BA. et al. Antibiotic failure mediated by a resistant subpopulation in *Enterobacter cloacae*. *Nat. Microbiol.* 1(6), 16053 (2016).

161. Adams MD, Nickel GC, Bajaksouzian S. et al. Resistance to colistin in *Acinetobacter baumannii* associated with mutations in the PmrAB two-component system. *Antimicrob. Agents Chemother.* 53(9), 3628–3634 (2009).

162. Beceiro A, Llobet E, Aranda J. et al. Phosphoethanolamine modification of lipid A in colistin-resistant variants of *Acinetobacter baumannii* mediated by the pmrAB two-component regulatory system. *Antimicrob. Agents Chemother.* 55(7), 3370–3379 (2011).

163. Gunn JS. The Salmonella PmrAB regulon: lipopolysaccharide modifications, antimicrobial peptide resistance and more. *Trends Microbiol.* 16(6), 284–290 (2008).

164. Moskowitz SM, Ernst RK, Miller SI. PmrAB, a two-component regulatory system of *Pseudomonas aeruginosa* that modulates resistance to cationic antimicrobial peptides and addition of aminoarabinose to lipid A. *J. Bacteriol.* 186(2), 575–579 (2004).

165. Cannatelli A, Di Pilato V, Giani T. et al. *In vivo* evolution to colistin resistance by PmrB sensor kinase mutation in KPC-producing *Klebsiella pneumoniae* is associated with low-dosage colistin treatment. *Antimicrob. Agents Chemother.* 58(8), 4399–4403 (2014).

166. Ah YM, Kim AJ, Lee JY. Colistin resistance in *Klebsiella pneumoniae*. *Int. J. Antimicrob. Agents* 44(1), 8–15 (2014).

167. Miller AK, Brannon MK, Stevens L. et al. PhoQ mutations promote lipid A modification and polymyxin resistance of *Pseudomonas aeruginosa* found in colistin-treated cystic fibrosis patients. *Antimicrob. Agents Chemother.* 55(12), 5761–5769 (2011).

168. Moskowitz SM, Brannon MK, Dasgupta N. et al. PmrB mutations promote polymyxin resistance of *Pseudomonas aeruginosa* isolated from colistin-treated cystic fibrosis patients. *Antimicrob Agents Chemother* 56(2), 1019–1030 (2012).

169. Jayol A, Nordmann P, Brink A, Poirel L. Heteroresistance to colistin in *Klebsiella pneumoniae* associated with alterations in the PhoPQ regulatory system. *Antimicrob. Agents Chemother.* 59(5), 2780–2784 (2015).

170. Cabot G, Zamorano L, Moya B. et al. Evolution of *Pseudomonas aeruginosa* Antimicrobial Resistance and Fitness under Low and High Mutation Rates. *Antimicrob. Agents Chemother*. 60(3), 1767–1778 (2016).

171. Arroyo LA, Herrera CM, Fernandez L, Hankins JV, Trent MS, Hancock RE. The pmrCAB operon mediates polymyxin resistance in Acinetobacter baumannii ATCC 17978 and clinical isolates through phosphoethanolamine modification of lipid A. *Antimicrob. Agents Chemother*. 55(8), 3743–3751 (2011).

172. Liu MC, Tsai YL, Huang YW. et al. Stenotrophomonas maltophilia PhoP, a two-component response regulator, involved in antimicrobial susceptibilities. *PLoS ONE* 11(5), e0153753 (2016).

173. Gunn JS. Bacterial modification of LPS and resistance to antimicrobial peptides. *J. Endotoxin Res.* 7(1), 57–62 (2001).

174. Clarke DJ. The Rcs phosphorelay: more than just a two-component pathway. *Future Microbiol.* 5(8), 1173–1184 (2010).

175. Erickson KD, Detweiler CS. The Rcs phosphorelay system is specific to enteric pathogens/commensals and activates *ydeI*, a gene important for persistent Salmonella infection of mice. *Mol. Microbiol.* 62(3), 883–894 (2006).

176. Farizano JV, Torres MA, Pescaretti Mde L, Delgado MA. The RcsCDB regulatory system plays a crucial role in the protection of *Salmonella enterica* serovar Typhimurium against oxidative stress. *Microbiology* 160(Pt 10), 2190–2199 (2014).

177. Ferrieres L, Clarke DJ. The RcsC sensor kinase is required for normal biofilm formation in *Escherichia coli* K-12 and controls the expression of a regulon in response to growth on a solid surface. *Mol. Microbiol.* 50(5), 1665–1682 (2003).

178. Guo XP, Sun YC. New insights into the non-orthodox two component rcs phosphorelay system. *Front. Microbiol.* 8, 2014 (2017).

179. Howery KE, Clemmer KM, Rather PN. The Rcs regulon in Proteus mirabilis: implications for motility, biofilm formation, and virulence. *Curr. Genet.* 62(4), 775–789 (2016).

180. Howery KE, Clemmer KM, Simsek E, Kim M, Rather PN. Regulation of the min cell division inhibition complex by the Rcs phosphorelay in *Proteus mirabilis*. *J. Bacteriol.* 197(15), 2499–2507 (2015).

181. Laubacher ME, Ades SE. The Rcs phosphorelay is a cell envelope stress response activated by peptidoglycan stress and contributes to intrinsic antibiotic resistance. *J. Bacteriol.* 190(6), 2065–2074 (2008).

182. Majdalani N, Gottesman S. The Rcs phosphorelay: a complex signal transduction system. *Ann. Rev. Microbiol.* 59, 379–405 (2005).

183. Mouslim C, Groisman EA. Control of the Salmonella *ugd* gene by three two-component regulatory systems. *Mol. Microbiol.* 47(2), 335–344 (2003).

184. Szczesny M, Beloin C, Ghigo JM. Increased osmolarity in biofilm triggers RcsB-dependent lipid A palmitoylation in *Escherichia coli*. *mBio* 9(4), pii:e01415–18 (2018).

185. Mikkelsen H, Ball G, Giraud C, Filloux A. Expression of *Pseudomonas aeruginosa* CupD fimbrial genes is antagonistically controlled by RcsB and the EAL-containing PvrR response regulators. *PLoS ONE* 4(6), e6018 (2009).

186. Pruss BM. Evaluation of CpxRA as a therapeutic target for uropathogenic *Escherichia coli* infections. Evaluation of CpxRA as a therapeutic target for uropathogenic *Escherichia coli* infections. *J. Bacteriol.* 199(18), pii:e00259–17 (2017). [Google Scholar]

187. Mikkelsen H, Sivaneson M, Filloux A. Key two-component regulatory systems that control biofilm formation in *Pseudomonas aeruginosa*. *Environ. Microbiol.* 13(7), 1666–1681 (2011).

188. Goodman AL, Merighi M, Hyodo M, Ventre I, Filloux A, Lory S. Direct interaction between sensor kinase proteins mediates acute and chronic disease phenotypes in a bacterial pathogen. *Genes Dev.* 23(2), 249–259 (2009).

189. Parkins MD, Ceri H, Storey DG. *Pseudomonas aeruginosa* GacA, a factor in multihost virulence, is also essential for biofilm formation. *Mol. Microbiol.* 40(5), 1215–1226 (2001).

190. Dingemans J, Poudyal B, Sondermann H, Sauer K. The Yin and Yang of SagS: distinct residues in the HmsP domain of SagS independently regulate biofilm formation and biofilm drug tolerance. *mSphere* 3(3), pii:e00192–18 (2018).

191. Petrova OE, Gupta K, Liao J, Goodwine JS, Sauer K. Divide and conquer: the *Pseudomonas aeruginosa* two-component hybrid SagS enables biofilm formation and recalcitrance of biofilm cells to antimicrobial agents via distinct regulatory circuits. *Environ. Microbiol.* 19(5), 2005–2024 (2017).

192. Gupta K, Marques CN, Petrova OE, Sauer K. Antimicrobial tolerance of *Pseudomonas aeruginosa* biofilms is activated during an early developmental stage and requires the two-component hybrid SagS. *J. Bacteriol.* 195(21), 4975–4987 (2013).

193. Petrova OE, Sauer K. SagS contributes to the motile-sessile switch and acts in concert with BfiSR to enable *Pseudomonas aeruginosa* biofilm formation. *J. Bacteriol.* 193(23), 6614–6628 (2011).

194. Poudyal B, Sauer K. The ABC of biofilm drug tolerance: the MerR-Like Regulator BrlR Is an Activator of ABC Transport Systems, with PA1874-77 Contributing to the Tolerance

of *Pseudomonas aeruginosa* Biofilms to Tobramycin. *Antimicrob. Agents Chemother.* 62(2), pii:e01981-17 (2018).

195. Chambers JR, Liao J, Schurr MJ, Sauer K. BrlR from *Pseudomonas aeruginosa* is a c-di-GMP-responsive transcription factor. *Mol. Microbiol.* 92(3), 471–487 (2014).

196. Liao J, Schurr MJ, Sauer K. The MerR-like regulator BrlR confers biofilm tolerance by activating multidrug efflux pumps in *Pseudomonas aeruginosa* biofilms. *J. Bacteriol.* 195(15), 3352–3363 (2013).

197. Liao J, Sauer K. The MerR-like transcriptional regulator BrlR contributes to *Pseudomonas aeruginosa* biofilm tolerance. *J. Bacteriol.* 194(18), 4823–4836 (2012).

198. Wu CJ, Huang YW, Lin YT, Ning HC, Yang TC. Inactivation of SmeSyRy two-component regulatory system inversely regulates the expression of SmeYZ and SmeDEF efflux pumps in *Stenotrophomonas maltophilia*. *PLoS ONE* 11(8), e0160943 (2016).

199. Faron ML, Ledeboer NA, Buchan BW. Resistance mechanisms, epidemiology, and approaches to screening for vancomycin-resistant enterococcus in the health care setting. *J. Clin. Microbiol.* 54(10), 2436–2447 (2016).

200. Mcguinness WA, Malachowa N, Deleo FR. Vancomycin resistance in *Staphylococcus aureus*. *Yale J. Biol. Med.* 90(2), 269–281 (2017).

201. Novotna GB, Kwun MJ, Hong HJ. *In vivo* characterization of the activation and interaction of the VanR-VanS two-component regulatory system controlling glycopeptide antibiotic resistance in two related streptomyces species. *Antimicrob. Agents Chemother.* 60(3), 1627–1637 (2015).

202. Evers S, Courvalin P. Regulation of VanB-type vancomycin resistance gene expression by the VanS(B)-VanR (B) two-component regulatory system in *Enterococcus faecalis* V583. *J. Bacteriol.* 178(5), 1302–1309 (1996).

203. Hong HJ, Hutchings MI, Buttner MJ. Vancomycin resistance VanS/VanR two-component systems. *Adv. Exp. Med. Biol.* 631, 200–213 (2008).

204. Hutchings MI, Hong HJ, Buttner MJ. The vancomycin resistance VanRS two-component signal transduction system of Streptomyces coelicolor. *Mol. Microbiol.* 59(3), 923–935 (2006).

205. Li L, Wang Q, Zhang H, Yang M, Khan MI, Zhou X. Sensor histidine kinase is a beta-lactam receptor and induces resistance to beta-lactam antibiotics. *Proc. Natl Acad. Sci. USA* 113(6), 1648–1653 (2016).

206. Ahn SJ, Burne RA. Effects of oxygen on biofilm formation and the AtlA autolysin of Streptococcus mutans. *J. Bacteriol.* 189(17), 6293–6302 (2007).

207. Senadheera MD, Guggenheim B, Spatafora GA. et al. A VicRK signal transduction system in Streptococcus mutans affects gtfBCD, gbpB, and ftf expression, biofilm formation, and genetic competence development. *J. Bacteriol.* 187(12), 4064–4076 (2005).

208. Stipp RN, Boisvert H, Smith DJ, Höfling JF, Duncan MJ, Mattos-Graner RO. CovR and VicRK Regulate Cell Surface Biogenesis Genes Required for Biofilm Formation in Streptococcus mutans. *PLoS ONE* 8(3), e58271 (2013).

209. Collins B, Curtis N, Cotter PD, Hill C, Ross RP. The ABC transporter AnrAB contributes to the innate resistance of Listeria monocytogenes to nisin, bacitracin, and various beta-lactam antibiotics. *Antimicrob. Agents Chemother.* 54(10), 4416–4423 (2010).

210. Mandin P, Fsihi H, Dussurget O. et al. VirR, a response regulator critical for Listeria monocytogenes virulence. *Mol. Microbiol.* 57(5), 1367–1380 (2005).

211. Kuroda M, Kuroda H, Oshima T, Takeuchi F, Mori H, Hiramatsu K. Two-component system VraSR positively modulates the regulation of cell-wall biosynthesis pathway in *Staphylococcus aureus*. *Mol. Microbiol.* 49(3), 807–821 (2003).

212. Chen H, Xiong Z, Liu K. et al. Transcriptional profiling of the two-component regulatory system VraSR in *Staphylococcus aureus* with low-level vancomycin resistance. *Int. J. Antimicrob. Agents* 47(5), 362–367 (2016).

213. Boyle-Vavra S, Yin S, Daum RS. The VraS/VraR two-component regulatory system required for oxacillin resistance in community-acquired methicillin-resistant *Staphylococcus aureus*. *FEMS Microbiol. Lett.* 262(2), 163–171 (2006).

214. Gardete S, Wu SW, Gill S, Tomasz A. Role of VraSR in antibiotic resistance and antibiotic-induced stress response in *Staphylococcus aureus*. *Antimicrob. Agents Chemother.* 50(10), 3424–3434 (2006).

215. Belcheva A, Golemi-Kotra D. A close-up view of the VraSR two-component system. A mediator of *Staphylococcus aureus* response to cell wall damage. *J. Biol. Chem.* 283(18), 12354–12364 (2008).

216. Mehta S, Cuirolo AX, Plata KB. et al. VraSR two-component regulatory system contributes to mprF-mediated decreased susceptibility to daptomycin in *in vivo*-selected clinical strains of methicillin-resistant *Staphylococcus aureus*. *Antimicrob. Agents Chemother.* 56(1), 92–102 (2012).

217. Yin S, Daum RS, Boyle-Vavra S. VraSR two-component regulatory system and its role in induction of pbp2 and vraSR expression by cell wall antimicrobials in *Staphylococcus aureus*. *Antimicrob. Agents Chemother.* 50(1), 336–343 (2006).

218. Martin PK, Bao Y, Boyer E. et al. Novel *locus* required for expression of high-level macrolide-lincosamide-streptogramin B resistance in *Staphylococcus aureus*. *J. Bacteriol.* 184(20), 5810–5813 (2002).

219. Dubrac S, Boneca IG, Poupel O, Msadek T. New insights into the WalK/WalR (YycG/YycF) essential signal transduction pathway reveal a major role in controlling cell wall metabolism and biofilm formation in *Staphylococcus aureus*. *J. Bacteriol.* 189(22), 8257–8269 (2007).

220. Martin PK, Li T, Sun D, Biek DP, Schmid MB. Role in cell permeability of an essential two-component system in *Staphylococcus aureus*. *J. Bacteriol.* 181(12), 3666–3673 (1999).

221. Zhang S, Li X, Wang X, Li Z, He J. The two-component signal transduction system YvcPQ regulates the bacterial resistance to bacitracin in Bacillus thuringiensis. *Arch. Microbiol.* 198(8), 773–784 (2016).

222. Kapoor G, Saigal S, Elongavan A. Action and resistance mechanisms of antibiotics: a guide for clinicians. *J. Anaesthesiol. Clin. Pharmacol.* 33(3), 300–305 (2017). • A concise and effective introduction to the mechanisms of antibiotic resistance.

223. Hancock RE. Peptide antibiotics. *Lancet* 349(9049), 418–422 (1997).

224. Hancock RE, Chapple DS. Peptide antibiotics. *Antimicrob. Agents Chemother.* 43(6), 1317–1323 (1999).

225. Bahar AA, Ren D. Antimicrobial peptides. *Pharmaceuticals* 6(12), 1543–1575 (2013).

226. Jana S, Deb JK. Molecular understanding of aminoglycoside action and resistance. *Appl. Microbiol. Biotechnol.* 70(2), 140–150 (2006).

227. Tran TB, Velkov T, Nation RL. et al. Pharmacokinetics/pharmacodynamics of colistin and polymyxin B: are we there yet? *Int. J. Antimicrob. Agents* 48(6), 592–597 (2016).

228. Kox LFF, Wösten M, Groisman EA. A small protein that mediates the activation of a two-component system by another two-component system. *EMBO J.* 19(8), 1861–1872 (2000).

229. Chen HD, Groisman EA. The biology of the PmrA/PmrB two-component system: the major regulator of lipopolysaccharide modifications. *Ann. Rev. Microbiol.* 67, 83–112 (2013).

230. Yuan J, Jin F, Glatter T, Sourjik V. Osmosensing by the bacterial PhoQ/PhoP two-component system. *Proc. Natl Acad. Sci. USA* 114(50), E10792–E10798 (2017).

231. Groisman EA. The pleiotropic two-component regulatory system PhoP–PhoQ. *J. Bacteriol.* 183(6), 1835–1842 (2001).

232. Ly NS, Yang J, Bulitta JB, Tsuji BT. Impact of two-component regulatory systems PhoP–PhoQ and PmrA-PmrB on colistin pharmacodynamics in *Pseudomonas aeruginosa*. *Antimicrob. Agents Chemother.* 56(6), 3453–3456 (2012).

233. Wright MS, Jacobs MR, Bonomo RA, Adams MD. Transcriptome remodeling of *Acinetobacter baumannii* during infection and treatment. *mBio* 8(2), pii:e02193–16 (2017).

234. Lo Sciuto A, Imperi F. Aminoarabinosylation of lipid A is critical for the development of colistin resistance in *Pseudomonas aeruginosa*. *Antimicrob. Agents Chemother.* 62(3), pii:e01820–17 (2018).

235. Chalabaev S, Chauhan A, Novikov A. et al. Biofilms formed by Gram-negative bacteria undergo increased lipid a palmitoylation, enhancing *in vivo* survival. *mBio* 5(4), pii:e01116–14 (2014).

236. Qiao Y, Srisuknimit V, Rubino F. et al. Lipid II overproduction allows direct assay of transpeptidase inhibition by beta-lactams. *Nat. Chem. Biol.* 13(7), 793–798 (2017).

237. Kohanski MA, Dwyer DJ, Collins JJ. How antibiotics kill bacteria: from targets to networks. *Nat. Rev. Microbiol.* 8(6), 423–435 (2010).

238. Falord M, Karimova G, Hiron A, Msadek T. GraXSR proteins interact with the VraFG ABC transporter to form a five-component system required for cationic antimicrobial peptide sensing and resistance in *Staphylococcus aureus*. *Antimicrob. Agents Chemother.* 56(2), 1047–1058 (2012).

239. Li M, Cha DJ, Lai Y, Villaruz AE, Sturdevant DE, Otto M. The antimicrobial peptide-sensing system aps of *Staphylococcus aureus*. *Mol. Microbiol.* 66(5), 1136–1147 (2007).

240. Achouak W, Heulin T, Pages JM. Multiple facets of bacterial porins. *FEMS Microbiol. Lett.* 199(1), 1–7 (2001).

241. Pages JM, James CE, Winterhalter M. The porin and the permeating antibiotic: a selective diffusion barrier in Gram-negative bacteria. *Nat. Rev. Microbiol.* 6(12), 893–903 (2008).

242. Li XZ, Plesiat P, Nikaido H. The challenge of efflux-mediated antibiotic resistance in Gram-negative bacteria. *Clin. Microbiol. Rev.* 28(2), 337–418 (2015).

243. Fernandez L, Hancock RE. Adaptive and mutational resistance: role of porins and efflux pumps in drug resistance. *Clin. Microbiol. Rev.* 25(4), 661–681 (2012).

244. Delcour AH. Outer membrane permeability and antibiotic resistance. *Biochim. Biophys. Acta* 1794(5), 808–816 (2009).

245. Blair JM, Richmond GE, Piddock LJ. Multidrug efflux pumps in Gram-negative bacteria and their role in antibiotic resistance. *Future Microbiol.* 9(10), 1165–1177 (2014).

246. Webber MA, Piddock LJV. The importance of efflux pumps in bacterial antibiotic resistance. *J. Antimicrob. Chemother.* 51(1), 9–11 (2003).

247. Colangeli R, Helb D, Sridharan S. et al. The Mycobacterium tuberculosis *iniA* gene is essential for activity of an efflux pump that confers drug tolerance to both isoniazid and ethambutol. *Mol. Microbiol.* 55(6), 1829–1840 (2005).

248. Alland D, Steyn AJ, Weisbrod T, Aldrich K, Jacobs WR., Jr Characterization of the Mycobacterium tuberculosis iniBAC promoter, a promoter that responds to cell wall biosynthesis inhibition. *J. Bacteriol.* 182(7), 1802–1811 (2000).

249. Zahrt TC, Deretic V. An essential two-component signal transduction system in Mycobacterium tuberculosis. *J. Bacteriol.* 182(13), 3832–3838 (2000).

250. Bretl DJ, Demetriadou C, Zahrt TC. Adaptation to environmental stimuli within the host: two-component signal transduction systems of Mycobacterium tuberculosis. *Microbiol. Mol. Biol. Rev.* 75(4), 566–582 (2011).

251. Curcic R, Dhandayuthapani S, Deretic V. Gene expression in mycobacteria: transcriptional fusions based on xylE and analysis of the promoter region of the response regulator mtrA from Mycobacterium tuberculosis. *Mol. Microbiol.* 13(6), 1057–1064 (1994).

252. Via LE, Curcic R, Mudd MH, Dhandayuthapani S, Ulmer RJ, Deretic V. Elements of signal transduction in Mycobacterium tuberculosis: *in vitro* phosphorylation and *in vivo* expression of the response regulator MtrA. *J. Bacteriol.* 178(11), 3314–3321 (1996).

253. Kundu M. The role of two-component systems in the physiology of Mycobacterium tuberculosis. *IUBMB Life* 70(8), 710–717 (2018).

254. Gorla P, Plocinska R, Sarva K. et al. MtrA response regulator controls cell division and cell wall metabolism and affects susceptibility of mycobacteria to the first line antituberculosis drugs. *Front. Microbiol.* 9, 2839 (2018).

255. Santajit S, Indrawattana N. Mechanisms of antimicrobial resistance in ESKAPE pathogens. *Biomed. Res. Int.* 2016, 3314 (2016).

256. Van Acker H, Van Dijck P, Coenye T. Molecular mechanisms of antimicrobial tolerance and resistance in bacterial and fungal biofilms. *Trends Microbiol.* 22(6), 326–333 (2014).

257. Singh S, Singh SK, Chowdhury I, Singh R. Understanding the mechanism of bacterial biofilms resistance to antimicrobial agents. *Open Microbiol. J.* 11, 53–62 (2017).

258. Hoiby N, Bjarnsholt T, Givskov M, Molin S, Ciofu O. Antibiotic resistance of bacterial biofilms. *Int. J. Antimicrob. Agents* 35(4), 322–332 (2010).

259. Stewart PS, William Costerton J. Antibiotic resistance of bacteria in biofilms. *Lancet* 358(9276), 135–138 (2001).

260. Stewart PS. Mechanisms of antibiotic resistance in bacterial biofilms. *Int. J. Med. Microbiol.* 292(2), 107–113 (2002).

261. Ridenhour BJ, Metzger GA, France M. et al. Persistence of antibiotic resistance plasmids in bacterial biofilms. *Evol. Appl.* 10(6), 640–647 (2017).

262. Mah TF. Biofilm-specific antibiotic resistance. *Future Microbiol.* 7(9), 1061–1072 (2012).

263. Olsen I. Biofilm-specific antibiotic tolerance and resistance. *Eur. J. Clin. Microbiol. Infect. Dis.* 34(5), 877–886 (2015).

264. Mulcahy H, Charron-Mazenod L, Lewenza S. Extracellular DNA chelates cations and induces antibiotic resistance in *Pseudomonas aeruginosa* biofilms. *PLoS Pathog.* 4(11), e1000213 (2008).

265. Kulasekara HD, Ventre I, Kulasekara BR, Lazdunski A, Filloux A, Lory S. A novel two-component system controls the expression of *Pseudomonas aeruginosa* fimbrial cup genes. *Mol. Microbiol.* 55(2), 368–380 (2005).

266. Hobbs M, Collie ES, Free PD, Livingston SP, Mattick JS. PilS and PilR, a two-component transcriptional regulatory system controlling expression of type 4 fimbriae in *Pseudomonas aeruginosa*. *Mol. Microbiol.* 7(5), 669–682 (1993).

267. Giraud C, Bernard CS, Calderon V. et al. The PprA–PprB two-component system activates CupE, the first non-archetypal *Pseudomonas aeruginosa* chaperone-usher pathway system assembling fimbriae. *Environ. Microbiol.* 13(3), 666–683 (2011).

268. Bernard CS, Bordi C, Termine E, Filloux A, De Bentzmann S. Organization and PprB-dependent control of the *Pseudomonas aeruginosa* tad *Locus*, involved in Flp pilus biology. *J. Bacteriol.* 191(6), 1961–1973 (2009).

269. Proctor RA, Von Eiff C, Kahl BC. et al. Small colony variants: a pathogenic form of bacteria that facilitates persistent and recurrent infections. *Nat. Rev. Microbiol.* 4(4), 295–305 (2006).

270. Evans TJ. Small colony variants of *Pseudomonas aeruginosa* in chronic bacterial infection of the lung in cystic fibrosis. *Future Microbiol.* 10(2), 231–239 (2015).

271. Poole K. Bacterial stress responses as determinants of antimicrobial resistance. *J. Antimicrob. Chemother.* 67(9), 2069–2089 (2012).

272. Poole K. Stress responses as determinants of antimicrobial resistance in Gram-negative bacteria. *Trends Microbiol.* 20(5), 227–234 (2012).

273. Poole K. Stress responses as determinants of antimicrobial resistance in *Pseudomonas aeruginosa*: multidrug efflux and more. *Can. J. Microbiol.* 60(12), 783–791 (2014).

Figures and Tables

Figure 1

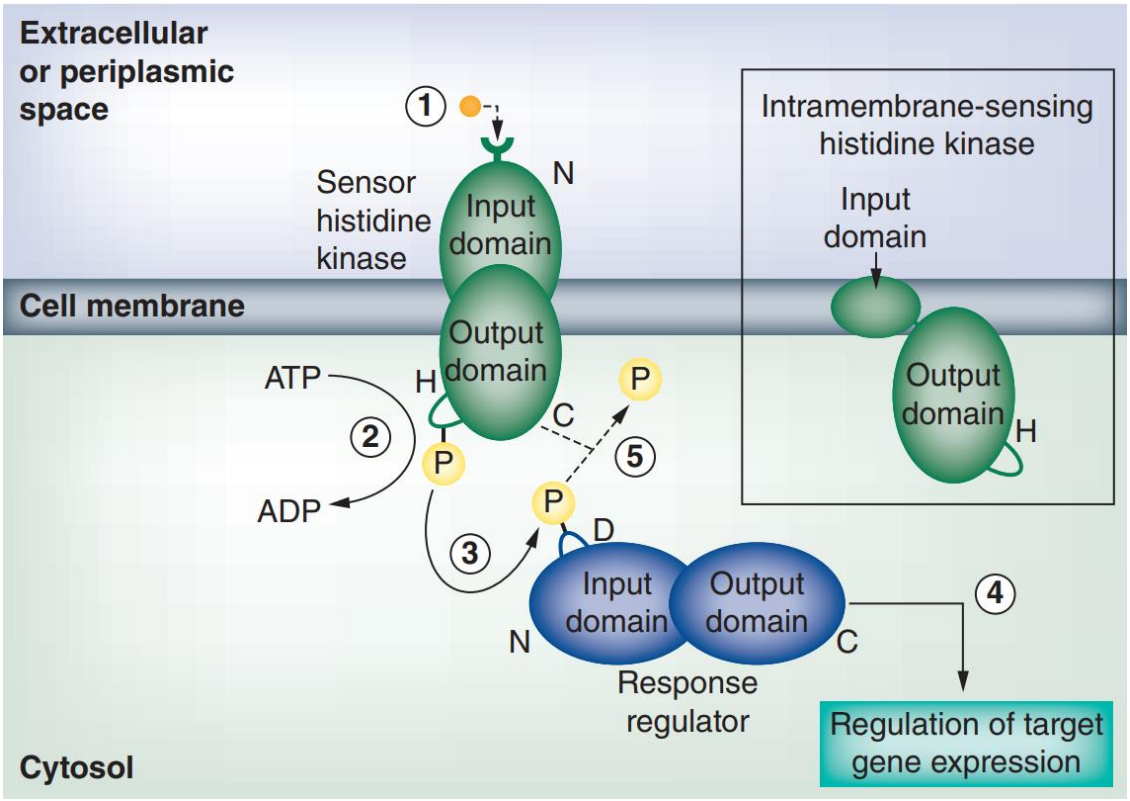

Figure 1. The basic process of two-component signal transduction. (1) An extracellular ligand (orange) binds to the N-terminal receptor of the sensor histidine kinase (green), embedded in the cell membrane. Binding of the ligand causes **(2)** the C-terminal kinase domain to hydrolyze adenosine triphosphate and phosphorylate a histidine residue. **(3)** The phosphate (yellow) is then transferred to an aspartate residue on the N-terminal domain of the cytosolic response regulator (blue). **(4)** This phosphorylation event activates the response regulator's C-terminal output domain, which leads to global transcriptional changes. **(5)** In some cases, the sensor histidine kinase also functions as a phosphatase, and terminates the response regulator's activation by removal of the phosphate. Inset to right: intramembrane-sensing histidine kinases lack an extracytoplasmic sensory domain and have recently been shown to recruit other sensory proteins in order to function.

Table 1. Summary of two-component regulatory systems that increase antibiotic resistance.

Two-component system	Regulation increasing antibiotic resistance	Antibiotic resistance(s)	Example species	Ref.
AarG	Increased expression of an aminoglycoside acetyltransferase Global transcriptional changes leading to increased intrinsic resistances	Aminoglycosides Tetracycline Chloramphenicol Ciprofloxacin	*Providencia stuartii*	[37]
AdeRS	Upregulation of AdeAB(C) efflux pump	Intrinsic resistance	*Acinetobacter baumannii*	[38–44]
AmgRS	Upregulation of MDR efflux pumps Activation of stress response protects membrane Mutations can give rise to SCVs	Aminoglycosides Intrinsic resistance	*Pseudomonas aeruginosa*	[45–48]
BaeSR	Upregulation of MDR efflux pumps	Ceftriaxone Intrinsic resistance	*A. baumannii* *Escherichia coli* *Salmonella enterica*	[38–40,42,49–52]
BfmRS	Increases formation of biofilm	Chloramphenicol Intrinsic resistance	*A. baumannii*	[1,38,39,53–56]
BlrAB	Activation of three β-lactamase genes	β-lactams	*Aeromonas species*	[57–59]
BraRS (BceRS, NsaRS)	Upregulation of MDR efflux pumps	Nisin Bacitracin	*Staphylococcus aureus* *Bacillus subtilis*	[60–66]
CesRK	Upregulation of cell-envelope related genes	β-lactams	*Listeria monocytogenes*	[67–69]
CesSR	Upregulation of cell-envelope related genes	Bacitracin Bacteriocins	*Lactococcus lactis*	[70]
CiaRH	Upregulation of cell-envelope related genes	β-lactams Cefotaxime Polymyxin B	*Streptococcus pneumoniae* Group B *Streptococcus*	[71–78]
ComDE	Increases formation of biofilm	Intrinsic resistance	*Streptococcus mutans*	[79,80]
CopRS	Decreased porin expression	β-lactams Carbapenems	*P. aeruginosa*	[81,82]
CprRS	Modification of lipid A by 4-aminoarabinose (via *arn* operon)	Polymyxins Aminoglycosides	*P. aeruginosa*	[83–88]

CpxAR	Decreased porin expression Upregulation of MDR efflux pumps	Chloramphenicol Amikacin Nalidixic acid Tetracycline	*Klebsiella pneumoniae* *E. coli*	[8,89–95]
CreBC	Activation of β-lactamase gene Increases formation of biofilm	β-lactams Intrinsic resistance	*P. aeruginosa*	[96–99]
CroRS	Upregulation PBP5	β-lactams	*Enterococcus* species	[100–106]
CzcRS	Decreased porin expression	β-lactams Carbapenems	*P. aeruginosa*	[82,107]
EnvZ/OmpR	Decreased porin expression Upregulation of MDR efflux pumps	β-lactams Intrinsic resistance	*E. coli* *A. baumannii* *Yersinia pseudotuberculosis* *S. enterica*	[89,90,108–122]
EvgAS	Upregulation of MDR efflux pumps	Intrinsic resistance	*E. coli* *Klebsiella pneumoniae* *Vibrio cholera* *P. aeruginosa*	[95,123–126]
fsr	Increases formation of biofilm via production of gelatinase	Intrinsic resistance	*Enterococcus faecalis*	[127]
GacSA	Increases formation of biofilm	Intrinsic resistance	*A. baumannii*	[128]
GraRS (aps)	Modification of teichoic acids via *D*-alanylation which reverses bacterial surface charge Upregulation of VraFG ABC transporter	Daptomycin Vancomycin Cationic antibiotics	*S. aureus*	[61,129–131]
hk11/rr11	Increases formation of biofilm	Intrinsic resistance	*S. mutans*	[132]
LiaSR	Regulation of cell wall stress responses Increases formation of biofilm	Vancomycin Bacitracin β-lactams Polymyxin B Nisin Intrinsic resistance	*B. subtilis* *Streptococcus species*	[34,60,71,133–137]

Two-component system	Regulation increasing antibiotic resistance	Antibiotic resistance(s)	Example species	Ref.
LisRK	Mechanism unknown	Nisin Cephalosporins	*L. monocytogenes*	[60,138,139]
LsrRS	Activation of ABC transporter LctFEG	Nukacin ISK-1	*S. mutans*	[60,61]
MisSR	Mechanism unknown; hypothesized upregulation of cell-envelope related proteins to protect the cell	Polymyxins Aminoglycosides	*Neisseria gonorrhoeae* *Neisseria meningitidis*	[140–142]
MtrAB	Upregulation of efflux pumps Regulation of a genetic switch to an MDR colony morphotype	Isoniazid Rifampicin Ethambutol Vancomycin	*Mycobacterium tuberculosis* *Mycobacterium smegmatis* *Mycobacterium avium*	[143–146]
NsrRS	Activation of NsrX, a gene hypothesized to interfere with nisin binding to lipid II	Nisin	*S. mutans*	[60,61]
ParRS	Modification of lipid A by 4-aminoarabinose (via *arn* operon)	Polymyxins Aminoglycosides	*P. aeruginosa*	[86–88,147]
PdtaRS	Mechanism unknown; hypothesized modification of 30S subunit of ribosome	Tetracycline Penimepicycline Blastocidin S	*M. smegmatis*	[148,149]
PhoBR	Decreased porin expression	Chloramphenicol Amikacin Nalidixic acid Tetracycline	*K. pneumoniae*	[150]
PhoPQ	Modification of lipid A by 4-aminoarabinose, phosphoethanolamine (via PmrAB), or palmitate (via PagP) Upregulation of efflux pumps (some species)	Polymyxins Aminoglycosides	*Enterobacter cloacae* *P. aeruginosa* *S. enterica* *K. pneumoniae* *Yersinia pestis*	[151–172]
PmrAB	Modification of lipid A by 4-aminoarabinose or phosphoethanolamine Mutations can give rise to SCVs in *P. aeruginosa*	Polymyxins Aminoglycosides	*A. baumannii* *S. enterica* *P. aeruginosa* *K. pneumoniae*	[39,153,157,161–164,167,168,171,173]

RcsBCD	Increases biofilm formation Regulates a gene required for 4-aminoarabinose modification of lipid A	Daptomycin Cationic antibiotics Intrinsic resistance	*E. coli* *S. enterica* *Proteus mirabilis*	[158,174–186]
RetS-GacSA	Increases formation of biofilm	Intrinsic resistance	*P. aeruginosa*	[187–189]
SagS	Upregulation of MDR efflux pumps Increases formation of biofilm via BfiSR TCS	Tobramycin Intrinsic resistance	*P. aeruginosa*	[190–197]
SmeRySy	Upregulation of SmeZ efflux pump	Aminoglycosides	*Stenotrophomonas maltophilia*	[198]
VanSR	Alters vancomycin target through several actions	Vancomycin	*S. aureus*	[199–204]
VbrKR	Activation of β-lactamase genes	β-lactams	*Vibrio parahaemolyticus*	[6,205]
VicKR	Increases formation of biofilm	Intrinsic resistance	*Streptococcus* species	[137,206–208]
VirRS	Upregulation of ABC transporter AnrAB	Nisin	*L. monocytogenes*	[60,209,210]
VraSR	Increases peptidoglycan synthesis and expression of PBP2	Methicillin Vancomycin Daptomycin Oxacillin β-lactams	*S. aureus*	[60,211–217]
WalKR (YycFG)	Mechanism unknown; hypothesized increased permeability or decreased efflux Increases formation of biofilm	Macrolides Lincosamides Intrinsic resistance	*S. aureus*	[218–220]
YvcPQ	Upregulation of MDR efflux pumps	Lantibiotics Bacitracin	*Bacillus thuringiensis*	[221]

The purpose of this table is to provide the reader with a list of two-component regulatory systems that can increase antibiotic resistance, the mechanisms by which resistance occurs, examples of antibiotics that can be affected, and examples of bacterial species in which one or more of these resistances can occur. Table entries that occupy the same row are not intended to be exclusively linked.
MDR: Multidrug resistance; SCV: Small colony variant; TCS: Two-component system.